PART I

A

Synthesis of 1,3,3-Trinitroazetidine via the Oxidative Nitration of N-p-Tosyl-3-azetidinone Oxime

and

PART II

Synthesis and Conformational Studies of Urea-Based Calix[4]arenes

by

HAMID YAZDEKHASTI

A Dissertation Submitted to the Graduate Faculty in Chemistry in Partial Fulfillment of the Requirements for the Degree of Doctor of Philosophy, The City University of New York

1995

This manuscript has been read and accepted for the Graduate Faculty in Chemistry in satisfaction of the dissertation requirement for the degree of Doctor of Philosophy.

4-28-95
Date

Chair of Examining Committee

4-28-95
Date

Executive officer

Supervisory Committee

The City University of New York

Abstract

PART I

Synthesis of 1,3,3-Trinitroazetidine via theOxidative Nitration of N-p-Tosyl-3-azetidinone Oxime

and

PART II

Synthesis and Conformational Studies of Urea-Based Calix[4]arenes

by

HAMID YAZDEKHASTI

Adviser: Professor Theodore Axenrod

PART I

The synthesis of 1,3,3-trinitroazetidine 1 has been accomplished. Alkylation of p-toluenesulfonamide with the tert-butyldimethylsilyl ethers of 1,3-dihalo-2-propanols in the presence of K_2CO_3 afforded the tert-butyldimethylsilyl ethers of 3-azetidinol. Cleavage of N-(p-toluenesulfonyl)-3-(t-butyldimethylsiloxy)azetidine with acetic acid gave N-(p-toluene-

sulfonyl)-3-azetidinol **42.** Subsequent oxidation with CrO_3/HOAc gave N-(p-toluenesulfonyl)-3-azetidinone **24.** Treatment of the ketone with hydroxylamine hydrochloride afforded N-(p-toluenesulfonyl)-3-azetidinone oxime **7.** In the final step this oxime was allowed to react with 99% HNO_3 to simultaneously nitrolyze the p-toluenesulfonyl group and oxidize the oxime moiety to produce 1,3,3-trinitroazetidine **1.**

PART II

The reaction of 1,3- and 1,4-bis(bromomethyl)benzene with the dianion of the 5-tert-butyltetrahydro-1,3,5-triazine 2(1H)one and 2-imidazolidone has been used to synthesize a series of 16- and 18-membered ring calixarene analogs which incorporate the cyclic urea units. The structures and conformations of these novel macrocyclic ring systems have been investigated in the solid state by x-ray crystallography and in solution by various NMR methods. The results indicate important conformational equilibria dominated by species having *syn* and *anti* alignments of the urea carbonyl groups. The interconversion of these conformers likely occurs by carbonyl group through the annulus rotation. AM1 semi-empirical molecular orbital geometry optimizations are consistent with these findings.

Acknowledgments

I would first like to express my sincere gratitude to my advisor, Theodore Axenrod for his guidance and his example over the past few years. He has taught me much about scientific thinking and the benefits of the continued pursuit of knowledge. I would also like to thank the members of my advisory committee, Professors L.H. Schwartz, S.H. Wilen, and H.E. Zieger for their time and helpful suggestions.

I would like to thank Professor Clara Watnick for her help, direction, invaluable discussions and suggestions relating to my projects.

I would like to also thank Professor H.L. Ammon for the x-ray crystallographic measurements and AM1 calculations.

It is with great pleasure that I acknowledge the technical staff of the Chemistry Department at The City College, particularly Joseph LaRubbio, Miguel Mieles and Hugo Schimatz for their friendship and assistance throughout the years. I am also grateful to Ramsey Pal for running all of the low resolution mass spectra. I would like to also acknowledge the Chemistry Department at The City College for the financial support.

Finally, I am truly grateful to my parents and my brother Reza who have been an inspiration to me and have given me much comfort and support.

To my parents and my brother

Table of Contents

PART II

Synthesis and Conformational Studies of Urea-Based Calix[4]arenes

CHAPTER 2

APPENDICES

List of Tables

List of Figures

PART I

Synthesis of 1,3,3-Trinitroazetidine

CHAPTER 1

1.0. Introduction

During the past two decades, there has been an accelerating effort toward the development of less sensitive and more powerful energetic materials for both civilian and military applications. This emphasis on decreased sensitivity stems from the desire to make the handling and manufacture of these materials safer, as well as the prevention of secondary detonation.[1,2]

The search for more powerful energetic material has focused on the synthesis of two classes of energetic compounds, carbocyclic polynitro cage and polynitro heterocyclic ring compounds containing both C-NO_2 and N-NO_2 groups.[1] Under active investigation as new high energy compounds are polynitrocubanes **2**,[2] polynitrobicyclododecane **3**,[4] polynitroadamantanes **4**,[3,4] polynitronorbornanes **5**,[1c] and various polynitro mono- and polycyclic polyazanitramines **6** (see Figure 1.1).[1b,4,5] Such materials are potentially

useful as explosives, propellants, fuels and binders in applications requiring materials which combine high-energy, high-density and reduced sensitivity properties.

Recently, the synthesis of 1,3,3-trinitroazetidine **1**, a member of the class of polynitro heterocyclic ring compounds, has captivated the interest of the energetic materials community, because of its many desirable properties.[11,21,22,25]

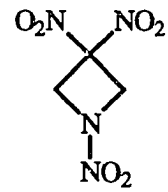

1

Among these are a low melting point (mp 101°C), which makes it steam castable (i.e., a decided advantage in that munitions can be melt-pour loaded as opposed to pressure loaded),[10] moderate density (1.84 g cm^{-3}), good thermal stability (>240°C) in addition to low impact sensitivity.[10] Infrared[6] and thermolysis[7] studies have been reported for this material as well as the experimental[8] and theoretical[9] examination of the energetics of its initial dissociation process. The objective of the present investigation is to develop an alternate synthesis of 1,3,3-trinitroazetidine **1** (TNAZ).

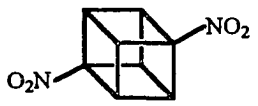

2

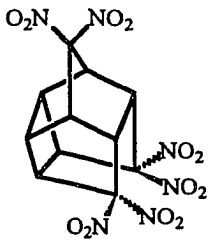

3

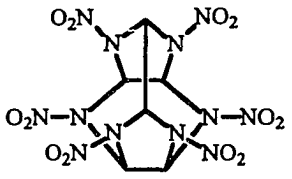

6

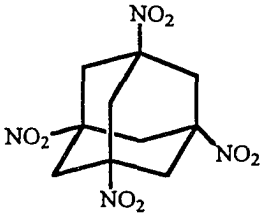

4

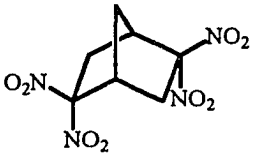

5

Figure 1.1. Some potential new energetic materials.

1.2. Background

The preparation of 1,3,3-trinitroazetidine **1** is presently focused upon the synthesis of 1,3-substituted azetidines with the expectation that these intermediates could be transformed into polynitro-substituted azetidines (i.e., 1,3,3-trinitroazetidine **1**).[11,12,13,14,15,16]

The synthesis of 1,3,3-trinitroazetidine **1** was initially reported in 1990 by Archibald et al.[11a] Their methodology involved a stepwise procedure for the introduction of C-nitro groups to the azetidine ring system. This synthetic design is illustrated in Scheme 1.

The first C-NO_2 group was introduced by sodium nitrite ion displacement of the mesylate of N-alkyl-azetidine **8**. Subsequent Kornblum[11b] oxidative nitration of the anion of the mononitro-N-alkyl-derivative of azetidine **9** with potassium ferrocyanide and sodium persulfate in the presense of a large excess of sodium nitrite ion, produced the N-alkyl-3,3-dinitroazetidine **10** (i.e., gem-dinitro groups). Oxidative nitrolysis of the N-alkyl-substituent using 98% HNO_3 in acetic anhydride resulted in the formation of 1,3,3-trinitroazetidine **1** in 60% yield. Despite the success of this approach the process suffers from a very poor yield (8%) early in this multi-step procedure.

Several strategies have been proposed for improving the preparation of 1,3,3-trinitro-azetidine **1**. These will be discussed in the following sections:

Marchand and coworkers[12] attempt to improve the above synthesis of 1,3,3-trinitroazetidine **1** is outlined in Scheme 2. The key intermediate in this synthesis, N-[(trifluoromethane)sulfonyl]-3-azetidinone **13**, was synthesized by the ozonolysis of N-[(trifluoromethane)sulfonyl]-3-ethylideneazetidine **12**.

The latter was obtained by the electrophilic addition of triflic anhydride (Tf_2O) across the C(3)-N σ-bond of a relatively inaccessible, and a highly strained bicyclic system (i.e., 1-aza-3-ethylbicyclo[1.1.0]butane **11**).

Scheme 1

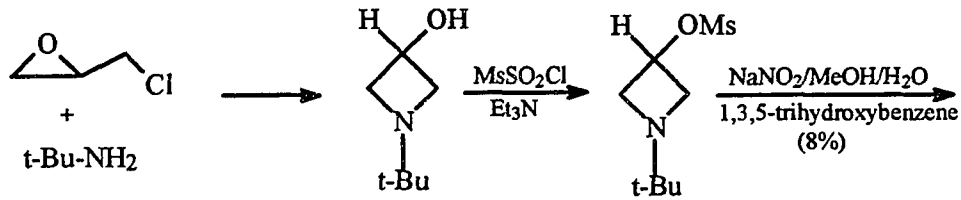

7 **8**

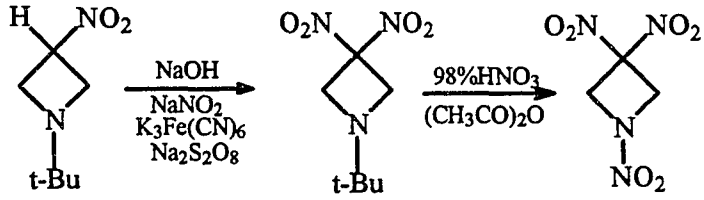

9 **10** **1**

Reaction of N-[(trifluoromethane)sulfonyl]-3-azetidinone oxime **14**, generated by oximation of the ketone **13**, with HNO_3 (100%) and H_2O_2 (90%) did not result in the formation of 1,3,3-trinitroazetidine **1** as expected, instead a

mixture of N-(trifluoromethanesulfonyl)-3,3-dinitroazetidine **15** and N-(trifluoromethanesulfonyl)-3-azetidinone **13** were obtained in 28% and 23% yield, respectively.

Scheme 2

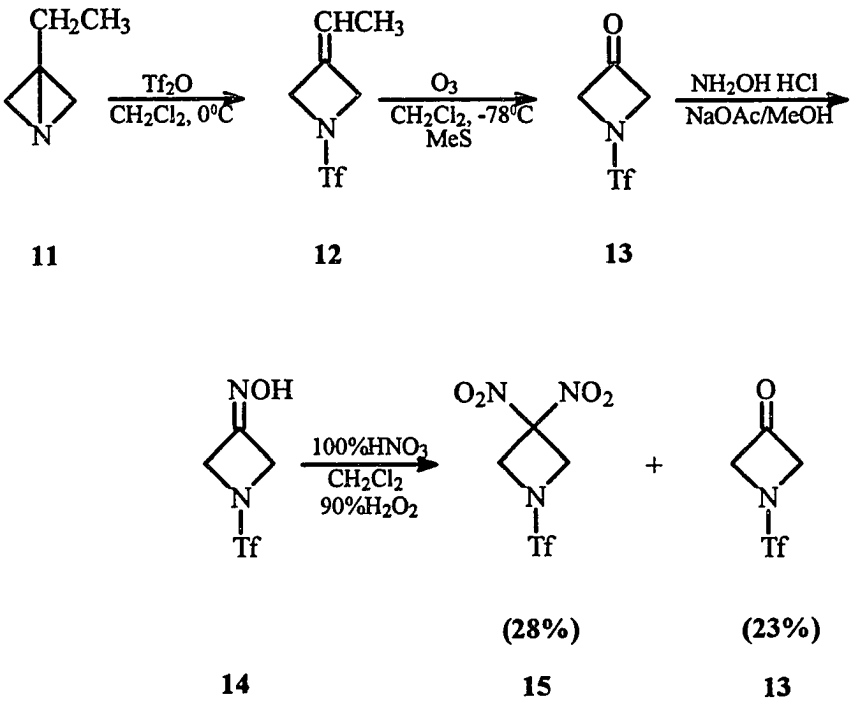

A modification of Archibald's[11] synthetic procedure, offered by Coburn and Hiskey[13] is shown in Scheme 3. Their goal was to circumvent the step involving the introduction of the first C-NO_2 group. Consequently, they

started with a nitro alcohol that served as the substrate for construction of the 3-nitro-substituted azetidine ring.

The 3-nitro derivative of N-t-butyl-azetidine **19**, a key intermediate in their strategy, was obtained in two steps. The reaction of t-butylamine and 2-(hydroxymethyl)-2-nitro-1,3-propanediol **16** gave the oxazine ring **17**, which was cleaved by ethanolic HCl to form compound **18**. Cyclization of **18** to the 3-nitro derivative of N-t-butyl-azetidine **19** was effected with Ph_3P/DEAD,[14a] a Mitsunobu type reaction.[14b] The oxidative nitration technique employed to form the gem-dinitro groups was identical to that of Archibald's original preparation of 1,3,3-trinitroazetidine **1** (see Scheme 2).

Scheme 3

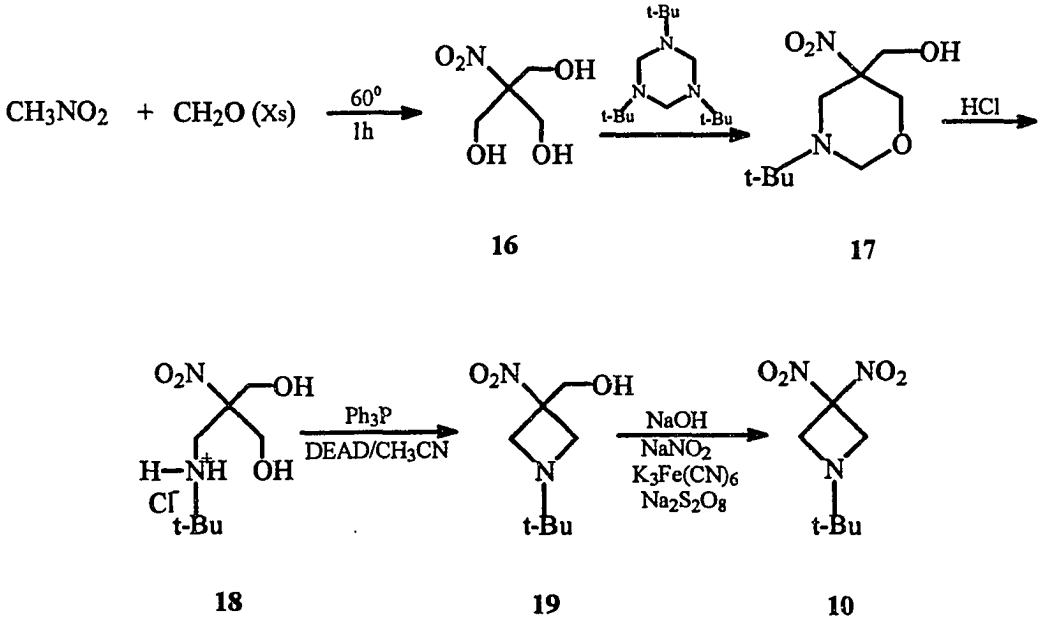

16 **17** **18** **19** **10**

Katritzky, Cundy and Chen[14c] reported a strategy for the synthesis of 1,3,3-trinitroazetidine **1** that appears strikingly parallel to our method[16] (i.e., the involvement of N-p-tosyl-3-azetidinone **24** as the intermediate in the synthesis of 1,3,3-trinitroazetidine **1**).

In their synthetic design, as illustrated in Scheme 4, N-benzhydryl-3-azetidinol **20** was oxidized with either Jones (i.e., chromic acid) or Swern (i.e., pyridine-sulfur trioxide/DMSO) oxidation methods to form ketone **21**. Hydrogenolysis ($Pd(OH)_2/C$) of ketone **21** resulted in the formation of 3-azetidinone hydrochloride **23**, which was allowed to react with tosyl chloride in pyridine to give, N-p-tosyl-3-azetidinone **24**. Reaction of the ketone **24** with hydroxylamine hydrochloride and sodium acetate in ethanol gave N-p-tosyl-3-azetidinone oxime **25**. The latter was subjected to nitric acid oxidation of the oxime moiety and the nitrolysis of the N-(p-toluenesulfonyl) group to obtain, 1,3,3-trinitroazetidine **1**.

Finally, Schechter and coworkers[15] proposed to synthesize 1,3,3-trinitroazetidine **1** from the condensation of tert-butylamine with nitroallyl acetate. The latter is generated from the reaction of sodium acetate and 2-nitro-1,3-propanediol. This synthetic plan is illustrated in Scheme 5.

Our own investigation to improve the synthesis of 1,3,3-trinitroazetidine **1** has centered on the introduction of the gem-dinitro groups through the oxidative nitration of an oxime moiety, and the simultaneous nitrolysis of an appropriate N-blocking group. This is outlined in Scheme 6. Transformations of this type have been reported for introduction of gem-dinitro groups in similar systems.[16,17,18]

Scheme 4

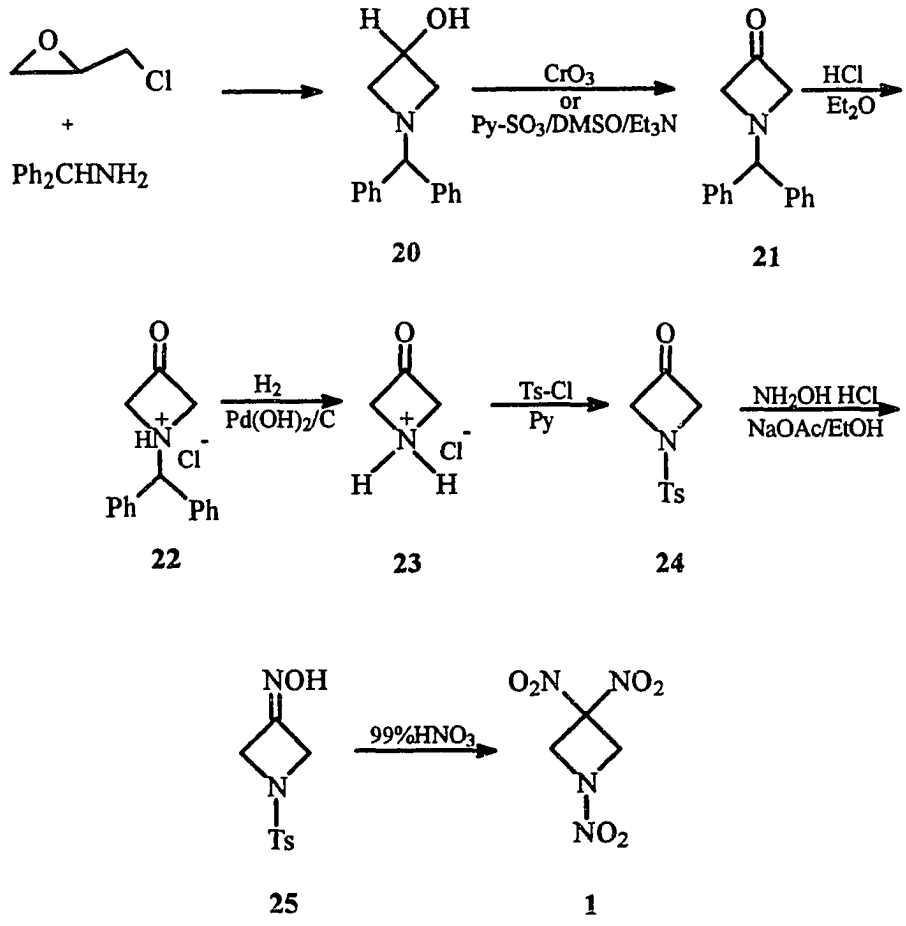

Scheme 5

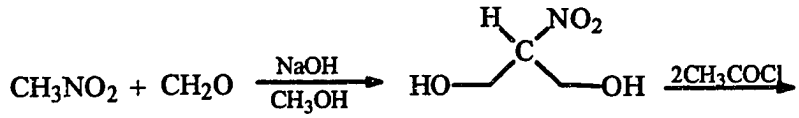

26

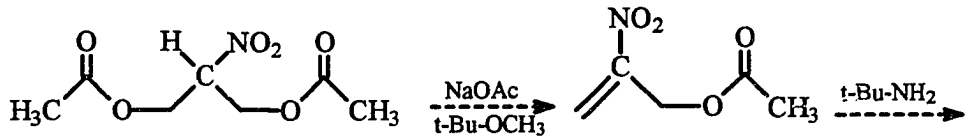

27 28

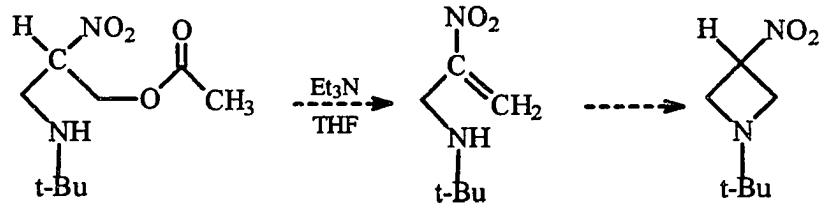

29 30 9

Scheme 6

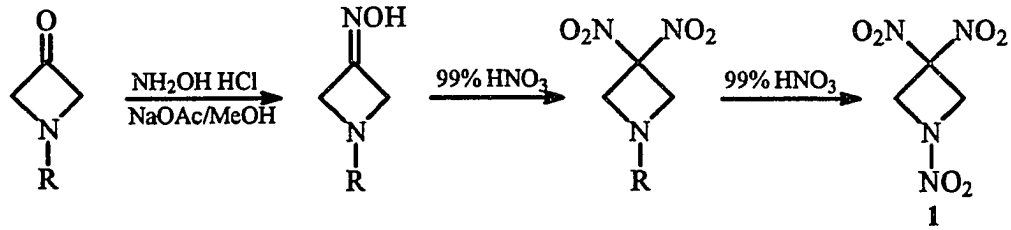

1

The feature that makes this method attractive is that the HNO_3 oxidation leading to the formation of the $C(NO_2)_2$ group is combined, in one pot, with the nitrolysis of the N-substituent group to produce the $N\text{-}NO_2$ function.[24] An added benefit of this approach is that all energetic nitro groups would be introduced in the final step of the synthesis which is desirable from a safety viewpoint. Essential to the success of this approach is the facile access to 1,3-substituted azetidines and the transformation of these intermediates into stable 3-azetidinones. Hence, methods of preparing 1,3-substituted azetidines were sought.

A literature review of the synthetic methods that are available for the synthesis of azetidines indicates that the chemistry of 1,3-substituted azetidines flourished after Gaertner[19] reported a simple method for their preparation from epichlorohydrin and sterically hindered amines (see Scheme 7). Since then, there have been relatively few, but nevertheless significant improvements in the synthesis of these interesting compounds. Okutnai, Kaneko and Masuda[20] conducted ring closures of hindered amines in acetonitrile and substantially decreased the time required for the cyclization and simultaneously increased the yield of product.

Scheme 7

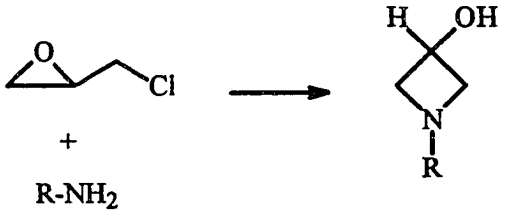

R= Bulky alkyl

Gaertner's method, however, fails completely for N-alkyl-substituents less bulky than an isopropyl group. Almost simultaneously with Gaertner's suggestion that substituents on the oxygen atom of N-alkyl-3-chloro-2-propanol would favor cyclization, Gaj and Moore[21] utilized the reaction of unhindered amines with ethers of 1,3-dihalo-2-propanol and prepared several N-(primary alkyl)-3-(methoxymethoxy)azetidines (see Scheme 8).

Scheme 8

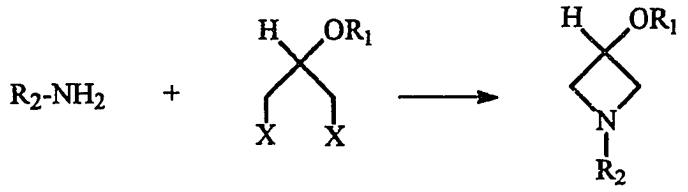

$R_1 = CH_2OCH_3$ X = Cl or Br
R_2 = Me, Et

Similarly, 3-(diphenylmethoxy) or (phenylmethoxy)methoxy ethers of 1-methyl and 1-ethylazetidinols (isolated as hydrochlorides) were prepared by Jenkins, Herndon and Cale[22] (see Scheme 9) by treatment of the appropriate ethers of 1,3-dichloro-2-propanol with unhindered amines. Subsequent hydrogenolysis of the corresponding ethers gave 1-methyl- and 1-ethylazetidinols, respectively.

Scheme 9

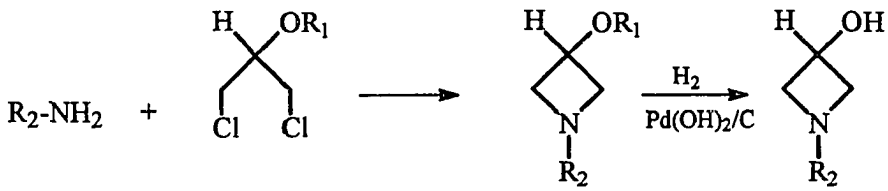

R_1 = $CHPh_2$,CH_2OCH_2Ph
R_2 = Me, Et

Tetrahydropyranyl and trimethylsilyl ethers of 3-azetidinol were also prepared by the Higgins group,[23,24] from the reaction of unhindered amines with the corresponding ethers of 1,3-dichloro-2-propanol or epichlorohydrin. The O-alkyl substitutents in this case were readily cleaved by warming in dilute acid to give the desired N-alkyl-3-azetidinols (see Scheme 10).

Scheme 10

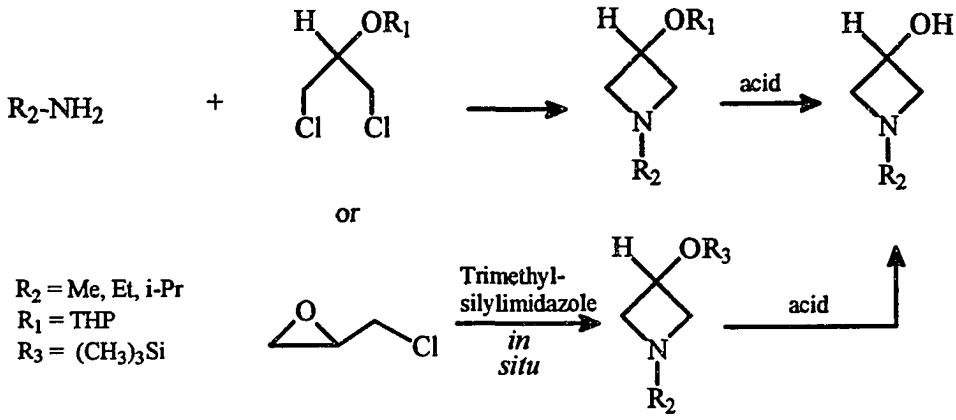

In view of the fact that N-alkyl-3-azetidinols are readily accessible from condensation of epichlorohydrin or an appropriately substituted 1,3-dihalo-2-propanols with amines, the study of several oxidative procedures for converting N-alkyl-3-azetidinols to the corresponding 3-azetidinones was undertaken. It is ultimately expected that the resulting ketone intermediates could be transformed into 1,3,3-trinitroazetidine **1** through the series of synthetic steps outlined in Scheme 6.

1.3. Results and Discussion

As our initial target the oxidation of N-(t-butyl)- and N-(t-octyl)-3-azetidinols was selected, since they are easily prepared according to known literature procedures.[19,25] This methodology is outlined in Scheme 11.

The attempted oxidation of either N-(t-butyl)- or N-(t-octyl)-3-azetidinol, using both the Jones and Swern oxidation methods, lead to the formation of ketone products. However, examination of the ^{1}H NMR spectrum of the oxidation of N-(t-butyl)-3-azetidinol **31a**, as illustrated in Figure 1.2, revealed the presence of two equal intensity t-butyl resonance signals of approximately equal intensity at δ0.74 and δ0.80, in addition to multiple signals from δ2.5-δ4.0. Similarly, the ^{13}C NMR spectrum, as illustrated in Figure 1.3, indicated the presence of two resonance signals at δ25.3, δ23.9, assigned to t-butyl carbons, and two resonance signals at δ201.7, δ202.8 due to carbonyl carbons.

Scheme 11

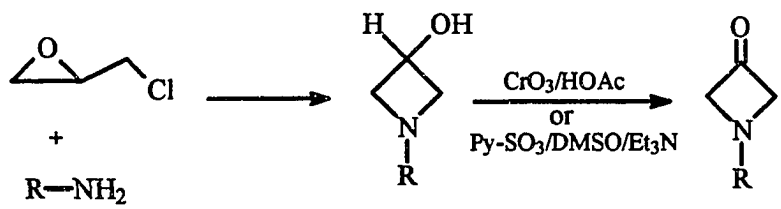

a, R = Me_3C
b, R = $(Me_3C)CH_2(CH_3)_2C$

31a,b **32a,b**

Analogously, the oxidation products of N-(t-octyl)-3-azetidinol **31b** exhibited a similar spectral pattern to that of **31a** oxidation products. For example, the ^{1}H NMR spectrum (see Figure 1.4) displayed multiple resonance signals at δ1.00 and δ4.00, which were assigned to the t-octyl and N-CH_2 protons of the oxidized reaction products, repectively. The study of the ^{13}C NMR (see Figure 1.5) spectrum of these products indicated the presence of signals at δ24.6, δ25.1 and δ25.3 due to the t-octyl carbons in addition to signals at δ201.43 and δ201.80 assigned to carbonyl carbons.

Clearly, the ^{1}H and ^{13}C NMR spectra of both oxidation products support the existence of more than one reaction product. The mass spectrum of the individual reaction products exhibited two molecular ion peaks each coinciding with N-(t-butyl)- and N-(t-octyl)-3-azetidinones and their respective dimers. This is illustrated for the N-(t-octyl)-3-azetidinol oxidation products in Figure 1.6. The chemical ionization mass spectrum indicated the presence of two molecular ions, one corresponding to N-t-octyl-3-azetidinone (M+1= 184) and the other ion peak to its dimeric product (M+1= 367). It is proposed that these dimeric mixtures arise from the self-condensation of the initially formed 3-azetidinones.

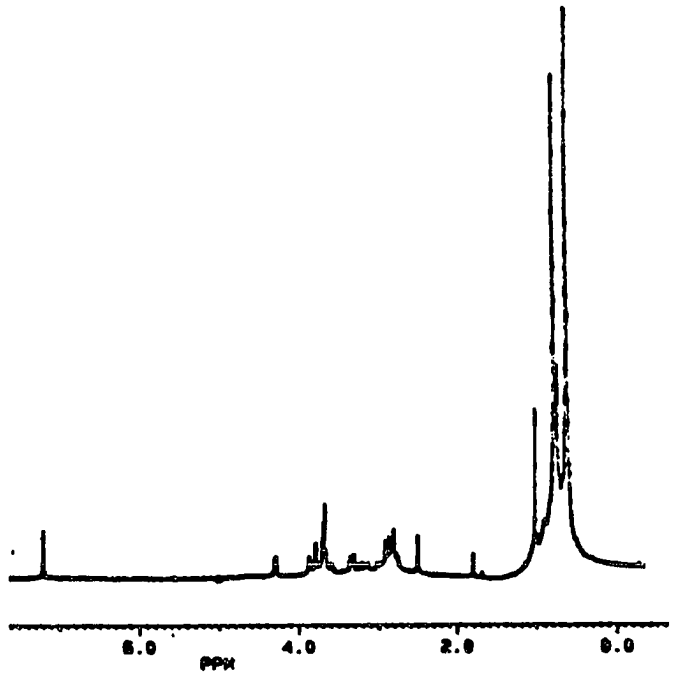

Figure 1.2. 300 MHz ^{1}H NMR spectrum of the oxidation reaction products of **31a** in $CDCl_3$.

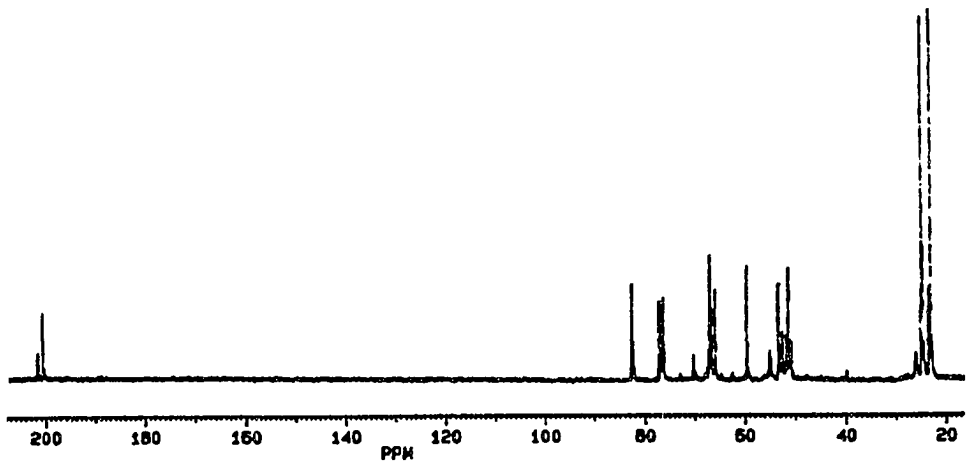

Figure 1.3. 75 MHz ^{13}C NMR spectrum of the oxidation reaction products of **31a** in $CDCl_3$.

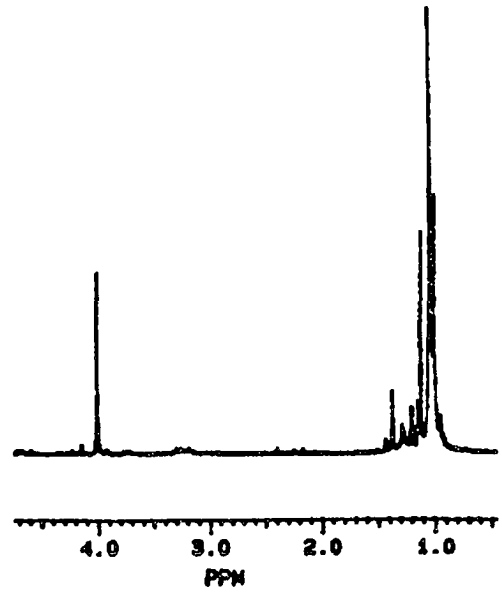

Figure 1.4. 300 MHz ^{1}H NMR spectrum of oxidation reaction produts of **32b** in $CDCl_3$.

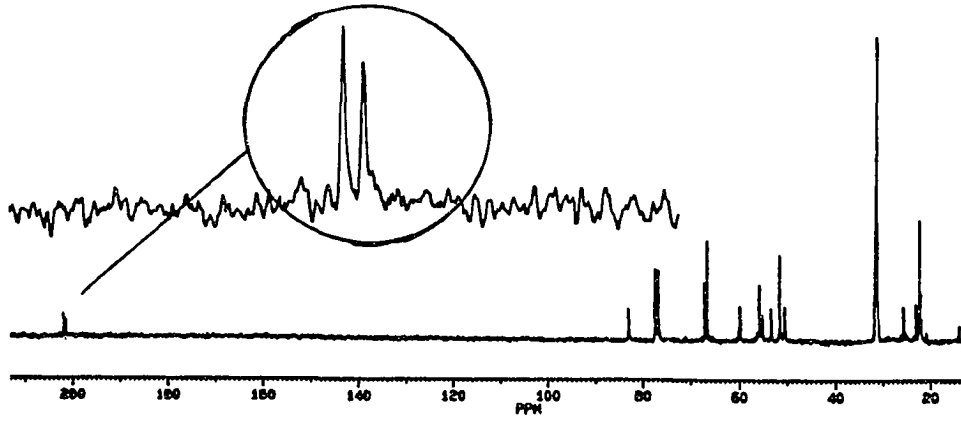

Figure 1.5. 75 MHz ^{13}C NMR spectrum of oxidation reaction products of **32b** in $CDCl_3$.

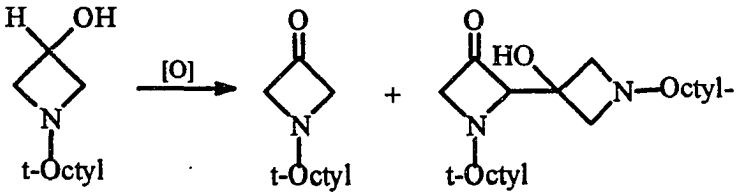

$(M+1)_{calc'd}$ **184**

$(M+1)_{calc'd}$ **367**

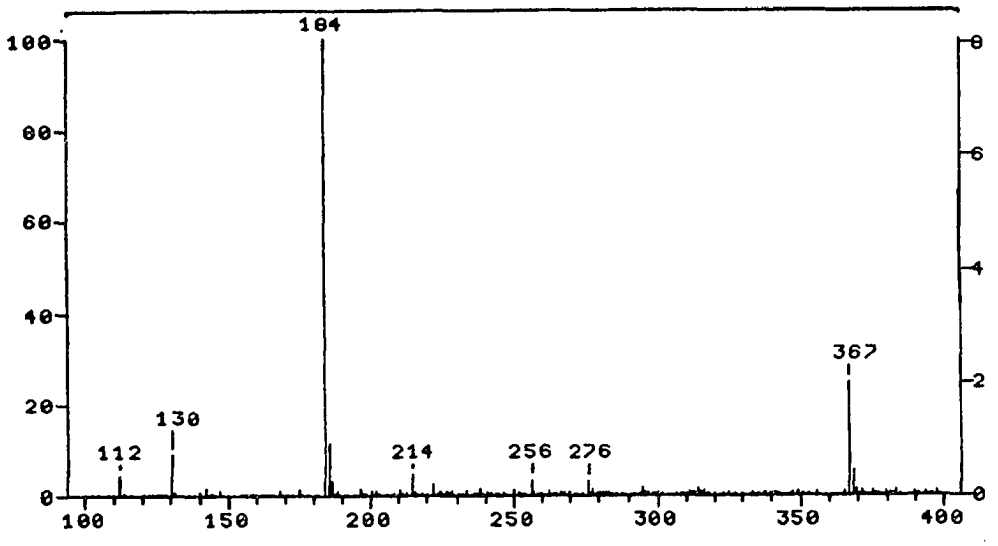

Figure 1.6. Chemical ionization mass spectrum (CI-NH_3) of the Swern oxidation product of N-(t-octyl)-3-azetidinol **32b**.

Morimoto and co-workers[35] also reported the oxidation of N-(benzhydryl)-3-azetidinol using pyridine-SO_3/Et_3N in DMSO similarly gave the corresponding 3-azetidinone **33a** and its dimer **33b** (see Scheme 12).

Scheme 12

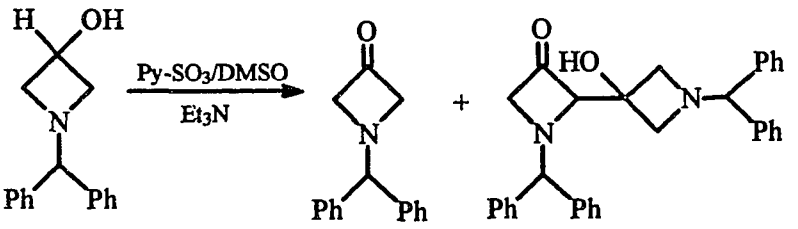

33a **33b**

In addition, they reported that N-(benzhydryl)-3-azetidinone **33a** is a stable solid, but when heated under reflux in methanol for 24 h it undergoes self-condensation to form the dimer **33b**. Furthermore, when a methanol solution of **33a** is heated at 50°C for 24 h in the presence of benzaldehyde the Aldol condensation product **33c** is obtained exclusively (see Scheme 13).

Scheme 13

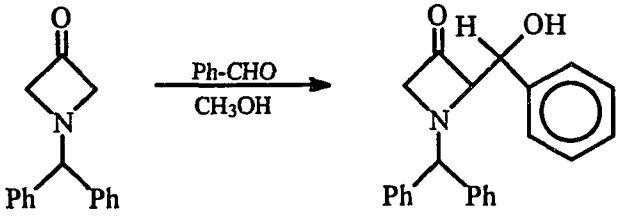

33a **33c**

Based on these observations as well as our own the facile condensation of N-(alkyl)-3-azetidinones may be explained in terms of the basicity of the ring nitrogen atom. This basicity is probably increased when the substituent that is

attached to the ring nitrogen is an alkyl group. The increased basicity of the ring nitrogen atom catalyzes the condensation of the ketone to form the dimer. This is illustrated in Scheme 14.

Scheme 14

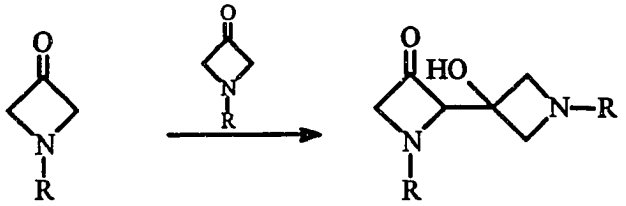

R = Alkyl

Both the chromium mediated and the pyridine-sulfur trioxide oxidation methods of N-alkyl-3-azetidinols were not satisfactory in getting the desired intermediate (i.e., N-(alkyl)-3-azetidinone), because of the instability of the latter. We focused our attention to those 3-azetidinones that had groups other than an alkyl group on the ring nitrogen atom.

Relatively few N-substituted-3-azetidinones have been reported in the literature. Examples in this regard generally fall into two categories: (a) they contain electron-withdrawing groups on the ring nitrogen (e.g., N-p-toluene-sulfonyl or N-CO_2Me), or (b) they possess an electron-donating substituent on the ring nitrogen atom. Moreover, a close examination of the literature

revealed that of the 3-azetidinones known, only those with electron-withdrawing groups appear to have sufficient stability to be isolated and stored. For example, N-(cyclohexyl)-3-azetidinone[26] is described as an unstable oil, while the N-benzyloxycarbonyl- **34**,[27] N-(p-toluenesulfonyl)- **35**,[28] N-(4-chlorophenyl)-carboxamido- **36**,[27] N-benzoyl- **37**,[27] and derivatives of 3-azetidinone as well as 3-azetidinone hydrochloride **38**[27] could be isolated as crystalline solids and stored for prolonged periods (see Figure 1.7).

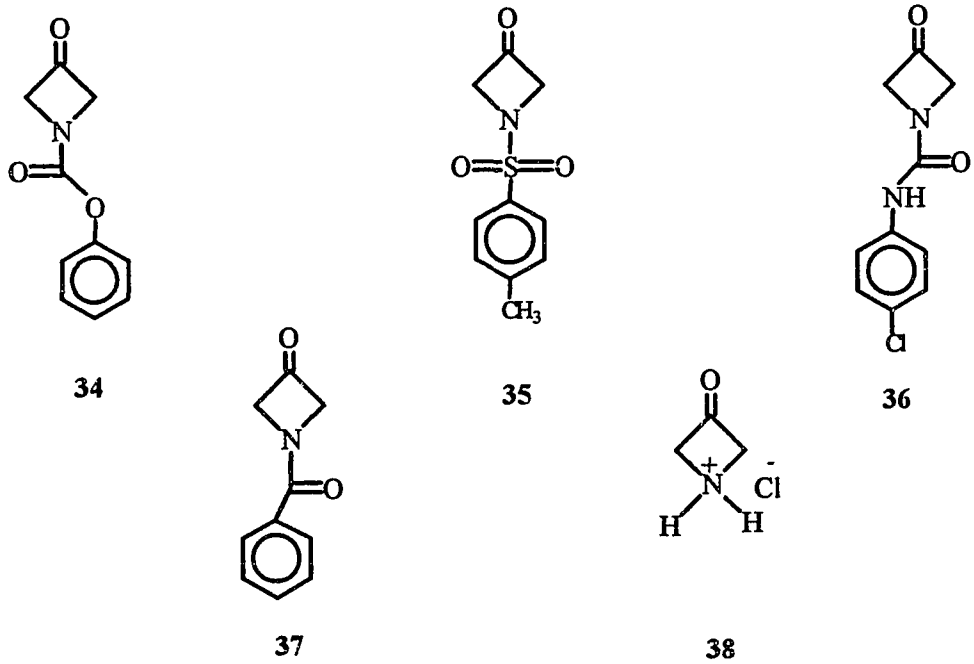

Figure 1.7. Structures of stable derivatives of 3-azetidinone reported in the literature.[27,28]

In light of the literature reports indicating enhanced stability of 3-azetidinones only when electron withdrawing groups are on the ring nitrogen atom, we selected N-(p-toluenesulfonyl)-3-azetidinone **24** as the key azetidine to investigate further. This compound could easily be prepared from glycine by the sequence of steps shown in Scheme 15. The Cu II promoted decomposition of diazoketone **41** gave ketone **24** (see Scheme 16), which demonstrated to be a stable compound.[28]

Scheme 15

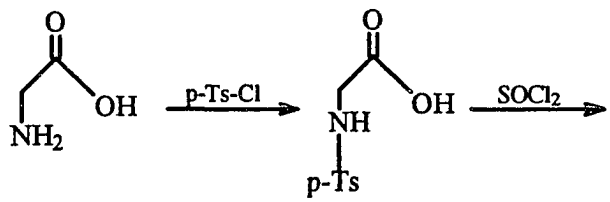

39

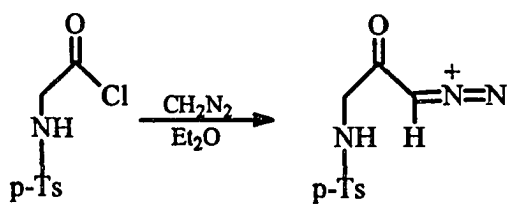

40 **41**

Scheme 16

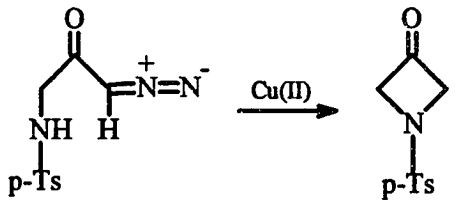

41 **24**

Although the Cu II promoted decomposition of diazoketone **41** proved to work well for the preparation of **24**, the use of diazomethane is not amenable to large scale work. Nevertheless, ketone **24** was quantitatively converted to its oxime **25** by the method of Corey, Melvin and Haslanger.[29] Treatment of this oxime with 99% HNO_3 afforded the gem-dinitro groups and simultaneously nitrolyzed the N-p-toluenesulfonyl functionality, hence yielding the desired 1,3,3-trinitroazetidine **1** in 40% yield. This is illustrated in Scheme 17.

Scheme 17

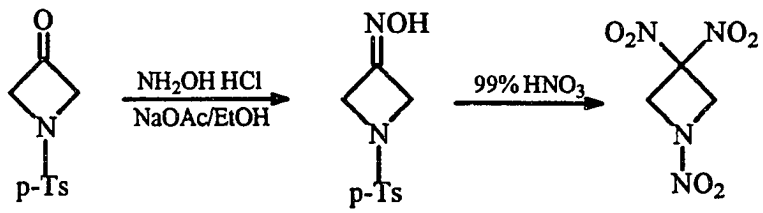

24 **25** **1**

The successful conversion of N-(p-toluenesulfonyl)-3-azetidinone **24** to 1,3,3-trinitroazetidine **1**, through oxime **25** directed us to explore convenient synthetic routes to N-(p-toluenesulfonyl)-3-azetidinone **24**. One such route is the oxidation of the corresponding alcohol **42**. Initially, however, it was established that this alcohol could be readily oxidized to ketone **24** and isolated as a stable compound. This was demonstrated by the $NaBH_4$ reduction of N-(p-toluenesulfonyl)-3-azetidinone **24** to N-(p-toluenesulfonyl)-3-azetidinol **42**, in 94% yield. Transformation of the alcohol **42** back to ketone **24** was effected in 74% yield, without difficulty by oxidation with CrO_3/HOAc. This is outlined in Scheme 18.

Scheme 18

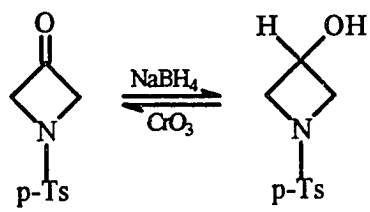

24 **42**

Consequently, we were encouraged to seek simpler methods of preparing **42** that could be adapted to large-scale work.

The base-induced intramolecular cyclization of bulky N-alkyl amino-oxiranes[19] is an important synthetic route to the azetidine ring system. This

methodology works well for the preparation of N-(p-toluenesulfonyl)-azetidine-2-methanol **43** and N-(p-toluenesulfonyl)-pyrrolidine-3-ol **45** depending on the substitution of the parent oxirane **44**.[30] This is illustrated in Scheme 19.

Scheme 19

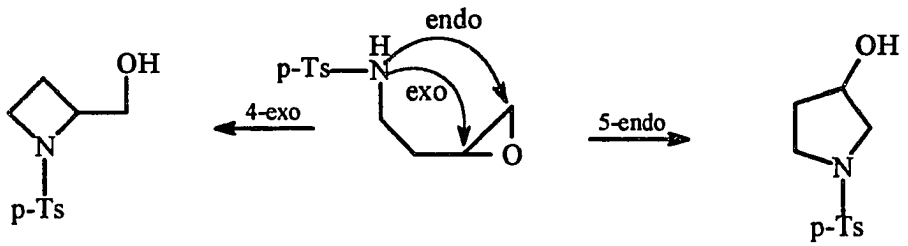

43 **44** **45**

However, in the case of N-(p-toluenesulfonyl)-2,3-epoxypropane **46**, cyclodimerization products are obtained instead of the anticipated N-(p-toluenesulfonyl)-3-azetidinol.[31] For example, as outlined in Scheme 20, the base-mediated reaction of p-toluenesulfonamide with either epichlorohydrin or 1,3-dihalo-2-propanols affords a mixture of the cyclodimerization products, *cis* and *trans*-N,N'-di-(p-toluenesulfonyl)-3,7-dihydroxy-1,5-diazacyclooctane **47**, and none of the desired N-(p-toluenesulfonyl)-3-azetidinol **42**. Presumably, the diazacyclooctanes are formed from the N-(p-toluenesulfonyl)-2,3-epoxypropane intermediate **46**. On the other hand, 1,3-disubstituted propanes do react with the p-toluenesulfonamide anion to give

azetidines.[32,33] The reaction of 3-(toluene-sulfonamido)-2,2-dimethylpropane-1-(toluenesulfonate) **48**, a neo-pentyl-like system with gem dimethyl substitution at the C-2 surprisingly, cyclizes smoothly to the azetidine **49**.[34,35]

Scheme 20

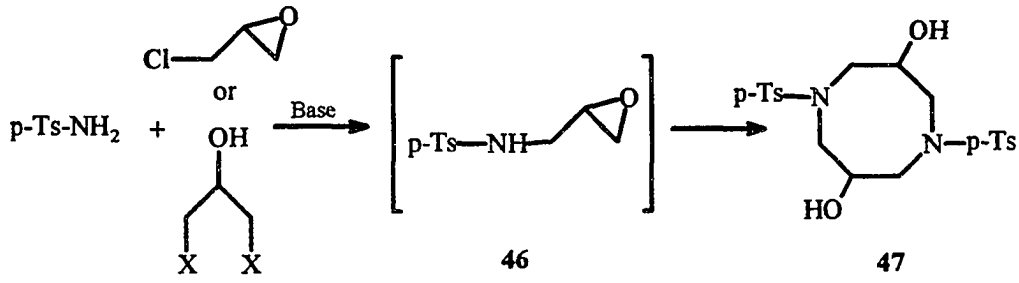

This is illustrated in Scheme 21. Therefore, the failure of 1,3-dihalo-2-propanols to form azetidines implies an intermediate oxirane (see Scheme 20) and cannot be attributed wholly to steric factors.

Scheme 21

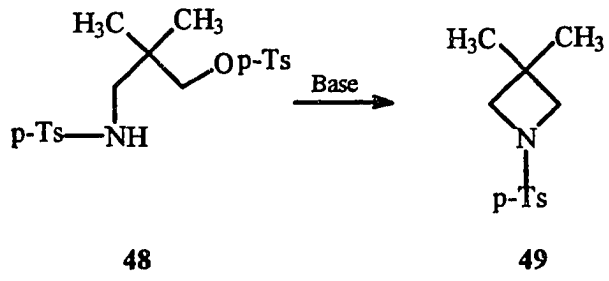

The importance of achieving optimum azetidine formation and avoiding cyclodimerization prompted us to investigate the reactions of sulfonamides

with a number of base stable ether derivatives of 1,3-disubstituted-2-propanols.[21,22,23,24] This approach is illustrated in Scheme 22.

Scheme 22

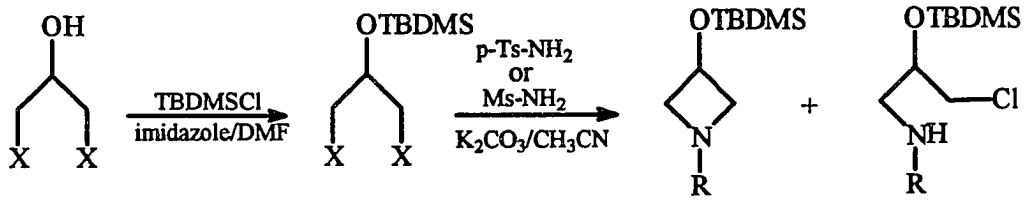

50a : x = Cl
50b : x = Br

51a : R = p-Ts
51b : R = Ms

52a: R = p-Ts

Therefore, the reaction of t-butyldimethylsilyl ether derivatives of 1,3-dihalo-2-propanols with methanesulfonamide and p-toluenesulfonamide in acetonitrile in the presence of potassium carbonate was studied under a variety of experimental conditions. These results are summarized in Table 1. The data confirm that when epoxide formation is prevented, the t-butyldimethylsilyl ethers of either 1,3-dichloro-2-propanol **50a** or 1,3-dibromo-2-propanol **50b** do, indeed, cyclize to the azetidine, albeit under extended heating. For example, ring closure of **50b** gave **51a** in 68% yield after heating for 27 h. Under the same conditions **50a** fails to appreciably cyclize to **51a**. After 90 h of heating **50a** can eventually be cyclized to **51a**. The rate of this cyclization, however, was judged too slow to be synthetically

useful. The addition of tetrabutylammonium iodide as a phase transfer catalyst had no significant rate-enhancing effect on these cyclization reactions. Azetidine ring-closure in the reaction of amines with either the tetrahydropyranyl or trimethylsilyl ethers of 1,3-dichloro-2-propanol is also reported to require extensive reaction times.[24]

Table 1.1. Comparison of yields and reaction times of t-butyldimethylsilyl ethers of 1,3-dihalo-2-propanols with sulfonamides to form azetidines.

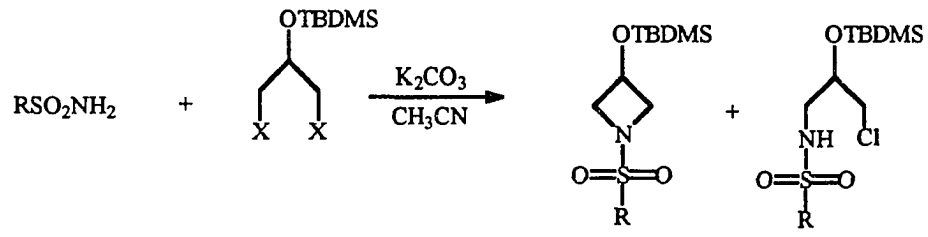

R	X	Y	Reflux time, h	Yield, %	
H_3C–C$_6$H$_4$–	Br	Br	27	68	—
H_3C–C$_6$H$_4$–	Cl	Cl	90	50	50[a]
H_3C–	Br	Br	27	66	—

[a]Estimated from analysis of NMR and MS spectra

In an alternate approach to investigate the possibility of shortening the reaction time, 3-amino-1,2-propanediol **53** was converted to the ditosyl derivative **54** by reaction with p-toluenesulfonyl chloride in pyridine. This was accompanied by the formation of the tritosylated 3-amino-1,2-propanediol **55**. Compounds **54** and **55** were isolated in 66% and 26% yield, respectively, after separation by silica gel chromatography. Compound **54** was then converted in 88% yield to its t-butyldimethylsilyl ether **56** using t-butyldimethylsilyl chloride and imidazole in dimethylformamide. Cyclization of **56** using lithium hydride as the base gave **51a** in 91% yield. This is outlined in Scheme 23.

Also, consistent with earlier observations, where an intermediate epoxide may intervene, the treatment of **54** with LiH/THF failed to give the desired azetidinol and only the cyclodimerization products, *cis* and *trans*-N,N'-di-(p-toluenesulfonyl)-3,7-dihydroxy-1,5-diazacyclooctane **47**, were obtained in 45% yield (see Scheme 24).

It is interesting to note that the reaction of the p-toluenesulfonyl derivative **55** with base affords exclusively, and not unexpectedly, the aziridine **57** in 94% yield, (see Scheme 25).

Scheme 23

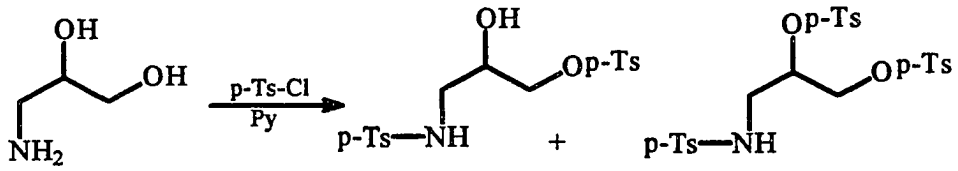

53 **54** **55**

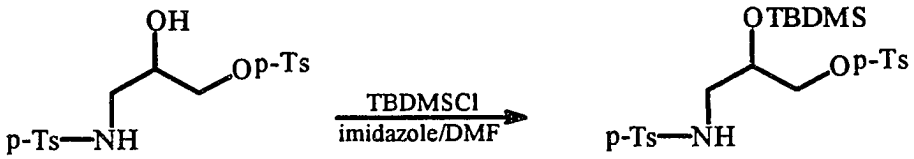

54 **56**

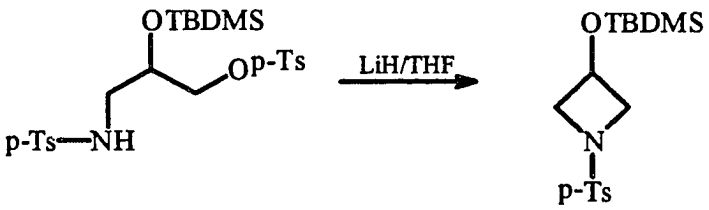

56 **51a**

Scheme 24

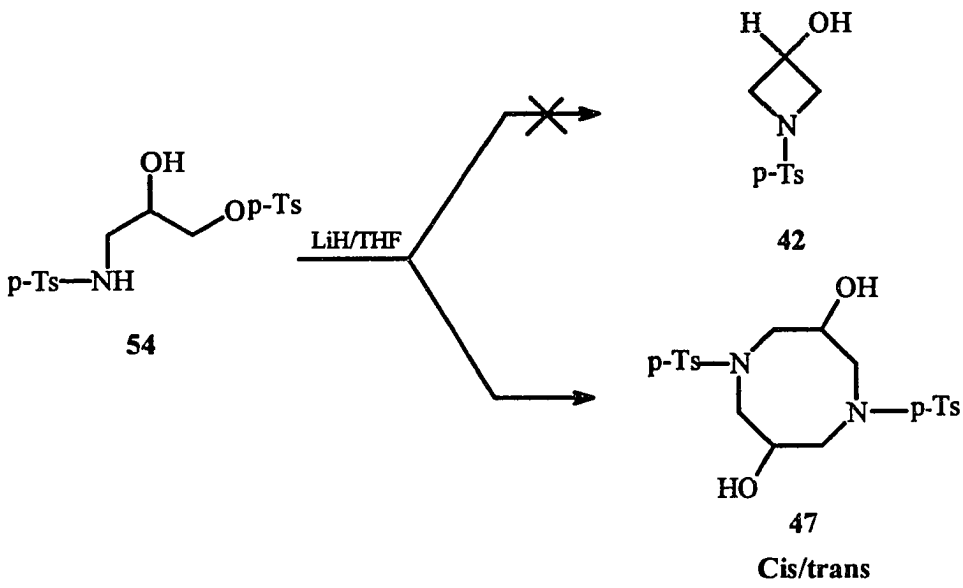

Scheme 25

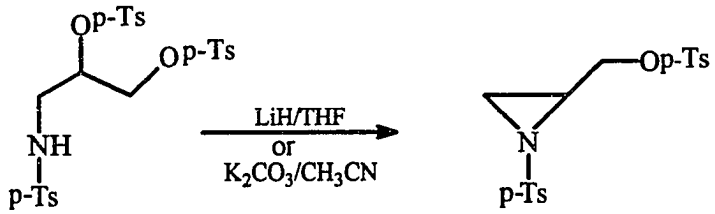

55 **57**

The overall synthesis of 1,3,3-trinitroazetidine **1** developed in this investigation may be summarized by the sequence of steps outlined in Scheme 26. Deprotection of **51a** afforded the N-p-tosyl-3-azetidinol **42** in near quantitative yields. Transformation of N-p-tosyl-3-azetidinol **42** to ketone **24** was effected in 74% yield by oxidation with CrO_3/HOAc and the

latter ketone on treatment with hydroxylamine afforded the N-(p-toluenesulfonyl)-3-azetidinone oxime **25** in nearly quantitative yields. In the final step this oxime was treated with 99% HNO_3 in refluxing methylene chloride to simultaneously nitrolyze the p-toluenesulfonyl group and oxidize the oxime function to produce the desired 1,3,3-trinitroazetidine **1** in 40% yield.

Scheme 26

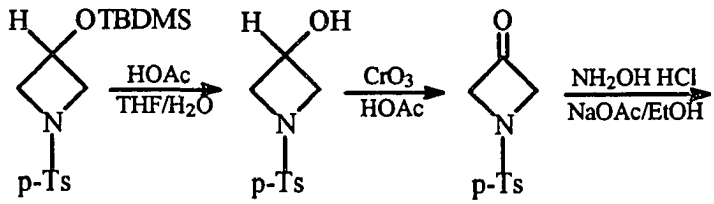

51a **42** **24**

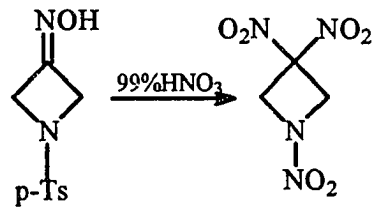

25 **1**

1.4. Conclusion

A new synthesis of 1,3,3-trinitroazetidine **1** has been developed. In this synthetic route HNO_3 oxidation of an oxime intermediate leading to the

formation of the $C(NO_2)_2$ group is combined, in one step, with the nitrolysis of the N-(p-toluenesulfonyl) group to introduce the $N\text{-}NO_2$ function. Significantly, all the energetic nitro groups are introduced in the final step of the sequence, which is an important safety consideration.

1.5.0. Experimental Section

1.5.1. General Methods

All reactions were carried out under a nitrogen atmosphere unless otherwise stated. Glassware was dried overnight in an oven at 120°C, removed from the oven, fitted with rubber septa, addition funnel, condenser, and flushed with nitrogen prior to use. Magnetic stiring bars were dried in an oven at 120°C and placed in their reaction vessels before the latter were flushed with nitrogen. Syringes were dried in an oven at 120°C and allowed to cool in a desiccator over calcium chloride prior to use.

Thin layer chromatographic analyses (TLC) was performed with Aldrich grade 60 silica gel plastic plates with 254-nm fluorescent indicator. Chromatographic column separations was performed using Aldrich grade 634, 100-200 mesh, 60Å silica gel, Davisil. Eluent mixtures for this procedure are reported as volume/volume percentages.

All ^{1}H and ^{13}C NMR spectra were measured in 5-mm tubes. Spectra were recorded on either Bruker NR 200 or NR 300 spectrometers at ambient temperature unless otherwise stated. Routine ^{13}C NMR spectra were recorded at 50 or 75 MHz with broad-band decoupling, a pulse angle of 45° and an acquisition time of 0.475 s for a 16K data table with a spectral width of 230 ppm. Routine ^{1}H NMR spectra were recorded at either 200 or 300 MHz with a pulse angle of 50° and an acquisition time of 2.0 s for a 16K data table with a spectral width of 14 ppm. Unless otherwise noted, spectra are reported in parts per million downfield from a tetramethylsilane as the internal standard. Data are reported as follows: chemical shift, multiplicity (s = singlet, d = doublet, t = triplet, q = quartet, m = multiplet, br = broad) and spin-coupling values are given in Hertz. ^{1}H and ^{13}C NMR spectra for all compounds are reproduced in Appendix A.

Low resolution EI and CI (NH_3) were recorded on a Finnigan-MAT model SSQ 70 mass spectrometer with an ionization voltage of 70eV; peaks are reported as m/z. High resolution mass spectra were measured on a JEOL HX110A mass spectrometer by FAB ionization mode using the peak matching technique. Melting points were measured on a Thomas Hoover apparatus and are uncorrected.

1.5.2. Solvents and Materials

All solvents and materials, unless otherwise specified, were obtained from Aldrich Chemical Co. and were used without further purification.

Chloroform-d_1 (99.8 atom %D), acetone-d_6 (99.8 atom %D) and dimethylsulfoxide-d_6 (99.5 atom %D) were obtained from Cambridge Isotopes Laboratory and contained 0.1% tetramethylsilane as an internal standard.

Tetrahydrofuran (THF) was obtained from Fisher Scientific Co., as reagent grade tetrahydrofuran and distilled from sodium-benzophenone ketyl intermediate prior to use.

1.5.3. Procedures

1,3,3-Trinitroazetidine (1). To a refluxing solution of **25** (24 mg, 0.1 mmol) in methylene chloride (20 mL) was added a solution of 99 % HNO_3 (2 mL), urea (20 mg) and ammonium nitrate (20 mg) in methylene chloride (20 mL). After the addition was completed the mixture was heated under reflux for an additional 30 min and then cooled to room temperature. The mixture was then poured over ice and the layers were separated. The organic phase was dried (Na_2SO_4), filtered and concentrated under reduced pressure to yield 1,3,3-trinitroazetidine **1** (8 mg, 40%) which was identified and characterized

by comparison of its physical and spectroscopic properties with an authentic sample; ^{1}H NMR (acetone-d_6): δ5.45 (s, 4H); ^{13}C NMR (acetone-d_6): δ64.7, 104.9. [see Appendix A; Figures A.1 and A.2 for the ^{1}H and ^{13}C NMR spectra, respectively].

N-(p-Toluenesulfonyl)-3-azetidinone (24). This compound was prepared by either the (a) oxidation of **42** or by the (b) bis(hexafluoroacetylacetonato) copper II catalyzed cyclization of N-(3-diazo-2-oxopropyl)-4-methyl benzenesulfonamide **41** derived from glycine.[30]

Method A. N-(p-Toluenesulfonyl)-3-azetidinone (24). The method of Chaterjee and Shoeb[27] was used. A mixture of **42** (30 mg, 0.132 mmol), concentrated H_2SO_4 (50 mg), CrO_3 (15 mg), HOAc (50 mg) in 0.50 ml of 15% aqueous acetone was maintained between 0-5°C for 2 h. The cold solution was then treated with 2 mL of water containing 2 drops of conc. NH_3 and the mixture was extracted with ether (2x3 mL). The organic layer was washed with water, dried over Na_2SO_4 and evaporated to give an oil (22 mg, 74%), which crystallized on standing, mp 149°C; ^{1}H NMR ($CDCl_3$): δ2.43 (s, 3H), 4.59 (s, 4H), 7.35 (d, J= 9 Hz, 2H), 7.76 (d, J= 9 Hz, 2H). ^{13}C NMR ($CDCl_3$): δ21.5, 72.4, 128.4, 130.0, 131.8, 145.0, 192.0. This material was identical with **24** prepared from the N-(3-diazo-2-oxopropyl)-p-

toluenesulfonamide.[28] [see Appendix A; Figures A.3, and A.4 for the ^{1}H, and ^{13}C NMR spectra, respectively].

N-(p-Toluenesulfonyl)-3-azetidinone oxime (25). N-(p-toluenesulfonyl)-3-azetidinone **24** was converted to the corresponding oxime using the method of Corey, Melvin and Haslanger.[29] To a solution of **24** (30 mg, 0.133 mmol) and NaOAc trihydrate (72 mg, 0.53 mmol) in methanol was added portionwise with stirring solid $NH_2OH{\cdot}HCl$ (17.7 mg, 0.27 mmol) and the resulting mixture was heated under reflux for 2 h. The reaction mixture was filtered and the cooled filtrate was concentrated under reduced pressure. The residue was partitioned between water (10 mL) and methylene chloride (15 mL). The organic phase was washed with saturated sodium bicarbonate (10 mL), brine, dried (Na_2SO_4) and filtered. The filtrate was concentrated in vacuo to give a solid. Recrystallization from CH_2Cl_2/hexane gave the oxime **25** as a colorless solid (29 mg, 90%): mp 171-173°C; ^{1}H NMR ($CDCl_3$): δ 2.41 (s, 3H), 2.43 (s, 3H), 3.20-3.70 (m, 8H), 4.1-4.3 (m, 2H), 7.32 (m, 2H), 7.68 (m, 2H); ^{13}C NMR ($CDCl_3$): δ21.5, 53.9, 54.1, 69.6, 127.3, 130.0, 134.4, 144.2; IR (KBr) 3295 cm^{-1} (br, s), 1600 cm^{-1} (w); LRMS (EI) Calcd for $C_{10}H_{12}SO_3N_2$ $(M)^{+}$240.0 found m/z 240.0. [see Appendix A; Figures A.5 and A.6 for the ^{1}H and ^{13}C NMR spectra, respectively].

Oxidation of N-tert-butyl-3-azetidinol (31a). The methods of (a) Chaterjee and Shoeb[37] (b) Morimoto, Okutani and Masuda[35] were used for the attempted preparations of N-t-butyl- and N-t-octyl-3-azetidinones. [see Appendix A; Figures A.7 and A.8 for the ^{1}H and ^{13}C NMR spectra of the oxidation products, respectively].

Oxidation of N-(tert-octyl)-3-azetidinol (31b). To a stirred solution of oxalyl chloride (407 mg, 3.21 mmol) in CH_2Cl_2 (4 mL) at -70°C was added dropwise over a 5-min period a solution of DMSO (211 mg, 2.70 mmol) in CH_2Cl_2 (4 mL). To this solution at -70°C was added dropwise a solution of N-(t-octyl)-3-azetidinol **31b** (500 mg, 2.70 mmol) in CH_2Cl_2 (5 mL). Stirring was continued at -70°C for an additional 45-min after which time a solution of triethylamine (546 mg, 5.40 mmol) in CH_2Cl_2 (2 mL) was added dropwise and the reaction mixture was allowed to warm up to room temperature. The resulting triethylamine hydrochloride was removed by filtration. The CH_2Cl_2 layer was washed with H_2O (2x5 mL), dried ($MgSO_4$) and concentrated under vacuum to give a solid (263 mg, 53%). The crude reaction product was characterized by its ^{1}H, ^{13}C NMR and MS (CI) spectra. [see Appendix A; Figure A.9, and A.10, for the ^{1}H, and ^{13}C NMR, respectively].

N-(p-Toluenesulfonyl)-3-azetidinol (42). This compound was prepared by two independent routes: (a) by $NaBH_4$ reduction of **24** obtained from the cyclization of the corresponding diazoketone[28] and (b) by deprotection of N-(p-toluenesulfonyl)-3-(t-butyldimethylsiloxy)azetidine **51a**.

Method A. N-(p-Toluenesulfonyl)-3-azetidinol (42). A solution of N-(p-toluenesulfonyl)-3-azetidinone **24** (101 mg, 0.449 mmol) in MeOH (10 mL) was prepared by slight warming. To this solution at room temperature was added all at once with swirling $NaBH_4$ (40 mg, 1.06 mmol). Swirling was continued at room temperature for an additional 10 min during which time hydrogen evolution ceased. The reaction mixture was poured onto crushed ice (*ca.*, 20 g) and the mixture was extracted with CH_2Cl_2 (2x15 mL). The CH_2Cl_2 solution was washed with water (15 mL), dried (Na_2SO_4) and concentrated on a rotary evaporator to give an oil (94 mg, 92%), which crystallized on standing: mp 106-107°C; ^1H NMR ($CDCl_3$): δ2.45 (s, 3H), 2.56 (s, 1H), 3.55 (m, 2H), 3.95 (m, 2H), 4.44 (m, 1H); ^{13}C NMR ($CDCl_3$): δ 21.5, 60.10, 60.40, 128.30, 129.80, 131.60, 144.20; HRMS (FAB) Calcd for $C_{10}H_{14}SO_3N$ $(M+1)^+$ 228.0694, found m/z 228.0695. [see Appendix A; Figures A.11 and A.12 for the ^1H and ^{13}C NMR spectra, respectively].

Method B. N-(p-Toluenesulfonyl)-3-azetidinol (42). A mixture of N-(p-toluenesulfonyl)-3-(t-butyldimethylsiloxy)azetidine **51a** (40 mg, 0.117 mmol) and acetic acid-water-THF 3:1:1 (1 mL) was stirred at ambient temperature for 36 h. The mixture was concentrated in vacuum and THF (5 mL) was added to the resulting residue. Removal of the THF under vacuum gave **42** (26 mg, 98%) as a colorless solid: mp 104-105°C; ^{1}H NMR ($CDCl_3$): δ2.42 (s, 3H), 2.56 (br, s, 1H), 3.52 (t, 2H), 3.93 (t, 2H), 4.41 (quintet, 1H), 7.33 (d, J=8.1 Hz, 2H), 7.67 (d, J=8.1, 2H); ^{13}C NMR ($CDCl_3$): δ21.5, 60.1, 60.4, 128.31, 129.73, 131.13, 144.28. [see Appendix A; Figures A.11 and A.12 for the ^{1}H and ^{13}C NMR spectra, respectively].

***Cis* and *trans*-N,N'-di-(p-toluenesulfonyl)-3,7-dihydroxy-1,5-diaza-cyclooctane (47).** To a suspension of LiH (19.2 mg, 2.40 mmol) in dry THF (40 ml) under a nitrogen atmosphere was added a solution of **53** (810 mg, 2.00 mmol) in THF (25 mL) and the resulting mixture was heated under reflux for 12 h. The mixture was cooled to room temperature and ice water added cautiously to destroy any excess LiH. The solvent was removed under reduced pressure and the residue partitioned between water (5 mL) and methylene chloride (5 mL). The organic layer was separated, dried ($MgSO_4$) and concentrated in vacuum to give **47** as an oil which crystallized on

standing. Recrystallization from ethanol gave **47** (203 mg, 45%): mp 198-212 °C; ^{1}H NMR ($CDCl_3$): δ2.41 (s, 3H), 2.43 (s, 3H), 3.20-3.70 (m, 8H), 4.1-4.3 (m, 2H), 7.32 (m, 2H), 7.68 (m, 2H); ^{13}C NMR ($CDCl_3$): δ21.5, 53.9, 54.1, 69.6, 127.3, 130.0, 134.4, 144.2. [see Appendix A; Figures A.13 and A.14 for the ^{1}H and ^{13}C NMR spectra, respectively].

The product obtained from the reaction of N-(p-toluenesulfonamido)-propane-2-ol-1-(p-toluenesulfonate) (**54**) with LiH/THF was identical with the stereoisomeric mixture of diazacyclooctane from the reaction of p-toluenesulfonamide with epichlorohydrin reported by Paudler.[31] LRMS (CI, NH_3) Calcd for $C_{20}H_{26}S_2O_5N_2$ $(M+18)^+$ 472, found m/z 472.

1,3-Dichloro-2-(t-butyldimethylsiloxy)propane (50a). To t-butyldimethylsilyl chloride (5.00 g, 31 mmol) and imidazole (3.90 g, 57 mmol), in dimethylformamide (10 mL) was added a solution of 1,3-dichloro-2-propanol (3.33 g, 26 mmol) in 5mL of DMF at 25°C. The reaction mixture was stirred for 24 h at ambient temperature and then concentrated under vacuum. Methylene chloride (20 mL) was added and the solution washed with water (4x10 mL). The organic layer was dried ($MgSO_4$) and concentrated under vacuum to give **50a** as a liquid (5.53 g, 88%); ^{1}H NMR ($CDCl_3$): δ0.101 (s, 6H), 0.884 (s, 9H), 3.57 (dd, J=1.9 Hz, 2.5 Hz, 4H), 3.97-4.04 (quintet, 1H);

^{13}C NMR ($CDCl_3$): δ-4.72, 18.05, 25.64, 45.85, 72.25; LRMS (CI, NH_3) Calcd for $C_9H_{24}ONSiCl_2$ $(M+18)^+$ 260, 262, 264 found m/z 260, 262, 264. [see Appendix A; Figures A.15 and A.16 for the ^1H and ^{13}C NMR spectra, respectively].

1,3-Dibromo-2-(t-butyldimethylsiloxy)propane (50b). This compound was prepared by the procedure described for the dichloro derivative **50a**. ^1H NMR ($CDCl_3$): δ0.98 (s, 9H), 0.88 (s, 6H), 3.45 (dd, J=2.0 Hz, 2.5 Hz, 4H), 3.96 (quintet, 1H); ^{13}C NMR ($CDCl_3$): δ-4.71, 17.97, 25.60, 35.39, 71.12. LRMS (CI, NH_3) Calcd for $C_9H_{24}ONSiBr_2$ $(M+18)^+$ 348, 350, 352 found m/z 348, 350, 352. [see Appendix A; Figures A.17 and A.18 for the ^1H and ^{13}C NMR spectra, respectively].

N-(p-Toluenesulfonyl)-3-(tert-butyldimethylsiloxy)azetidine (51a). This compound was prepared by cyclization of **56** with (a) LiH in THF and (b) by treatment of 1,3-dibromo-2-(t-butyldimethylsiloxy)propane **50b** with K_2CO_3 in acetonitrile.

Method A. To a suspension of LiH (13.4 mg, 1.7 mmol) in dry THF (50 mL) under a nitrogen atmosphere was added a solution of **56** (710 mg, 1.4 mmol) in THF (20 mL) all at once. The resulting mixture was heated under reflux for 12 h, cooled to room temperature and ice-cold water (1 mL) was

added cautiously to destroy the excess LiH. The solvent was removed under reduced pressure and the residue partitioned between water (10 mL) and methylene chloride (10 mL). The organic phase was separated, dried ($MgSO_4$) and concentrated in vacuo to give 448 mg (91 %) of **51a** as a colorless solid: mp 100-102°C; ^1H NMR ($CDCl_3$): δ-0.083 (s, 6H), 0.737 (s, 9H), 3.46 (t, 2H), 3.91 (t, 2H), 4.37 (quintet, 1H), 7.34 (d, J=8.1 Hz, 2H), 7.67 (d, J=8.3 Hz, 2H). ^{13}C NMR ($CDCl_3$): δ-5.14, 17.65, 21.52, 25.44, 60.70, 128.37, 129.63, 131.53, 143.99; HRMS (FAB) Calcd for $C_{16}H_{28}SiSO_3N$ $(M+1)^+$ 342.1559, found m/z 342.1552. [see Appendix A; Figures A.19, and A.20 for the ^1H, and ^{13}C NMR spectra, respectively].

Method B. To a solution of p-toluenesulfonamide (103.4 mg, 0.602 mmol) in 7 mL of acetonitrile containing suspended anhydrous potassium carbonate (183 mg, 1.32 mmol) was added a solution of 1,3-dibromo-2-(t-butyldimethylsiloxy)propane **50b** (200 mg, 0.602 mmol) in CH_3CN (2 mL) all at once. The resulting mixture was then heated under reflux for 27 h. The mixture was cooled to room temperature and the solvent removed under reduced pressure. The residue was partitioned between water (10 mL) and methylene chloride (10 mL). The organic phase was washed sequentially with 5% NaOH, (5 mL) water (5 mL) and finally dried ($MgSO_4$) and concentrated

in vacuum to give 139 mg (68 %) of **51a** as a colorless solid: mp 101-103°C; ^{1}H NMR ($CDCl_3$): δ-0.083 (s, 6H), 0.737 (s, 9H), 3.46 (t, 2H), 3.91 (t, 2H), 4.37 (quintet, 1H), 7.34 (d, J=8.1 Hz, 2H), 7.67 (d, J=8.3 Hz, 2H); ^{13}C NMR ($CDCl_3$): δ-5.14, 17.65, 21.52, 25.44, 60.40, 60.70, 128.37, 129.63, 131.53, 143.99; HRMS (FAB) Calcd for $C_{16}H_{28}SiSO_3N$ $(M+1)^+$ 342.1559, found m/z 342.1552. [see Appendix A; Figures A.19, and A.20 for the ^{1}H, and ^{13}C NMR spectra, respectively].

N-(Methanesulfonyl)-3-(t-butyldimethylsiloxy)azetidine (51b). To a solution of methane sulfonamide (64.4 mg, 0.680 mmol) in acetonitrile (7 mL) containing suspended anhydrous potassium carbonate (156 mg, 1.13 mmol) was added a solution of 1,3-dibromo-2-(t-butyldimethylsiloxy)propane **50b** (210 mg, 0.680 mmol) in CH_3CN (3 mL) all at once. The resulting mixture was then heated under reflux for 27 h. The mixture was cooled to room temperature and the solvent removed under reduced pressure. The residue was partitioned between water (10 mL) and ethyl acetate (10 mL). The organic phase was washed with 5% NaOH (5 mL) followed by water (5 mL), and finally dried ($MgSO_4$) and concentrated in vacuum to give **51b** (106 mg, 66%) as a brown oil which after chromatography on silica gel and elution with pentane gave a colorless crystalline solid: mp 45°C; ^{1}H NMR ($CDCl_3$): δ

-0.068 (s, 6H), 0.819 (s, 9H), 3.71 (t, 2H), 3.98 (t, 2H), 4.50 (quintet, 1H). ^{13}C NMR ($CDCl_3$): δ -5.18, 17.72, 25.49, 35.51, 60.16, 60.22; LRMS (CI, NH_3) Calcd for $C_{10}H_{27}SiSO_3N$ $(M+18)^+$ 283 found m/z 283. [see Appendix A; Figures A.21 and A.22 for the ^1H and ^{13}C NMR spectra, respectively].

1-(p-toluenesulfonamido)-3-chloro-2-(t-butyldimethylsiloxy)propane (52a) and N-(p-toluenesulfonyl)-3-(t-butyldimethylsiloxy)azetidine (51a). To a solution of p-toluenesulfonamide (105.4 mg, 0.613 mmol) in acetonitrile (10 mL) containing suspended anhydrous potassium carbonate (186 mg, 1.35 mmol) was added a solution of 1,3-dichloro-2-(t-butyldimethylsiloxy)propane **50a** (149 mg, 0.613 mmol) in CH_3CN (3 mL) all at once. The resulting mixture was heated under reflux for 90 h. After that time, the mixture was cooled to room temperature and the solvent removed under reduced pressure. The residue was partitioned between water (8 mL) and methylene chloride (10 ml). The organic phase was washed with water (5 mL), followed by 10% aqueous HCl (5 mL), dried ($MgSO_4$) and concentrated in vacuum to give 128 mg of a 1:1 mixture of 1-(p-toluenesulfonamido)-3-chloro-2-(t-butyldimethylsiloxy)propane **52a** and N-(p-toluenesulfonyl)-3-(t-butyldimethylsiloxy)-azetidine **51a.** [see Appendix A; Figures A.20 and A.21 for the ^1H and ^{13}C NMR spectra, respectively].

3-(p-toluenesulfonamido)propane-2-ol 1-(p-toluenesulfonate) (54) and **3-(p-Toluenesulfonamido)-1,2-propane-di-(p-toluenesulfonate) (55).**To a stirred solution of 3-amino-1,2-propane-diol **53** (1.34 g, 14.7 mmol) in dry pyridine (20 mL) maintained at ice-temperature was added a solution of p-toluenesulfonyl chloride (5.60 g, 29.4 mmol) in pyridine (10 mL) over a 2 h period. The resulting yellow suspension was refrigerated overnight, acidified with ice-cold 6N HCl and then extracted with methylene chloride (3x20 mL). The combined organic layers were washed with 5% aqueous $NaHCO_3$ (2x10 mL) solution, dried over $MgSO_4$ and concentrated in vacuo to give a syrupy residue. Silica gel chromatography (chloroform-methanol 95:5) of this residue afforded **54** as a viscous oil. Crystallization from ethyl acetate-hexane gave **54** (3.88 g, 66%) as a colorless solid: mp 96-98°C; ^{1}H NMR ($CDCl_3$): δ2.41, (s, 3H), 2.43 (s, 3H,), 2.93-3.00 (m, 4H), 3.94-4.03 (m, 1H), 4.00 (s, 1H,), 7.70-7.79 (m, 4H); ^{13}C NMR ($CDCl_3$): δ21.52, 21.66, 44.81, 68.02, 70.78, 127.05, 127.96, 129.86, 130.05, 132.08, 136.15, 143.82, 145.37; HRMS (FAB) Calcd for $C_{17}H_{22}O_6S_2N$ $(M+1)^+$ 400.0889, found m/z 400.0901. [see Appendix A; Figures A.23 and A.24 for the ^{1}H and ^{13}C NMR spectra, respectively].

Compound **55** was also obtained from the silica gel chromatography as a solid. Recrystallization from absolute ethanol gave a colorless solid: mp 108-110°C; ^{1}H NMR ($CDCl_3$): δ2.43, (s, 3H), 2.46 (s, 3H), 2.47 (s, 3H), 3.11 (m, 2H), 4.09 (m, 2H), 4.66 (quintet, 1H, CH), 4.86 (t, 1H, NH), 7.30-7.35 (m, 4H), 7.57-7.68 (m, 4H); ^{13}C NMR (CD_2Cl_2): δ21.63, 21.82, 43.11, 67.80, 77.05, 127.32, 128.30, 130.24, 130.42, 132.73, 146.08, 146.23; HRMS (FAB) Calcd for $C_{24}H_{28}O_8S_3N$ $(M+1)^+$ 554.0977, found m/z 554.0980. [see Appendix A; Figures A.25 and A.26 for the ^{1}H and ^{13}C NMR spectra, respectively].

3-(p-Toluenesulfonamido)propane-2-(t-butyldimethylsiloxy)-1-(p-toluenesulfonate) (56). To a solution of t-butyldimethylsilyl chloride (380 mg, 2.52 mmol) and imidazole (315 mg, 4.63 mmol) in DMF (5 mL) was added a solution of 3-(p-toluenesulfonamido)propane-2-ol-1-(p-toluenesulfonate) **54** (820 mg, 2.1 mmol) in 5 ml of DMF at 25°C. The reaction mixture was stirred for 24 h at ambient temperature and then concentrated under vacuum. Methylene chloride (10 mL) was added and the solution was extracted with water (4x5 mL). The organic layer was dried over $MgSO_4$ and concentrated under vacuum to give **56** as a colorless liquid (951 mg, 88%); ^{1}H NMR ($CDCl_3$): δ0.01 (s, 6H), 0.77 (s, 9H), 2.39 (s, 3H), 2.42 (s, 3H), 2.84-2.99 (m,

2H), 3.82-3.96 (m, 5H), 4.71 (t, 1H, NH), 7.24-7.33 (m, 4H).[13] C NMR ($CDCl_3$): δ4.91, 17.81, 21.45, 21.59, 25.53, 43.32, 68.63, 70.32, 126.99, 127.89, 129.76, 129.92, 132.39, 136.21, 143.66, 145.08; HRMS (FAB) Calcd for $C_{23}H_{37}SiO_6S_2N$ $(M+1)^+$ 514.1753, found m/z 514.1758. [see Appendix A; Figures A.27 and A.28 for the ^1H and ^{13}C NMR spectra, respectively].

N-(p-Toluenesulfonyl)-2-(methyl-p-toluenesulfonate)aziridine (57). This compound was prepared by cyclization of 3-(p-toluenesulfonamido)-1,2-propane-di(p-toluenesulfonate) **55** with (a) LiH in THF and (b) K_2CO_3 in acetonitrile.

Method A. To a suspension of LiH (10.5 mg, 1.32 mmol) in dry THF (55 mL) under a nitrogen atmosphere was added a solution of **55** (610 mg, 1.1 mmol) in THF (15 mL) and the resulting mixture was heated under reflux for 12 h. The reaction mixture was cooled to room temperature and ice-cold water (1 mL) was added cautiously to destroy the excess LiH. The solvent was removed under reduced pressure and the residue partitioned between water (10 ml) and methylene chloride (10 mL). The organic phase was separated, dried ($MgSO_4$) and concentrated in vacuum to give **57** as a colorless oil (335 mg, 80 %); ^1H NMR ($CDCl_3$): δ2.18 (d, J= 4.3 Hz, 2H),

2.43 (s, 3H), 2.46 (s, 3H), 2.68 (d, J=7.0 Hz, 2H), 3.00 (quintet, 1H), 4.00 (dd, J=5.1Hz, 1H), 7.31-7.36 (d, J=6.0 Hz, 4H), 7.70-7.85 (d, J=8.34H, N-Ar-H). ^{13}C NMR ($CDCl_3$): δ21.56, 31.02, 36.68, 68.44, 127.86, 128.00, 129.71, 129.86, 132.72, 134.51, 139.92 144.87, 145.10; HRMS (FAB) Calcd for $C_{17}H_{20}S_2O_5N$ $(M+1)^+$ 382.0783, found m/z 382.0786. [see Appendix A; Figures A.29 and A.30 for the ^1H and ^{13}C NMR spectra, respectively].

Method B. To a suspension of K_2CO_3 (30 mg, 0.220 mmol) in CH_3CN (5 mL) was added a solution of **55** (100 mg, 0.180 mmol) in CH_3CN (5 mL) and the resulting mixture was heated under reflux for 18 h. The solvent was removed under reduced pressure and the residue partitioned between water (10 mL) and ethyl acetate (10 mL). The organic phase was separated, dried ($MgSO_4$) and concentrated in vacuum to give **56** as a colorless oil (65 mg, 94 %). Compound **56** had spectral properties identical with the material obtained from the LiH reaction.

PART II

Synthesis and Conformational Studies of Urea-Based Calix[4]arenes

CHAPTER 2

2.0 Introduction

The synthesis and chemistry of macrocyclic compounds has attracted considerable attention in recent years because of their unusual structures, conformational properties and ability to act as hosts to both neutral molecules and ionic species.[38,39] The host-guest phenomenon warrants study as a mimic of enzyme-substrate interactions in biological systems as well as the study of in-vitro chemical reactions brought about by preorganization of reagents. This is illustrated schematically in Figure 2.1.

Most of the compounds that can act as hosts have macrocyclic structures with three-dimensional cavities that can accommodate the guest molecules. Examples include crown ethers, cryptands, cyclophanes, spherands and calixarenes (see Figure 2.2). These examples are typical of supramolecular

species that can recognize, transform and translate guest molecules via the formation of inclusion complexes.

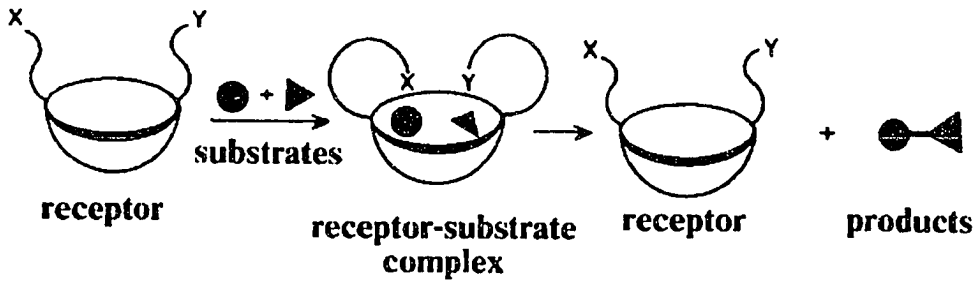

Figure 2.1. Schematic representation of receptor-substrate complex.[57]

Despite the fact that carbonyl groups of amides and esters play dominating roles in biological systems, macrocycles incorporating these groups have received little attention compared to their polyoxo, polysulfo, and polyaza congeners. Even fewer examples are known that involve cyclic urea units as binding sites either solely or in combination with other functional groups. Cram and co-workers[40-44] have synthesized a variety of macrocycles incorporating the tetrahydropyrimidinone unit. In fact, a spherand constituted of this unit is reported to be the strongest complexer of alkyammonium ions (see Figure 2.3).[39] More recently, Pratt, Sutherland and Newton[46] have described the synthesis of a novel macrocycle also incorporating the tetrahydropyrimidinone unit (see Figure 2.3).

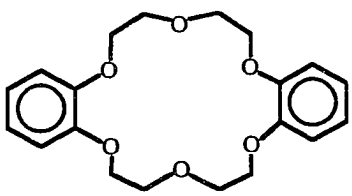

Crown ether

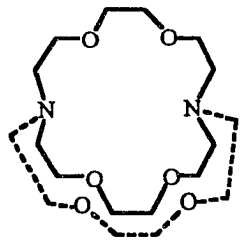

Cryptand

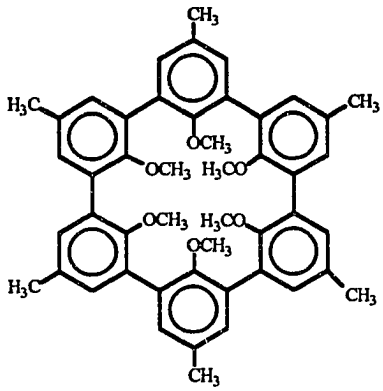

Spherand

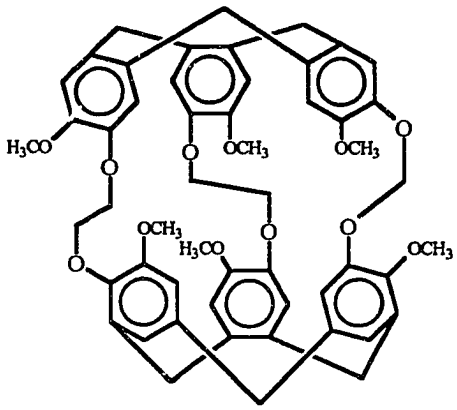

Cyclophane

Figure 2.2. Some examples of supramolecular species.

In addition to the biological rationale for studying such systems, it has been established that urea oxygen is less sterically hindered and a stronger complexing group than methoxy units.[39,45]

In the present investigation the study of the chemistry and NMR properties of a series of novel macrocycles incorporating cyclic urea units was undertaken. These macrocycles are analogs of the calix[4]arenes,[47] in which two of the aryl groups have been replaced by urea units incorporated in the triazone and imidazolidone ring systems, respectively. The structures of these

systems are shown in Schemes 3 and 4 (pp. 48 and 49). It was of interest to investigate the conformational behavior of such molecular assemblies.

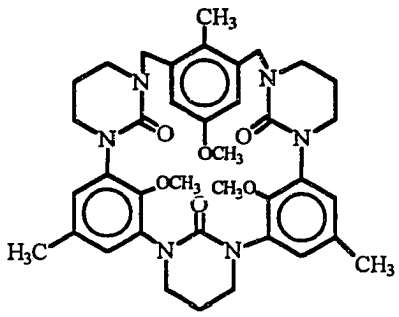

Spherand

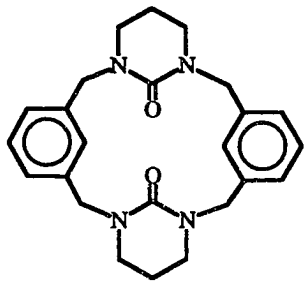

Calixarene

Figure 2.3. Macrocycles containing urea units.

In order to understand the factors which shape these molecules, the spatial structures and various interactions contributing to the formation of a particular comformation must be well-characterized. In the solid state the most direct and powerful method for the determination of three-dimensional structures is x-ray diffraction, provided single crystals are available. However, in the liquid phase almost all important intramolecular or intermolecular interactions leading to the stabilization (or destabilization) of a particular molecular geometry occur between atoms or groups that are situated in close proximity (i.e., a few angstroms) to each other. Thus, high resolution NMR spectroscopy is extremely useful for the study of such phenomenona, because

NMR parameters such as chemical shift, spin-coupling and Nuclear Overhauser effects are sensitive to short-range interactions.

2.1. Background

Calixarenes, are phenol-formaldehyde oligomers which are conformationally mobile.[48] The most common types of calixarenes are calix[4]arene, calix[5]arene, calix[6]arene, calix[7]arene and calix[8]arene which contain four, five, six, seven, and eight phenol units connected via methylene bridges, respectively (see Figure 2.4). They are obtained either by acid-catalyzed or base-induced condensation of p-substituted phenols and formaldehyde. This is illustrated in Scheme 1.

Scheme 1

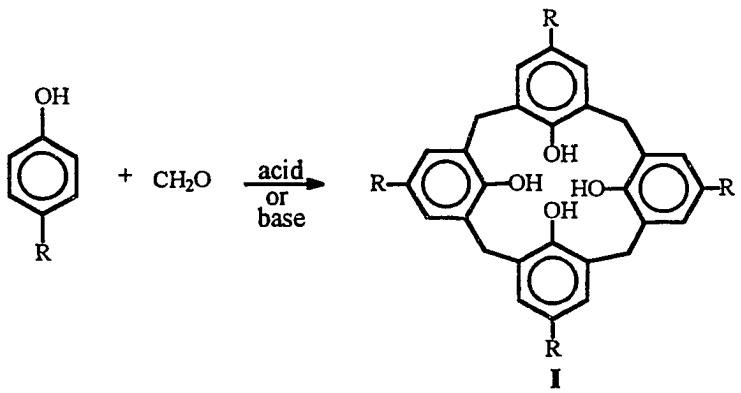

I

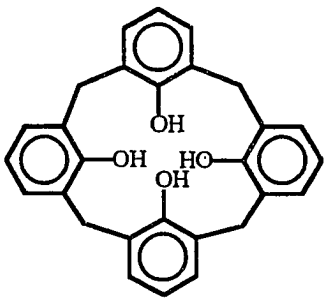

Calix[4]arene

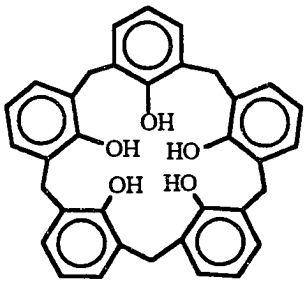

Calix[5]arene

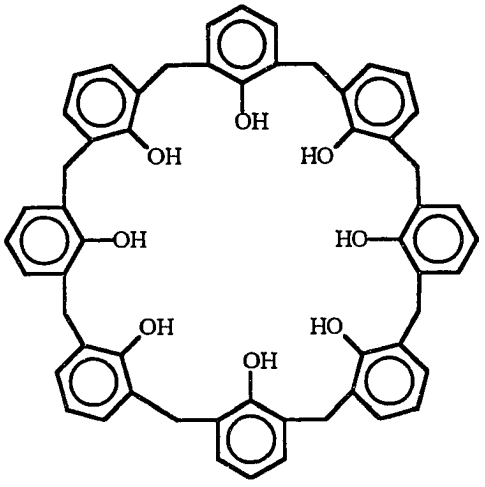

Calix[8]arene

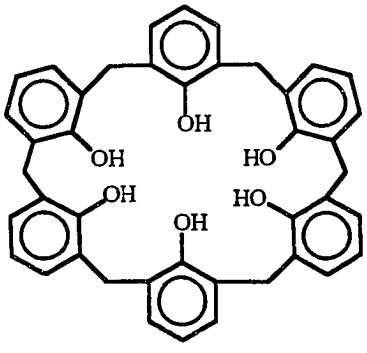

Calix[6]arene

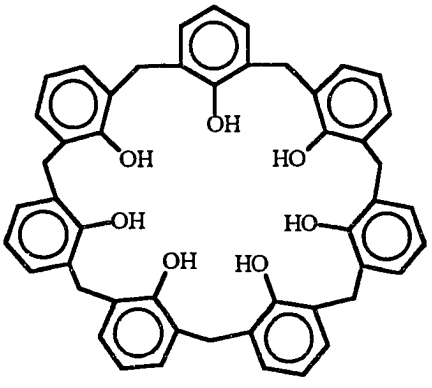

Calix[7]arene

Figure 2.4. Representatives of calix[n]arenes.

Calixarenes form complexes with a variety of small molecules that bind in the molecular cavity of the host in much the same way as is observed in cyclodextrin host-guest complexes.[60,61] They differ from cyclodextrins, however, in that they are synthetic molecules and thus, have greater possibility for controlled design and functionality.[48]

2.2. Conformational Characteristics of Calix[4]arenes

The possible existence of calix[4]arene type molecules in four "up-down" forms was first considered by Cornforth[73] in the 1950s (see Figure 2.5). The subsequent designation of these structures as conformers followed from the development of the concepts of conformational analysis due to Barton.

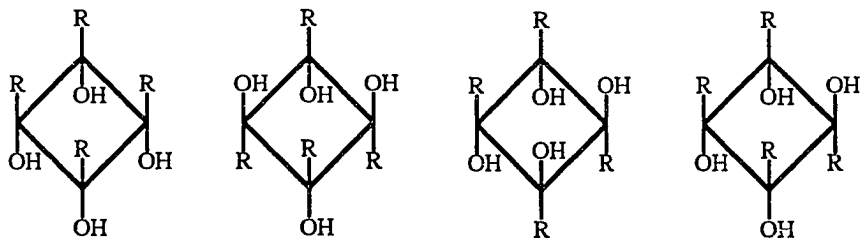

Figure 2.5. Rotational distereomers of a cyclic-tetramer proposed by Cornforth.[73]

The smallest of the known calixarenes are the cyclic tetramers, designated as calix[4]arenes **I**. Calix[4]arenes exist in a number of different conformations, some of which are not useful as hosts, as they lack a definable

cavity. The four forms considered as important species were later named by Gutsche,[49] as the **cone, partial cone, 1,2-alternate** and **1,3-alternate** conformers, shown in Figure 2.6.

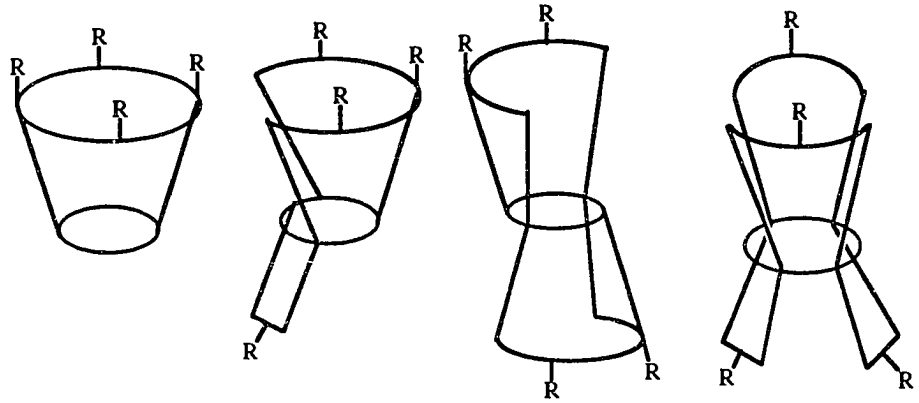

Figure 2.6. Pseudo three-dimensional representations of calix[4]arenes conformers.[58]

These four conformations of calix[4]arenes are interconvertable by rotations of the aryl groups around the axis that passes through the meta carbon atoms bonded to the bridging methylene groups. By analogy with the calixarenes which have been extensively studied,[51,57] similar types of conformations may also be considered for the urea-based calixarene macrocycles. These are provisionally designated as the cone, partial cone, 1,3-alternate and the 1,2-alternate forms and are illustrated in Figure 2.7 for the 16-membered triazone-calixarene analog **2a**.

It is recognized that some of these conformations may have only fleeting existence or by present methods may not be unambiguously distinguishable. These four designations also may not be sufficient to accommodate all possible conformations. If one considers species having their carbonyl oxygens pointed in the same and opposite directions and the aryl groups similarly oriented partially, or completely, the necessity for defining other types of conformations escalates. However, these four forms will be used as guide in attempting to define the shapes of the molecules explored in this study (see Figure 2.8).

2.3. NMR Spectral Characteristics of Calix[4]arene

Dynamic ^{1}H NMR measurements of several calix[4]arenes[49-51] have shown that the parent ring system is conformationally mobile and exists preferentially in the cone conformation at room temperature, interconverting at a rate of *ca.* 100 $sec.^{-1}$ Various ethers including methyl, ethyl, allyl, benzyl and trimethylsilyl derivatives as well as the acetates have been prepared.[52] All but the methyl ethers are conformationally rigid at room temperature. The preferred conformations in most cases are the cone and partial cone, depending on the derivatives formed (i.e. methyl and ethyl ethers favor the partial cone; benzyl and trimethylsilyl ethers favor the cone).[52]

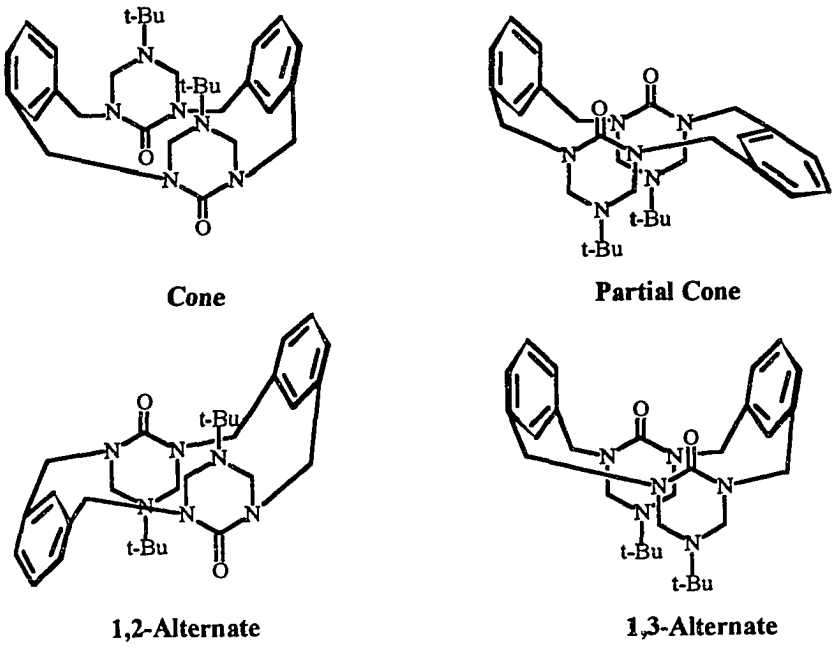

Figure 2.7 Some possible conformations of the 16-membered bis-triazone-calixarene analog **2a**.

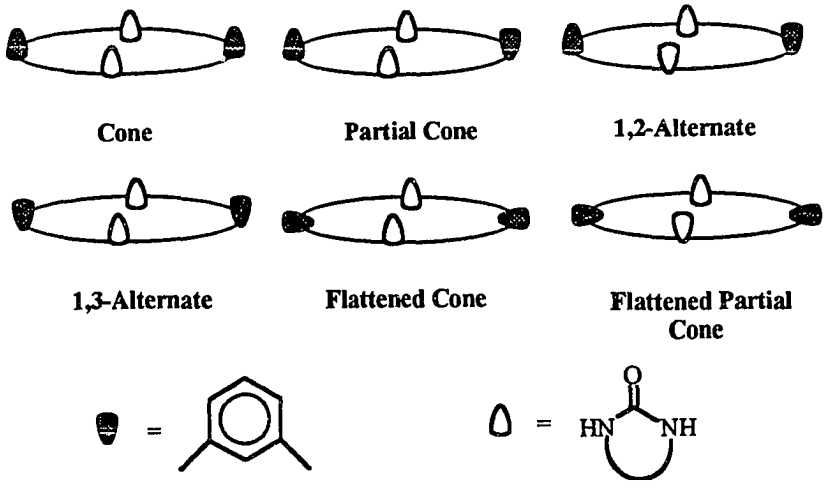

Figure 2.8. Iconographic representation of conformations.

NMR spectral characteristics of calix[4]arenes are specific for each conformer. Using p-t-butylcalix[4]arene as an illustrative example, Tables 1 and 2 compare the ^{1}H and ^{13}C NMR spectral patterns that are predicted for each conformer.[52]

Table 2.1. ^{1}H NMR features predicted for different conformations of p-tert-butylcalix[4]arene.

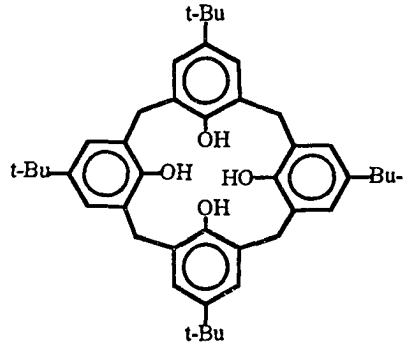

Conformation	Ar-H	Ar-CH_2	$C(CH_3)_3$
Cone	One singlet	One pair of doublets (J=12 Hz)	One singlet
Partial cone	Two singlets and two doublet or four singlets ratio (1:1:1:1)	Two pairs of doublets (J=12 Hz), ratio (1:1) or one pair of doublets (J=12 Hz) and one singlet, ratio (1:1)	Three singlets ratio (1:2:1)
1,2-Alternate	Two singlets ratio (1:1)	One singlet and one pair of doublets (J=12 Hz), ratio (1:1)	One singlet
1,3-Alternate	One singlet	One singlet	One singlet

Table 2.2 ^{13}C NMR signals predicted for different conformations of p-tert-butylcalix[4]arene.

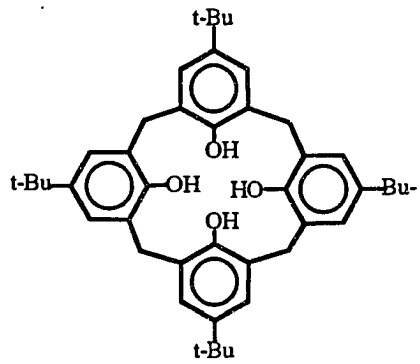

Conformation	Ar-C	Ar-$\underline{C}H_2$	$C(\underline{C}H_3)_3$	$\underline{C}(CH_3)_3$
Cone	4	1	1	1
Partial cone	12	2	3	3
1,2-Alternate	4	2	1	1
1,3-Alternate	4	1	1	1

Inspection of the tables reveals that the ^{1}H NMR spectrum will generally be a better probe of the presence of different conformations than the ^{13}C NMR spectrum because in the former each of the four conformers displays a distinctively different pattern not found in the ^{13}C NMR spectrum.[57] This is illustrated in the ^{1}H NMR spectrum shown in Figure 2.9 for the tetrabenzoate derivative of p-tert-butylcalix[4]arene. On occasion, however, the ^{13}C NMR spectra can provide useful corroboratory information.[52]

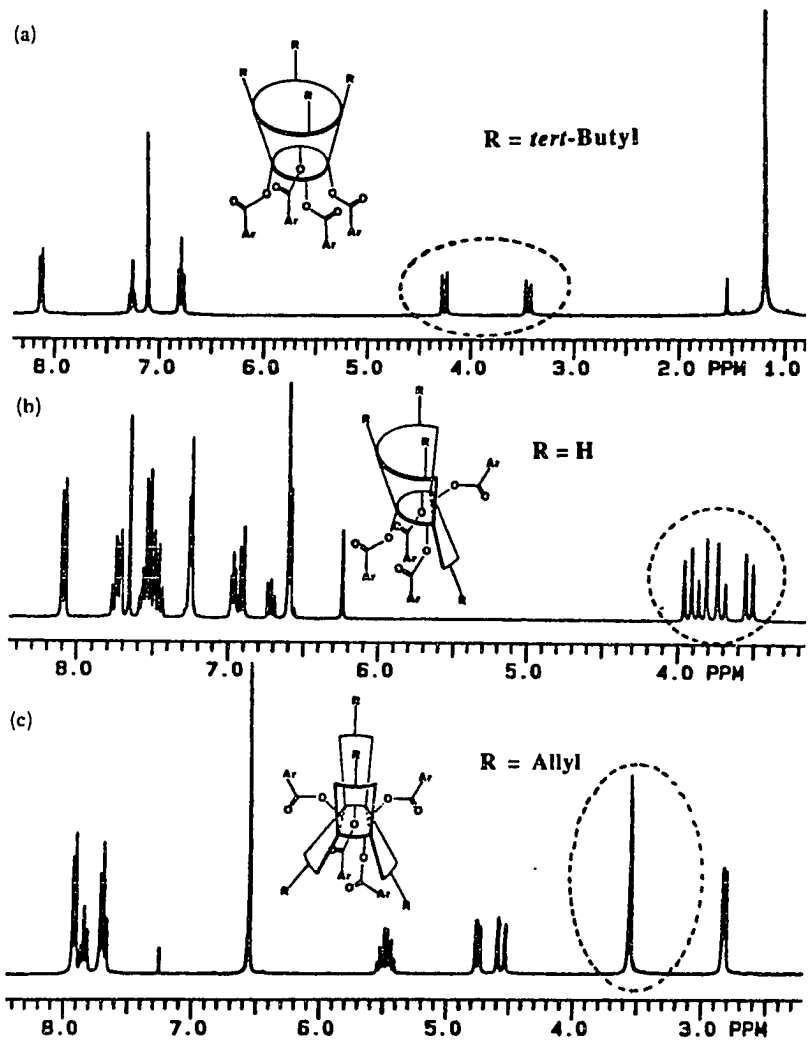

Figure 2.9. Comparison of the ^{1}H NMR spectra exhibited by different conformations of calixarene tetrabenzoate derivatives (a) p-tert-butylcalix[4]arene in the cone conformation; (b) calix[4]arene in the partial cone; (c) p-allylcalix[4]arene in the 1,3-alternate conformation.[57]

Similarly, the predicted ^{1}H NMR spectral patterns for each conformer in the case of triazone-calixarene analogs **2a-c** are summarized in Tables 3, 4 and 5, respectively.

Table 2.3. ^{1}H NMR resonance signals predicted for different conformations of macrocycle **2a**.

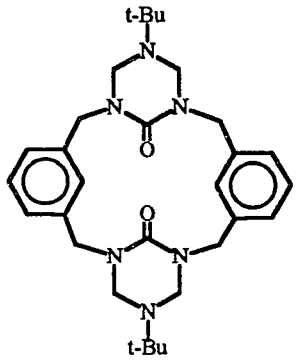

2a

Conformation	Ar-CH_2	N-CH_2-N
Cone	Two pairs of doublets	Two pairs of doublets
Partial cone	Four pairs of doublets	Four pairs of doublets
1,2-Alternate	Four pairs of doublets	Four pairs of doublets
1,3-Alternate	Two pairs of doublets	Two pairs of doublets

Table 2.4. ^{1}H NMR resonance signals predicted for different conformations of macrocycle **2b**.

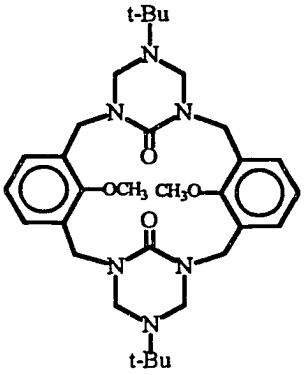

Conformation	Ar-CH_2	N-CH_2-N	CH_3O
Cone	Two pairs of doublets	Two pairs of doublets	One singlet
Partial cone	Four pairs of doublets	Four pairs of doublets	Two singlets
1,2-Alternate	Four pairs of doublets	Four pairs of doublets	One singlet
1,3-Alternate	Two pairs of doublets	Two pairs of doublets	One singlet

Table 2.5. ^{1}H NMR resonance signals predicted for different conformations of macrocycle **2c**.

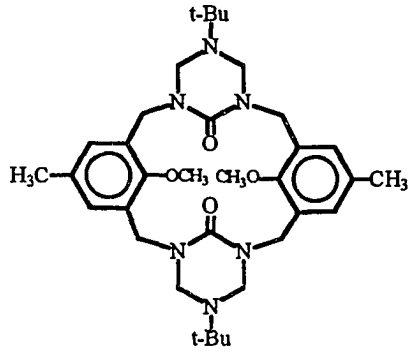

Conformation	Ar-CH_2	N-CH_2-N	CH_3O	Ar-CH_3
Cone	Two pairs of doublets	Two pairs of doublets	One singlet	One singlet
Partial cone	Four pairs of doublets	Four pairs of doublets	Two singlets	Two singlets
1,2-Alternate	Four pairs of doublets	Four pairs of doublets	One singlet	One singlet
1,3-Alternate	Two pairs of doublets	Two pairs of doublets	One singlet	One singlet

2.4. Synthesis and Proof of Structure of Urea-based Calixarene analogs

5-tert-Butyltetrahydro-1,3,5-triazine-(1H)one **1** was conveniently prepared from tert-butylamine, aqueous formaldehyde and urea (see Scheme 2).[53]

Scheme 2

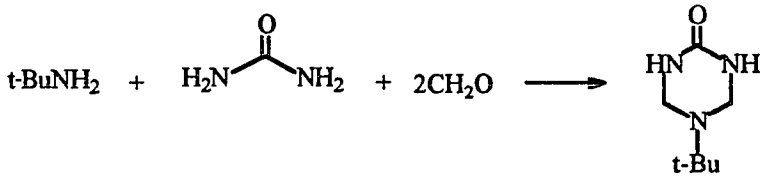

1

Reaction of the disodium salt of **1** with 1,3-bis(bromomethyl)benzene in refluxing tetrahydrofuran (THF) gave the cyclized product **2a**[68] in 54% yield. Similarly, the reaction of the disodium salt of **1** with 2,6-bis-(bromomethyl)-anisole[66] and 2,6-bis(bromomethyl)-4-methylanisole[65] gave mixtures of products from which the corresponding 16-membered macrocycles **2b**, and **2c** were isolated in 11% and 6% yield, respectively (see Scheme 3).

In a completely analogous fashion, when the disodium salt of **1** was allowed to react with 1,4-bis(bromomethyl)benzene in refluxing tetrahydrofuran (THF), the 18-membered macrocycle **3** was obtained in 3%

yield. Additionally, treatment of the disodium salt of 2-imidazolidone **4** with 1,3-bis(bromomethyl)benzene or 1,4-bis(bromomethyl)benzene gave the corresponding 16- and 18-membered macrocyclic derivatives **8** and **9** in 13% and 0.3% yield, respectively (see Scheme 4).

Scheme 3

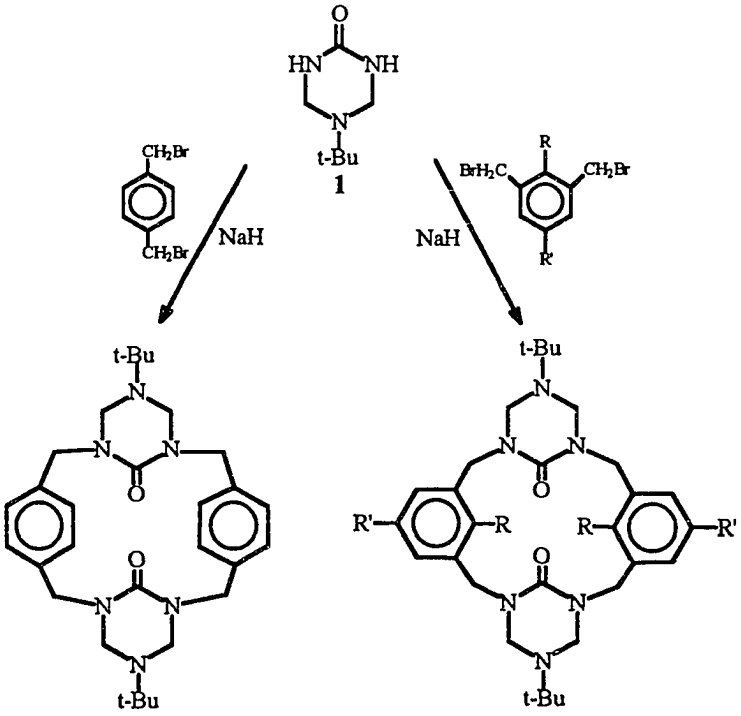

2a : R = R' = H
2b : R = OCH_3, R' = H
2c ; R = OCH_3, R' = CH_3

Scheme 4

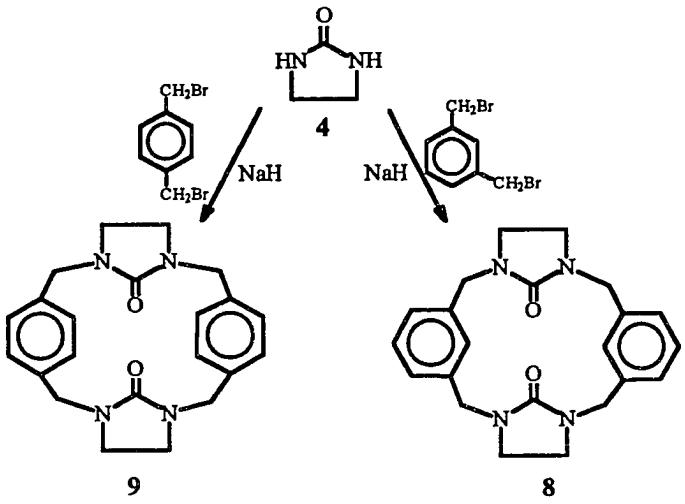

Finally, to aid in making spectral assignments the deuterium labeled-d_8 analog **10** of macrocycle **2b** was prepared (see Scheme 5). The key intermediate **14** for this sequence was obtained by the series of steps shown in Scheme 6.

Scheme 5

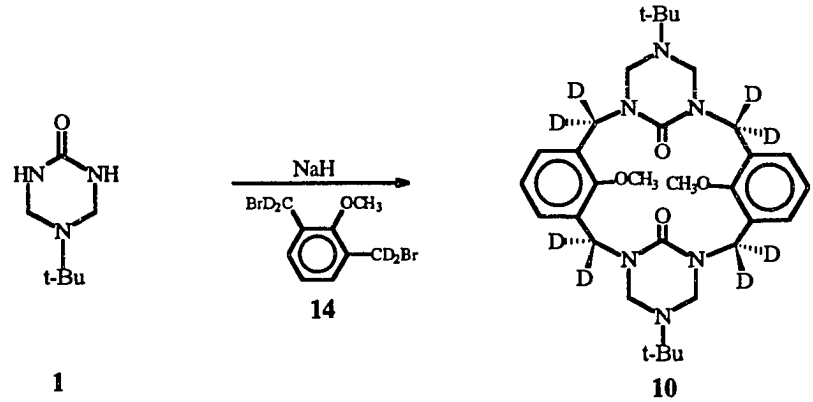

Oxidation of 2,6-dimethylanisole with potassium permanganate gave the 2-methoxy-1,3-benzenedicarboxylic acid **11**. Conversion of **11** to its ethyl ester derivative **12** was achieved using anhydrous ethanol and H_2SO_4. Reduction of **12** with $LiAlD_4$ in ether gave 2,6-bis(hydroxymethyl-d_2)anisole **13**. Subsequent treatment of **13** with thionyl bromide afforded 2,6-bis(bromo-methyl-d_2)anisole **14** (see Scheme 6).

Scheme 6

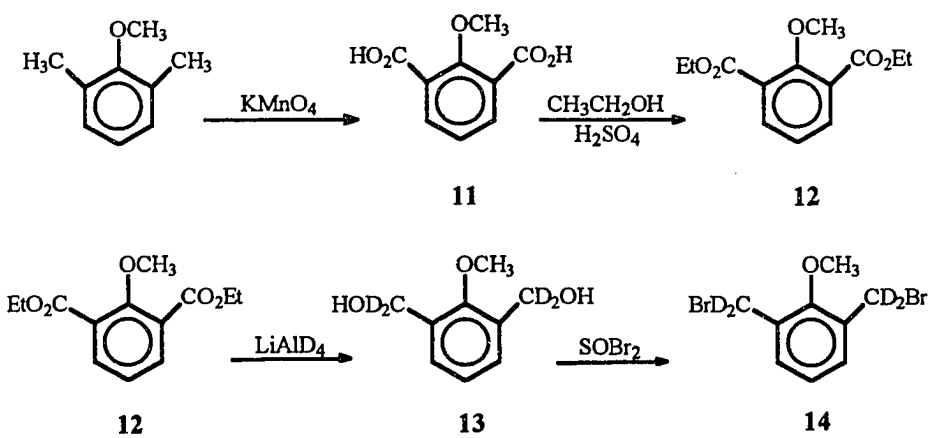

The structures of the urea-based calixarene analogs prepared in this investigation were established by mass spectral determination of elemental composition and by ^1H and ^{13}C NMR spectroscopy.

2.5. Results and Discussion of the X-ray Structures of the 16-Membered Urea-based Calix[4]arene Analogs 2a-c

X-ray crystallographic determination showed that in the solid state macrocyle **2a** adopts a flattened partial cone-like conformation with the two aromatic rings and the attached benzyl carbons approximately perpendicular to the cone axis. The triazone units are essentially parallel to each other with their respective carbonyl units pointing in opposite directions. This is schematically represented in Figure 2.10. The ORTEP diagram of the x-ray analysis is illustrated in Figure 2.11.

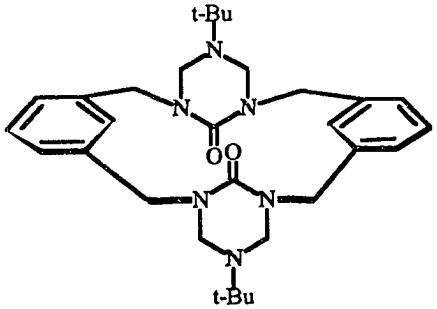

Distorted Cone-like 2a(*anti*)

Figure 2.10. Conformation of macrocycle **2a** adopted in the solid state.

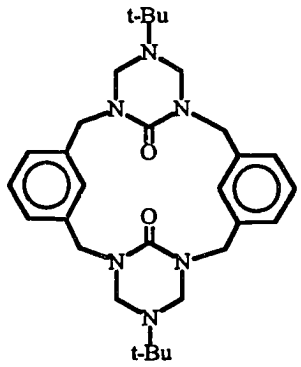

2a

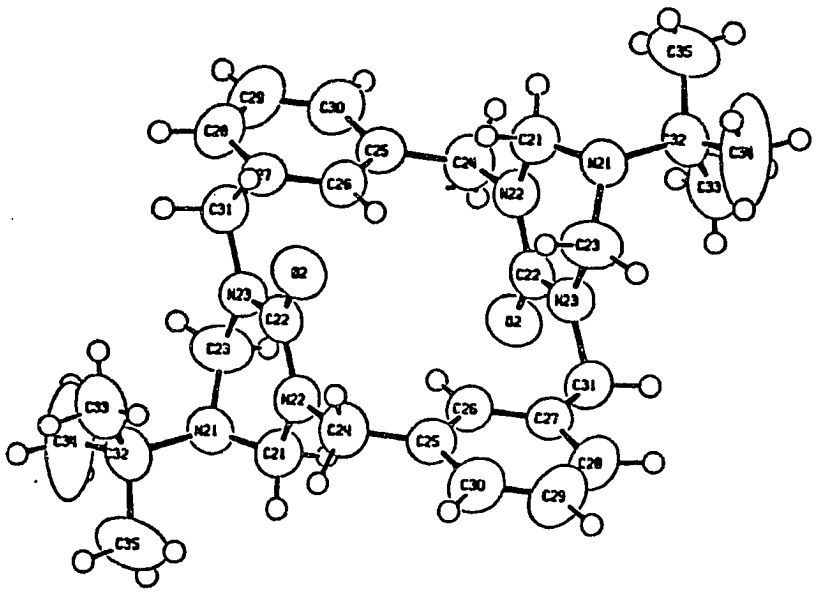

Figure 2.11. ORTEP representation of macrocycle **2a**.

The ORTEP diagram of **2b** is shown in Figure 2.13 and that of **2c** is shown in Figure 2.14. The x-ray crystallographic determinations show the conformations adopted by **2b** and **2c** to be essentially the same, but different from that of **2a**. In both cases the triazone units are parallel to each other, but in contrast to **2a** which adopts the *anti* conformation having the urea carbonyl

groups oriented in the opposite direction, in **2b** and **2c** the *syn* conformation having the carbonyl oxygen atoms pointing in the same direction is favored. The probable steric demand of the two methoxy groups in the cavity prevent the coplanarity of the aromatic rings found in **2a**. Compared with **2a**, one aromatic ring in **2b** and **2c** is partially rotated about the axis that passes through the meta carbon atoms joining the bridging benzyl CH_2 groups. This results in canting of the two aryl groups in each molecule. The aryl groups occupy approximately perpendicular planes with one of the methoxy groups pointing into the cavity and the other pointing in the opposite direction from the triazone carbonyl groups (see Figure 2.12). Molecular models show the cavity-enforced methoxy group appears to be close to the orthogonal π cloud of the facing aromatic ring.

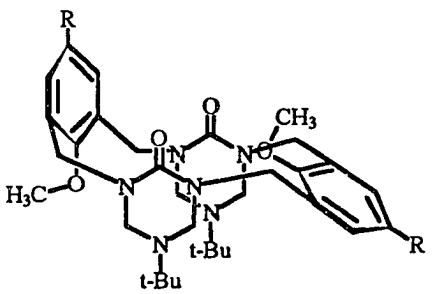

2b (*syn*): R=H
2c (*syn*): R=CH_3

Figure 2.12. Conformation of macrocycles **2b** and **2c** adopted in the solid state.

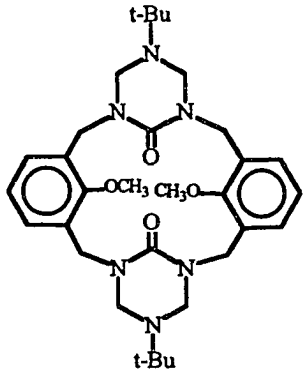

2b

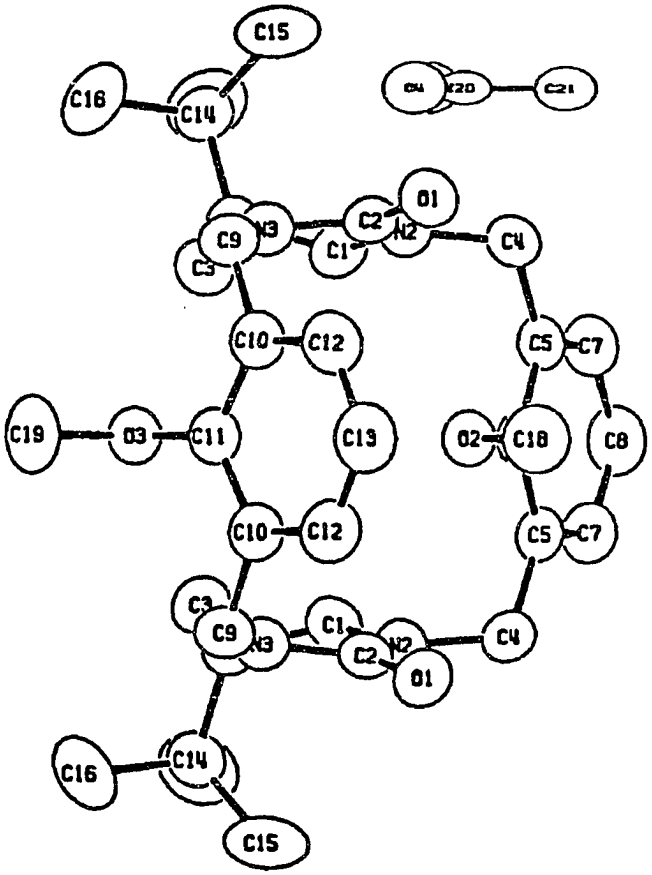

Figure 2.13. ORTEP representation of macrocycle **2b**.

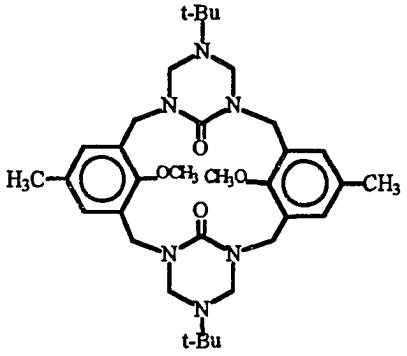

2c

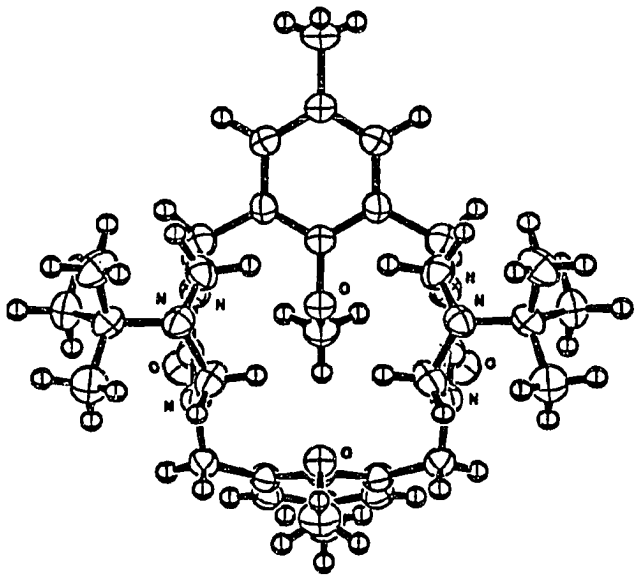

Figure 2.14. ORTEP representation of macrocycle **2c**.

2.6. Results and Discussion of the NMR Spectra of the 16-Membered Urea-based Calix[4]arene Analogs

The ^1H NMR spectra of macrocycle **2a** recorded at 300K and 250K, measured in $CDCl_3$ are illustrated in Figures 2.15 and 2.16, respectively. In the room temperature spectrum of **2a** in $CDCl_3$, the 16 aliphatic methylene

protons are seen as broad signals at δ5.8, δ4.2 and δ3.7 with an intensity ratio of 1:2:1, respectively.

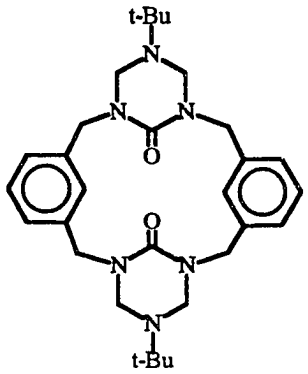

2a

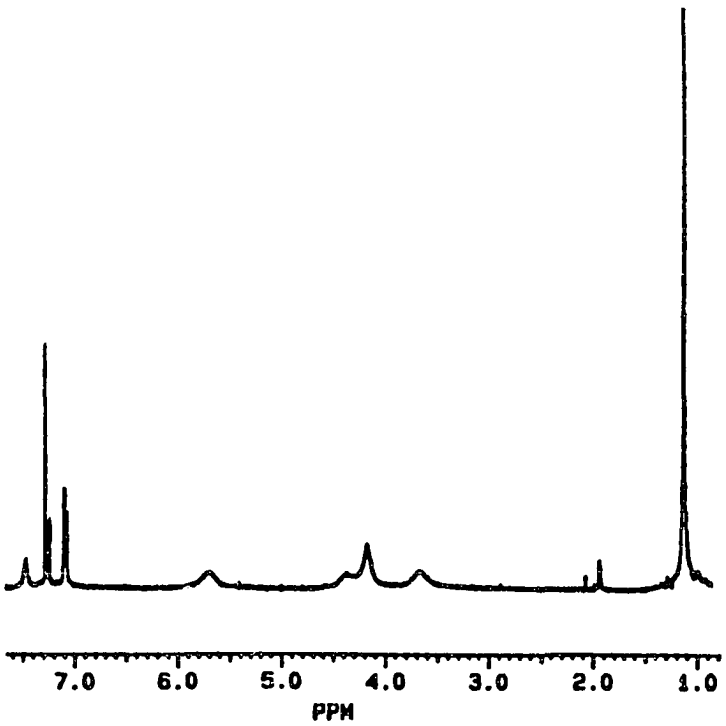

Figure 2.15. 200 MHz ^{1}H NMR spectrum of macrocycle **2a** measured in $CDCl_3$ at 300K.

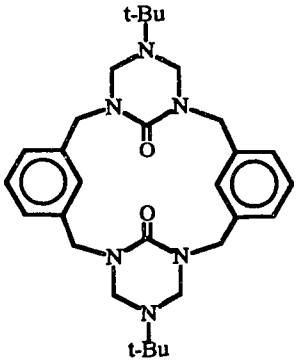

2a

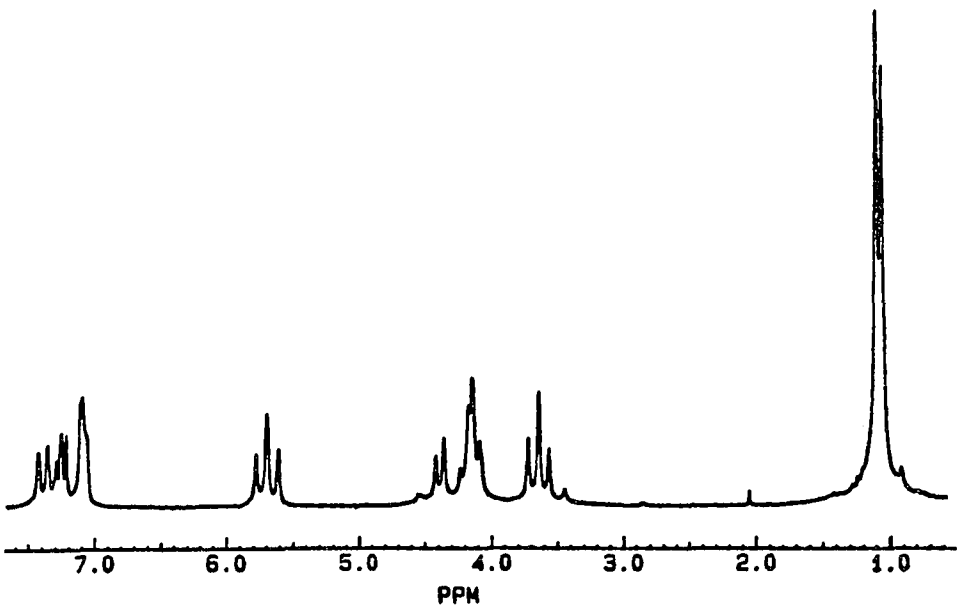

Figure 2.16. 200 MHz ^{1}H NMR spectrum of macrocycle **2a** measured in $CDCl_3$ at 250K.

On the basis of the ^1H-^1H homonuclear shift and ^1H-^{13}C heteronuclear shift correlated two-dimensional NMR spectroscopy techniques, the signals at δ5.8 and δ3.7 are assigned to the benzylic protons and the others at δ4.2 to the heterocyclic ring methylene protons. The contour plots of the ^1H-^1H homonuclear shift and the ^1H-^{13}C heteronuclear shift correlated spectra of macrocycle **2a** recorded at 250K are illustrated in Figures 2.17 and 2.18, respectively. These correlated data are summarized in Tables 2.6 and 2.7.

Table 2.6. Correlated ^1H-^1H chemical shifts in macrocycle **2a** measured in $CDCl_3$ at 250K.

δ^{1}H-δ^{1}H, ppm	δ^{1}H-δ^{1}H, ppm
5.81	3.76
7.45 5.73	5.73 3.68
5.73	3.76
7.38 5.64	4.20 3.68
5.73	
7.12 5.64	

Table 2.7. Correlated ^{1}H-^{13}C chemical shift assignments signals in macrocycle **2a** measured in $CDCl_3$ at 300K and 250K.

	300K		250K	
C/H assignment	**$\delta^{1}H$, ppm**	**$\delta^{13}C$, ppm**	**$\delta^{1}H$, ppm**	**$\delta^{13}C$, ppm**
CH_3-(t-butyl)	1.10	28.4	1.14 1.27	28.3 28.5
Ph-CH_2	3.70(br) 5.80(br)	48.8	3.65 5.68 } J = 16.2 Hz	48.3 48.6
C_q-(t-butyl)		54.0		53.7 54.1
N-CH_2-N	4.20(br)	62.4	4.20 complicated multiplet	61.8 62.3
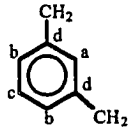				
C_a	7.5	123.8	7.5 7.4	123.2 124.9
C_b	7.0	126.0	7.3 multiplet	125.6 126.4
C_c	7.2	128.1	7.1	128.1 128.2
C_d		139.2		138.5 138.7
C=O		155.6		155.2 155.3

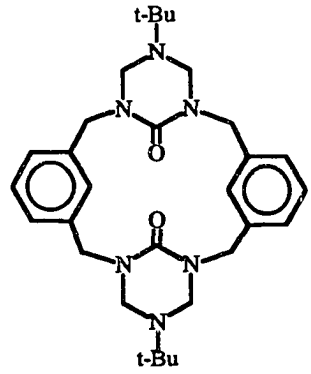

2a

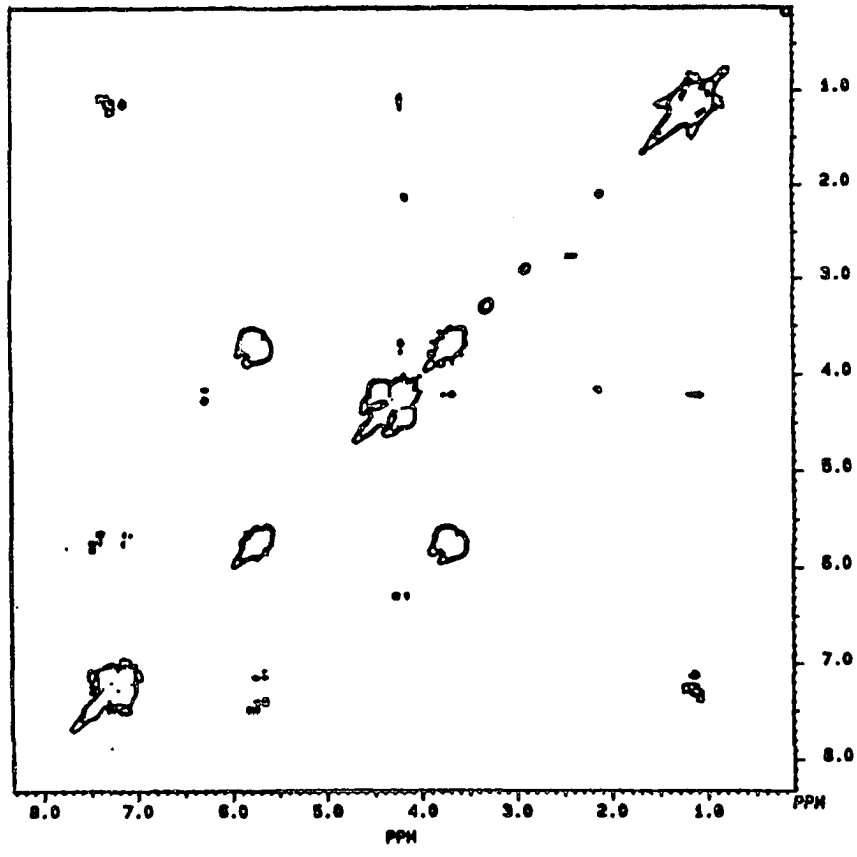

Figure 2.17. Contour plot of 200 MHz ^{1}H-^{1}H correlated spectrum of macrocycle **2a** measured in $CDCl_3$ at 250K.

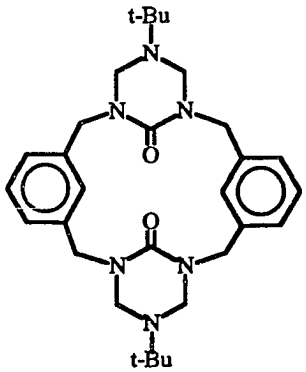

2a

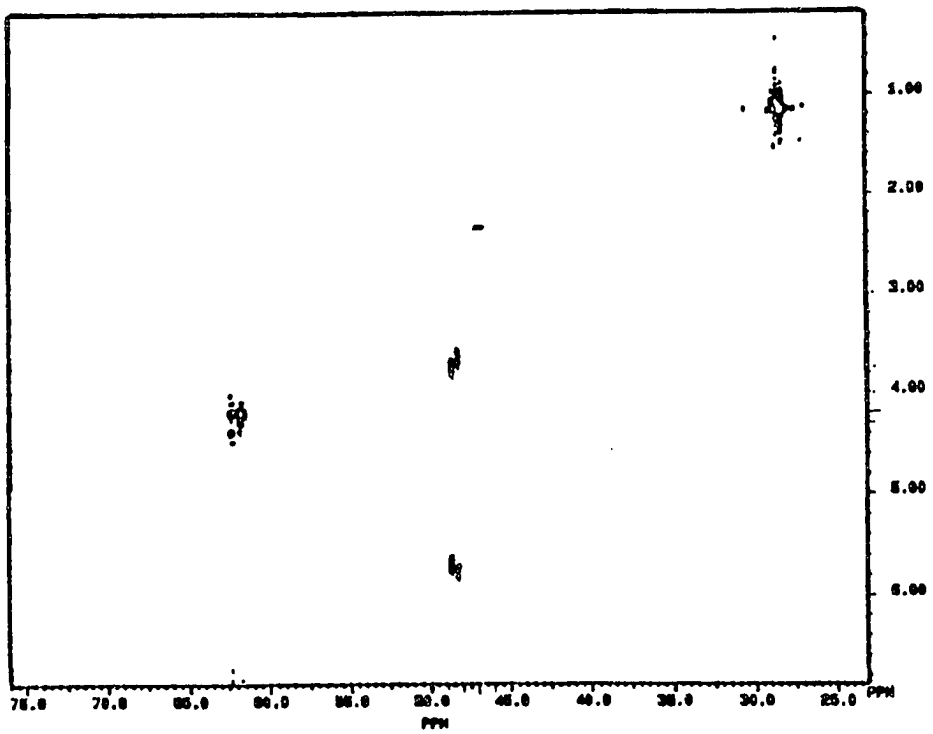

Figure 2.18. Contour plot of 200/50 MHz ^{1}H-^{13}C correlated spectrum of macrocycle **2a** measured in $CDCl_3$ at 250K.

In the low-temperature spectrum of macrocycle **2a** recorded at 250K and illustrated in Figure 2.19, the broad signals assigned to the benzyl protons in the room temperature spectrum centered at δ5.7 and δ3.7 appear as two sets of equal intensity AB systems. These signals coalesce at room temperature and finally at 375K the individual A and B proton signals coalesce. Temperature-dependent behavior is also noted for the N-CH_2-N protons assigned to the triazone portion of the molecule at δ4.2. At low temperature the latter signal appears as two sets of AB systems. In addition, two sets of approximately equally intense tert-butyl resonances appear at δ1.14 and δ1.27 in place of the one signal at δ1.10 in the room temperature spectrum.

Similarly, in the low-temperature ^{13}C spectrum, as indicated in Table 2.7, all signals are doubled. For example, the signals assigned to the benzylic carbons at δ48.8 and at δ62.4 for the N-CH_2-N carbons at room temperature (see Figure 2.20) now appear at δ48.3, δ48.6 and at δ61.8, δ62.3, respectively (see Figure 2.21). This suggests the slow interconversion of two conformers on the NMR time scale.

At higher temperatures, as may be seen in Figure 2.22, coalescence of signals is observed in the ^1H NMR spectrum. In DMSO-d_6 solution at 375K the two broad signals at δ5.8 and δ3.7 have flattened into the baseline and a new

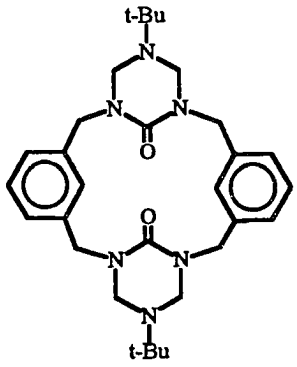

2a

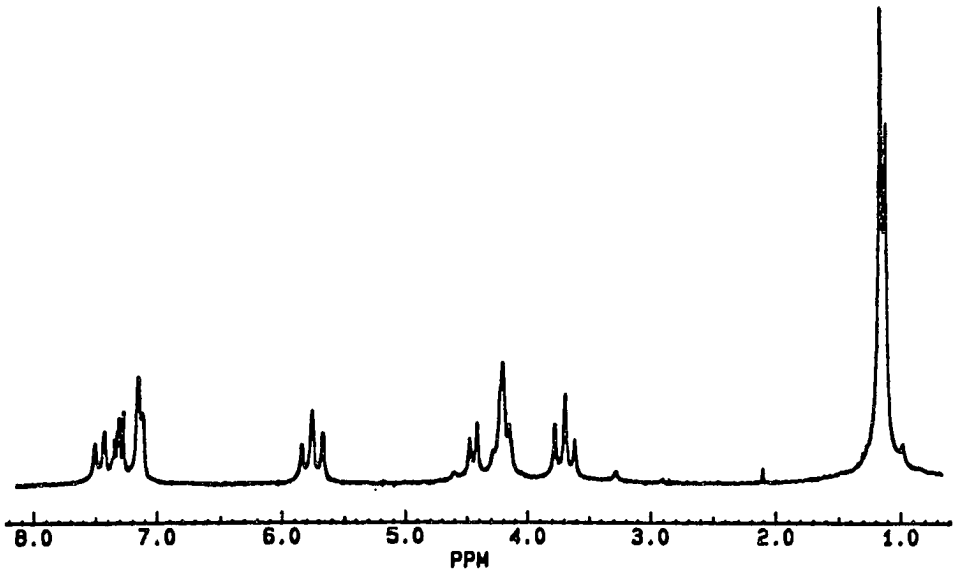

Figure 2.19. 200 MHz ^{1}H NMR spectrum of macrocycle **2a** measured in $CDCl_3$ at 250K.

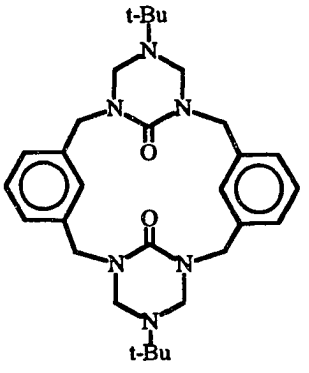

2a

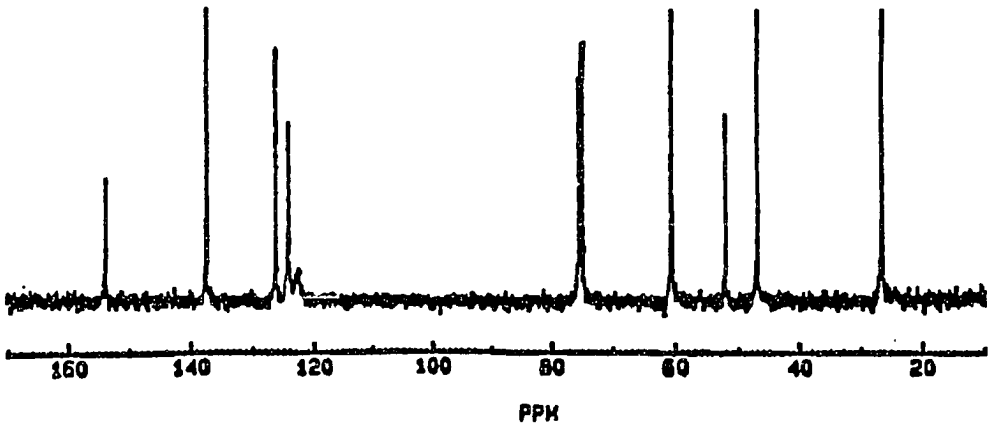

Figure 2.20. 50 MHz ^{13}C NMR spectrum of macrocycle **2a** measured in $CDCl_3$ at 300K.

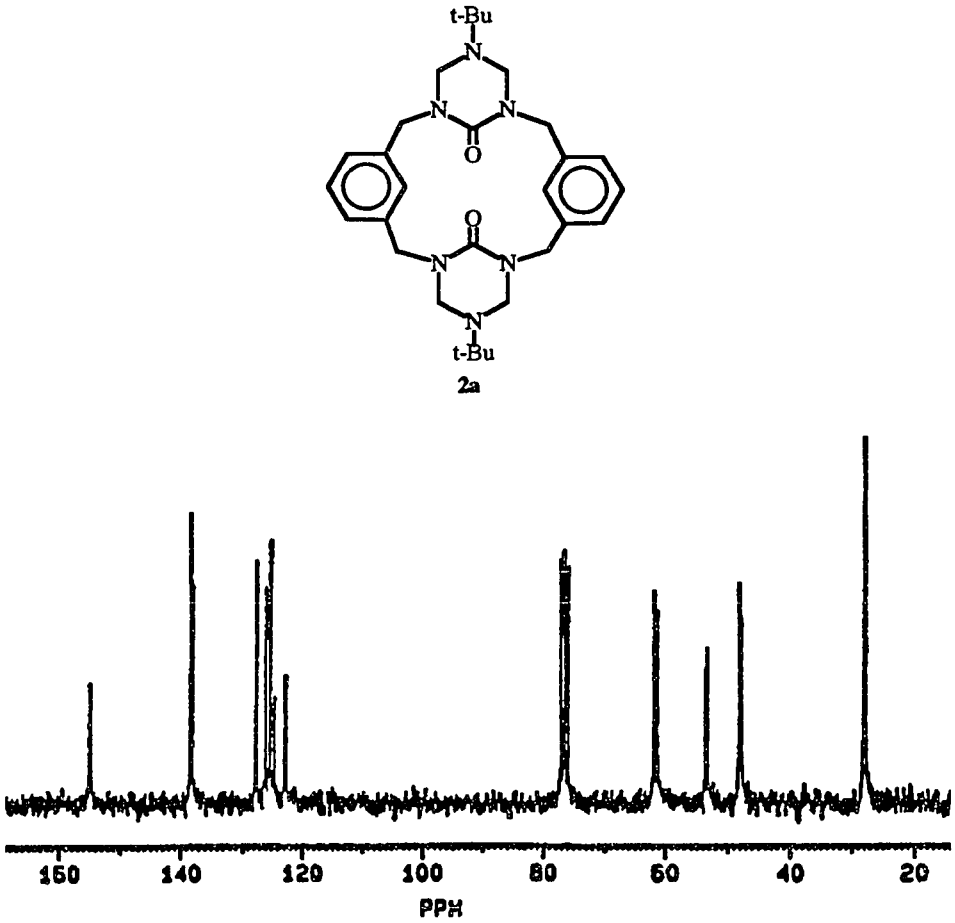

Figure 2.21. 50 MHz ^{13}C NMR spectrum of macrocycle **2a** measured in $CDCl_3$ at 250K.

broad signal begins to emerge at δ4.6. The other broad shoulder at δ4.8 has sharpened considerably. This coalescence process continues in DMSO-d_6 as the temperature is raised to 405K yielding a sharp signal due to the N-CH_2-N groups at δ4.2 and a much sharpened benzylic proton singlet at δ4.5.

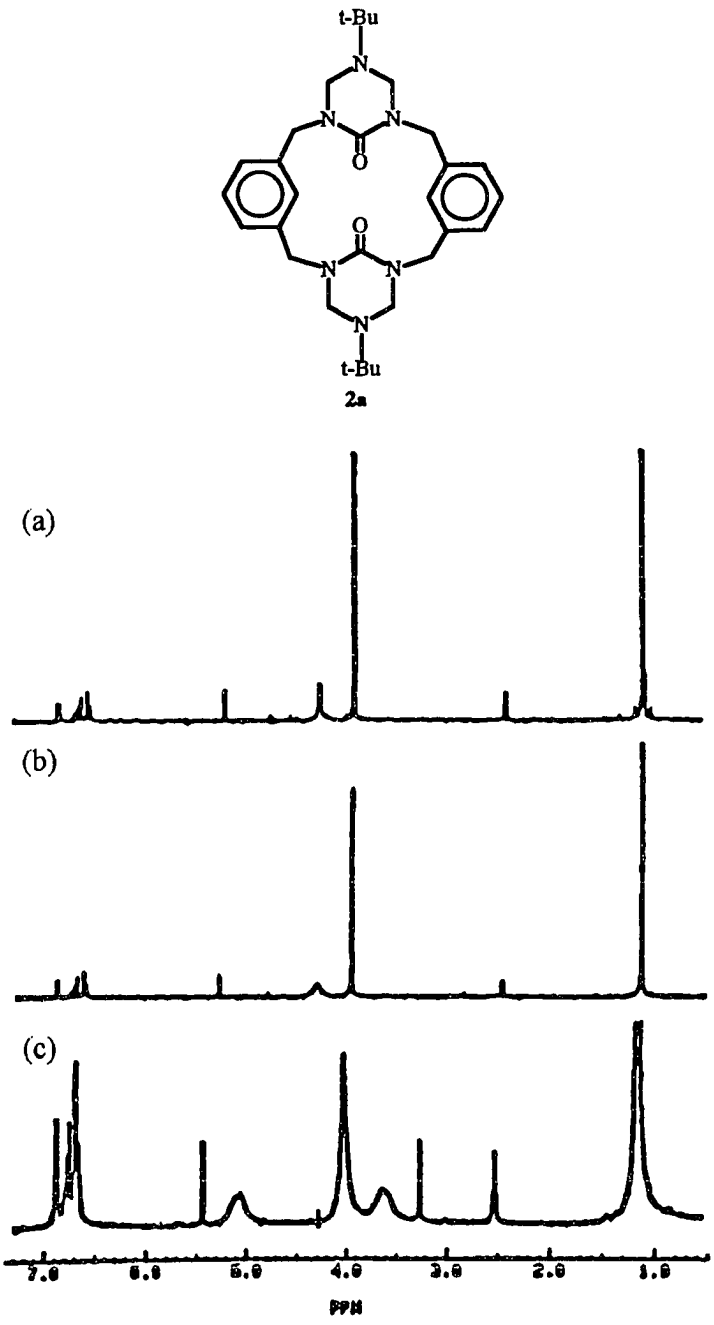

Figure 2.22. 200 MHz ^{1}H NMR spectra of macrocycle **2a** at (a) 405K (b) 375K and (c) 300K measured in DMSO-d_6.

The temperature dependence behavior observed in the ^{1}H and ^{13}C NMR spectra of macrocycle **2a** shows the ring system to be conformationally mobile. From the two equal intensity sets of signals for the tert-butyl, benzyl and the N-CH_2-N groups at low temperature, one may conclude that two approximately equally-populated conformations are present.

These NMR observations can be accommodated by a conformational equilibrium involving three species such as the *syn* and *anti* conformers shown in Figure 2.23. These resemble approximately the cone, partial cone and the 1,2-alternate forms familiar to calix[4]arene conformational analysis. The interconversion of the forms could conceivably come about by a process involving carbonyl oxygen through the annulus rotation that leads to the other conformation and averages the different heterocyclic methylene and benzylic protons equivalent on the NMR time scale. Consideration of molecular models suggests that this ring system should be sufficiently flexible to permit such rotation. Rotation of the t-butyl group through the center of the ring would also interconvert these conformers, but this process is deemed to be sterically more demanding with a higher energy barrier and hence less likely.

Alternatively, the conformational mobility of this system can be viewed in terms of the ease with which the C-1 carbons of the aryl units can pass

through the annulus. Such a process illustrated in Figure 2.24 would lead to two different forms for a conformer having, for example, oppositely directed carbonyl groups as in the so-called partial cone and the 1,2-alternate forms.

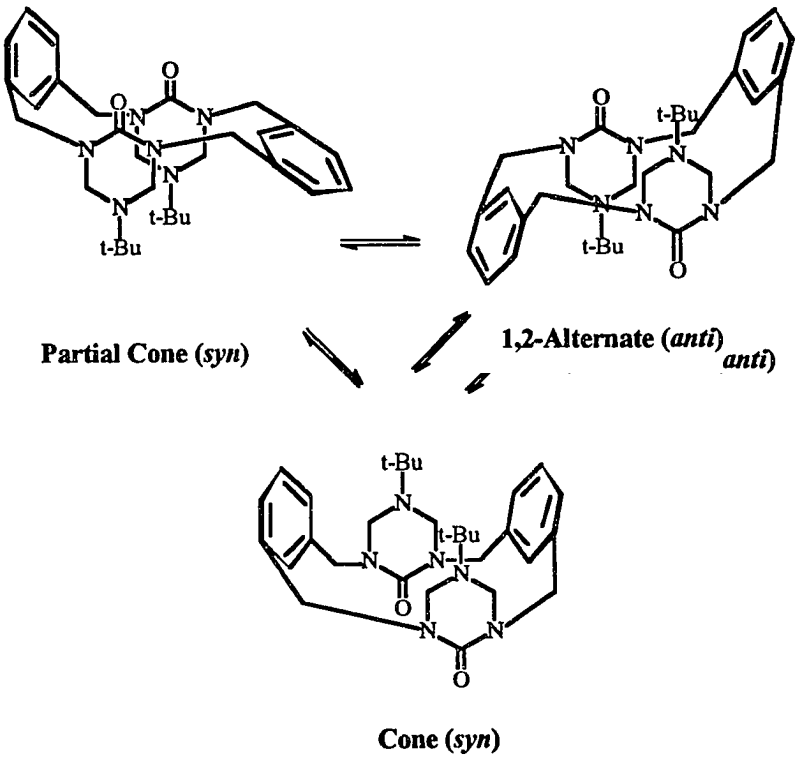

Figure 2.23. Conformational equilibria in macrocycle **2a**.

In this connection it is interesting to note in the ambient temperature spectrum the broad appearance of the C-1 carbon resonances. Such rotation (i.e., aryl C-1 through the annulus rotation) could also interconvert the forms.

Based on the x-ray structure we propose that at low temperature **2a** exists as a slowly interconverting mixture of *syn* and *anti* conformers, as shown in

Figure 2.25. This conformational equilibrium involving substantially equal amounts of the *syn* and *anti* forms agrees with the *anti* conformation observed in the solid state deduced from x-ray crystallography considerations.

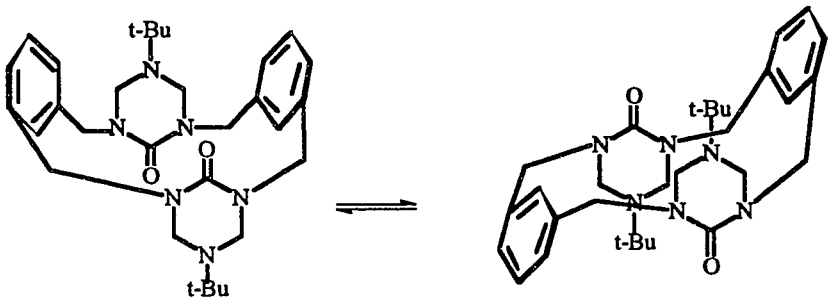

Partial Cone (*anti*) **1,2-Alternate (*anti*)**

Figure 2.24. Conformational equilibria in macrocycle **2a**.

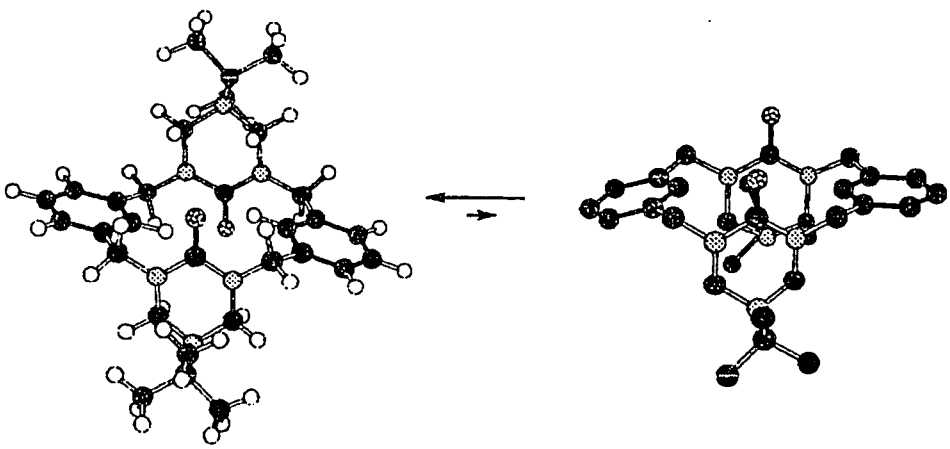

anti *syn*

Figure 2.25. Conformational equilibrium in **2a**. Hydrogen atoms in the *syn*-conformer were omittted for clarity.

In the case of macrocycles **2b** and **2c** the ^{1}H and ^{13}C NMR spectra are similarly consistent with the presence of two conformations. However, the two conformations are unequally populated. The ratio of the major to the minor conformation in these systems is about 10:1. The ^{1}H NMR spectra of **2b** and **2c** are essentially identical, attesting to similar conformations. The ^{1}H-^{1}H correlation data and assignments of resonance signals for ^{13}C-^{1}H correlations in macrocycles **2b** and **2c** are summarized in Tables 2.8 and 2.9, respectively.

Table 2.8. Correlated ^{1}H-^{1}H chemical shifts for macrocycles **2b** and **2c** measured in $CDCl_3$ at 300K.

2b	**2c**
$\delta^{1}H$-$\delta^{1}H$, ppm	**$\delta^{1}H$-$\delta^{1}H$, ppm**
7.47 / 7.00	7.28 / 3.75
7.00 / 6.86	6.80 / 2.30
5.91 / 3.40	5.82 / 3.36
5.67 / 3.30	5.64 / 3.30
4.90 / 4.30	4.90 / 4.32
4.70 / 3.76	4.68 / 3.75
4.30 / 3.76	4.28 / 3.75
3.76 / 3.58	3.75 / 3.30
3.62 / 3.26	

As may be seen in the ^{1}H NMR spectrum of macrocycle **2b** illustrated in Figure 2.26, the major conformation exhibits a single signal due to tert-butyl hydrogens and two singlets for the methoxy protons at δ2.8 and δ3.8. This indicates that the two heterocyclic ring units as a whole are in identical chemical environments, while the two aromatic rings are not. The benzylic hydrogens display two AB systems centered at δ3.3 and δ5.6 and at δ3.8 and δ4.7. There are also what appear to be two AB patterns due to the heterocyclic ring methylene hydrogens. These spectral features would arise if the two aromatic rings were oriented in different directions thereby, placing the benzyl or N-CH_2-N groups on one side of the ring in a different environment from the similar groups on the other half of the macrocyclic ring. The substantial difference in chemical shift of the two methoxy groups in **2b** ($\Delta\delta = 1$) clearly indicates different environments for these groups and at least one of these methoxy groups shows a chemical shift typical of the resonance expected for anisole.[65] This substantial chemical shift difference can be accounted for by the interaction of the methoxy group of one aromatic unit with the transannular π-cloud of an approximately perpendicular facing aromatic ring. This interaction places the methoxy unit in a shielding environment and results in an upfield shift. The ^{1}H NMR spectrum of **2c** also

Table 2.9. Carbon/Hydrogen assignments of resonance signals in macrocycles **2b** and **2c** measured in $CDCl_3$ at 300K.

	2b		2c	
C/H assignment	**δ^1H, ppm**	**δ^{13}C, ppm**	**δ^1H, ppm**	**δ^{13}C, ppm**
CH_3-(t-butyl)	1.20	29.0	1.21	1.21
CH_3-(aryl)			2.23 2.28	29.7 20.6
Ph-CH_2	3.30 5.67 } J= 14.7 Hz	45.7	3.30 5.64 } J= 14.0 Hz	45.7
	4.70 3.76 } J= 14.2 Hz	47.8	4.68 3.75 } J= 14.5 Hz	47.7
C_q-(t-butyl)		54.0		54.0
CH_3O	2.86 3.77	60.8 60.3	2.86 3.74	60.7 60.4
N-CH_2-N	3.76 3.70 } J= 12.0 Hz	61.4	3.75 3.60 } J= 12.0 Hz	61.4
	4.90 4.30 } J= 12.3 Hz	65.7	4.90 4.32 } J= 12.3 Hz	65.7
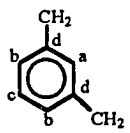				
C_a		157.7 159.3		157.1 159.1
C_b	7.02 7.46		7.27 6.81	134.1 131.4
C_c	6.70 7.02	130.9 133.7		132.4 131.1
C_d		132.4 131.1		131.8 130.7
C=O		155.3		155.4

shows the same features (see Figure 2.27). The two methoxy signals in **2c** are widely dispersed and appear at δ2.9 and δ3.8 indicating a conformation that

places these groups in rather different environment. This reasoning is further reinforced by the appearance in the spectrum of two singlets for non-equivalent aryl methyl groups at δ2.20 and δ2.25.

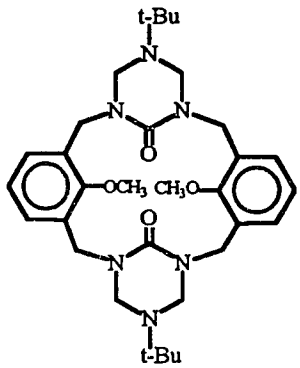

2b

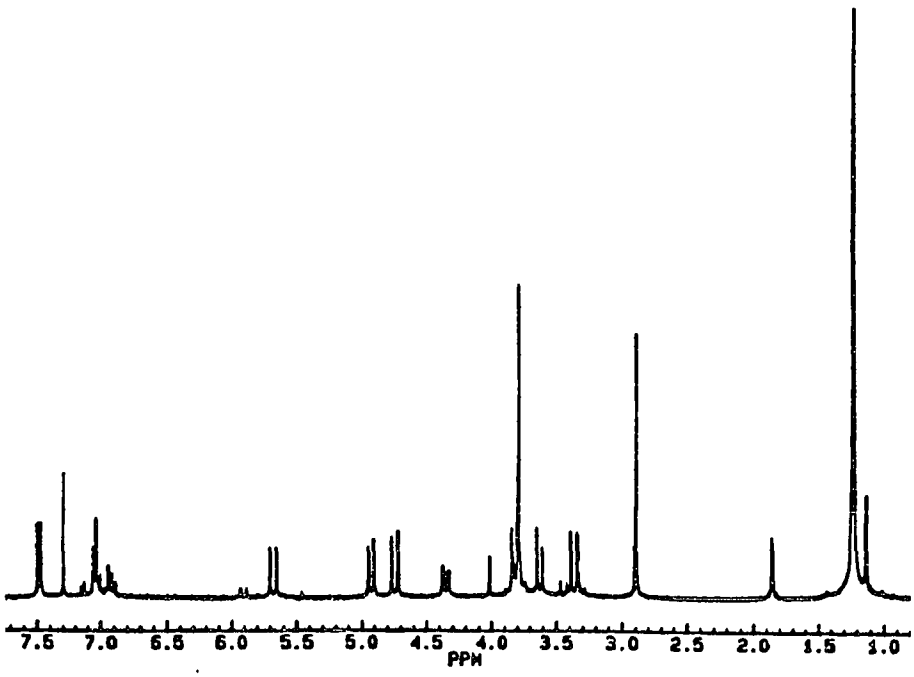

Figure 2.26. 300 MHz ^{1}H NMR spectrum of macrocycle **2b** measured in $CDCl_3$ at 300K.

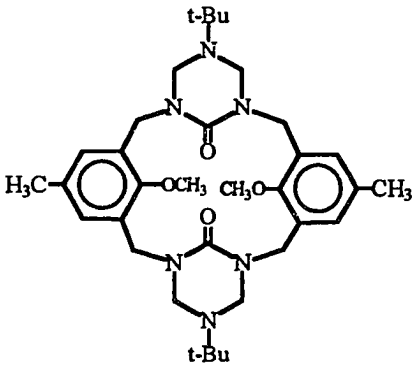

2c

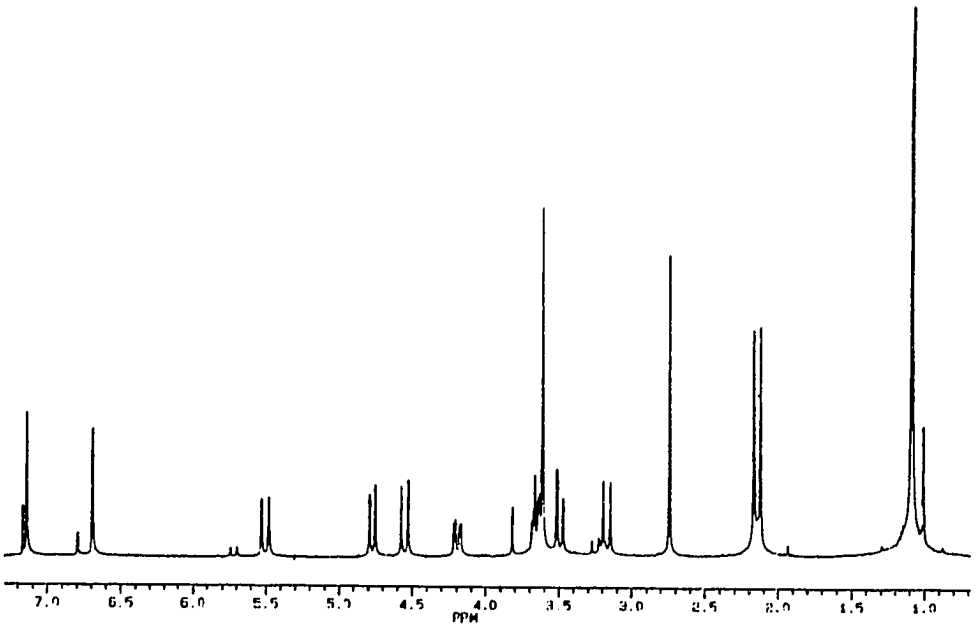

Figure 2.27. 300 MHz ^{1}H NMR spectrum of macrocycle **2c** measured in $CDCl_3$ at 300K.

Based on these observations, it may be inferred that the major conformations for both macrocycles **2b** and **2c** at room temperature in $CDCl_3$

solution are partial cone (*syn*) conformers shown in Figure 2.28. Less rigorously based, but reasonable, the presence in this equilibrium of the minor conformation represented as the *anti* form. This is supported by the presence of the methoxy signal present at δ4.0. Although the difference in chemical shift is evidently substantially less than in the *syn* form. In principle, this equilibrium would be conceptually the same as that postulated for **2a** except that the stability of the *syn* and *anti* forms differ significantly.

On the other hand, the combination of ^{1}H and ^{13}C NMR spectra of macrocycles **2b** and **2c** do not permit the definitive assignment of the *anti* conformer in the minor species present. This conformer would require two tert-butyl resonances which in addition to a minor set of aromatic methyls are not obvious in the ambient temperature spectra. An alternative explanation that can not be dismissed is that the minor conformation here is due to one or the other of species that resemble a distorted cone, 1,2-alternate or something intermediate between these forms. A more certain identification of the minor conformer is for the present hindered by the severely overlapping signals in the ^{1}H NMR spectra as well as the small quantity of material available for study.

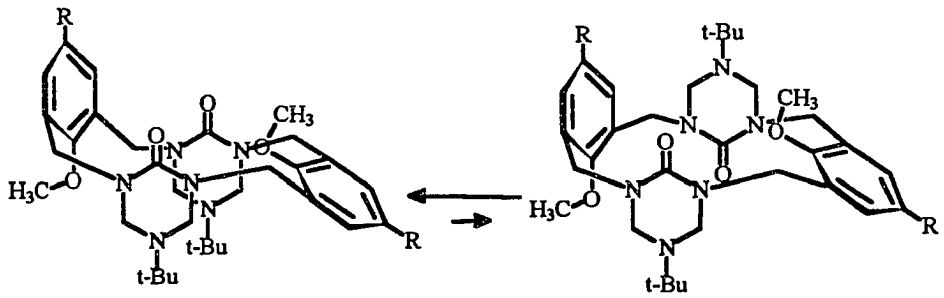

Partial Cone (*syn*) **1,2-Alternate (*anti*)**

2b: R=H
2c: R=CH$_3$

Figure 2.28. Conformational equilibrium showing major (*syn*) and possible minor (*anti*) conformers for macrocycles **2b** and **2c** in $CDCl_3$.

The NMR spectral results commensurate with the x-ray crystallographic conclusions that lead to the assignment of the major conformation as the partial cone-like (*syn*) conformer. This conformation is also consistent with the structure inferred in $CDCl_3$ solution where the ^1H NMR chemical shifts found for one of the methoxy groups in both **2b** and **2c** were found to be unusually shielded (i.e., δ2.7 ppm).

Another class of urea-based calixarene analogs that has been studied in this work is derived from imidazolidone. The ^1H NMR spectrum of macrocycle **8** at room temperature in $CDCl_3$ also exhibits broad signals at δ5.2, δ3.8 and δ3.3 with an intensity ratio of 1:1:2. By analogy with macrocycle **2a** the signals at δ5.2 and δ3.8 are assigned to the benzylic

protons and the other signals at δ3.3 to the heterocyclic ring methylene groups. The ^{1}H NMR spectrum is illustrated in Figure 2.29.

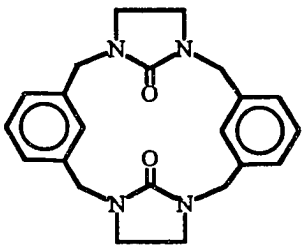

8

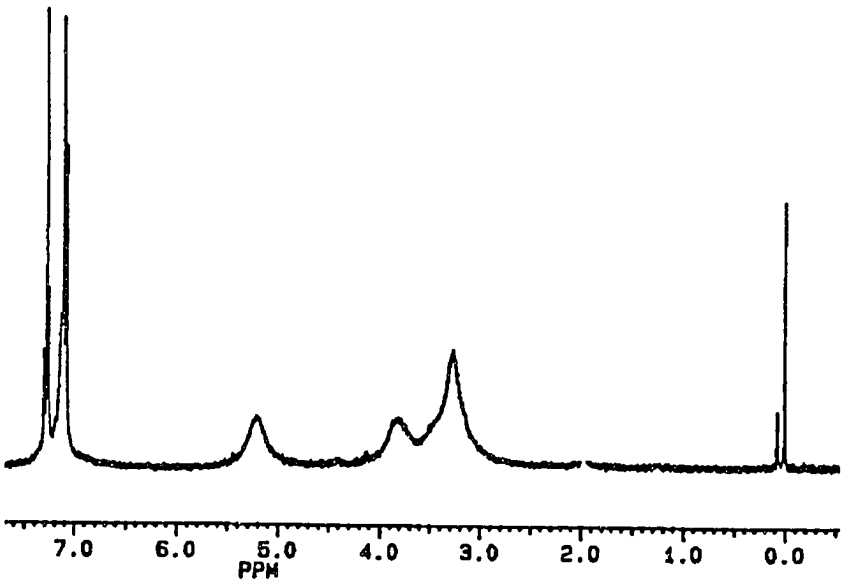

Figure 2.29. 300 MHz ^{1}H NMR spectrum of macrocycle **8** measured in $CDCl_3$ at 300K.

The complete carbon/hydrogen assignment of resonance signals in macrocycle **8** is summarized in Table 2.10.

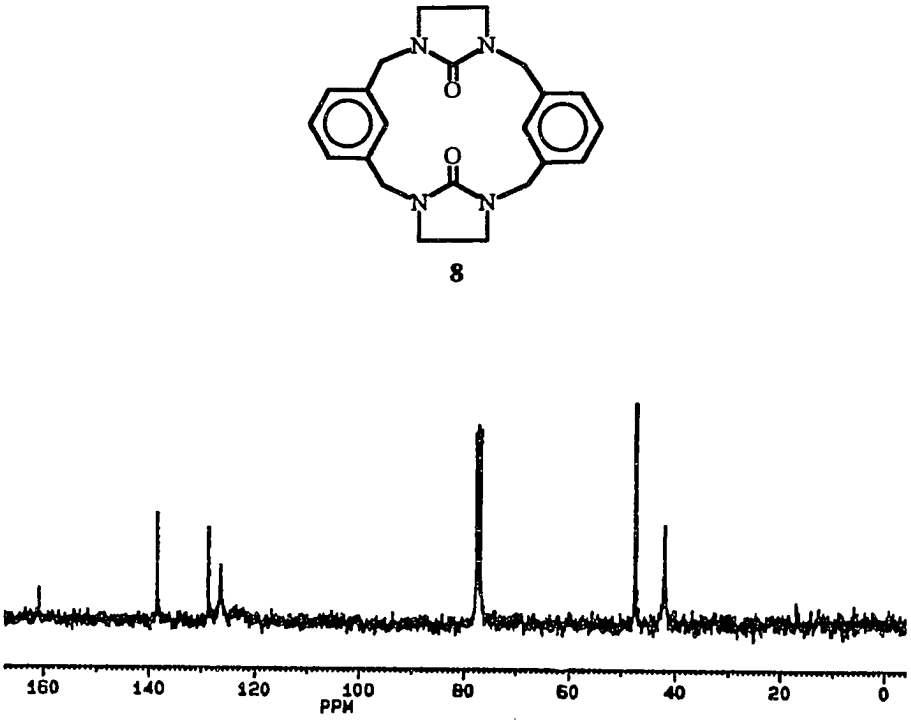

8

Figure 2.30. 75 MHz ^{13}C NMR spectrum of macrocycle **8** measured in $CDCl_3$ at 300K.

The room temperature ^{13}C NMR spectrum exhibits individual and sharp signals for the benzylic carbons at δ47.2 and at δ41.8 for the N-CH_2-CH_2-N carbons. This ^{13}C NMR spectrum is illustrated in Figure 2.30. Attention should also be called to the broad signal assigned to the aryl C-1 carbon resonance.

At low-temperature both the ^{1}H and ^{13}C NMR spectra indicate the existence of a slowly interconverting conformational equilibrium similar to

that of macrocycle **2a**. In the ^1H NMR spectrum, shown in Figure 2.31 the broad signals previously assigned to the benzylic protons in the regions of δ5.2, δ3.8 appear as two sets of equal intensity AB systems. One A_2B_2 system is also noted for the N-CH_2-CH_2-N protons.

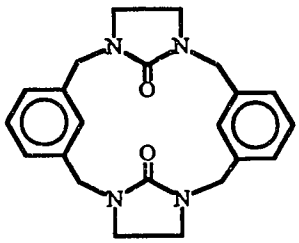

8

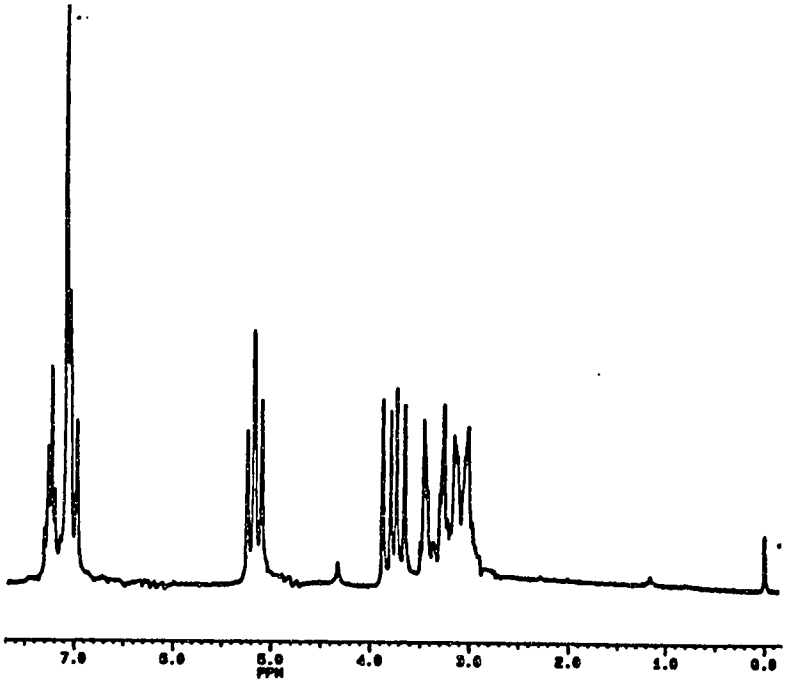

Figure 2.31. 200 MHz ^1H NMR spectrum of macrocycle **8** measured in $CDCl_3$ at 250K.

Analogously, in the low temperature ^{13}C NMR spectrum all signals are doubled. For example, the signals assigned to the benzylic carbons at δ47.2 and the N-CH_2-CH_2-N carbons at δ41.8 in the room temperature ^{13}C NMR spectrum now appear at δ46.9, δ46.7 and at δ41.7, δ41.0, respectively (see Figure 2.33). This reinforces the earlier conclusion regarding the slow interconversion of the conformers on the NMR time-scale. Moreover, from the ratios in the spectra it may be concluded that the two conformers involved have comparable stabilities.

By analogy with **2a** with which **8** is very closely related in structure and apparent NMR behavior, it may be postulated that a similar equilibrium between *syn* and *anti* forms exists. This is illustrated in Figure 2.32.

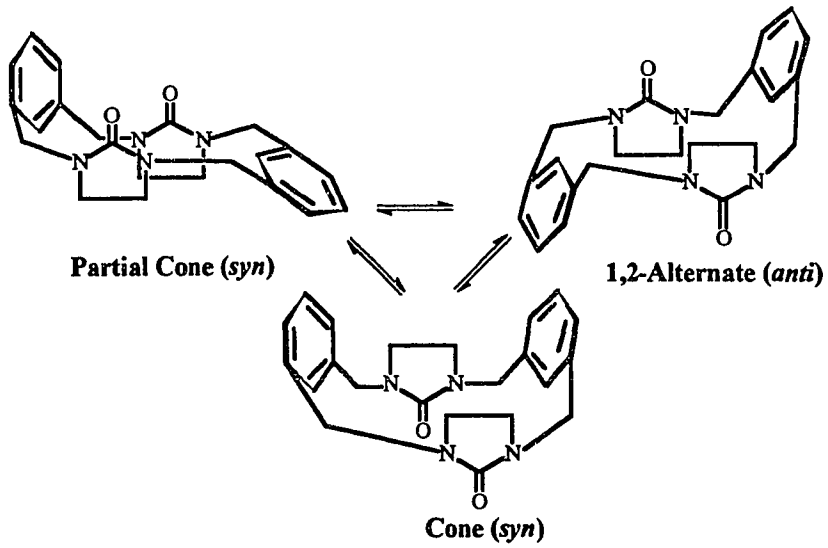

Figure 2.32. Conformational equilibria in macrocycle **8**.

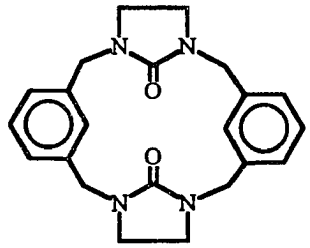

8

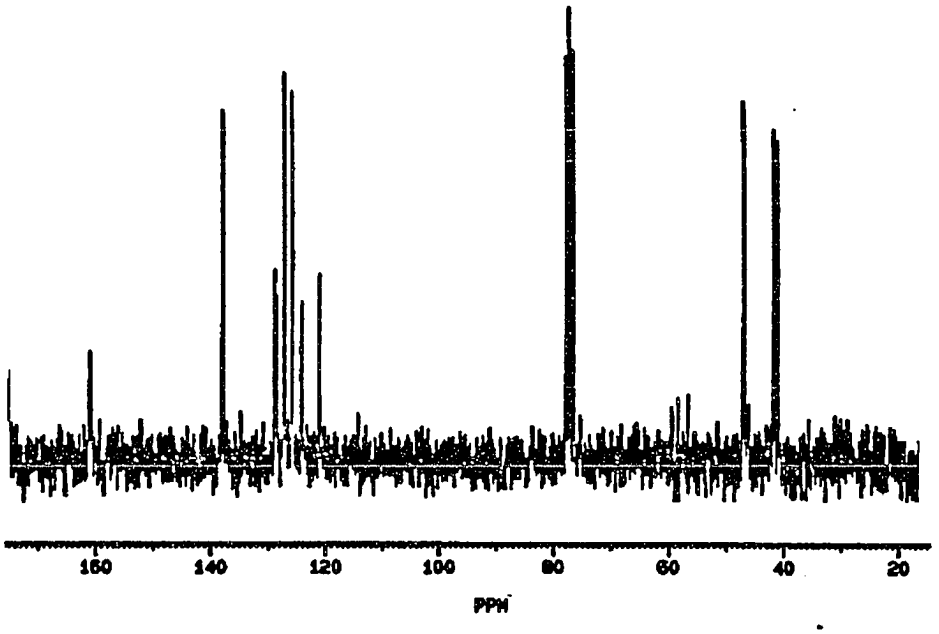

Figure 2.33. 50 MHz ^{13}C NMR spectrum of macrocycle **8** measured at 250K measured in $CDCl_3$.

Table 2.10. Carbon/Hydrogen assignments in macrocycle **8** measured in $CDCl_3$ at 300K and 250K.

	300K		250K	
C/H assignment	**δ^1H, ppm**	**δ^{13}C, ppm**	**δ^1H, ppm**	**δ^{13}C, ppm**
N-CH_2CH_2N	3.30(br)	41.8	3.10 3.34	41.0 41.7
Ph-CH_2 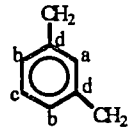	3.80(br) 5.20(br)	47.2	3.68 5.11 J = 15.6 3.82 5.21 J = 15.3	46.7 46.9
C_a	7.13 complicated multiplet	123.3	7.10 complicated multiplet	120.9 123.9
C_b		126.3		125.6 126.9
C_c		128.5		128.4 128.6
C_d		139.4		137.6 137.7
C=O		160.7		160.9 160.7

2.7. Confirmation of Spectral Assignments in Macrocyles 2b and 2c

In order to eliminate any ambiguity and verify the signal assignments in the ^{1}H NMR spectra of macrocycles **2b** and **2c**, the benzyl labeled-d_8 analog **10** of macrocycle **2b** was prepared.

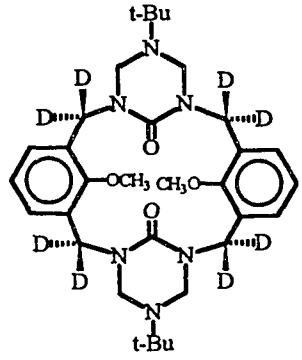

10

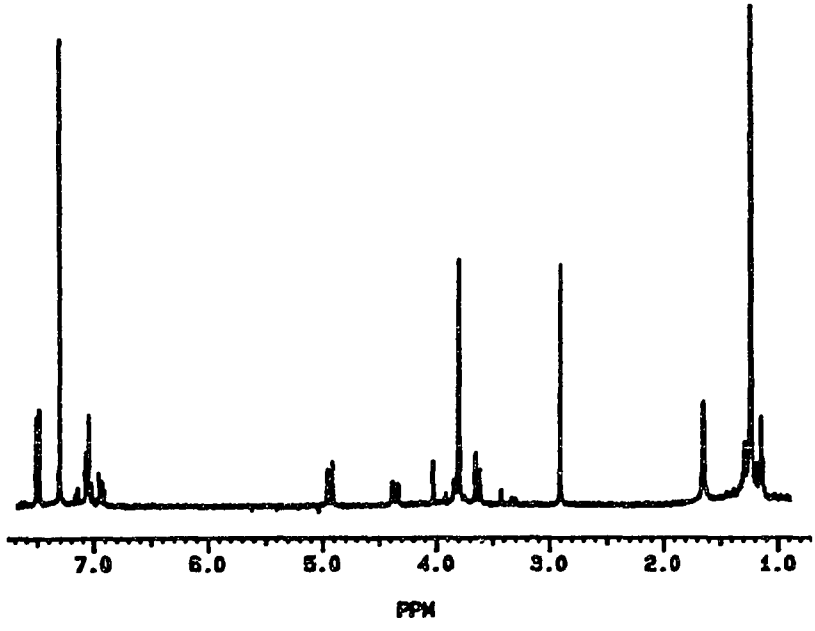

Figure 2.34. 300 MHz ^{1}H NMR spectrum of macrocycle **10** measured in $CDCl_3$.

As may be seen from the ^1H NMR spectrum, illustrated in Figure 2.34, the deuterated analog **10** exhibits a methyl resonance for the tert-butyl group atδ1.2. Two AB patterns centered at δ3.6, δ4.9 (J= 12 Hz) and at δ3.8, δ4.3 (J = 15 Hz) are assigned to the N-CH_2-N protons. Two methoxy signals appear at δ3.8 and δ2.9. Clearly, the absence of signals at δ3.3 and δ5.6 and at δ3.8 and δ4.7 are consistent with and confirms the original assignment of the benzylic and triazone ring methylene protons in **2b**.

2.8. Solvent effects and Conformational Equilibria

It is well-known that NMR chemical shifts of nuclei in organic molecules are sensitive to the environment surrounding them. This environment is a composite of the chemical and/or stereochemical structure of the molecule as well as the solvent medium in which it is dissolved. Solvent effects and their influence on NMR chemical shifts may be separated into two categories (a) specific and (b) non-specific. Hydrogen-bonding, protonation, molecular association and ionic interactions are examples of the former type while the latter which are produced especially by electronic interactions between the dipole moments of the solute and solvent molecules include van der Waals effects, neighboring anisotropic susceptibility and electric fields effects. Changes in solute NMR chemical shifts induced by different solvents are a

physical effect of the latter and are sensitive indicators of molecular surrounding. Analysis of the solvent-induced chemical shift changes observed for these calixarene analogs should provide insight into the nature and geometric structure of these molecules in solution.

Substances dissolved in aromatic solvents generally give resonance signals at higher fields than when dissolved in aliphatic solvents. This is attributed to the time-dependent association of the anisotropic fields around the aromatic ring with the substrate.[69] Bauer and Gutsche[57,58] used the ASIS technique to study the interaction of calixarenes with toluene and chloroform. They concluded that in non-polar solvents such as chloroform, toluene, benzene, bromobenzene and carbon disulfide the barrier to conformational interconversion increases in going from bromobenzene to chloroform. Similarly, in more polar (i.e., high dielectric) solvents such as acetone and acetonitrile a significant decrease in the conformational interconversion is typically observed and this becomes particularly pronounced in basic, hydrogen-bonding solvents such as pyridine. This difference was attributed to the differing abilities of the calix[4]arene to form endo-calix (i.e., binding of the solvent in the cavity of the calixarene) complexes with the solvent.[57,58]

A study of solvent-induced shifts (ASIS) was initially undertaken to simplify overlapping resonance signals. In addition, solvent effect studies provided an opportunity to probe changes in the conformational equilibria arising from the interaction between the solvent and the urea-based-calixarene analogs. A profound change was observed when the ^{1}H NMR spectrum of **2a** was measured in either $CDCl_3$-C_6D_6 (3:1) and toluene-d_8 at 250K. The ^{1}H NMR spectral changes observed for **2a** in $CDCl_3$ and $CDCl_3$:C_6D_6 (3:1) or toluene-d_8 at 250K are shown in Figures 2.35 and 2.36, respectively.

The ^{1}H NMR spectrum of **2a** measured in $CDCl_3$ solution indicated the presence of two conformational isomers in equal amounts. The ratios of the two conformers in the presence of increasing amounts of C_6D_6 changed to 2:1 and 5:1, respectively (see Figure 2.35). However, when the spectrum of macrocycle **2a** was measured in toluene-d_8 a more pronounced effect on the population of conformational isomers was observed (see Figure 2.36).

The ^{1}H NMR spectrum in toluene-d_8 is consistent with the spectral pattern expected for the cone and the 1,3-alternate conformations. This is evident by the presence of a single AB system for the benzyl- and the heterocyclic-methylene protons at 240K. It appears that intermolecular dipole-dipole interactions between the associated host and solvent molecules lead to a

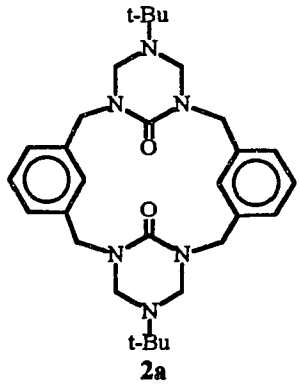

2a

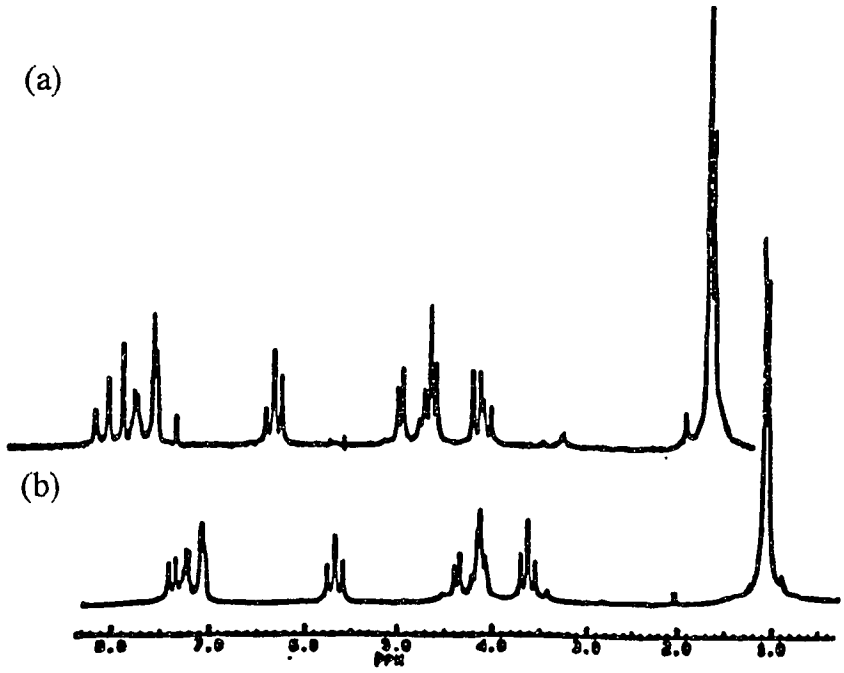

Figure 2.35. 200 MHz ^{1}H NMR spectra of macrocycle **2a** measured in (a) $CDCl_3$:C_6D_6 (3:1) and (b) $CDCl_3$ at 250K.

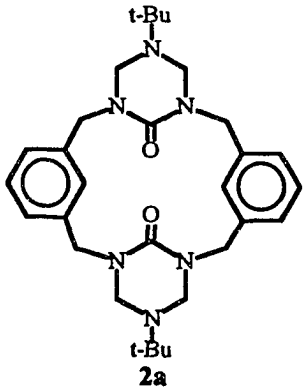

2a

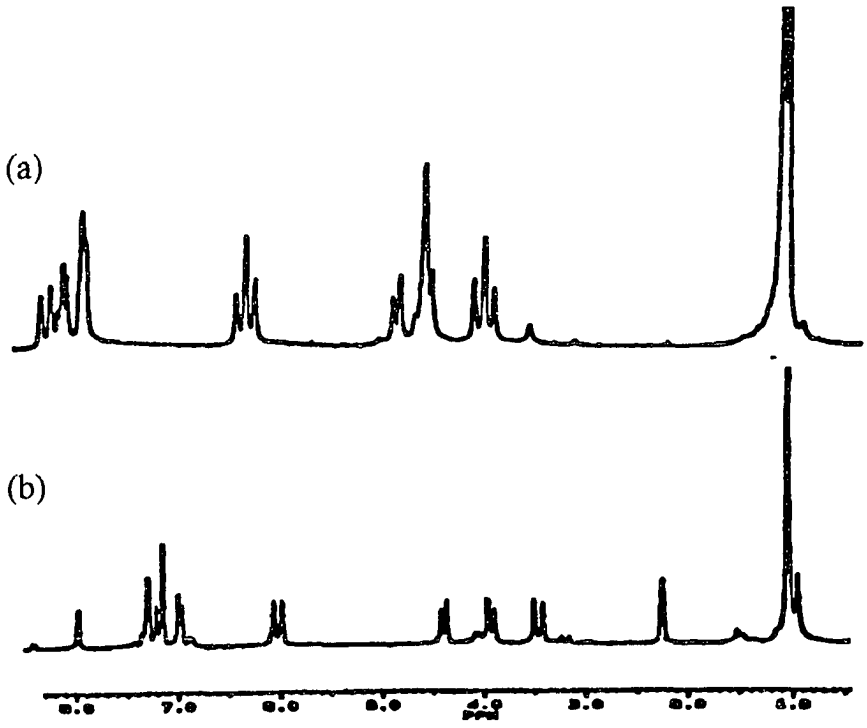

Figure 2.36. 200 MHz ^{1}H NMR spectra of macrocycle **2a** measured in (a) $CDCl_3$ and (b) toluene-d_8 at 240K.

complex formation in which one orientation of the host molecule is more favored than the other. This gives rise not only to pronounced shifts in the resonance frequencies of the most affected proton (e.g., see tert-butyl signal ratios in both solvent systems) but also to major changes in the conformer populations. This behavior could be explained in terms of preferential stabilization of the conformer with the higher dipole moment (i.e., cone or 1,3-alternate conformations, see Figure 2.37).

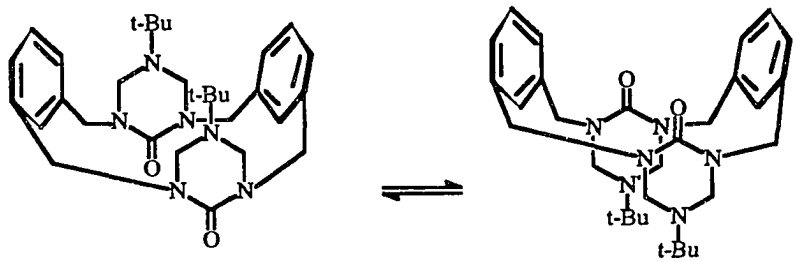

Figure 2.37. Possible conformations of macrocycle **2a**.

The ^{1}H NMR spectrum of macrocycle **2b** measured in C_6D_6 solution is illustrated in Figure 2.38. The major NMR spectral change observed, when compared to the $CDCl_3$ NMR spectrum is the upfield shift in the methoxy signals. The methoxy signals for **2b** appear at δ2.8 and δ3.8 in $CDCl_3$ and at δ3.0 and δ3.3 in C_6D_6. No other change in the chemical shifts of either the benzyl- or the heterocyclic ring protons was observed for **2b** (see Figure 2.38). The ^{1}H NMR spectrum of **2c** also showed the same upfield shift of

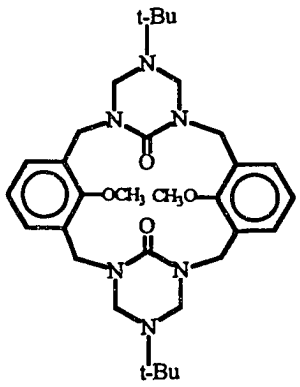

2b

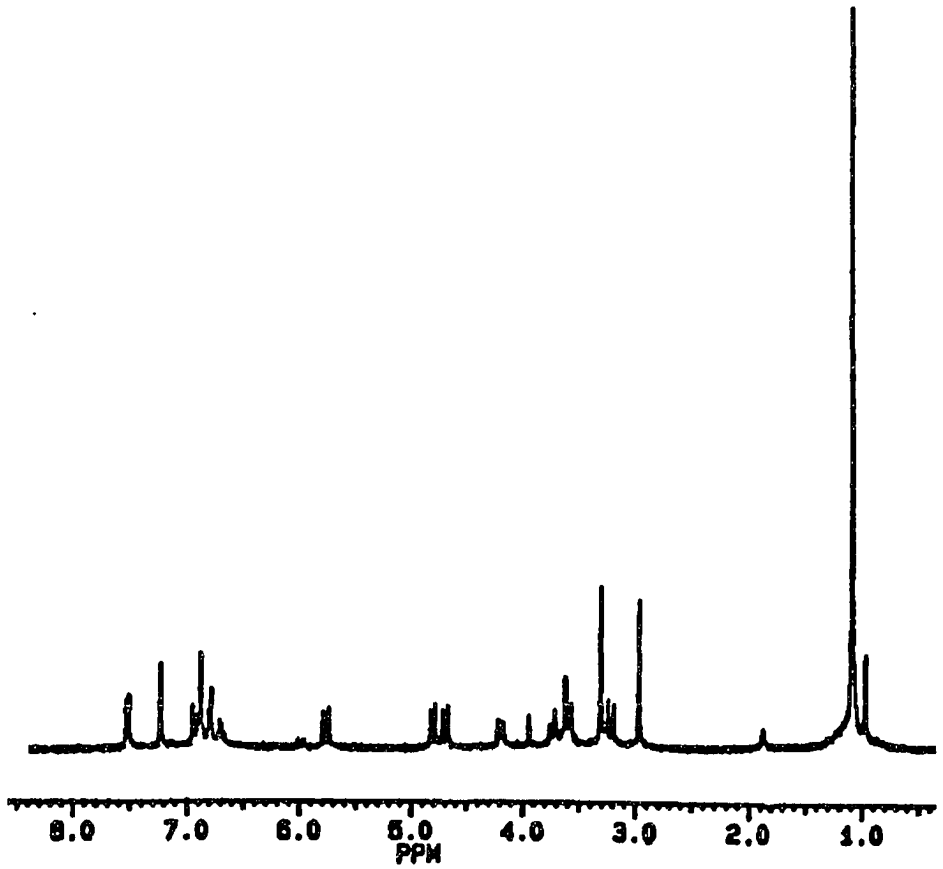

Figure 2.38. Anisotropic effect of C_6D_6 on the methoxy groups in macrocycle **2b**.

both methoxy signals. Similarly, the methoxy signals for **2c** appear at δ2.9 and δ3.8 in $CDCl_3$ and at δ3.0 and δ3.1 in C_6D_6. The $CDCl_3$ spectrum also shows two singlets at δ2.20 and δ2.25 for the non-equivalent aryl methyl groups. The chemical shifts of these methyl signals are unaffected by the presence of C_6D_6.

Based on these NMR spectral results, it may be suggested that the major conformations for both **2b** and **2c** at room temperature in $CDCl_3$ and C_6D_6 solutions are similar and perhaps are best represented by the form illustrated in Figure 2.39. These macrocycles have dipole moments whose magnitudes depend sensitively on the prevailing conformation. It is therefore reasonable to expect that intermolecular macrocycle-solvent interaction may lead to a preferred conformation as appears to be the case with **2a**.

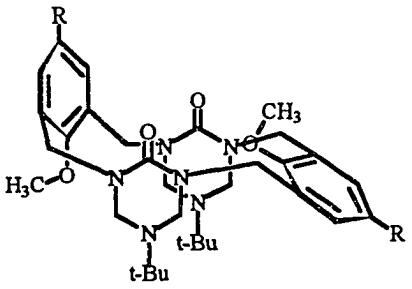

2b: R=H
2c: R=CH_3
Partial Cone (*syn*)

Figure 2.39. Dominant conformation of macrocycles **2b** and **2c** in the presence of non-polar solvents.

2.9. Results and Discussion of the NMR Spectra of the 18-Membered Urea-based Calix[4]arene Analogs

Ring enlargement of **2a** by two atoms gives the 18-membered macrocycle **3** whose room temperature ^1H NMR spectrum is illustrated in Figure 2.40. The ^1H NMR spectrum of macrocycle **3** similarly indicates the presence of two conformations in the ratio of 3:1 at ambient temperature.

The ^1H-^1H homonuclear and ^1H-^{13}C heteronuclear two-dimensional correlation spectra are shown in Figures 2.41 and 2.42 and summarized in Tables 11 and 12, respectively. The major conformer of macrocycle **3** exhibits a methyl resonance for the tert-butyl group at δ1.21. An AB pattern centered at δ3.2 and δ5.4 (J= 14.0 Hz) assigned to the benzyl protons. A second AB system at δ3.7 and δ4.0 (J = 10.8 Hz) is due to the N-CH_2-N protons and a singlet for the aromatic protons appears at δ7.09. The minor conformer shows a methyl resonance for the tert-butyl group at δ1.25. An AB pattern at δ3.5 and δ5.0 (J = 14.9 Hz) is assigned to the benzyl protons. A AB system at δ4.2 and δ4.3 (J = 10.6 Hz) due to the N-CH_2-N protons and a singlet at δ7.30 due to the aromatic protons.

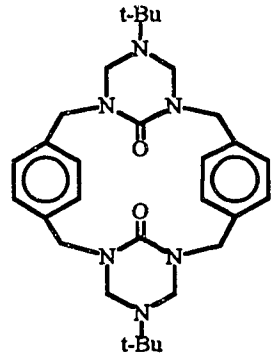

3

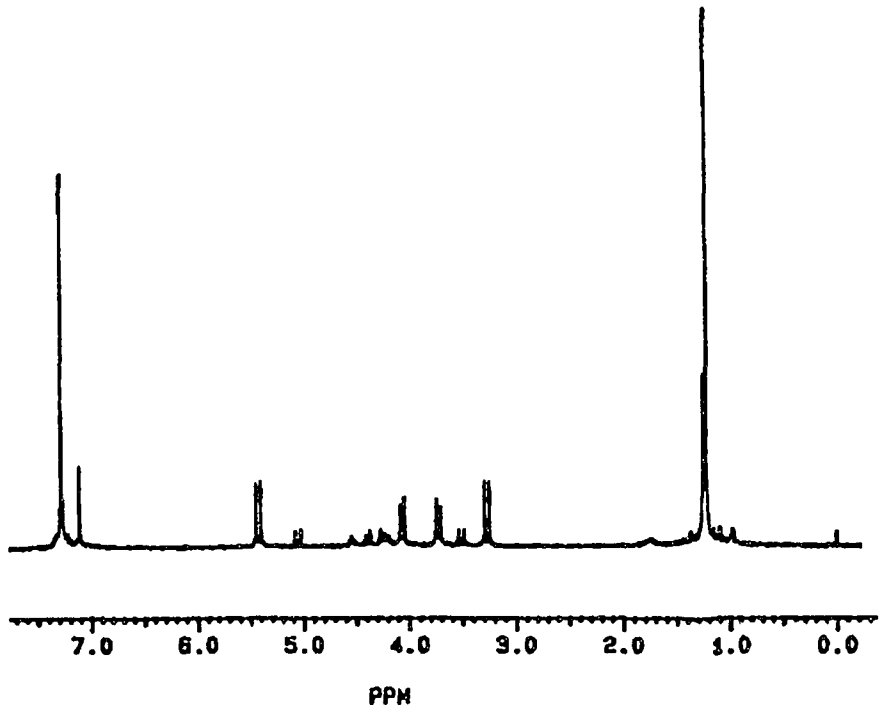

Figure 2.40. 300 MHz ^{1}H NMR spectrum of macrocycle **3** measured in $CDCl_3$.

Table 2.11. Correlated ^1H-^1H chemical shift in macrocycle **3** measured in $CDCl_3$.

δ^1H-δ^1H, ppm
3.30
5.44 / 3.73
5.00 / 3.73
4.22

Table 2.12. Carbon/Hydrogen assignments of resonance signals in macrocycle **3** measured in $CDCl_3$ at 300K.

Carbon/Hydrogen	δ^1H, ppm	$\delta^{13}C$, ppm
CH_3-(t-butyl)	1.21 1.25	28.5 28.7
Ph-CH_2	3.20, 5.40 J= 14.9 Hz 3.50, 5.00 J= 14.0 Hz	49.1 49.5
C_q-(t-butyl)		54.1 53.9
N-CH_2-N	3.70, 4.00 J= 10.8 Hz 4.20, 4.30 J= 10.6 Hz	61.8 63.4
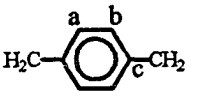		
C_a	7.09	127.8
C_b	7.30	128.8
C_c		137.3
C=O		157.0 156.6

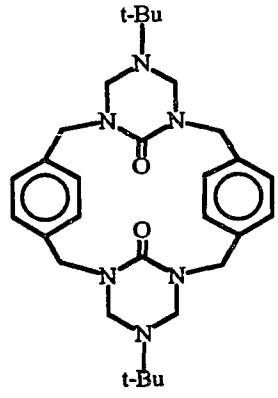

3

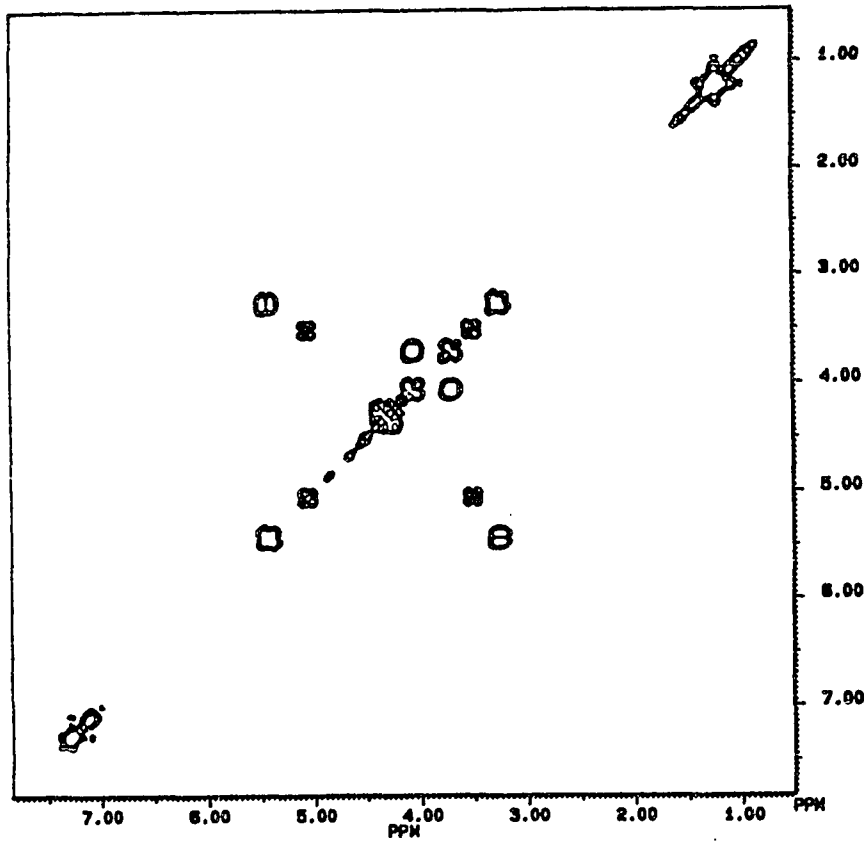

Figure 2.41. Contour plot of 300 MHz ^1H-^1H correlated spectrum of macrocycle **3** measured in $CDCl_3$ at 300K.

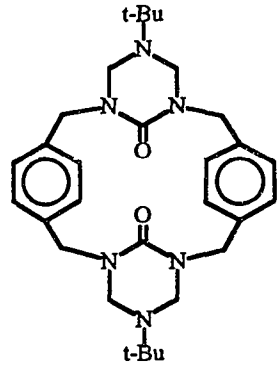

3

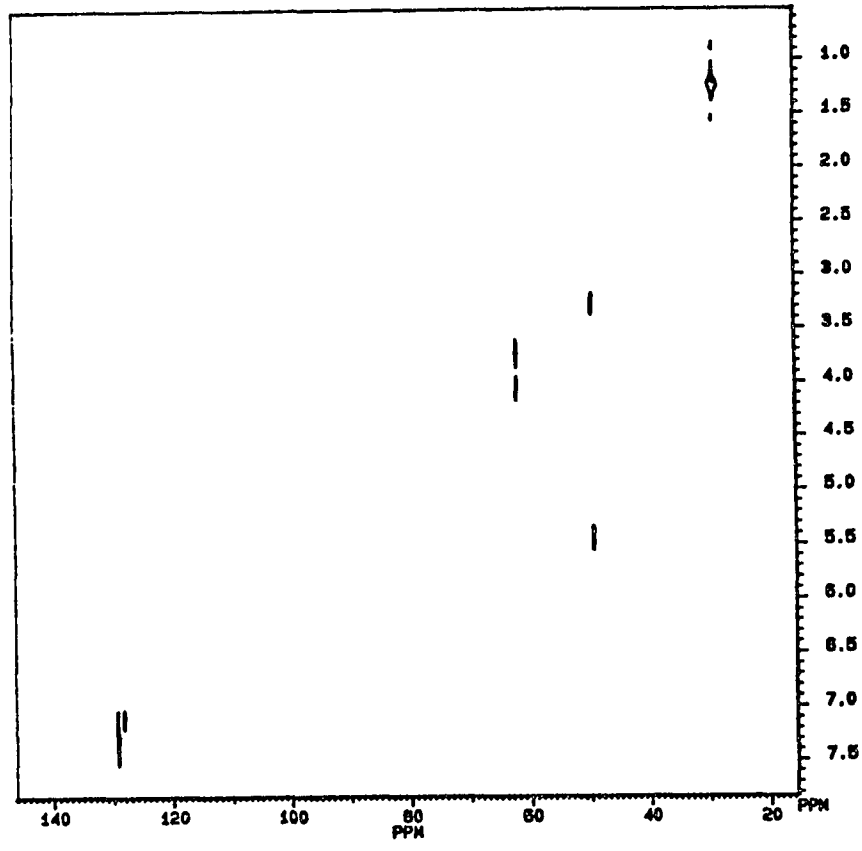

Figure 2.42. Contour plot of 75 MHz ^{1}H-^{13}C correlated spectrum of macrocycle **3** measured in $CDCl_3$ at 300K.

The ^{13}C NMR spectrum is also consistent with the presence of a major and minor conformation. For example, resonances due to the major conformer occur at δ28.7 (CH_3), δ49.1 (Ar-$\underline{C}H_2$), δ54.1 ($\underline{C}(CH_3)_3$), δ61.8 (N-$\underline{C}H_2$-N), and at δ157.0 (C=O), while the minor conformer exhibits signals at δ28.5 (CH_3), δ49.5 (Ar-$\underline{C}H_2$-), δ53.9 ($\underline{C}(CH_3)_3$), δ63.4 (N-$\underline{C}H_2$-N) and at δ156.6 (C=O). The aromatic region exhibits three carbon signals at δ127.8, δ128.8, and δ137.3 (see Figure 2.44), which also suggest the presence of more than one conformation.

Thus, these observations are consistent with the conformational equilibrium involving species **3** (*anti*) and **3** (*syn*) which interconvert presumably by passage of the carbonyl group through the annulus of the macrocycle (see Figure 2.43). Moreover, in contrast to macrocycle **2a** the ratio of these conformers remains unchanged in going from chloroform to aromatic solvents.

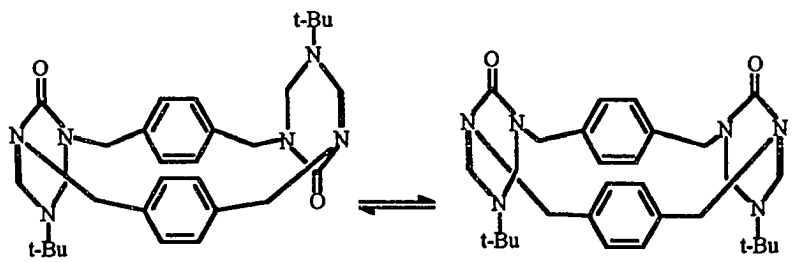

Figure 2.43. Conformational equilibria of macrocycle **3**.

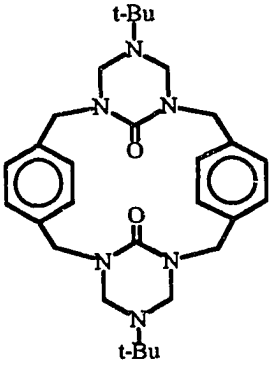

3

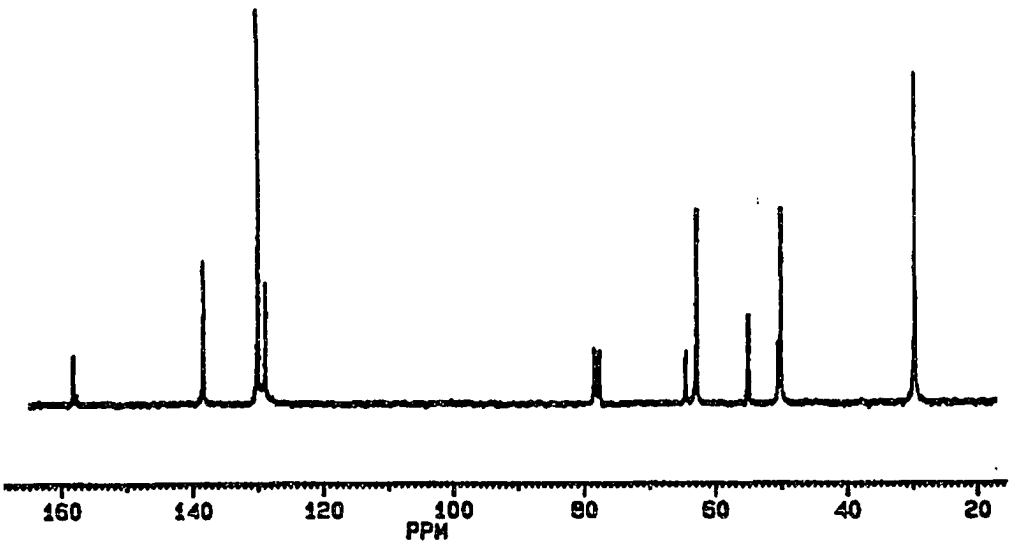

Figure 2.44. 75 MHz ^{13}C NMR spectrum of macrocycle **3** measured in $CDCl_3$ at 300K.

Crystals of **3** having sufficient quality for x-ray analysis have until now defied successful preparation. It is therefore unclear whether the **3** (*syn*) or **3** (*anti*) conformer is the dominant one in the solid state.

In the case of macrocycle **9** (i.e., the eighteen-membered macrocyle), where the 2-imidazolidone ring **4** was substituted for the triazone ring **1** somewhat different results are obtained. The room temperature ^{1}H NMR spectrum of macrocycle **9**, as illustrated in Figure 2.45, exhibits a well defined AB pattern at δ3.4 and δ5.0 (J = 14.1 Hz) assigned to the benzyl protons. One A_2B_2 system is also noted for the N-CH_2-CH_2-N protons at δ3.2 and δ2.6. The ^{1}H NMR spectrum of this macrocycle remains unchanged as the temperature is lowered to 250K.

The ^{13}C NMR spectrum displays two carbon resonances at δ48.0 and at δ40.4. These signals are assigned to the benzylic and the imidazolidone ring carbons, respectively. The ^{13}C NMR spectrum is shown in Figure 2.46. The chemical shift assignments of resonance signals are summarized in Table 2.13.

The behavior observed in the ^{1}H NMR spectrum of **9** can be interpreted in terms of (1) a single predominant conformation in solution or (2) a rapid exchange between two conformations (e.g., *syn* and *anti*-**9**) that is essentially

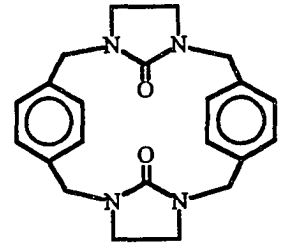

9

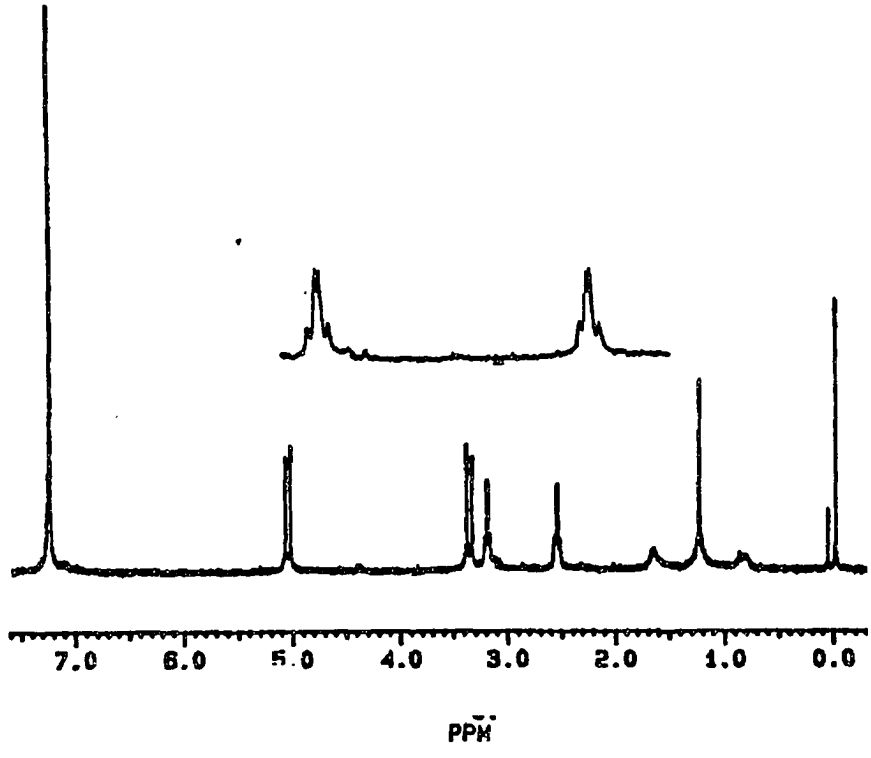

Figure 2.45. 300 MHz ^{1}H NMR spectrum of macrocycle **9** measured in $CDCl_3$ at 300K.

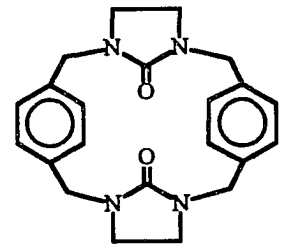

9

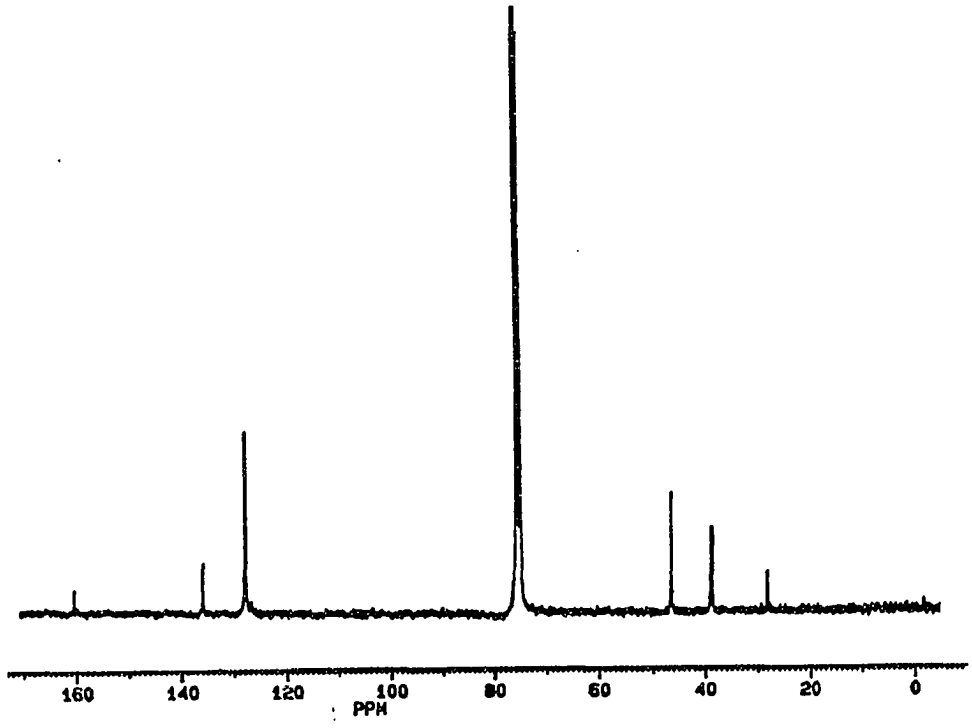

Figure 2.46. 75 MHz ^{13}C NMR spectrum of macrocycle **9** measured in $CDCl_3$ at 300K.

unaltered at 250K. Interestingly enough, the AM1 calculated heats of formation of conformer stability (i.e., *syn* and *anti*-**9**) (see Table 2.14) predicts the existence of two equally-populated *syn* and *anti* conformers in equilibrium. These conformations are illustrated in Figure 2.47.

Table 13. Carbon/Hydrogen assignments of resonance signals in macrocycle **9** measured in $CDCl_3$ at 300K.

C/H assignment	δ^1H (ppm)	δ^{13}C (ppm)
N-CH_2-CH_2-N	3.20 3.60	40.4
Ph-CH_2	3.40 5.00 } J= 14.1 Hz	48.0
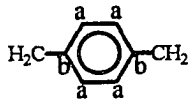		
C_a	7.26	129.5
C_b		137.5
C=O		162.0

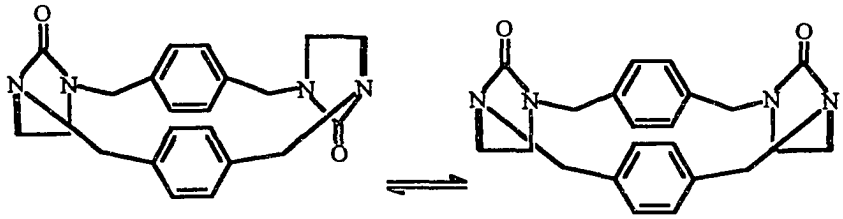

9(*anti*) **9**(*syn*)

Figure 2.47. Conformational equilibria in macrocycle **9**.

2.10. Calculations of Conformer Stability

The relative stabilities of the *syn* and *anti* conformations of the urea-based calixarene analogs have been investigated with AM1 semi-empirical molecular orbital procedure.[70] The x-ray structure of **2a** formed the starting point for AM1-geometry optimization of the anti-conformer. All other preliminary models were constructed with MacroModel 4.5[71] and optimized with the MM2 force field of Macromodel prior to AM1 optimization. The similarity of the x-ray and AM1-optimized structures of *anti*-**2a** can be found in the 0.157 rms deviation from a least-squares fit of the 38 C, N and O common atoms in both structures. Chem3D[72] drawings of the optimized models are shown in Figures 2.48-2.52 and the AM1 heats of formation are listed in Table 2.14.

The calculated heats of formation of the *syn* and *anti* conformations of **2a** are essentially identical, suggesting that the *anti* conformation found in the crystal structure of **2a** is favored by crystal packing energies. These heats of formation are in accord with the NMR data for two conformations of approximately equal population. In *anti*-**2a**, the two benzene rings are almost perpendicular to the cylinder axis and the cross-cylinder H...H separation is 2.9-3.0 Å (2.90 Å in the AM1-optimized model; 2.97 Å in the x-ray structure

with C-H= 1.084 Å). The H...H van der Waals separation of two touching hydrogens is about 2.4 Å (2x 1.2 Å).

Table 2.14. AM1 heats of formation (kcal mol^{-1}).

Model	ΔH_f
anti-**2a**	37.4
syn-**2a**	37.3
2b/2c	39.7
anti-**3**	42.3
syn-**3**	41.0
anti-**8**	34.7
syn-**8**	32.9
anti-**9**	34.7
syn-**9**	34.9

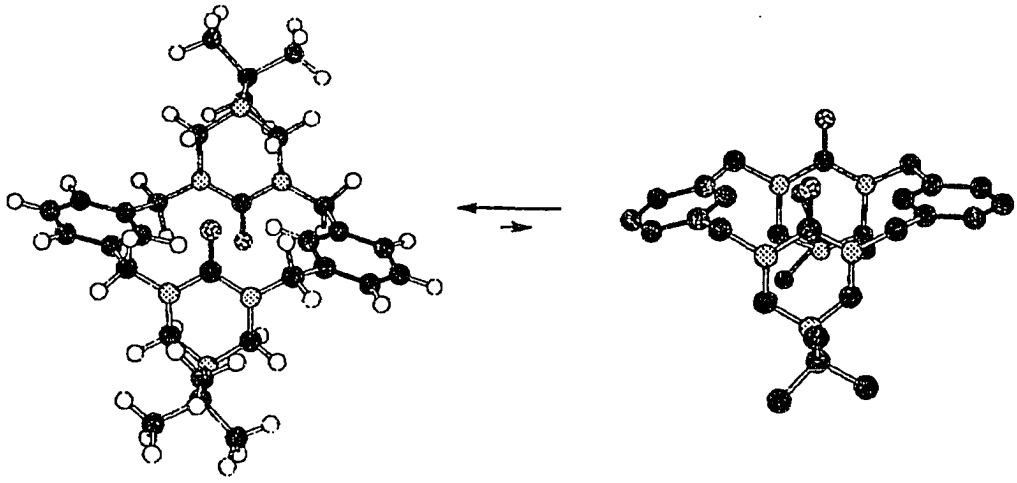

anti-**2a** *syn*-**2a**

Figure 2.48. AM1-optimized conformational equilibria in **2a**. Hydrogen atoms in the syn-conformer were omitted for clarity.

A similar conformation for macrocycles **2b** and **2c** is precluded because it would require both methoxy groups to point into the center of the cylinder. In macrocycle **2c**, the shortest distance from the inward pointing benzene hydrogen to the benzene ring on the opposite side of the cylinder of 4.01 is substantially larger than the van der Waals H...C distance of about 2.9 Å (1.2 + 1.7 Å).

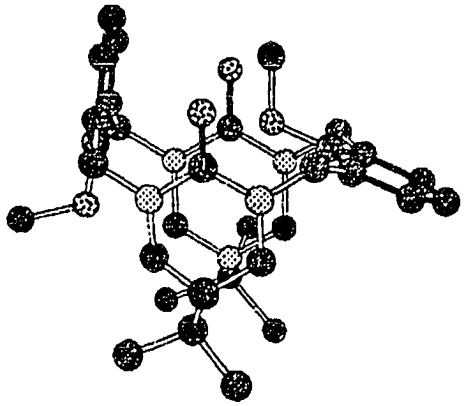

Figure 2.49. AM1 optimized model for the major conformation of **2b** and **2c**. Hydrogen atoms have been omitted for clarity.

The *syn* and *anti* models of macrocycle **3**, viewed down the cylinder axes, are shown in Figure 2.50. The benzene rings are almost perfectly parallel to the cylinder axis in *anti*-**3**, while in *syn*-**3** the benzene rings are slightly canted inward. The cross-cylinder benzene...benzene separations are substantially larger than the van der Waals separation (2 x 1.7 = 3.4 Å). If one assumes

that the difference in the AM1 calculated heats of formation of 1.3 kcal mol^{-1} is the same as the difference in free energies, an equilibrium constant of approximately 9 in favor of the *syn*-**3** is calculated at 298K. This is in reasonable agreement with the 3:1 conformer ratio from NMR data.

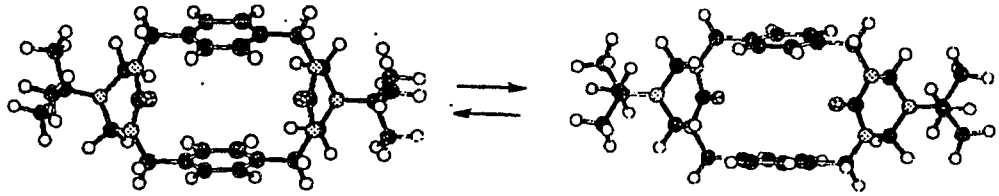

syn-**3** (major) *anti*-**3** (minor)

Figure 2.50. AM1-optimized conformational equilibria in macrocycle **3**. The view is down the cylinder axis.

The relative stabilities of the *syn* and *anti* conformers of macrocycles **8** and **9** were similar to those found for macrocycles **2a** and **3**, respectively.

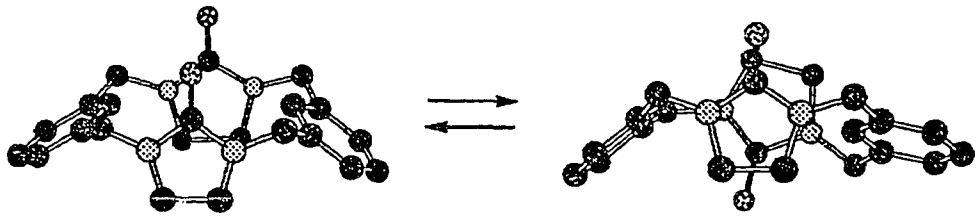

syn-**8** *anti*-**8**

Figure 2.51. AM1-optimized conformational equilibria in macrocycle **8**. Hydrogen atoms have been omitted for clarity.

The calculated heats of formation of *syn* and *anti* conformations of **8** are essentially identical, suggesting in a similar manner to macrocycle **2a**, two equally populated *syn* and *anti* conformers in equilibrium.

In the case of macrocycle **9** the AM1 heats of formation suggests the presence of two equally-populated *syn* and *anti* conformers.

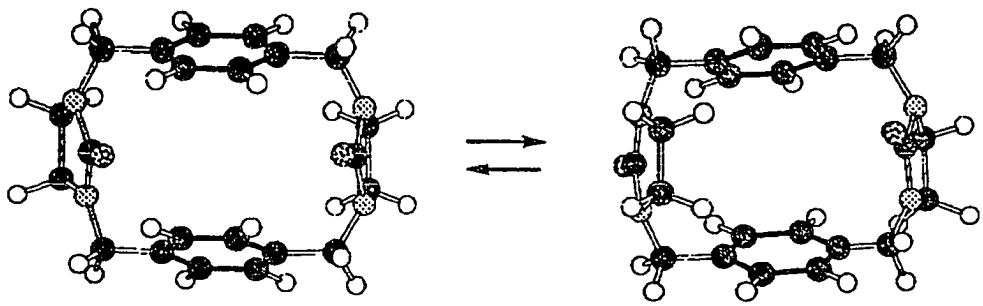

syn-**9** *anti*-**9**

Figure 2.52. Conformational equilibria in macrocycle **9**. The view is down the cylinder axis.

2.11. Conclusion

A series of calix[4]arene analogs incorporating the cyclic urea units have been synthesized and their structures studied by x-ray crystallography, dynamic NMR and computational methods.

2.12. Experimental Section

2.12.1. General Methods

All reactions were carried out under a nitrogen atmosphere unless otherwise stated. Glassware was dried overnight in an oven at 120°C, removed from the oven, fitted with a rubber septum or addition funnel, a condenser and flushed with nitrogen prior to use. Syringes were dried in an oven at 120°C and allowed to cool in a desiccator over calcium chloride prior to use.

Thin layer chromatography (TLC) was performed with Aldrich grade 60 silica gel plastic plates (250μm) with a 254-nm fluorescent indicator. Column chromatographic separations was performed using Aldrich grade 634, 100-200 mesh, 60Å silica gel, Davisil. Eluent mixtures for this procedure are reported as volume/volume percentages.

All ^{1}H and ^{13}C NMR spectra were measured in 5-mm tubes. Spectra were recorded on either Bruker NR 200 or NR 300 spectrometers at ambient temperature unless otherwise stated. Routine ^{13}C NMR spectra were recorded at 50 or 75 MHz with broad band decoupling, a pulse angle of 45° and an acquisition time of 0.475 s for a 16K data table with a spectral width of 230 ppm. Routine ^{1}H NMR spectra were recorded at either 200 or 300 MHz with a pulse angle of 50° and an acquisition time of 2.0 s for a 16K data table with a spectral width of 14 ppm. Unless otherwise noted, spectra are reported in

parts per million downfield from a tetramethylsilane as the internal standard. Data are reported as follows: chemical shift, multiplicity (s = singlet, d = doublet, t = triplet, q = quartet, m = multiplet, br = broad) and spin-coupling values are given in Hertz.

A typical homonuclear-correlated spectrum was acquired with spectral widths in F_1 of 380.5 Hz and in F_2 of 761.0 Hz. The acquisition involved eight transients with a 1 s delay between the transients for each of 128 different t_1 evolution times. The FIDs were zero-filled from 256W to 512W in F_1. A sine-bell enhancement was used prior to double Fourier transformation.

A typical carbon-proton correlated 2D spectrum was acquired with a spectral width of 2336.4 Hz at 50 MHz in the F_2 domain and 500 Hz in the F_1 domain. The spectra were acquired with 1K data points in F_2 and 256W in F_1 with 120 transients (two dummy scans) over 128 experiments. The delay between scans was 1.5 s. The values of the polarization transfer and the refocusing delays were 3.6 and 1.8 ms, respectively. The t_2 data were collected and transformed after being exponentially weighted using a line broadening factor of -3 Hz. The t_1 interferograms were multiplied by a sine-bell function before Fourier transformation as a magnitude spectrum.

Low resolution EI and CI (NH_3) mass spectra were recorded on a Finnigan-MAT model SSQ 70 mass spectrometer with an ionization voltage of 70eV; peaks are reported as m/z. High resolution mass spectra were measured on a JEOL HX110A mass spectrometer by FAB ionization mode using the peak matching technique. Samples were ionized from a 3-nitrobenzyl alcohol matrix using Xe as the FAB gas. Melting points were measured on a Thomas Hoover apparatus and are uncorrected.

Spectra for all compounds are reproduced in Appendices **B**, and **C**, respectively. The ORTEP representations of macrocyles **2a-c** are reproduced in Appendix **D**.

2.12.2. Solvents and Materials

All solvents and materials, unless otherwise specified, were obtained from Aldrich Chemical Co. and were used without further purification.

Chloroform-d_1 (99 atom % D), acetone-d_6 (99.8 atom % D), dimethyl-sulfoxide-d_6 (99.5 atom % D) were obtained from Cambridge Isotopes Laboratory and contained 0.1% tetramethylsilane as internal standard.

Deuterium oxide (99.9 atom % D, D_2O) was obtained from Cambridge Isotopes Laboratory.

Tetrahydrofuran (THF) was obtained from Fisher Scientific Co., as reagent grade solvent, and was distilled from sodium-benzophenone ketyl immediately prior to use.

2.12.3. Procedures

5-tert-Butyltetrahydro-1,3,5-triazine-2(1H)one 1. To a mixture of urea (30 g, 0.500 mol) and of 37% aqueous formaldehyde (80.0 g, 2.65 mol) was added tert-butyl amine (35.8 g, 0.490 mol) dropwise over a 5-min period. The mixture was stirred at 55°C for 24 h and an additional 20 h at room temperature. The mixture was diluted with acetone (200 mL) and stored in the freezer for 2 h during which time crystallization occurred. Filtration afforded a colorless solid which was recrystallized from ethanol (23.6 g, 30%): mp 205-207°C; ^{1}H NMR ($CDCl_3$): δ1.17 (s, 9H, $C(CH_3)_3$), 4.31 (s, 4H, N-CH_2-N), 5.10 (br, s, 2H, N-H); ^{13}C NMR (D_2O): δ26.83, 54.20, 56.06, 157.70. [see Appendix B; Figures B.1 and B.2 for the ^{1}H and ^{13}C NMR spectra, respectively].

2-Imidazolidone (Ethyleneurea) (4). This compound was purchased from Aldrich Chemical Co. ^{1}H NMR ($CDCl_3$): δ3.52 (s, 4H, CH_2), 5.74 (br, s, 2H, NH); ^{13}C ($CDCl_3$): δ40.8, 165.6.

[see Appendix B; Figures B.3 and B.4 for the ^{1}H and ^{13}C NMR spectra, respectively].

Compounds **5, 6** and **7** were prepared according to the method of Koenig, Lein, Stuckler, Kaneda and Cram.[65]

2,6-Bis(hydroxymethyl)-4-methylphenol (5). To a solution of K_2CO_3 (30 g, 217 mmol) in 300 mL of water was added p-cresol (20.0 g, 185 mmol) and 37% aqueous formaldehyde (60 mL, 740 mmol). The solution was stirred at 50°C for 3.5 h, cooled to room temperature and a stream of CO_2 was passed into the yellow solution until it turned cloudy. The mixture was extracted with ethyl acetate (2x30 mL), the combined extracts were dried ($MgSO_4$) and the solvent was removed under reduced pressure. The residue was recrystallized from 50 mL of $CHCl_3$ at -20°C to give (13.9 g, 45%) of product: mp 123-124°C; ^{1}H NMR (acetone-d_6): δ2.18 (s, 3H, CH_3), 4.66 (s, 4H, CH_2O), 6.86 (s, 2H, ArH); ^{13}C NMR (acetone-d_6): δ20.55, 62.15, 127.50, 128.45, 152.32.[65]

[see Appendix B; Figures B.5 and B.6 for the ^{1}H and ^{13}C NMR spectra, respectively].

2,6-Bis(hydroxymethyl)-4-methylanisole (6). A mixture of 2,6-bis-(hydroxymethyl)-4-methylphenol (13.9 g, 83 mmol) **5**, K_2CO_3 (16.6 g ,120

mmol) and $(CH_3)_2SO_4$ (11.3 g, 0.090 mol) in acetone (420 mL) was stirred under N_2 at 25°C for 24 h. The resulting mixture was filtered and the solvent evaporated under reduced pressure. The residue was taken up in $CHCl_3$ (20 mL) and washed with water (2x15 mL). The organic layer was separated, dried ($MgSO_4$) and concentrated under vacuum to give a residue which was recrystallized at -20°C from a minimum amount of $CHCl_3$ (12.6 g, 84%) of **6**: mp 103-104°C; ^1H NMR ($CDCl_3$): δ2.30 (s, 3H, CH_3), 3.78 (s, 3H, OCH_3), 4.64 (s, 4H, CH_2O), 7.10 (s, 2H, ArH); ^{13}C NMR ($CDCl_3$): δ 20.40, 55.36, 62.22, 110.18, 129.10, 129.58.[65]

[see Appendix B; Figures B.7 and B.8 for the ^1H and ^{13}C NMR spectra, respectively].

2,6-Bis(bromomethyl)-4-methylanisole (7). To a solution of 2,6-bis-(hydroxymethyl)-4-methylanisole (10 g, 55 mmol) **6** in $CHCl_3$ (350 mL) stirred at 25°C under a nitrogen atmosphere was added a solution of $SOBr_2$ (15.0 g, 72 mmol) in $CHCl_3$ (50 mL) over a 10 minute period. The solution was stirred for 1 h, washed successively with saturated aqueous $NaHCO_3$ (25 mL) and saturated aqueous Na_2SO_3 (25 mL). The organic layer was separated and dried ($MgSO_4$). Evaporation of the solvent gave **7** (16.9 g, 100%) as an oil, which solidified on standing: mp 66-68°C; ^1H NMR ($CDCl_3$): δ2.26 (s,

3H, CH_3), 3.94 (s, 3H, CH_3O), 4.46 (s, 4H, CH_2Br), 7.12 (2H, s, Ar-H); ^{13}C NMR ($CDCl_3$): δ20.48, 27.56, 62.10, 132.10, 132.66, 134.45, 154.31.[65] [see Appendix B; Figures B.9 and B.10 for the ^1H and ^{13}C NMR spectra, respectively].

2-Methoxy-1,3-benzenedicarboxylic acid (11). Potassium permanganate (37.0 g, 234 mmol) was added in small portions to a stirred refluxing solution of 2,6-dimethylanisole (5.0 g, 37 mmol) in pyridine (37 mL) and water (74 mL). Stirring was continued at room temperature for 12 h after which time the precipitated MnO_2 was removed by filtration and washed several times with a total of 200 mL of hot water. The filtrate was reduced under vacuum to *ca.*, 50 mL. The residue was acidified with ice-cold concentrated HCl (10.2 mL). The colorless precipitated dicarboxylic acid was collected by filtration, washed with a minimum amount of ice water *ca.*, 5 mL and dried in vacuo. Recrystallization from methanol gave **11** (5.9 g 82%) as a colorless crystalline solid: mp 227-229°C; ^1H NMR (DMSO-d_6): δ13.2 (br, 2H, COOH), 3.79 (s, 3H, OCH_3), 7.20-7.40 (m, 1H, Ar-H), 7.78-7.80 (m, 2H, Ar-H); ^{13}C NMR (DMSO-d_6): δ62.89, 123.49, 127.69, 133.37, 157.87, 167.15; LRMS (CI, NH_3): Calcd for $C_9H_{12}NO_5$ $(M+18)^+$ 214, found m/z 214. [see

Appendix B; Figures B.11 and B.12 for the ^{1}H and ^{13}C NMR spectra, respectively].

2-Methoxy-1,3-benzenedicarboxylic diethyl ester (12). To a stirred solution of 2-methoxy-1,3-benzenedicarboxylic acid **11** (3.90 g, 20 mmol) in absolute alcohol (20 mL) was added concentrated H_2SO_4 (2 mL). The solution was heated under reflux for 14 h after which time it was cooled to room temperature and concentrated to half its volume (~9 mL). The residue was poured into ice-water (16 mL), and extracted with diethyl ether (4x15 mL). The organic layer was washed with 10% sodium carbonate (10 mL), dried ($MgSO_4$) and concentrated in vacuo to give **12** (4.00 g, 80%) as an oil. ^{1}H NMR ($CDCl_3$): δ1.41 (t, 6H, $CO_2CH_2\underline{C}H_3$), 3.94 (s, 3H, OCH_3), 4.40 (q, 4H, $CO_2\underline{C}H_2CH_3$), 7.21-7.23 (m, 1H, Ar-H), 7.90-7.93 (m, 2H, Ar-H); ^{13}C NMR ($CDCl_3$): δ13.95, 61.06, 63.37, 123.20, 126.75, 134.50, 159.11, 165.46; LRMS (CI, NH_3): Calcd for $C_{13}H_{20}NO_5$ $(M+18)^+$ 270, found m/z 270.

[see Appendix B; Figures B.13 and B.14 for the ^{1}H and ^{13}C NMR spectra, respectively].

2,6-Bis(hydroxymethyl-d_2)anisole (13). To a solution of **12** (4.1 g, 16 mmol) in anhydrous diethyl ether under a nitrogen atmosphere was added in

one portion lithium aluminum deuteride (1.1 g, 0.026 mol) and the resulting suspension heated under reflux for 14 h. The reaction mixture was quenched in sequence with H_2O (0.93 mL), 15% NaOH (0.93 mL) and H_2O (1.8 mL), filtered and the filtrate concentrated under vacuum to give **13** (2.51g, 91 %) as a colorless solid: mp 88-90°C; ^{1}H NMR (acetone-d_6): δ 2.82 (br, 2H, OH), 3.76 (s, 3H, OCH_3), 7.08-7.11 (m, 1H, Ar-H), 7.36-7.38 (m, 2H, Ar-H); ^{13}C NMR (acetone-d_6): δ58.86-59.47, 62.24, 124.88, 128.62, 135.79, 156.50; LRMS (EI): Calcd for $C_9H_8O_3D_4$ $(M)^+$ 172, found m/z 172.

[see Appendix B; Figures B.15 and B.16 for the ^{1}H and ^{13}C NMR spectra, respectively].

2,6-Bis(bromomethyl-d_2)anisole (14). To a stirred solution of **13** (2.40 g, 14 mmol) in $CHCl_3$ (85 mL) at 25°C under a nitrogen atmosphere was added a solution of $SOBr_2$ (3.84g, 0.018mol) in $CHCl_3$ (10 mL) over a 10 minute period. The solution was stirred for 2 h, washed successively with saturated aqueous $NaHCO_3$ (15 mL) and saturated aqueous Na_2SO_3 (15 mL). The organic layer was separated and dried ($MgSO_4$). Evaporation of the solvent gave **14** (3.31 g, 80%) as an oil which solidified on standing: mp 80-82°C;^{1}H NMR ($CDCl_3$): δ4.03 (s, 3H, OCH_3), 7.11 (m, 1H, Ar-H), 7.37 (m, 2H, Ar-

H); ^{13}C NMR ($CDCl_3$): 27.11, 62.22, 125.10, 131.78, 132.18, 156.55; LRMS (CI, NH_3): Calcd for $C_9H_{10}OD_4NBr_2$ 314, 316, 318, found m/z 314, 316, 318. [see Appendix B; Figures B.17 and B.18 for the ^1H and ^{13}C NMR spectra, respectively].

Compound **15** was prepared according to the method of Newmann and Vogtle.[66]

2,6-Bis(bromomethyl)anisole (15). To a stirred solution of 2,6-bis(dimethyl)anisole (30.0 g, 220 mmol) in CCl_4 (300 mL) was added N-bromosuccinimide (82.3 g, 0.46 mol). The reaction flask was irradiated with a 250-watt lamp for 2 h (until succinimide was floating on the surface of the solvent). After cooling the reaction mixture to room temperature the solid succinimide was filtered and the filtrate concentrated under vacuum. Recrystallization from anhydrous diethyl ether gave **15** (30 g, 50%) as a crystalline solid: mp 84-85°C; ^1H NMR ($CDCl_3$): δ3.87 (s, 3H, OCH_3), 4.53 (s, 4H, CH_2Br), 7.11 (m, 1H, Ar-H), 7.36 (s, 2H, Ar-H); ^{13}C NMR ($CDCl_3$): δ27.45, 62.20, 125.02, 131.90, 132.19, 156.54.

[see Appendix B; Figures B.19 and B.20 for the ^1H and ^{13}C NMR spectra, respectively].

Cyclization of 1,3-bis(bromomethyl)benzene to macrocycle (2a). To a suspension of NaH (460 mg, 19.2 mmol) in THF (180 mL) was added triazone **1** (1.00 g, 6.4 mmol). The reaction mixture was heated under reflux for 1h and then allowed to cool to room temperature and a solution of 1,3-bis(bromomethyl)benzene (1.69 g, 6.4 mmol) in THF (50 mL) was injected all at once into the reaction mixture. The reaction mixture was heated under reflux for an additional 18 h, allowed to cool to room temperature and the remaining NaH destroyed with H_2O (Caution !). After evaporation of the solvent the residue was taken up in $CHCl_3$ (50 mL) and the $CHCl_3$ layer was washed with brine (25 mL), dried ($MgSO_4$) and evaporated to yield a colorless solid which was recrystallized from ethyl acetate to yield **2a** (700 mg, 54%) as a colorless solid: mp 214-218°C; ^{1}H NMR ($CDCl_3$, -23°C): δ 1.11 (s, 9H, $C(CH_3)_3$), 1.14(s, 9H, $C(CH_3)_3$), 4.15-4.35 (m, 8H, N-CH_2-N), 3.65 (m, 4H, Ar-CH_2), 5.68 (m, 4H, Ar-CH_2), 7.20-7.50 (m, 6H, Ar-H); ^{13}C NMR, ($CDCl_3$, -23°C): δ28.25, 28.49, 53.73, 54.09, 61.72, 62.24, 48.55, 48.20, 123.18, 124.93, 125.62, 126.41, 128.05, 128.07, 138.45, 138.74, 155.25; HRMS (FAB) Calcd for $C_{30}H_{43}O_2N_6$ $(MH)^+$ 519.3447, found m/z 519.3451.

[see Appendix B; Figures B.21 and B.22 for the ^{1}H and ^{13}C NMR spectra at 300K and 250K, respectively].

[see Appendix C; Figures C.1 and C.2 for the COSY and HETCORR spectra at 300K, repectively].

[see Appendix D; Figure D.1 for the ORTEP representation].

Cyclization of 2,6-bis(bromomethyl)anisole to macrocycle (2b). A suspension of NaH (460 mg, 19.2 mmol) and triazone **1** (1.00 g, 6.4 mmol) in THF (250 mL) was heated under reflux for 1 h. After cooling the reaction mixture to room temperature a solution of 2,6-bis(bromomethyl)anisole **15** (1.88g, 6.4mmol) in THF (100 mL) was added dropwise over a 40 min period. The resulting mixture was heated under reflux for 21 h after which time the remaining NaH was destroyed with ice cold H_2O (Caution !). Evaporation of the solvent resulted in a syrupy residue which was taken up in CH_2Cl_2 (50 mL). The organic layer was washed with brine (25 mL), dried ($MgSO_4$) and evaporated to yield a yellow amorphous solid. Silica gel chromatography (acetone/hexane 1:4) of this residue afforded **2b** (110 mg, 11%): mp 247-249°C; ^{1}H NMR ($CDCl_3$): δ1.10 (s, 9H, $C(CH_3)_3$), 1.21 (s, 9H, $C(CH_3)_3$), 2.77 (s, 3H, CH_3O), 3.73 (s, 3H, CH_3O), 3.60 (d, J=12 Hz, 4H, N-CH_2-N), 4.90 (d, J=12.5 Hz, 4H, N-CH_2-N), 3.70 (d, J=12 Hz, 4H, N-

CH_2-N), 4.20, (m, 4H, N-CH_2-N), 3.30, (d, J=15 Hz, 4H, Ar-CH_2, major), 5.63 (d, J=15 Hz, 4H, Ar-CH_2), 3.42, (d, J=13.9 Hz, 4H, Ar-CH_2, minor), 5.87 (d, J=13.9 Hz, 4H, Ar-CH_2, minor), 3.76 (m, 4H, Ar-CH_2), 4.72 (d, J=14 Hz, 4H, Ar-CH_2), 6.89-7.46 (m, 6H, Ar-H); ^{13}C NMR ($CDCl_3$): δ29.00, 29.67, 53.98, 60.35, 60.77, 61.39, 65.66, 47.78, 45.70, 133.66, 130.94, 123.22, 122.51, 132.35, 131.13, 157.66, 159.32; HRMS (FAB) Calcd for $C_{32}H_{47}O_4N_6$ $(MH)^+$ 579.3659, found m/z 579.3662.

[see Appendix B; Figures B.26 and B.27, for the ^{1}H and ^{13}C NMR spectra at 300K, respectively].

[see Appendix C; Figures C.3 and C.4 for the COSY and HETCORR spectra at 300K, repectively].

[see Appendix D; Figure D.2 for the ORTEP representation].

Cyclization of 2,6-bis(bromomethyl)-4-methylanisole to macrocycle (2c). A suspension of triazone **1** (1.00 g, 6.4 mmol) and NaH (460 mg, 19.2 mmol) in THF (300mL) was heated under reflux for 1 h and then allowed to cool to room temperature. A solution of 2,6-bis(bromomethyl)-4-methylanisole **7** (1.88 g, 6.4 mmol) in THF (150 mL) was added dropwise over a 60 min period. The resulting mixture was heated under reflux for 18 h, allowed to cool to room temperature and ice-cold water added to destroy

excess NaH (Caution !). After evaporation of the solvent the mixture was taken up in $CHCl_3$ (50 mL) and the solution washed with brine (25 mL). The organic layer was dried ($MgSO_4$) and evaporated under reduced pressure. Silica gel chromatography (acetone/hexane 1:4) of this residue afforded pure **2c** (125 mg, 5.9%): mp 261-263°C; ^1H NMR ($CDCl_3$): δ1.12, (s, 9H, $C(CH_3)_3$), 1.20 (s, 9H, $C(CH_3)_3$) 2.86 (s, 3H, OCH_3), 3.77 (s, 3H, CH_3O), 2.24, (s, 3H, Ar-CH_3), 2.28 (s, 3H, Ar-CH_3), 3.60, (d, J=13 Hz, 4H, N-CH_2-N), 4.90 (d, J=12 Hz, 4H, N-CH_2-N), 3.75 (m, 4H, N-CH_2-N), 4.30 (d, J=15 Hz, 4H, N-CH_2-N), 3.75 (m, 4H, Ar-CH_2), 4.65 (d, J=14 Hz, 4H, Ar-CH_2), 3.27 (d J=15 Hz, 4H, Ar-CH_2, major), 5.60 (d, J=15 Hz, 4H, Ar-CH_2, major), 3.40 (d, J=14 Hz, 4H, Ar-CH_2, minor), 5.83 (d, J=14 Hz, 4H, Ar-CH_2, minor), 4.47 (d J=14 Hz, 4H, Ar-CH_2), 3.80 (m, 4H, Ar-CH_2), 6.80 (s, 4H, Ar-H), 7.30 (s, 4H, Ar-H); ^{13}C NMR ($CDCl_3$): δ29.00, 29.67, 53.92, 60.35, 60.77, 62.00, 65.00, 47.71, 45.73, 134.14, 131.39, 132.35, 131.13, 131.78, 130.69,155.34, 156. HRMS (FAB) Calcd for $C_{34}H_{52}O_4N_6$ $(MH)^+$ 607.3972, found m/z 607.3971.

[see Appendix B; Figures B.29 and B.30 for the ^1H and ^{13}C NMR spectra at 300K, respectively].

[see Appendix C; Figures C.5 and C.6 for the COSY and HETCORR spectra at 300K, repectively].

[see Appendix D; Figure D.3 for the ORTEP representation].

Cyclization of 1,4-bis(bromomethyl)benzene to macrocycle (3). A suspension of triazone **1** (1.00 g, 6.4 mmol) and NaH (460 mg, 19.2 mmol) in THF (300 mL) was heated under reflux for 1 h and then allowed to cool to room temperature. A solution of 1,4-bis(bromomethyl)benzene (1.68 g, 6.4mmol) in THF (50 mL) was added dropwise over a 20-min period to the ice-cold reaction mixture. After the addition was completed the resulting mixture was heated under reflux for 18 h, cooled to room temperature and ice-cold water was added to destroy excess NaH (Caution !). After removal of the solvent the residue was taken up in $CHCl_3$ (60 mL) and the solution washed with brine (25 mL). The organic layer was dried ($MgSO_4$) and concentrated under reduced pressure to give an amorphous solid. Silica gel chromatography (ethyl acetate/hexane 4:1) of this amorphous solid afforded **3** (119 mg, 2.3%): mp 220-222°C; ^1H NMR ($CDCl_3$): δ1.22, (s, 9H, $C(CH_3)_3$) 1.25 (s, 9H, $C(CH_3)_3$), 3.72, (d J=10.7 Hz, 4H, N-CH_2-N, major), 4.05 (d, J=10.8 Hz, 4H, N-CH_2-N, major), 4.20 (d J=10.8 Hz, 4H, N-CH_2-N, minor) 4.36 (d J=10.6 Hz, 4H, N-CH_2-N, minor) 3.26 (d, J=14.0 Hz, 4H, Ar-CH_2,

major), 5.41 (d, J=14.0 Hz, 4H, Ar-CH_2, major), 3.50 (d, J= 14.9 Hz, 4H, Ar-CH_2, minor), 5.04 (d, J=14.9 Hz, 4H, Ar-CH_2, minor), 7.11 (s, 4H, Ar-H), 7.28 (s, 4H, Ar-H); ^{13}C NMR ($CDCl_3$): δ 28.72, 28.54, 53.94, 54.07, 63.45, 61.81, 49.50, 49.08, 137.24, 128.86, 127.78, 157.07; HRMS (FAB) Calcd for $C_{30}H_{43}O_2N_6$ $(MH)^+$ 519.3447, found m/z 519.3447.

[see Appendix B; Figures B.31 and B.32 for the ^1H and ^{13}C NMR spectra at 300K, respectively].

[see Appendix C; Figures C.7 and C.8 for the COSY and HETCORR spectra at 300K, repectively].

Cyclization of 1,3-bis(bromomethyl)benzene to macrocycle (8). A suspension of 2-imidazolidone **4** (550 mg, 6.4 mmol) and NaH (460 mg, 19.2 mmol) in THF (300 mL) was heated under reflux for 1 h. The mixture was cooled to room temperature and a solution of 1,3-bis(bromomethyl)benzene (1.68 g, 6.4 mmol) in THF (100 mL) was added dropwise over a 40 min period. This mixture was heated under reflux for an additional 18 h, allowed to cool to room temperature and ice-cold water was added to destroy excess NaH (Caution !). After evaporation of the solvent, the mixture was taken up in $CHCl_3$ (50 mL) and the solution was washed with brine (25 mL). The organic layer was dried ($MgSO_4$) and evaporated under reduced pressure.

Silica gel chromatography (ethyl acetate/acetone 9:1) of this residue afforded **8** (311 mg, 13%): mp 272-274°C; ^{1}H NMR ($CDCl_3$): δ3.00-3.40 (m, 4H, m, 4H, N-CH_2-CH_2-N), 3.63-3.85 (m, 4H, Ar-CH_2), 5.08-5.23 (m, 4H, Ar-CH_2), 6.98-7.25 (m, 4H, Ar-H); ^{13}C NMR ($CDCl_3$): δ41.02, 41.72, 46.69, 46.86, 120.87, 123.94, 125.58, 126.90, 128.38, 128.60, 137.62, 137.71, 160.70, 160.90; HRMS (FAB) Calcd for $C_{22}H_{25}O_2N_4$ $(MH)^+$ 377.1978, found m/z 377.1986.

[see Appendix B; Figures B.33, B.34 and B.36 and B.36 for the ^{1}H and ^{13}C NMR spectra at 300K and 250K, respectively].

Cyclization of 1,4-bis(bromomethyl)benzene to macrocycle (9). A suspension of 2-imidazolidone **4** (550 mg, 6.4 mmol) and NaH (460 mg, 19.2 mmol) in THF (350 mL) was heated under reflux for 1 h. The resulting mixture was cooled to room temperature and a solution of 1,4-bis(bromomethyl)benzene (1.68 g, 6.4 mmol) in THF (50 mL) was added dropwise over a 30-min period. The mixture was heated under reflux for an additional 18 h, allowed to cool to room temperature and ice cold water was added to destroy excess NaH (Caution !). After evaporation of the solvent the mixture was taken up in $CHCl_3$ (50 mL) and the resulting solution washed with brine (25 mL). The organic layer was dried ($MgSO_4$) and evaporated

under vacuum. Silica gel chromatography (ethyl acetate /hexane, 7:3) of this residue afforded pure **9** (7.0 mg, 0.32%): mp 277-280°dC; ^{1}H NMR ($CDCl_3$): δ2.56 (m, 4H, N-CH_2CH_2-N), 3.22 (m, 4H, N-CH_2CH_2-N), 3.37 (d, J=14.1 Hz, 4H, Ar-CH_2), 5.05 (d, J=14.1, 4H, Ar-CH_2), 7.27 (s, 8H, Ar-H); ^{13}C NMR ($CDCl_3$): δ40.35, 47.98, 137.52, 129.37, 161.92, 161.90; HRMS (FAB) Calcd for $C_{22}H_{25}O_2N_4$ $(MH)^+$ 377.1978, found m/z 377.1974.

[see Appendix B; Figures B.37 and B.38 for the ^{1}H and ^{13}C NMR spectra at 300K, respectively].

[see Appendix C; Figure C.9 for the COSY and Figures C.10 and C.11 for the HETCORR spectra at 300K].

Cyclization of 2,6-bis(bromomethyl-d_2)anisole to Macrocycle (10). A suspension of triazone **1** (380 mg, 2.4 mmol) and NaH (647 mg, 2.7 mmol) in THF (200 mL) was heated under reflux for 2 h and then allowed to cool to room temperature. A solution of 2,6-bis(bromomethyl-d_2)anisole (0.722 g, 2.42 mmol) **14** in THF (10 mL) was added dropwise over a 60-min period to the ice cold reaction mixture. After the addition was completed the reaction mixture was heated under reflux for 18 h, allowed to cool to room temperature and ice-cold water was added to destroy excess NaH (Caution !). After removal of the solvent, silica gel chromatography (methanol/ethyl

acetate 7:93) of this residue gave a colorless viscous oil. This oil was further purified by preparative thin-layer chromatography (2000μ) (methanol/ethyl acetate 7:93) to afford 44 mg of a colorless viscous oil; ^{1}H NMR ($CDCl_3$): δ 1.20 (s, 9H, $C(CH_3)_3$), 2.87 (s, 3H, OCH_3), 3.80 (s, 3H, OCH_3), 3.60, (d, J=12 Hz, 4H, N-CH_2N), 3.75 (m, 4H, N-CH_2-N), 4.30 (d J=15 Hz, 4H, N-CH_2-N), 4.90 (d J=12 Hz, 4H, N-CH_2-N), 6.87-7.47 (m, 6H, Ar-H); ^{13}C NMR ($CDCl_3$): δ 29.65, 54.04, 60.40, 60.78, 61.91, 65.56, 122.51, 123.26, 130.94, 131.21, 132.17, 133.60, 155.40; LRMS (CI, NH_3) calcd for $C_{32}H_{42}O_4N_7D_8$ $(M+18)^+$ 604, found m/z 604.

[see Appendix B; Figures B.39 and B.40 for the ^{1}H and ^{13}C NMR spectra at 300K, respectively].

APPENDIX A

^{1}H and ^{13}C Magnetic Resonance Spectra

^{1}H and ^{13}C magnetic resonance spectra for all compounds are reproduced in this section.

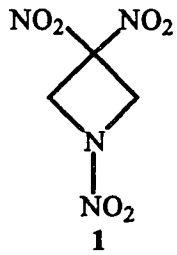

1

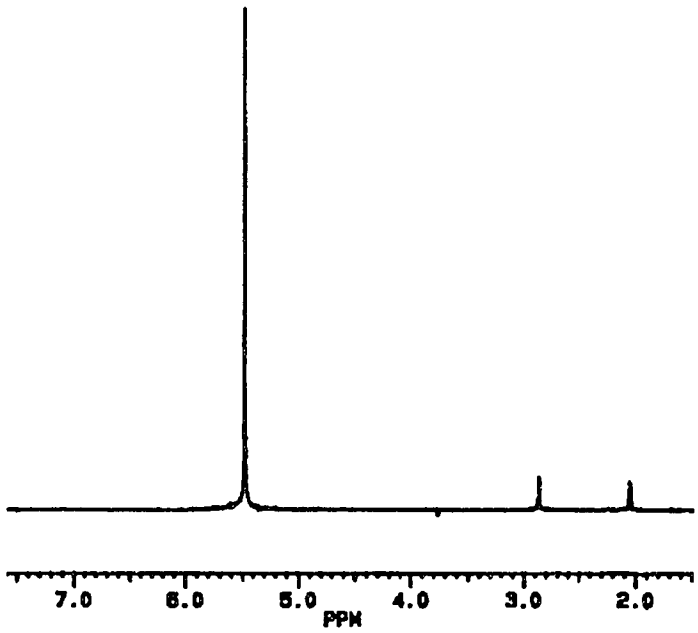

Figure A.1. 300 MHz ^{1}H NMR spectrum of 1,3,3-trinitroazetidine **1** measured in acetone-d_6.

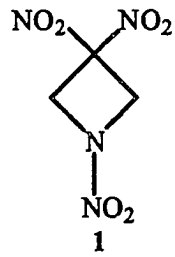

1

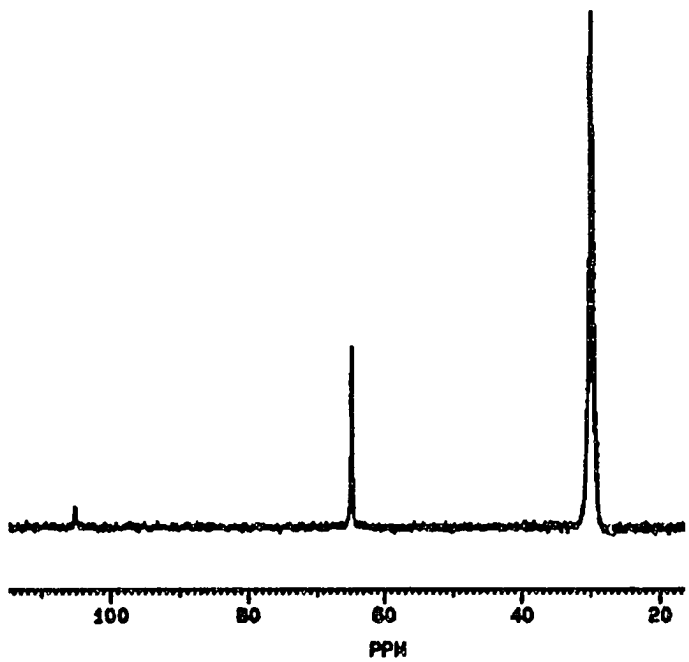

Figure A.2. 75 MHz ^{13}C NMR spectrum of 1,3,3-trinitroazetidine **1** measured in acetone-d_6.

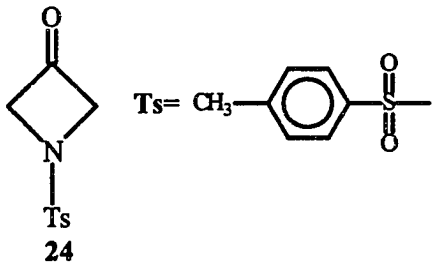

24

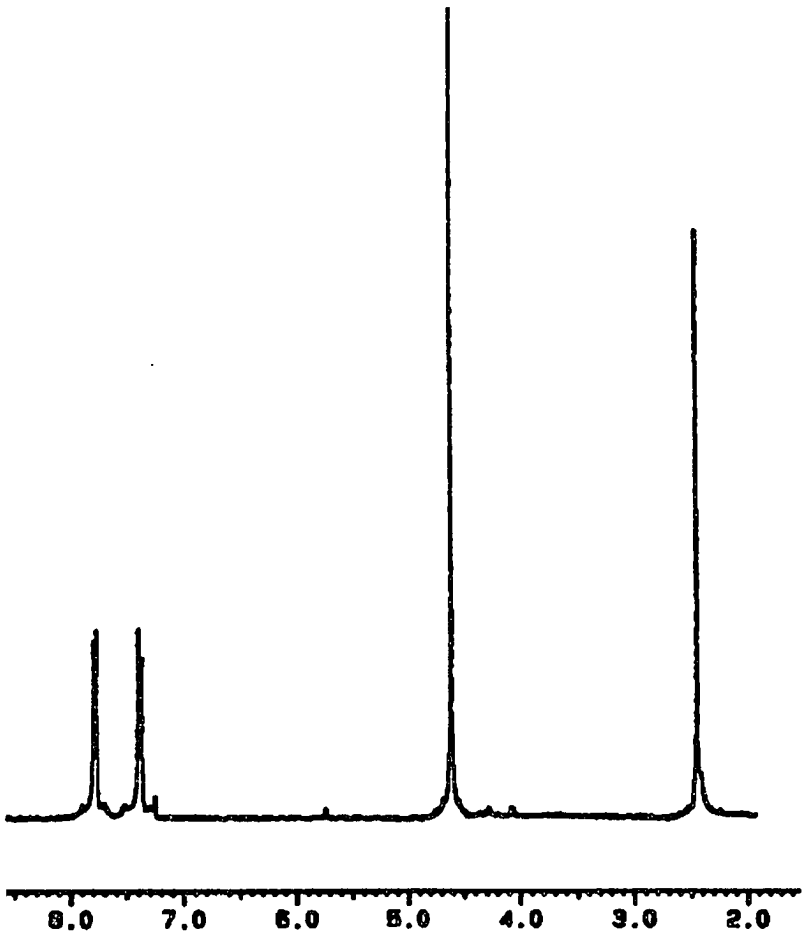

Figure A.3. 300 MHz ^{1}H NMR spectrum of N-(p-toluenesulfonyl)-3-azetidinone **24** measured in $CDCl_3$.

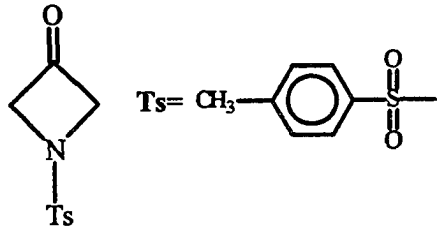

24

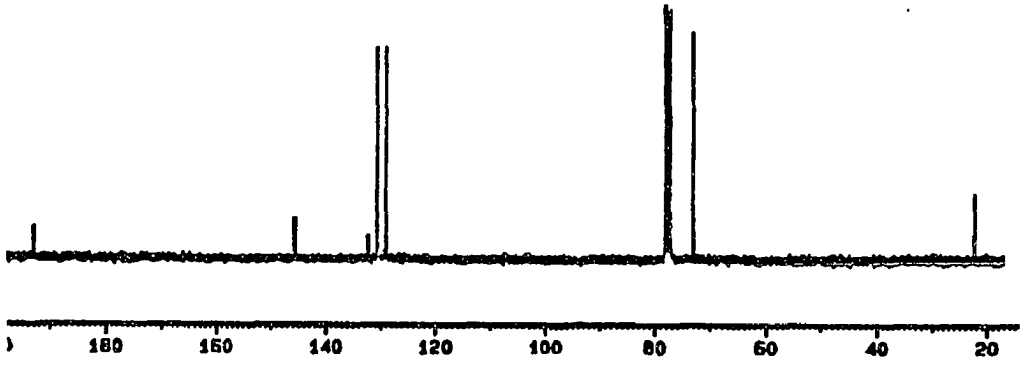

Figure A.4. 75 MHz ^{13}C NMR spectrum of N-(p-toluenesulfonyl)-3-azetidinone **24** measured in $CDCl_3$.

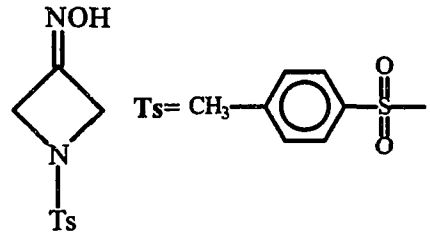

25

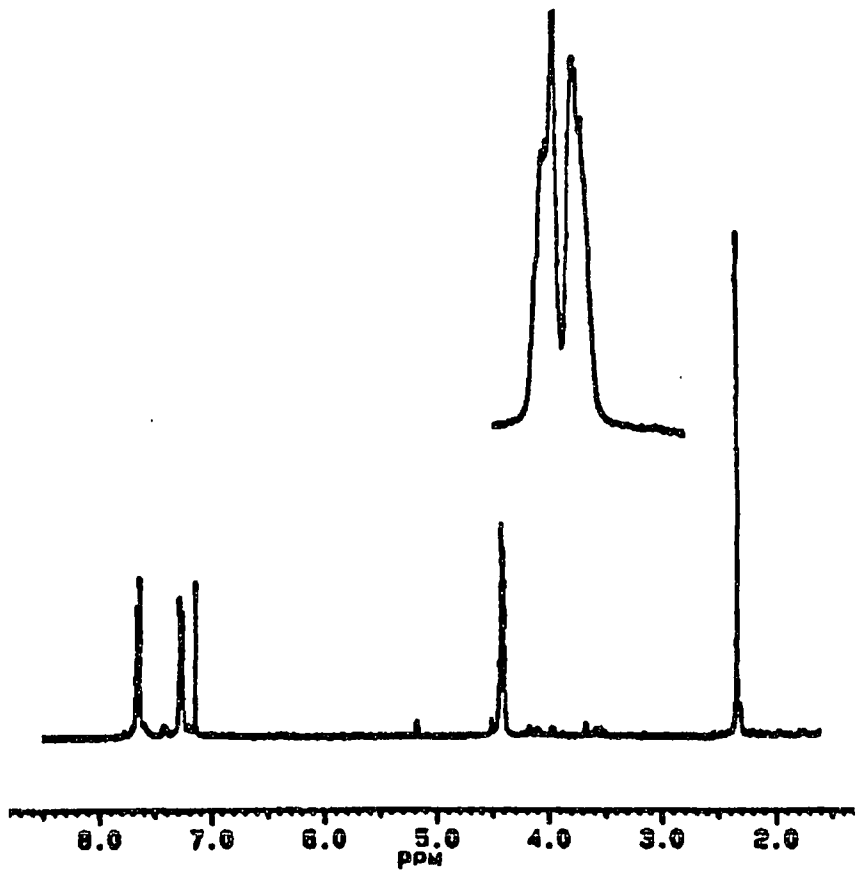

Figure A.5. 300 MHz ^{1}H NMR spectrum of N-(p-toluenesulfonyl)-3-azetidinone oxime **25** measured in $CDCl_3$.

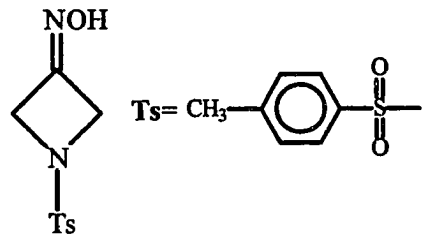

25

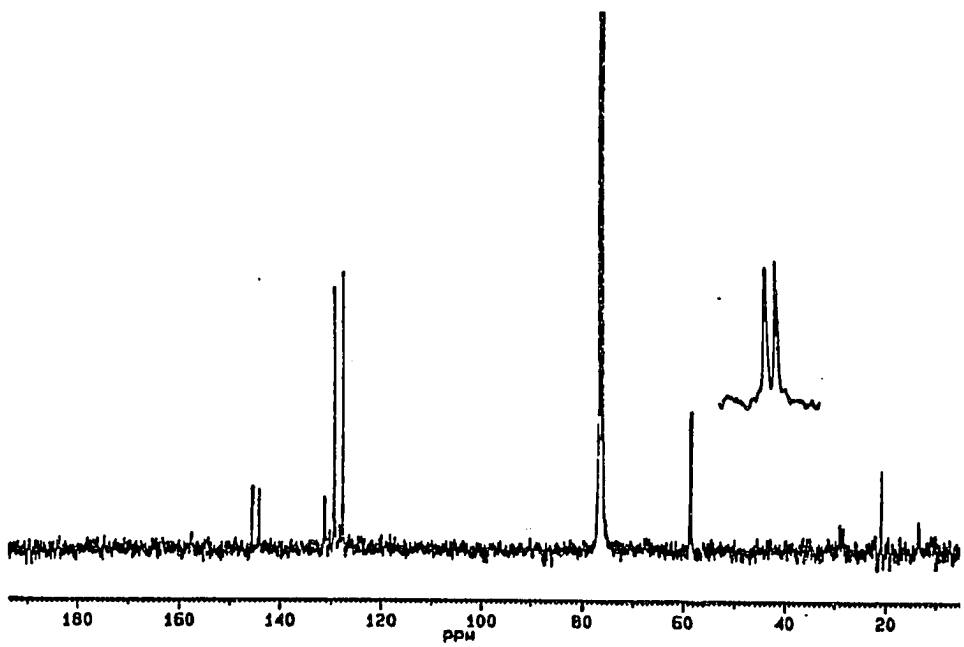

Figure A.6. 75 MHz ^{13}C NMR spectrum of N-(p-toluenesulfonyl)-3-azetidinone oxime **25** measured in $CDCl_3$.

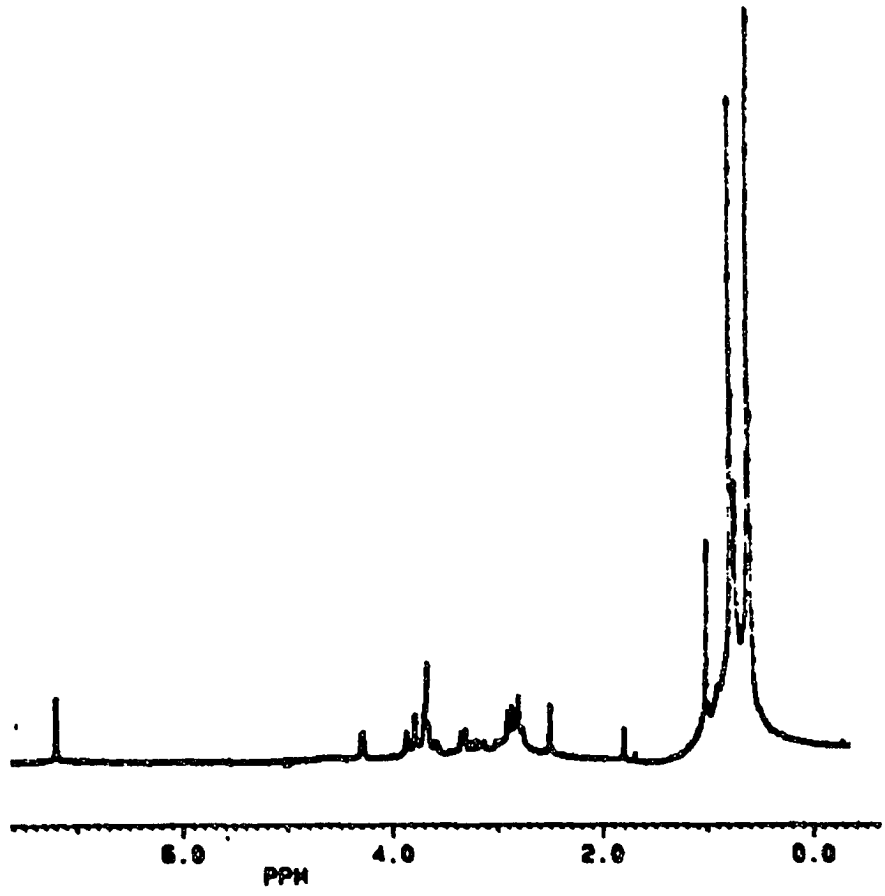

Figure A.7. 300 MHz ^{1}H NMR spectrum of the oxidation products of N-(tert-butyl)-3-azetidinol **31a** measured in $CDCl_3$.

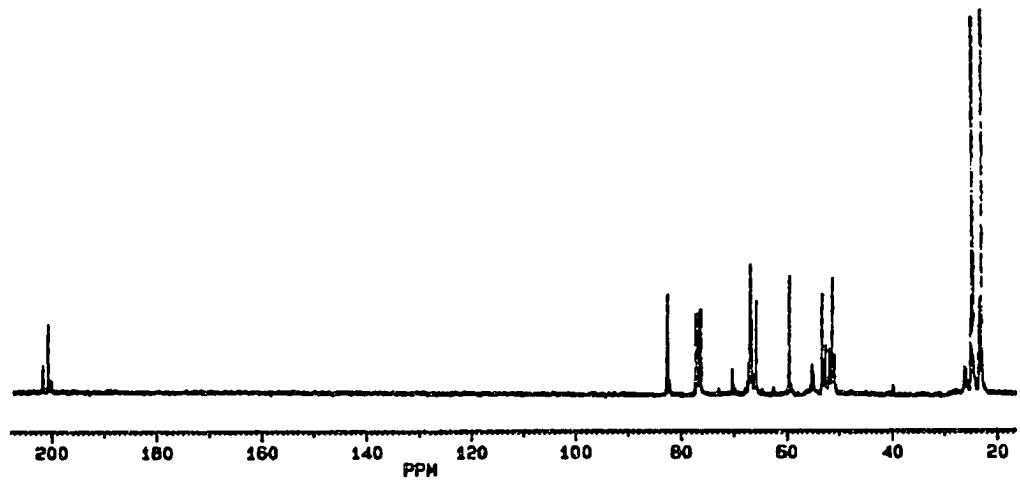

Figure A.8. 75 MHz ^{13}C NMR spectrum of spectrum of the oxidation products of N-(tert-butyl)-3-azetidinol **31a** measured in $CDCl_3$.

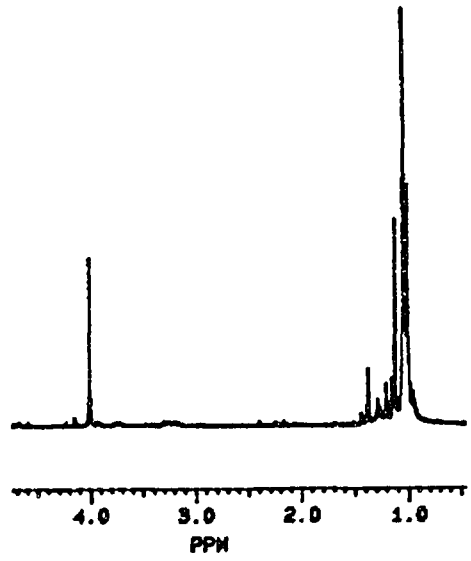

Figure A.9. 300 MHz ^{1}H NMR spectrum of spectrum of the oxidation products of N-(tert-octyl)-3-azetidinol **31b** measured in $CDCl_3$.

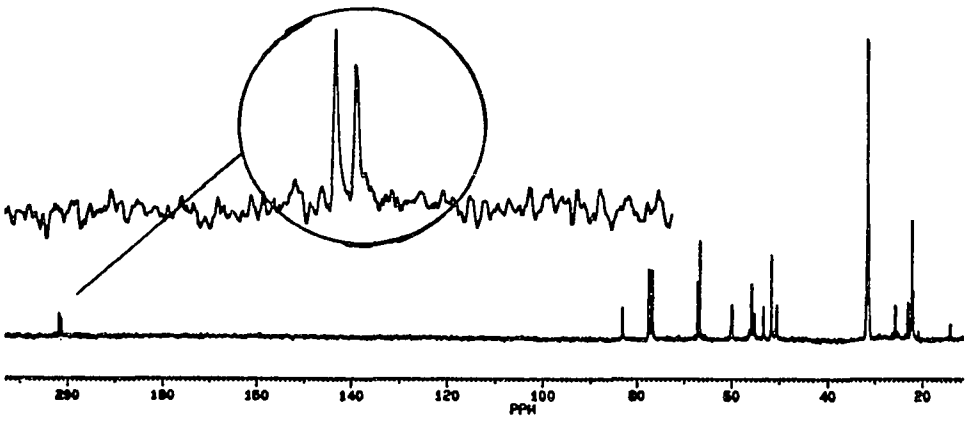

Figure A.10. 75 MHz ^{13}C NMR spectrum of the oxidation products of N-(tert-octyl)-3-azetidinol **31b** measured in $CDCl_3$.

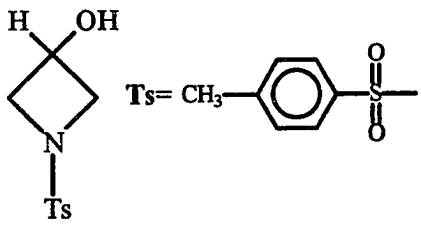

42

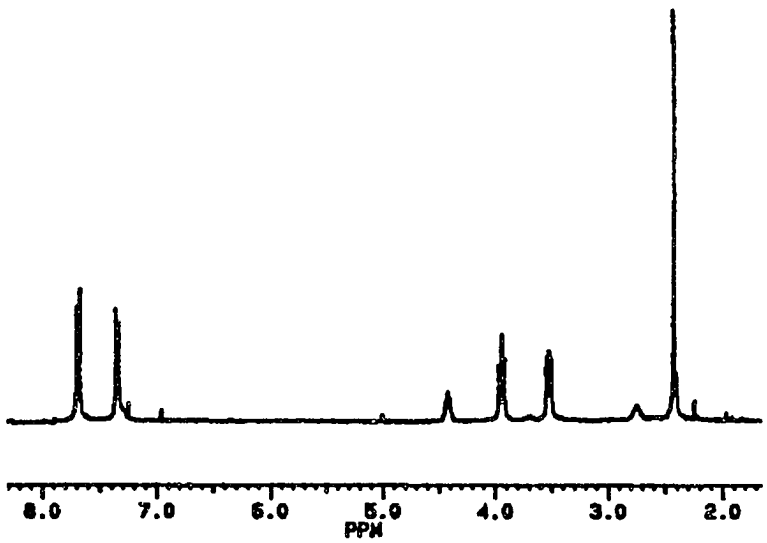

Figure A.11. 300 MHz ^{1}H NMR spectrum of N-(p-toluenesulfonyl)-3-azetidinol **42** measured in $CDCl_3$.

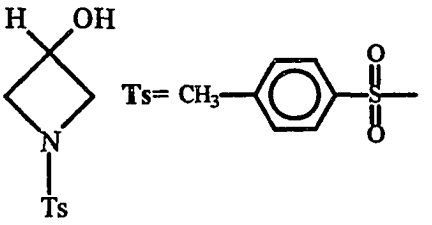

42

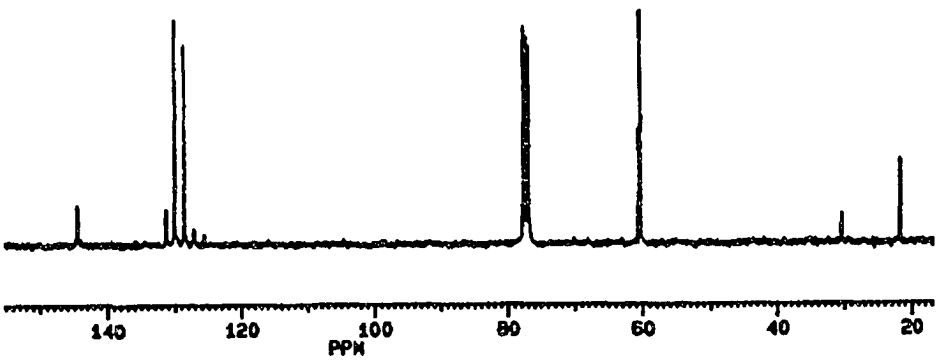

Figure A.12. 75 MHz ^{13}C NMR spectrum of N-(p-toluenesulfonyl)-3-azetidinol **42** measured in $CDCl_3$.

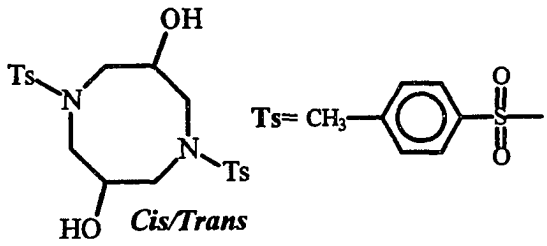

47

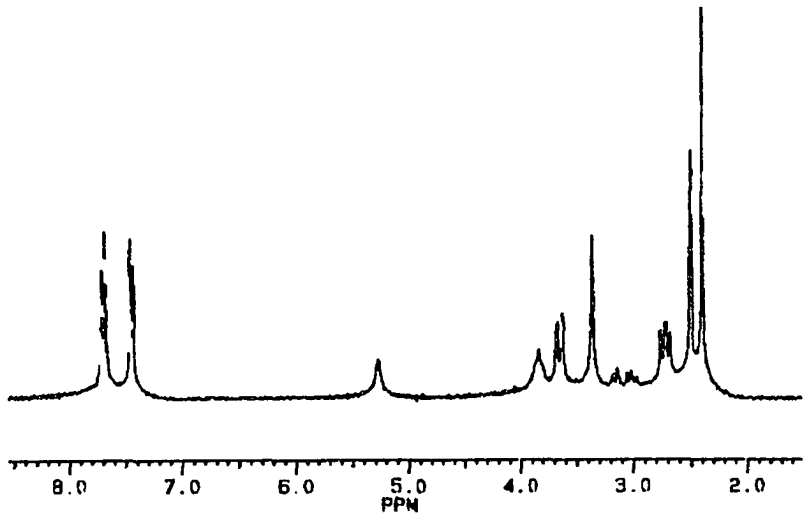

Figure A.13. 300 MHz ^{1}H NMR spectrum of *cis* and *trans*-N,N'-(p-toluene-sulfonyl)-3,7-dihydroxy-1,5-diazcyclooctane **47** measured in DMSO-d_6.

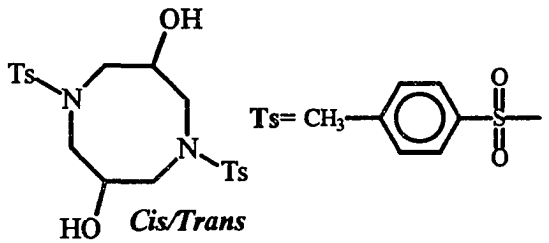

47

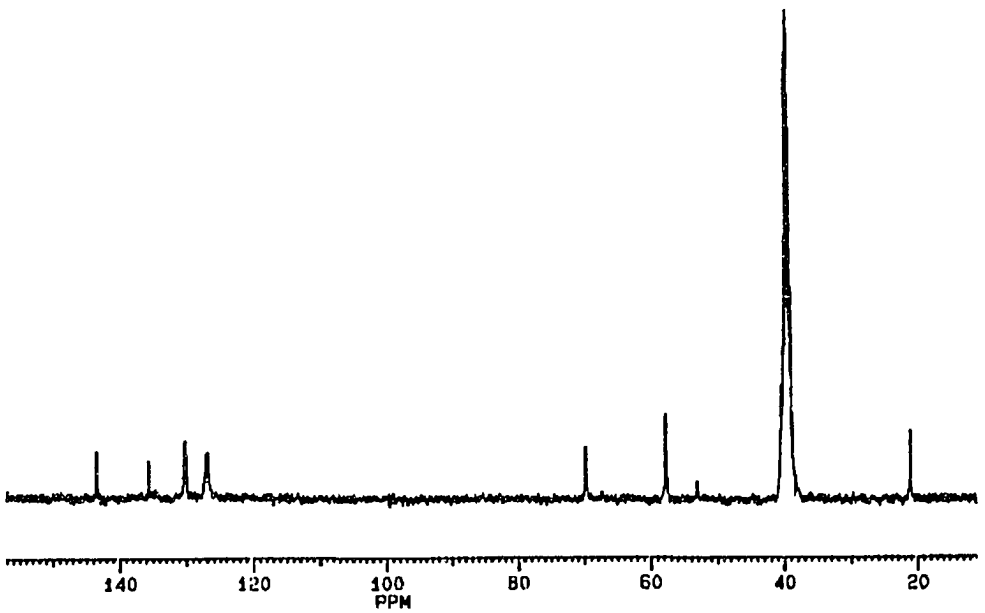

Figure A.14. 75 MHz ^{13}C NMR spectrum of *cis* and *trans*-N,N'-(p-toluene-sulfonyl)-3,7-dihydroxy-1,5-diazcyclooctane **47** measured in DMSO-d_6.

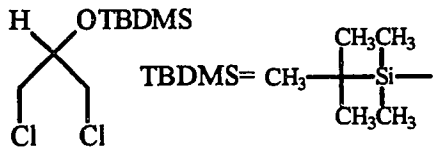

50a

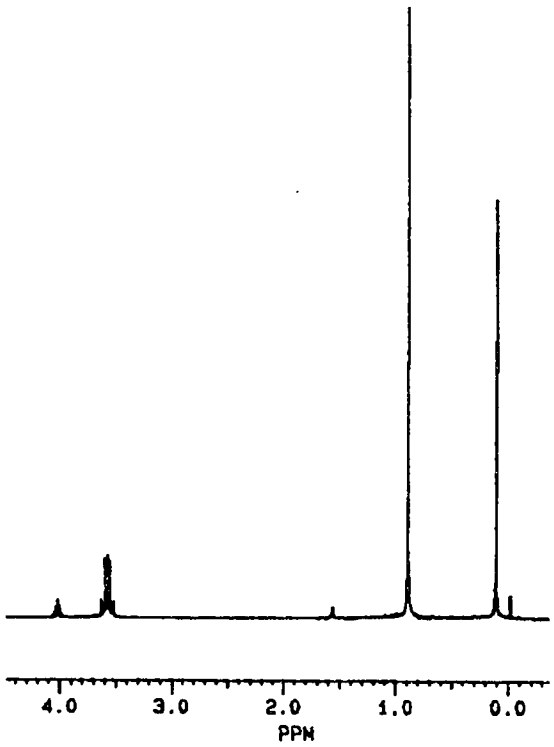

Figure A.15. 300 MHz ^{1}H NMR spectrum of 1,3-dichloro-2-(t-butyldimethylsiloxy)propane **50a** measured in $CDCl_3$.

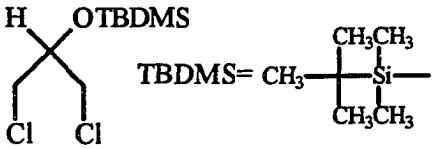

50a

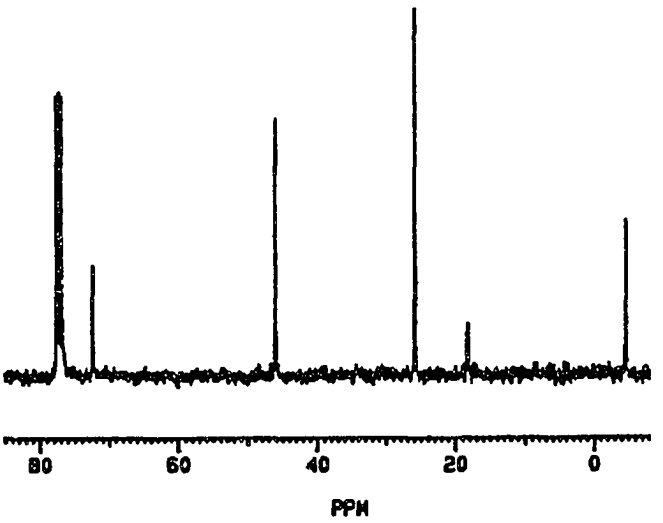

Figure A.16. 75 MHz ^{13}C NMR spectrum of 1,3-dichloro-2-(t-butyldimethylsiloxy)propane **50a** measured in $CDCl_3$.

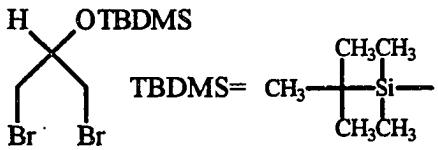

50b

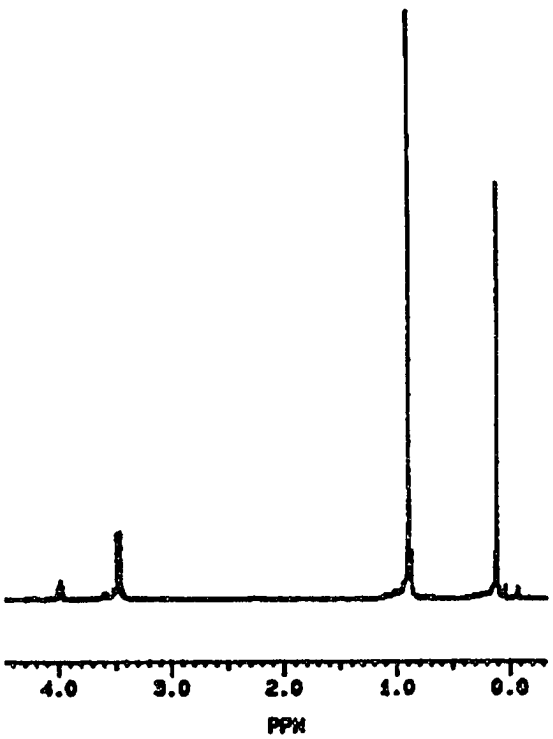

Figure A.17. 300 MHz ^{1}H NMR spectrum of of 1,3-dibromo-2-(t-butyldimethylsiloxy)propane **50b** measured in $CDCl_3$.

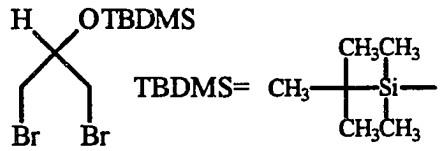

50b

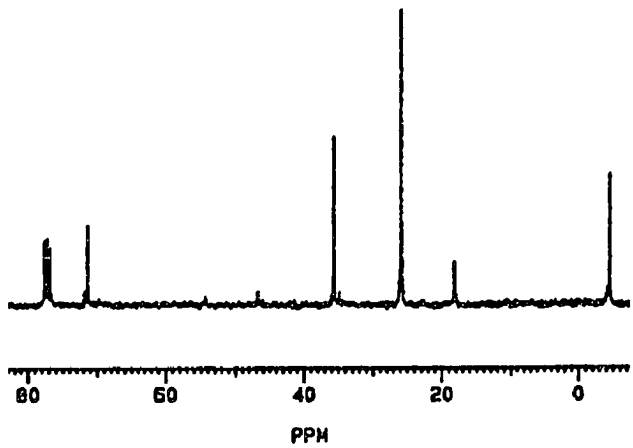

Figure A.18. 75 MHz ^{13}C NMR spectrum of of 1,3-dibromo-2-(t-butyldimethylsiloxy)propane **50b** measured in $CDCl_3$.

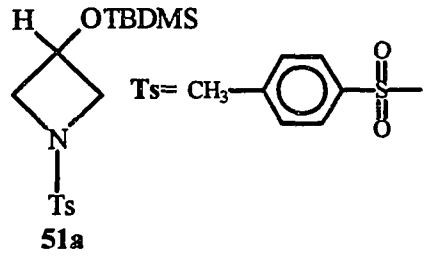

51a

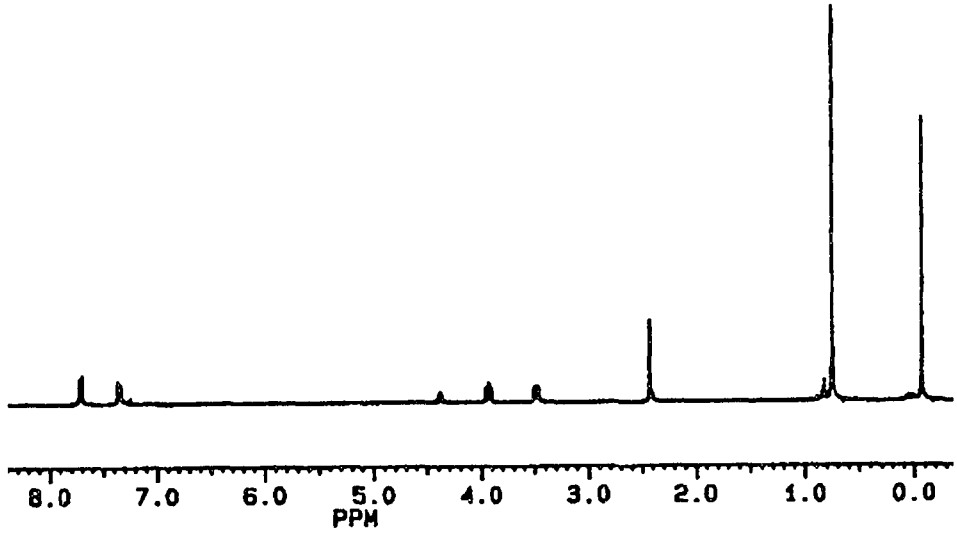

Figure A.19. 300 MHz ^{1}H NMR spectrum of N-(p-toluenesulfonyl)-3-(tert-butyldimethylsiloxy)azetidine **51a** measured in $CDCl_3$.

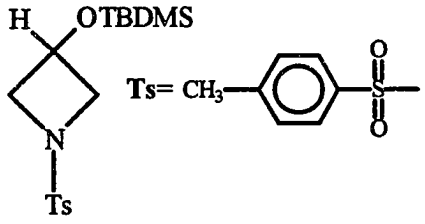

51a

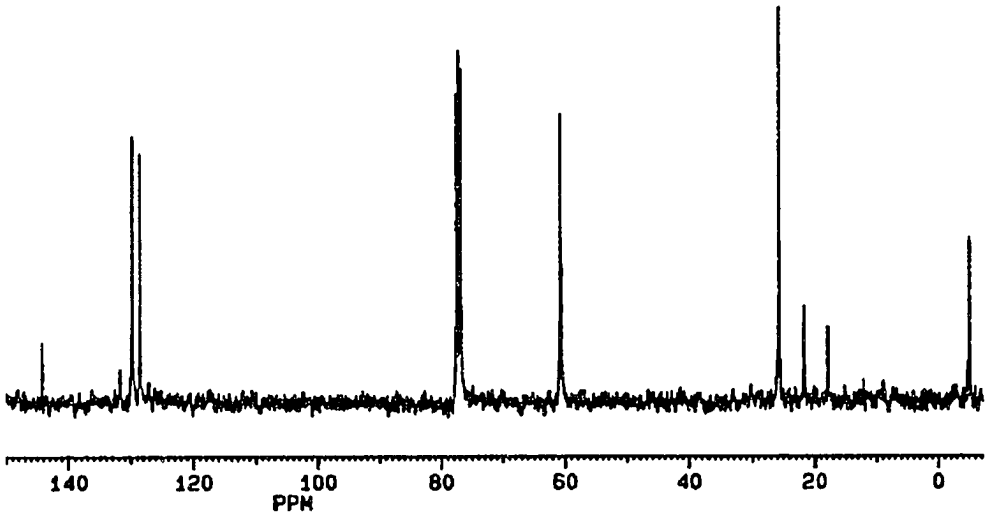

Figure A.20. 75 MHz ^{13}C NMR spectrum of N-(p-toluenesulfonyl)-3-(tert-butyldimethylsiloxy)azetidine **51a** measured in $CDCl_3$.

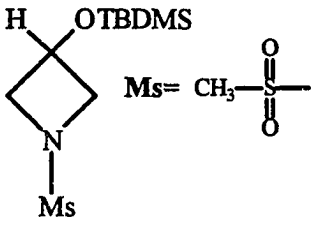

51b

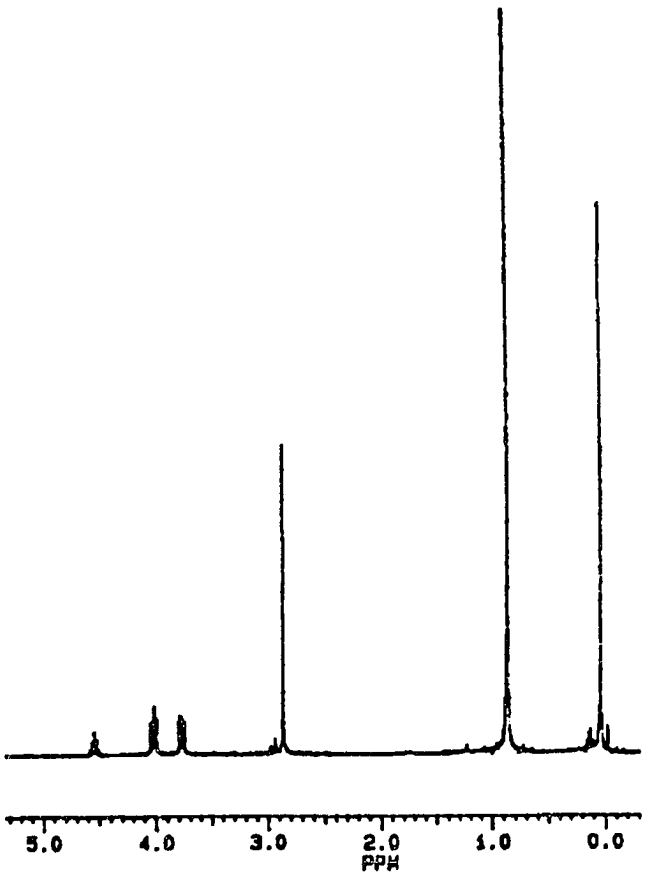

Figure A.21. 300 MHz ^{1}H NMR spectrum of N-(methansulfonyl)-3-(tert-butyldimethylsiloxy)azetidine **51b** measured in $CDCl_3$.

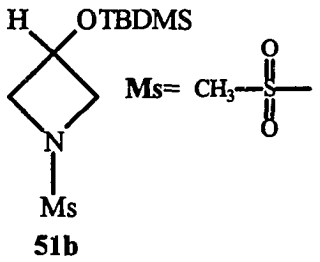

51b

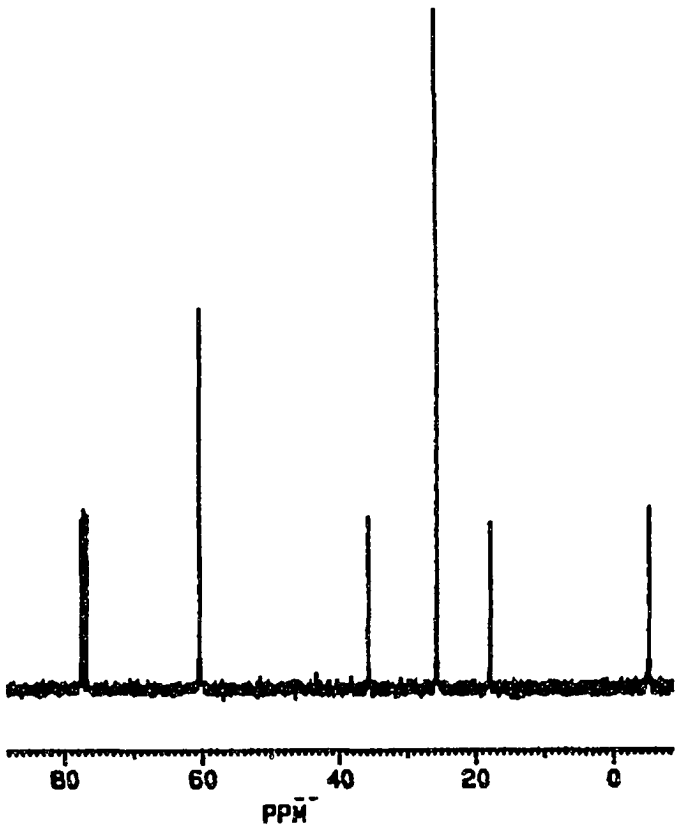

Figure A.22. 75 MHz ^{13}C NMR spectrum of N-(methansulfonyl)-3-(tert-butyldimethylsiloxy)azetidine **51b** measured in $CDCl_3$.

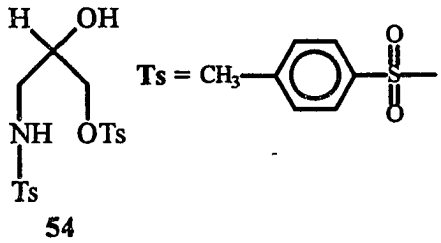

54

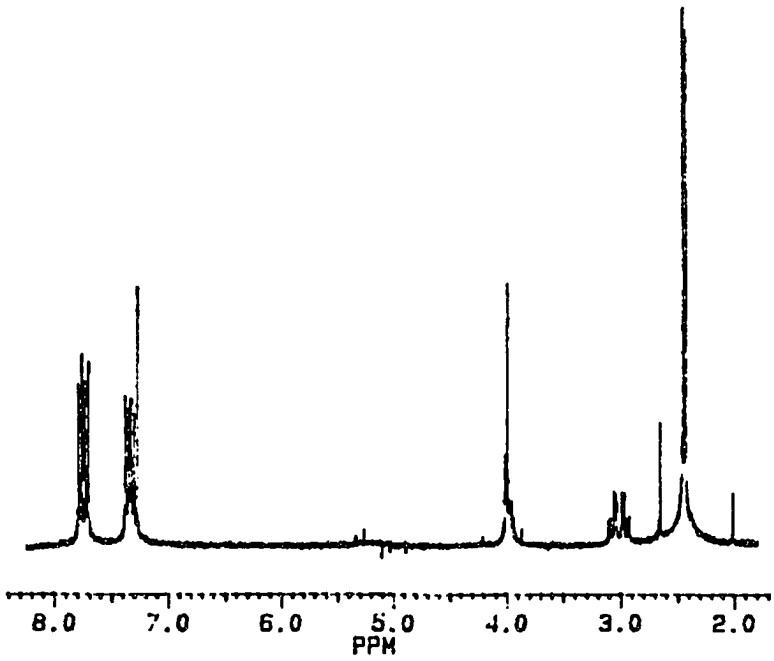

Figure A.23. 300 MHz ^{1}H NMR spectrum of 3-(p-toluenesulfonamido)-propane-2-ol 1-(p-toluenesulfonate) **54** measured in $CDCl_3$.

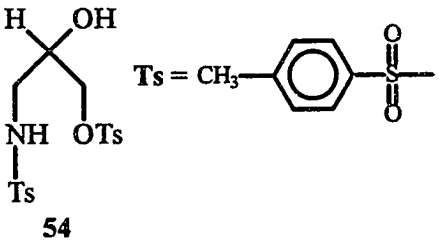

54

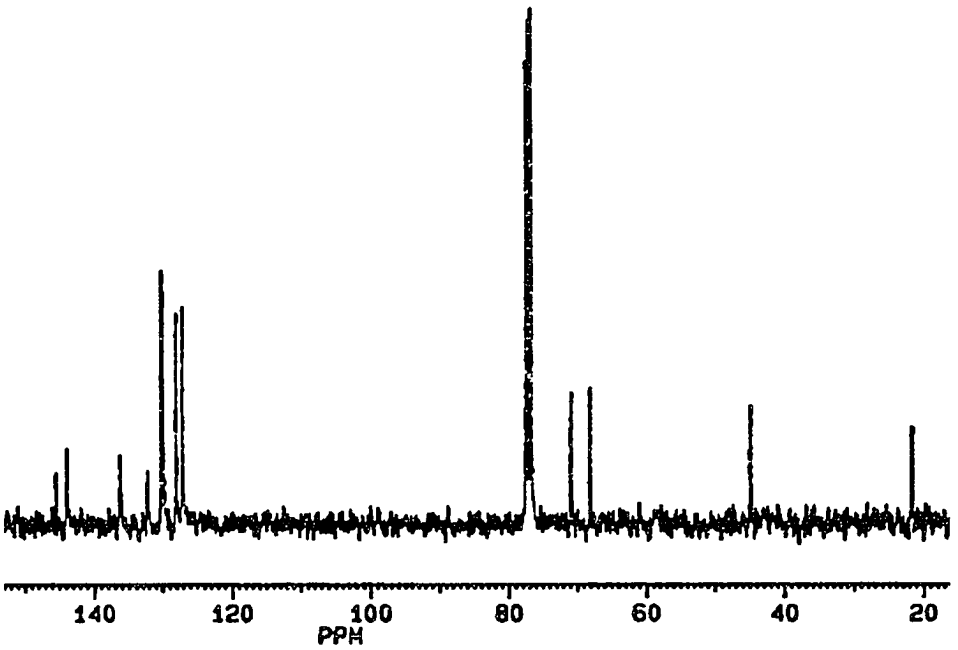

Figure A.24 75 MHz ^{13}C NMR spectrum of 3-(p-toluenesulfonamido)-propane-2-ol-1-(p-toluenesulfonate) **54** measured in $CDCl_3$.

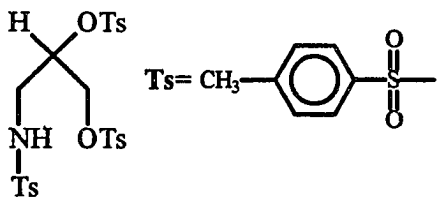

55

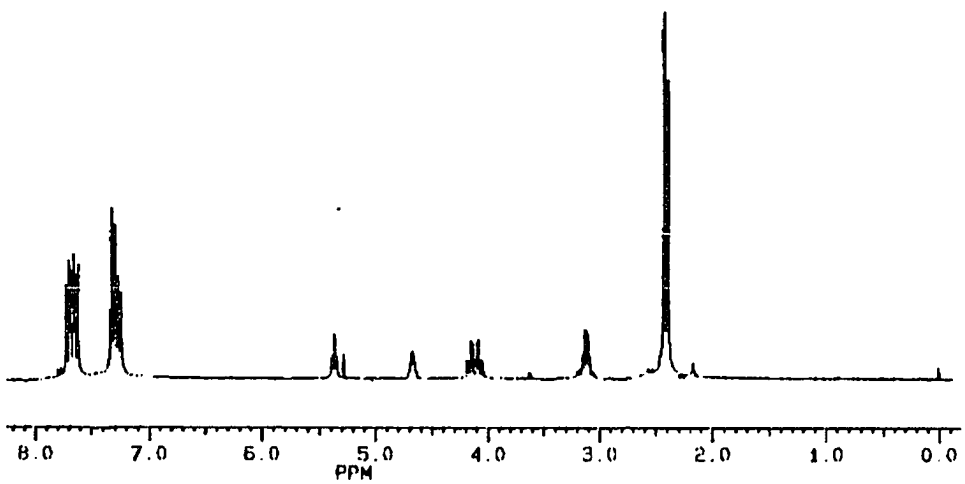

Figure A.25. 300 MHz ^{1}H NMR spectrum of 3-(p-toluenesulfonamido)-1,2-propane-di-(p-toluenesulfonate) **55** measured in $CDCl_3$.

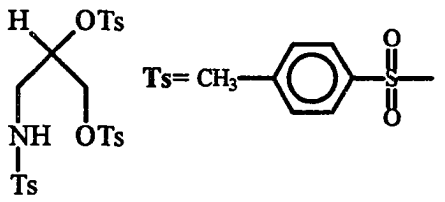

55

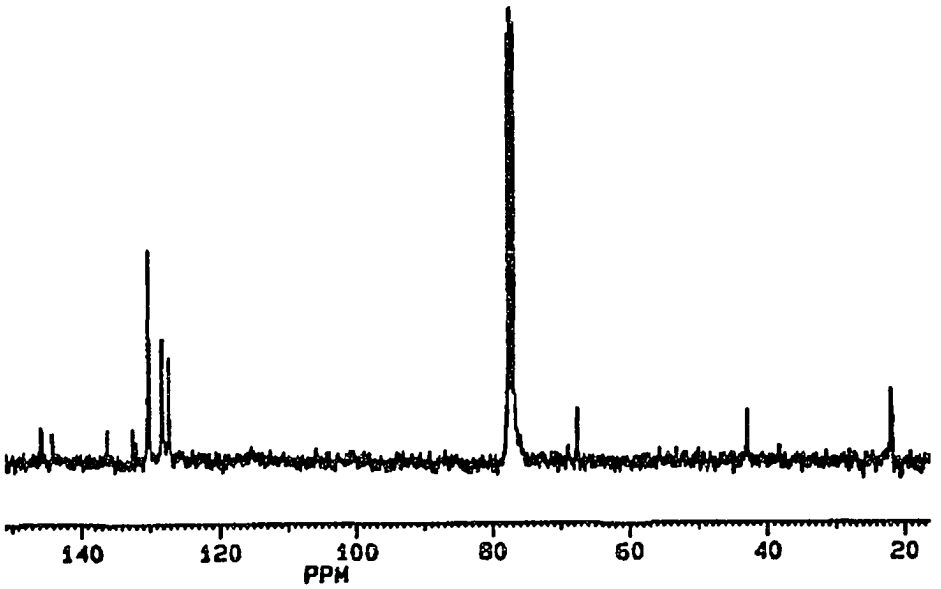

Figure A.26. 75 MHz ^{13}C NMR spectrum of 3-(p-toluenesulfonamido)-1,2-propane-di-(p-toluenesulfonate) **55** measured in $CDCl_3$.

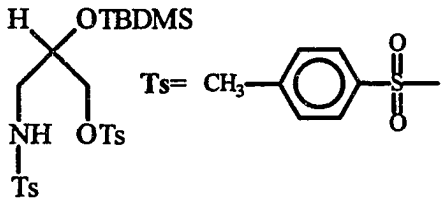

56

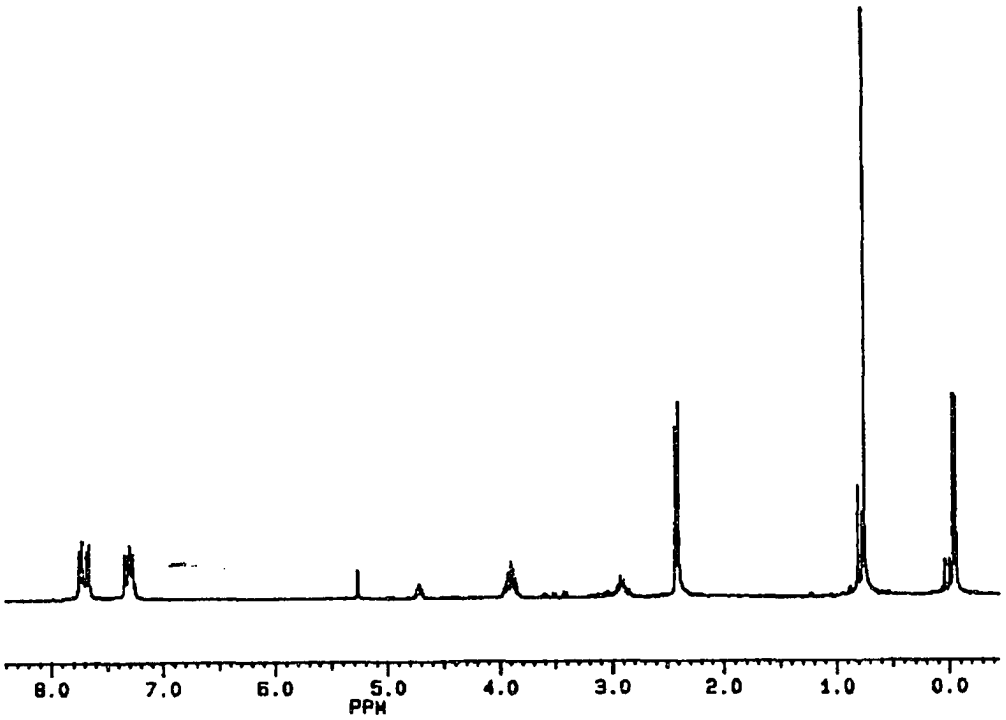

Figure A.27. 300 MHz ^{1}H NMR spectrum of 3-(p-toluenesulfonamido)-propane-2-(t-butyldimethylsiloxy)-1-(p-toluenesulfonate) **56** measured in $CDCl_3$.

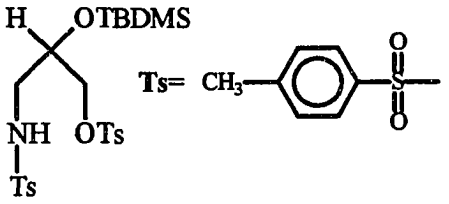

56

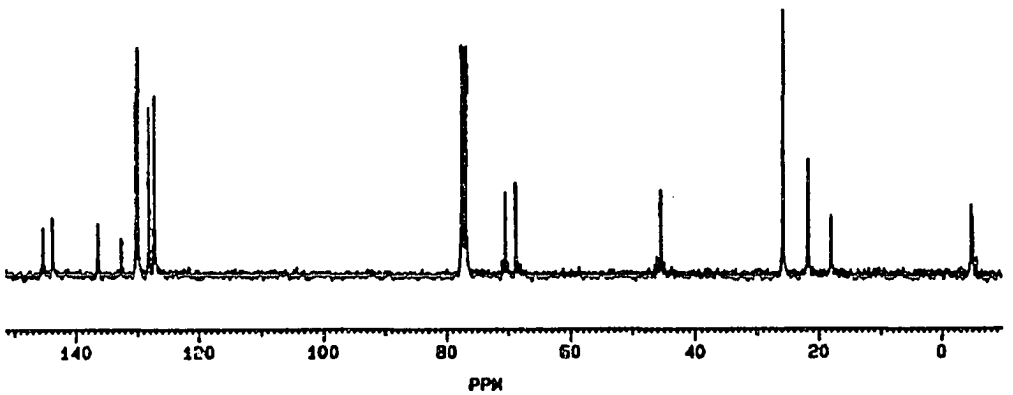

Figure A.28. 75 MHz ^{13}C NMR spectrum of 3-(p-toluenesulfonamido)-propane-2-(t-butyldimethylsiloxy)-1-(p-toluenesulfonate) **56** measured in $CDCl_3$.

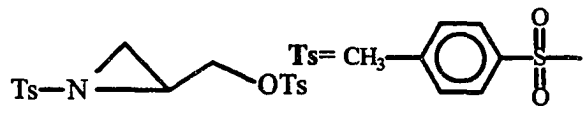

57

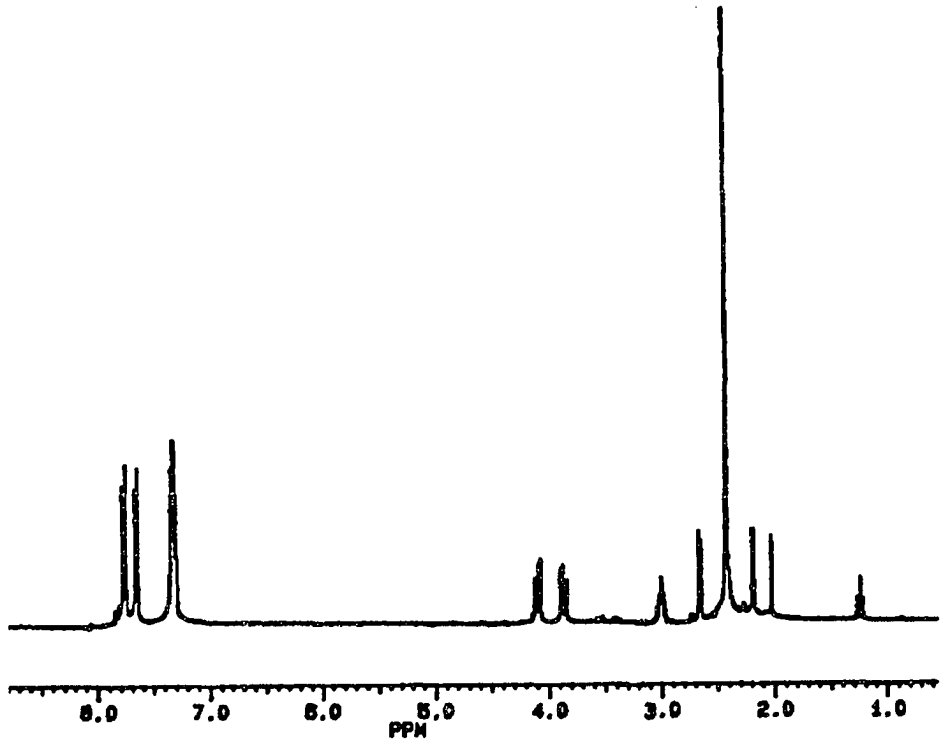

Figure A.29. 300 MHz ^{1}H NMR spectrum of N-(p-toluenesulfonyl)-2-(methyl-p-toluenesulfonate)aziridine **57** measured in $CDCl_3$.

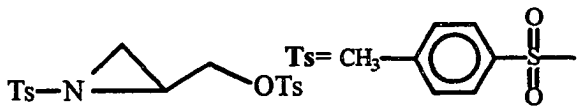

57

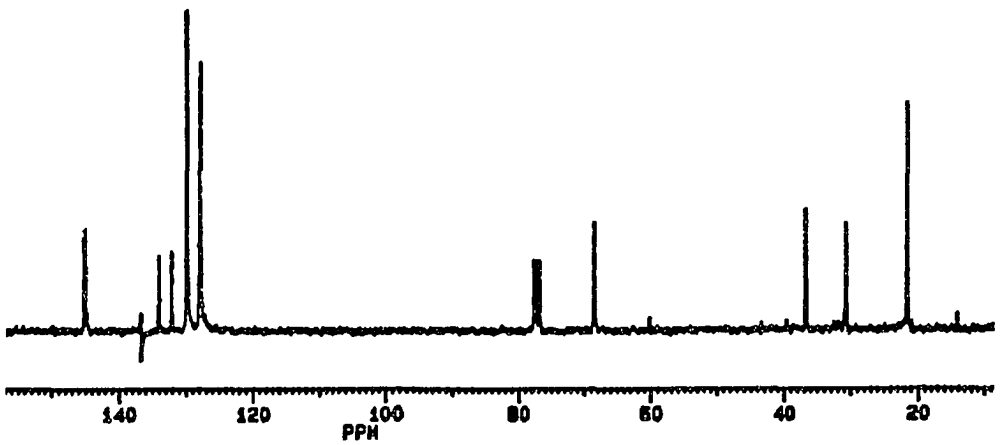

Figure A.30. 75 MHz ^{13}C NMR spectrum of N-(p-toluenesulfonyl)-2-(methyl-p-toluenesulfonate)aziridine 57 measured in $CDCl_3$.

APPENDIX B

^{1}H and ^{13}C Magnetic Resonance Spectra

^{1}H and ^{13}C magnetic resonance spectra for all compounds are reproduced in this section.

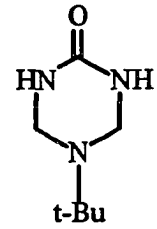

1

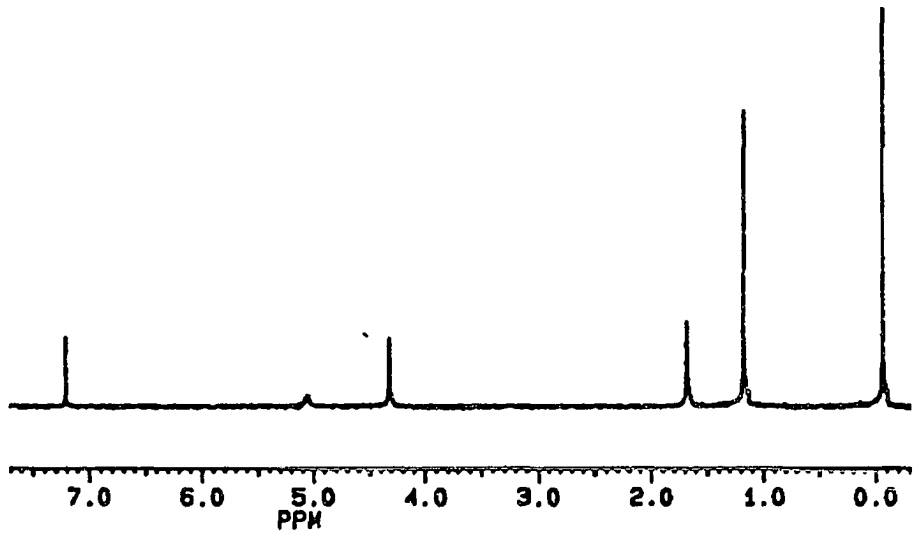

Figure B.1. 300 MHz ^{1}H NMR spectrum of 5-tert-Butyltetrahydro-1,3,5-triazine-2(1H)one **1** measured in $CDCl_3$.

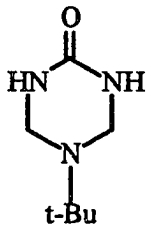

1

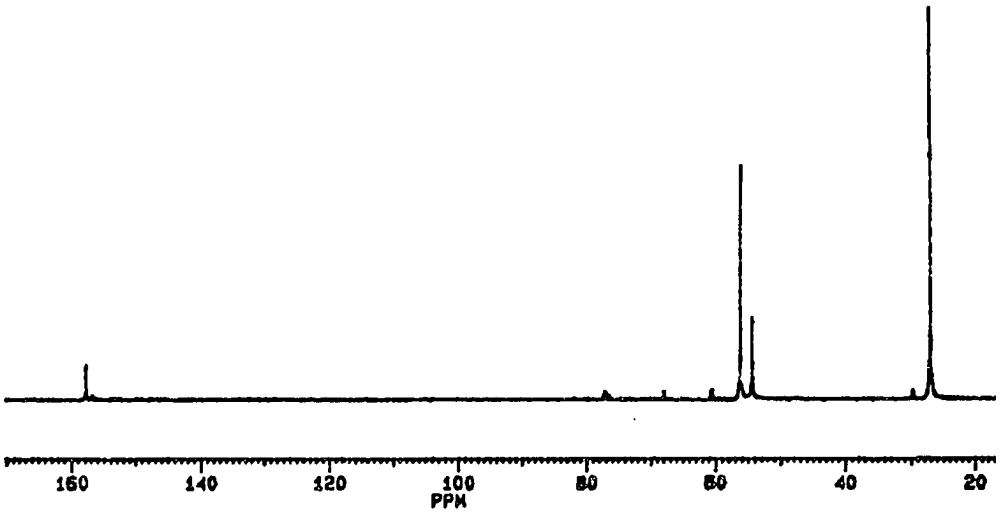

Figure B.2. 75 MHz ^{13}C NMR spectrum of 5-tert-Butyltetrahydro-1,3,5-triazine-2(1H)one **1** measured in D_2O.

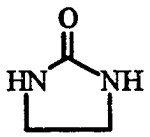

4

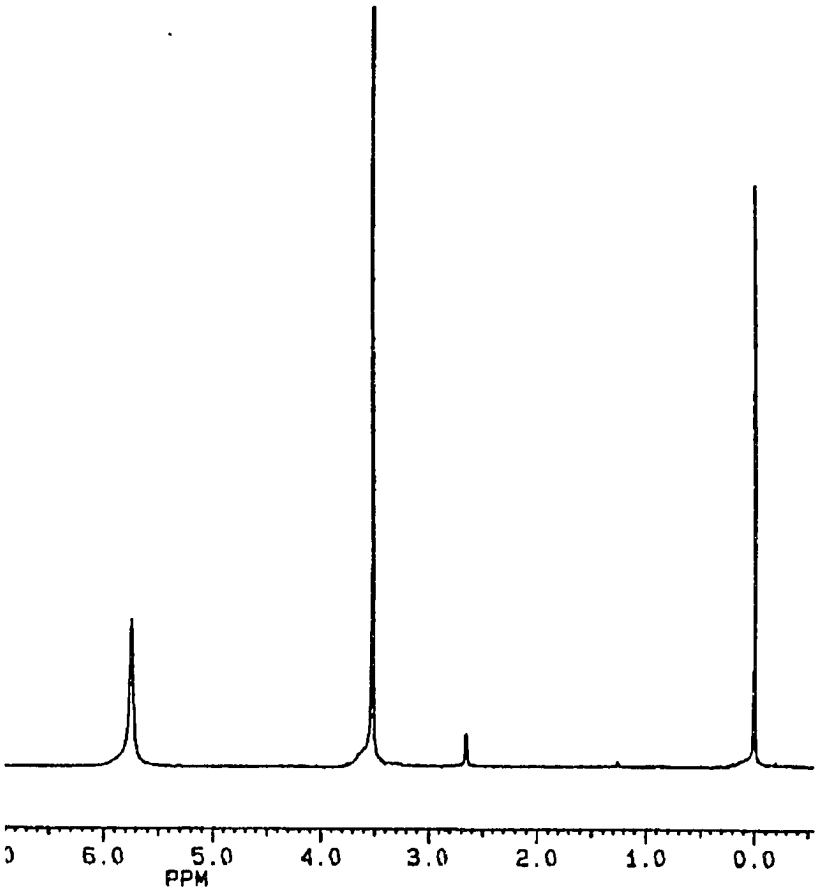

Figure B.3. 300 MHz ^{1}H NMR spectrum of 2-Imidazolidone **4** measured in $CDCl_3$.

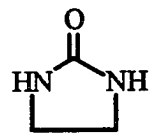

4

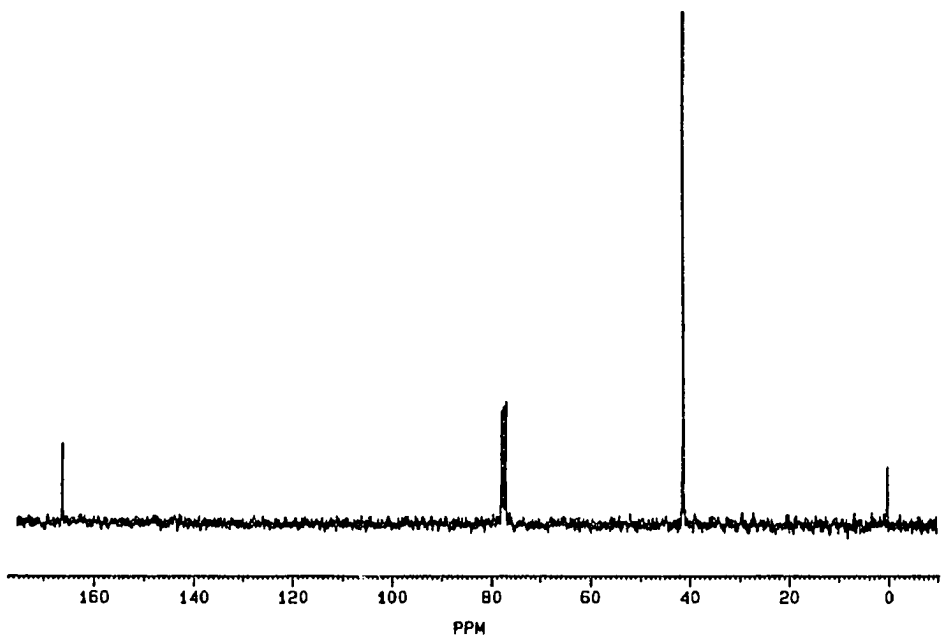

Figure B.4. 75 MHz ^{13}C NMR spectrum of 2-Imidazolidone **4** measured in $CDCl_3$.

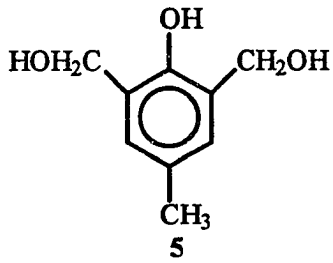

5

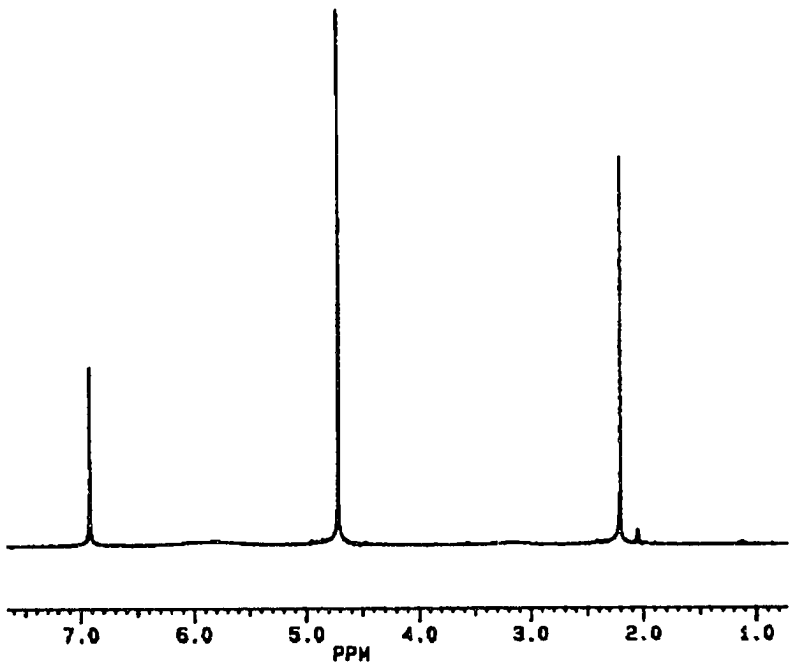

Figure B.5. 300 MHz ^{1}H NMR spectrum of 2,6-bis(hydroxymethyl)-4-methylphenol **5** measured in acetone-d_6.

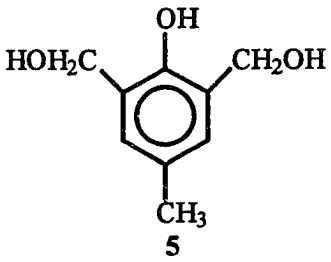

5

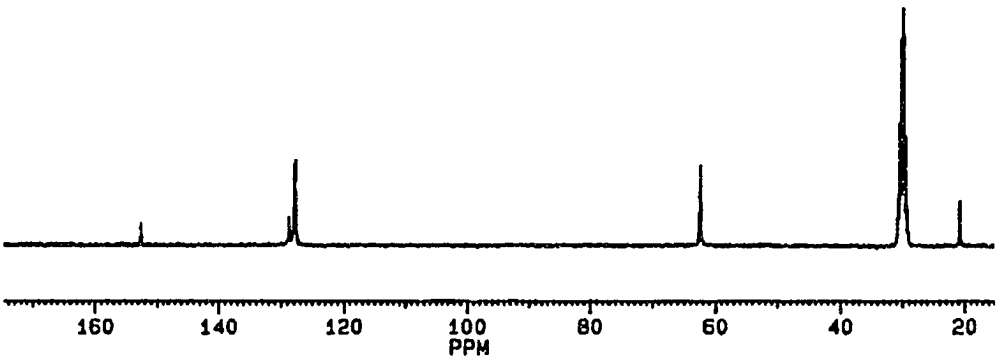

Figure B.6. 75 MHz ^{13}C NMR spectrum of 2,6-bis(hydroxymethyl)-4-methylphenol **5** measured in acetone-d_6.

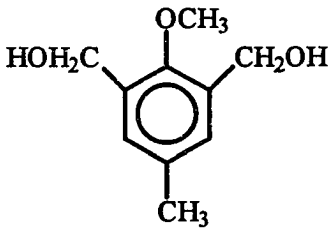

6

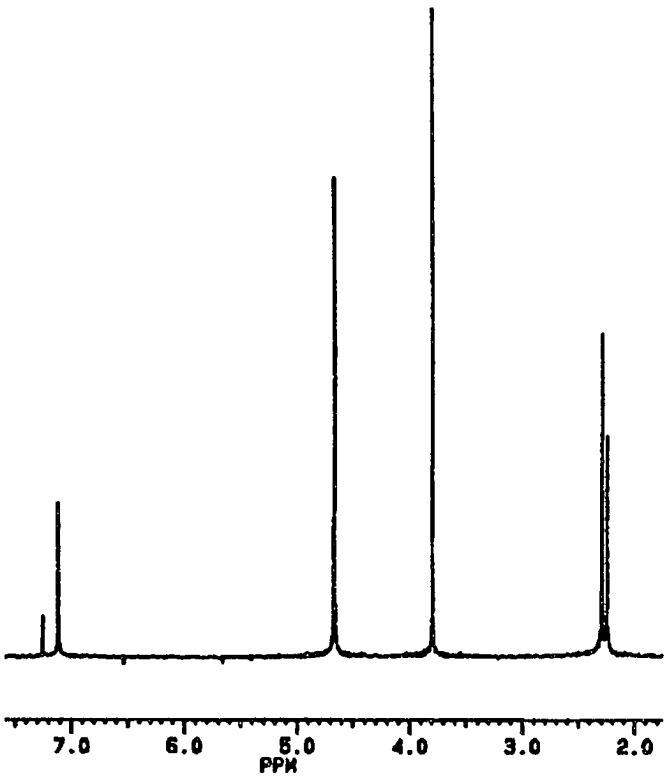

Figure B.7. 300 MHz ^{1}H NMR spectrum of 2,6-bis(hydroxymethyl)-4-methylanisole **6** measured measured in $CDCl_3$.

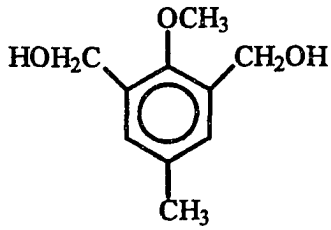

6

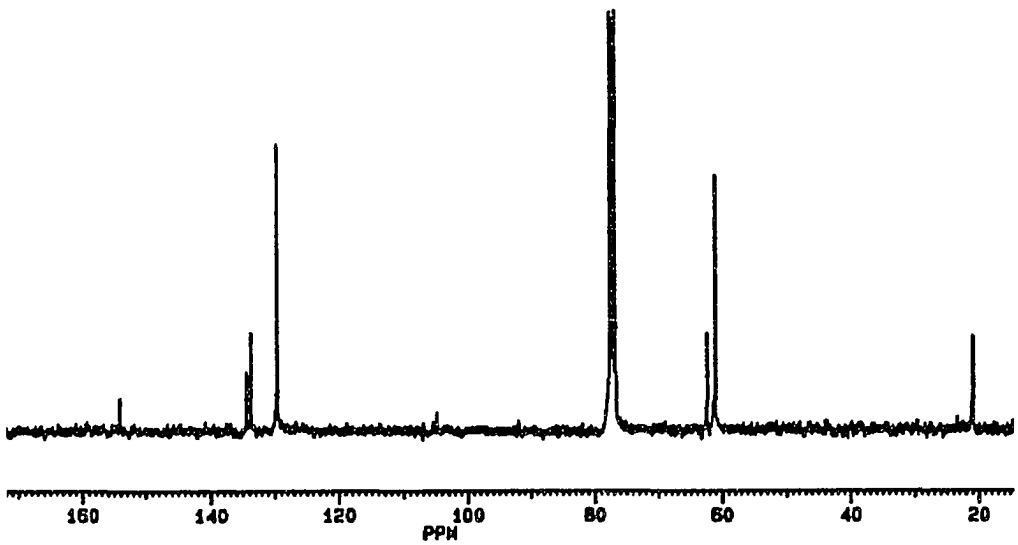

Figure B.8. 75 MHz ^{13}C NMR spectrum of 2,6-bis(hydroxymethyl)-4-methylanisole **6** measured in $CDCl_3$.

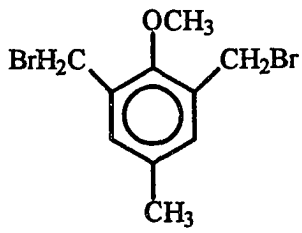

7

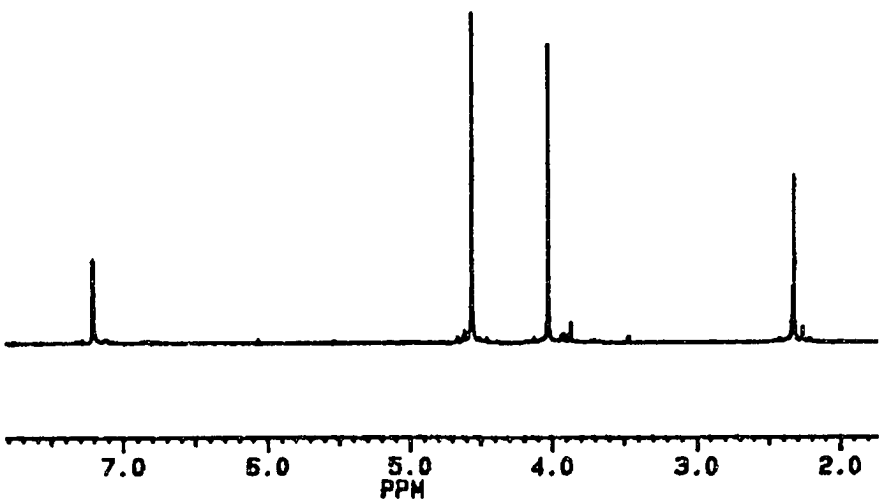

Figure B.9. 300 MHz ^{1}H NMR spectrum of 2,6-bis(bromomethyl)-4-metylanisole **7** measured in $CDCl_3$.

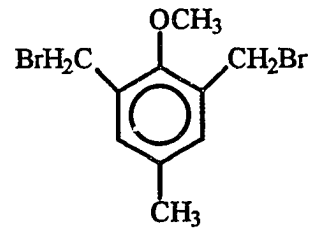

7

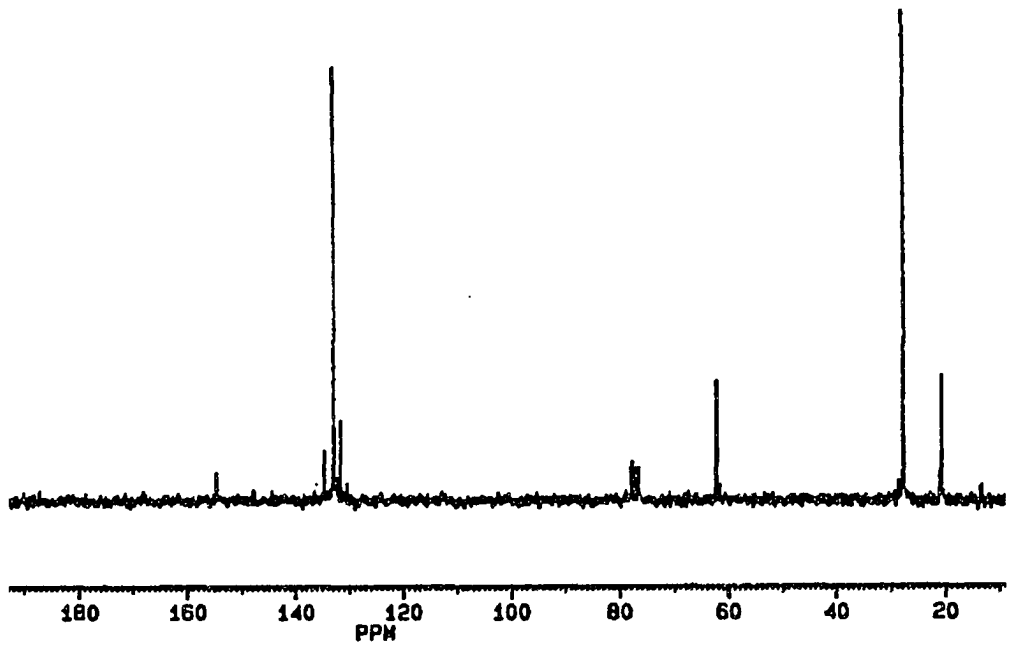

Figure B.10. 75 MHz ^{13}C NMR spectrum of 2,6-bis(bromomethyl)-4-metylanisole 7 measured in $CDCl_3$.

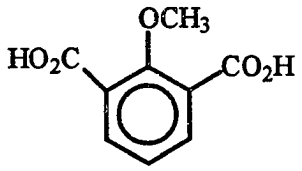

11

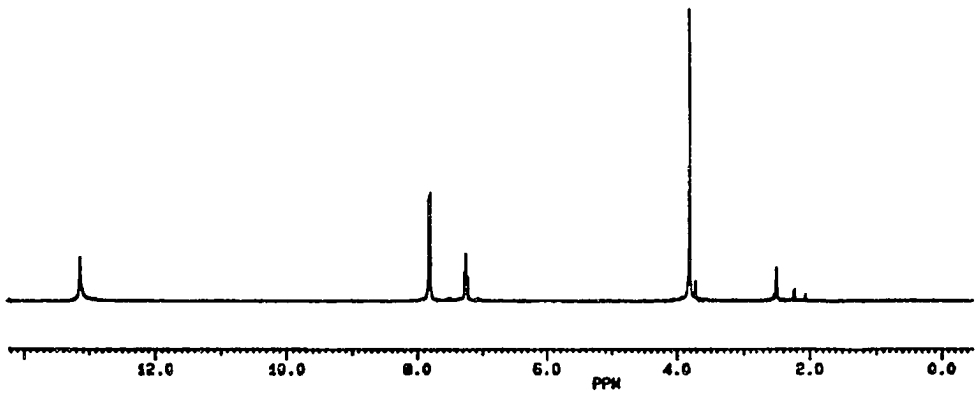

Figure B.11. 300 MHz ^{1}H NMR spectrum of 2-Methoxy-1,3-benzene-dicarboxylic acid **11** measured in DMSO-d_6.

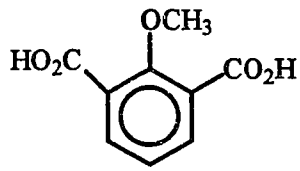

11

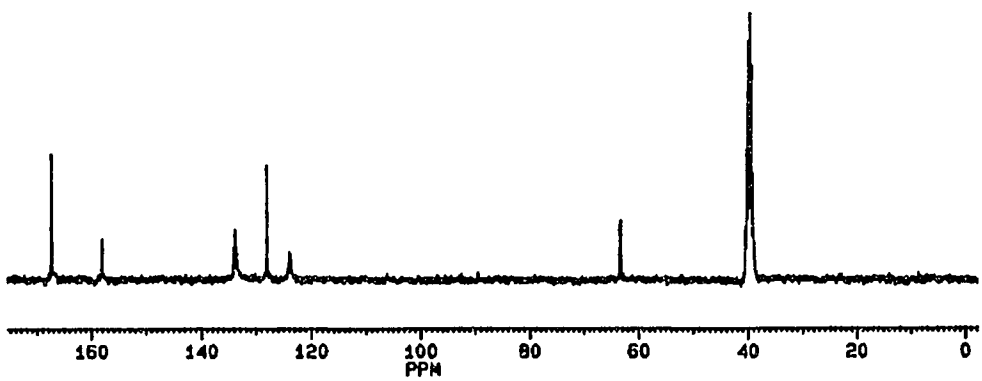

Figure B.12. 75 MHz ^{13}C NMR spectrum of 2-Methoxy-1,3-benzene-dicarboxylic acid **11** measured in DMSO-d_6.

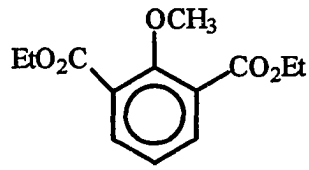

12

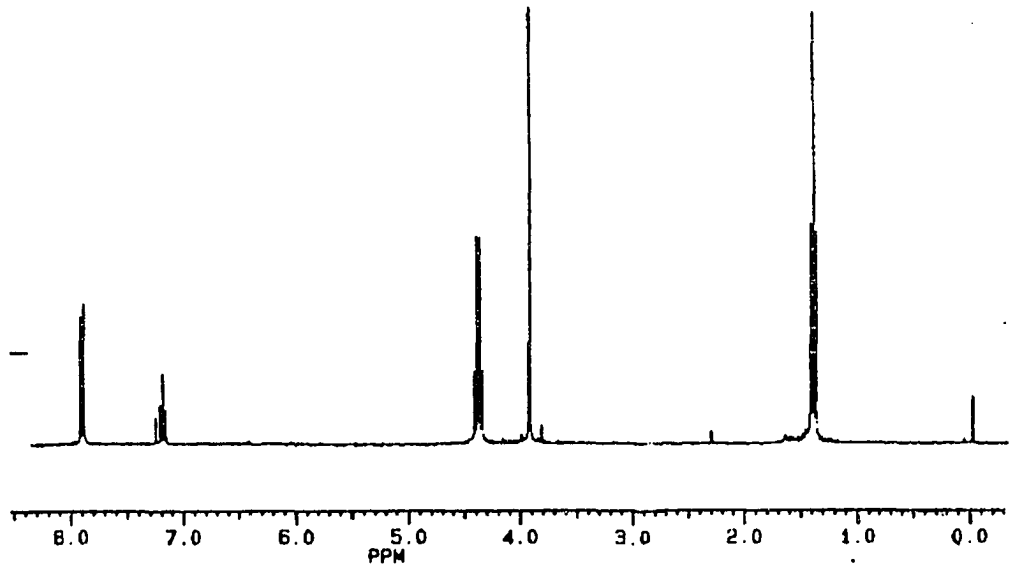

Figure B.13. 300 MHz ^{1}H NMR spectrum of 2-methoxy-1,3-benzene-dicarboxylic ethylester **12** measured in $CDCl_3$.

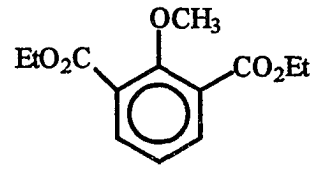

12

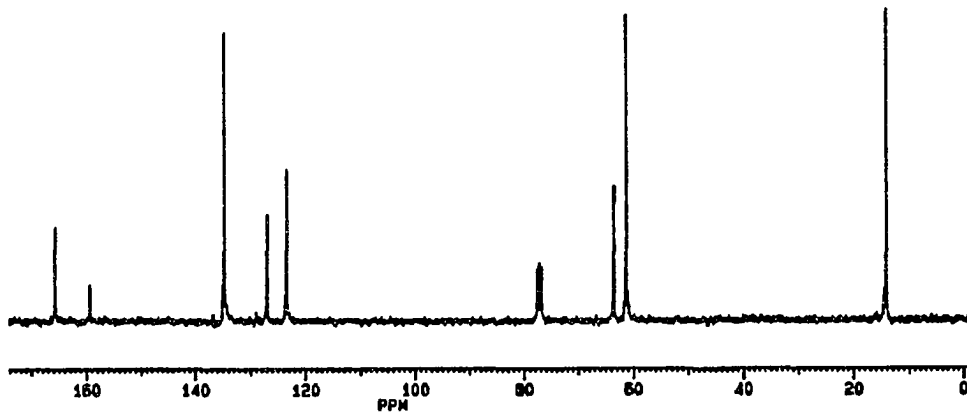

Figure B.14. 75 MHz ^{13}C NMR spectrum of 2-methoxy-1,3-benzene-dicarboxylic ethyl ester **12** measured in $CDCl_3$.

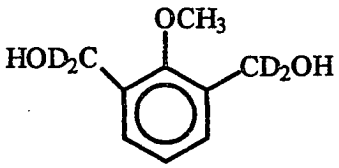

13

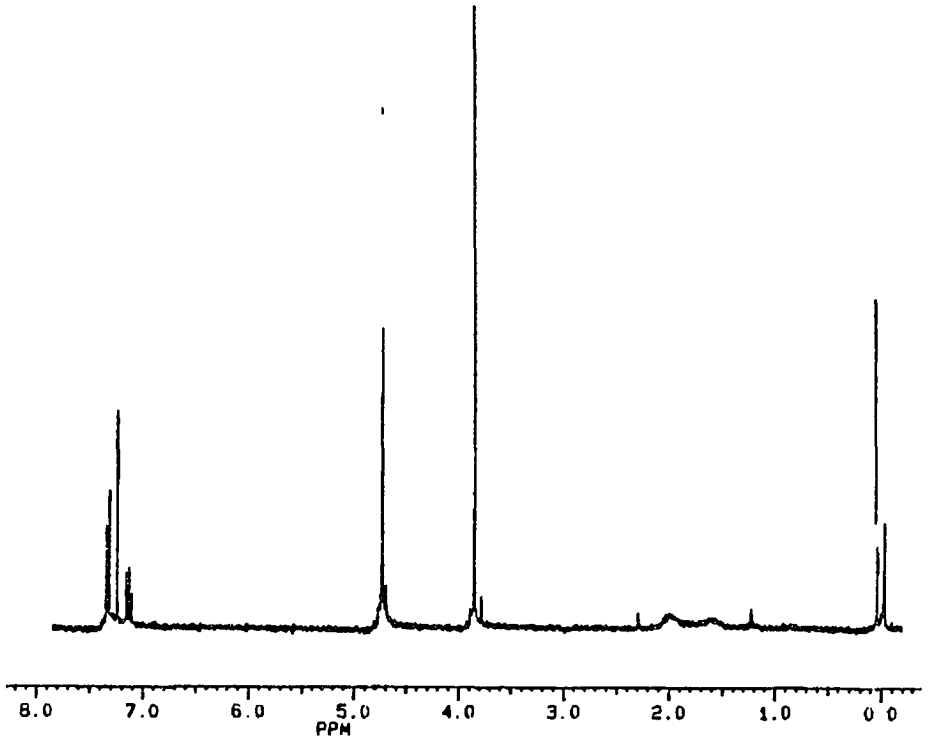

Figure B.15. 300 MHz ^{1}H NMR spectrum of 2,6-bis(hydroxymethyl-d_2)anisole **13** measured in $CDCl_3$.

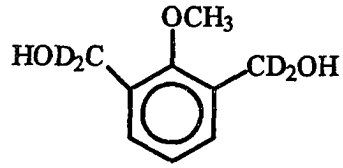

13

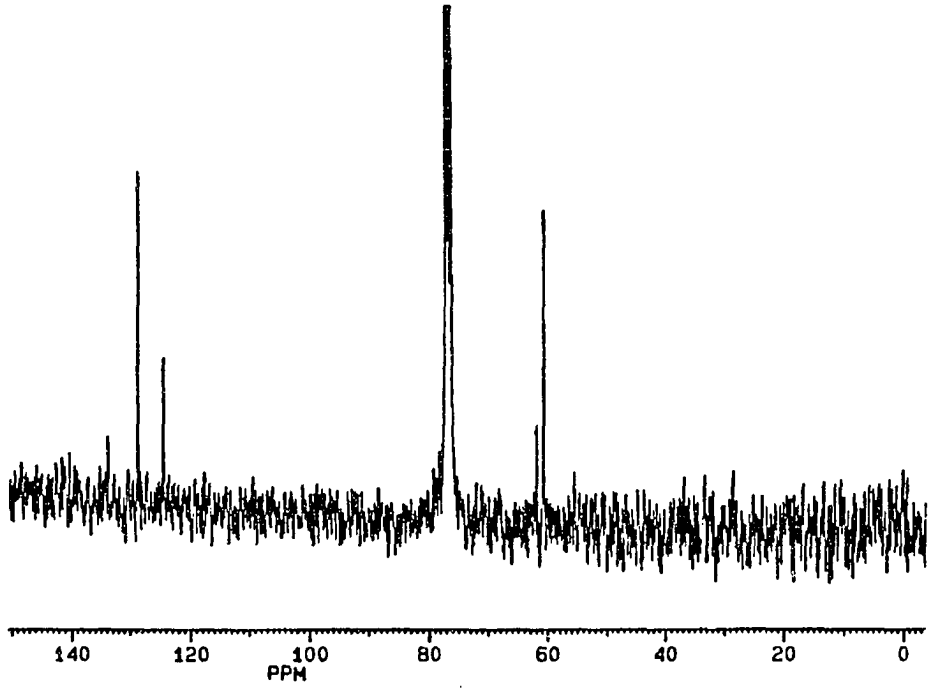

Figure B.16. 75 MHz ^{13}C NMR spectrum of 2,6-bis(hydroxymethyl-d_2)anisole **13** measured in $CDCl_3$.

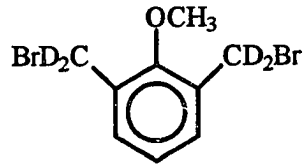

14

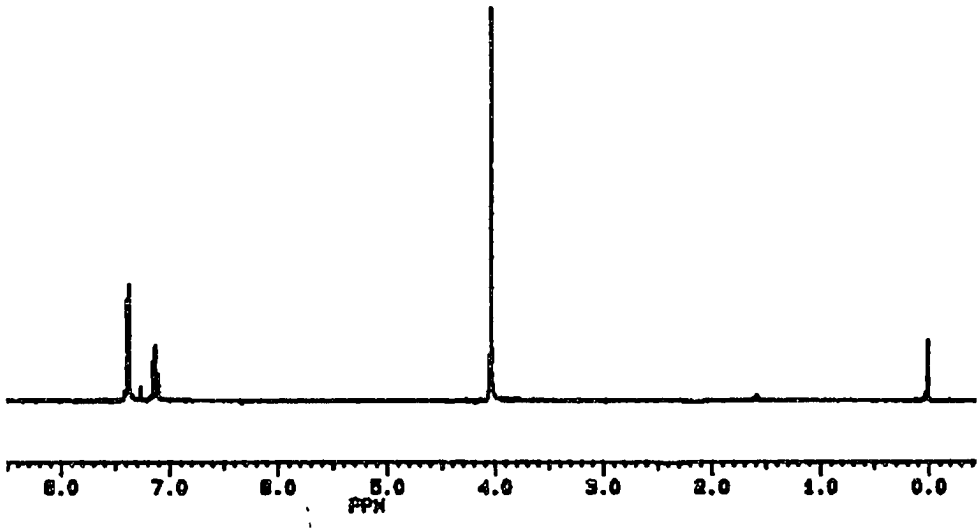

Figure B.17. 300 MHz ^{1}H NMR spectrum of 2,6-bis(bromomethyl-d_2)anisole **14** measured in $CDCl_3$.

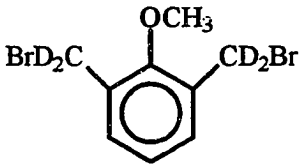

14

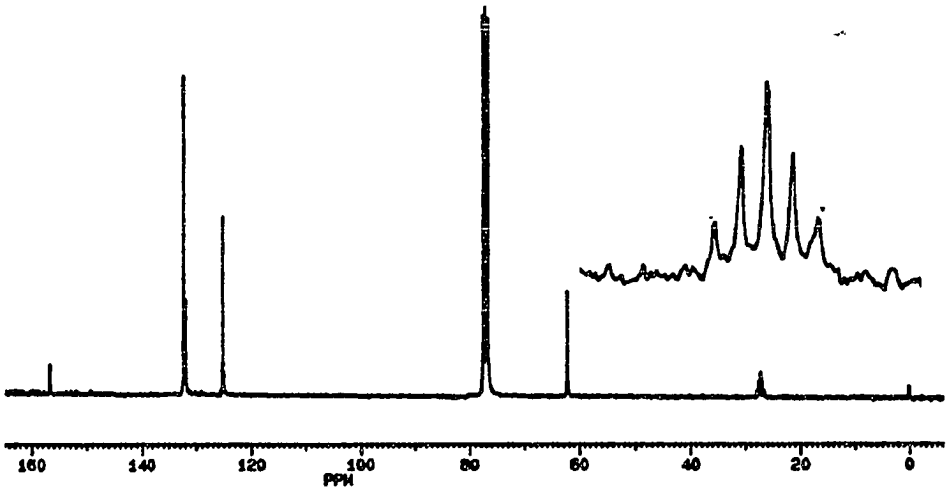

Figure B.18. 75 MHz ^{13}C NMR spectrum of 2,6-bis(bromomethyl-d_2)anisole **14** measured in $CDCl_3$.

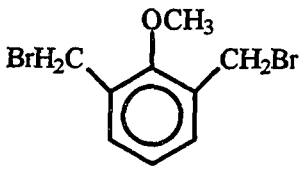

15

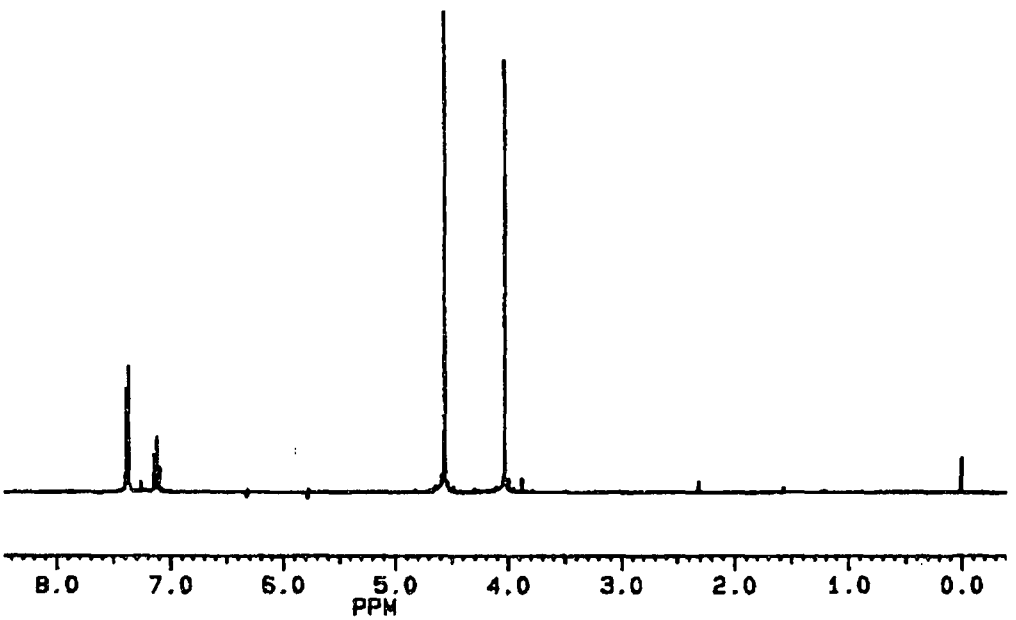

Figure B.19. 300 MHz ^{1}H NMR spectrum of 2,6-bis(bromomethyl)anisole **15** measured in $CDCl_3$.

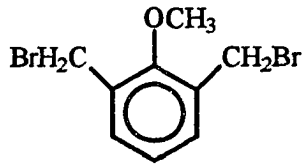

15

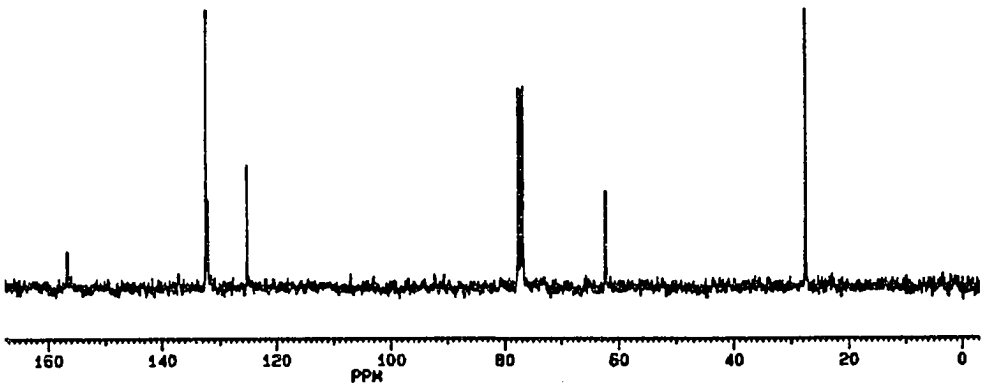

Figure B.20. 75 MHz ^{13}C NMR spectrum of 2,6-bis(bromomethyl)anisole **15** measured in $CDCl_3$.

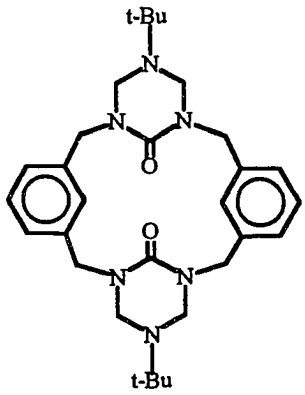

2a

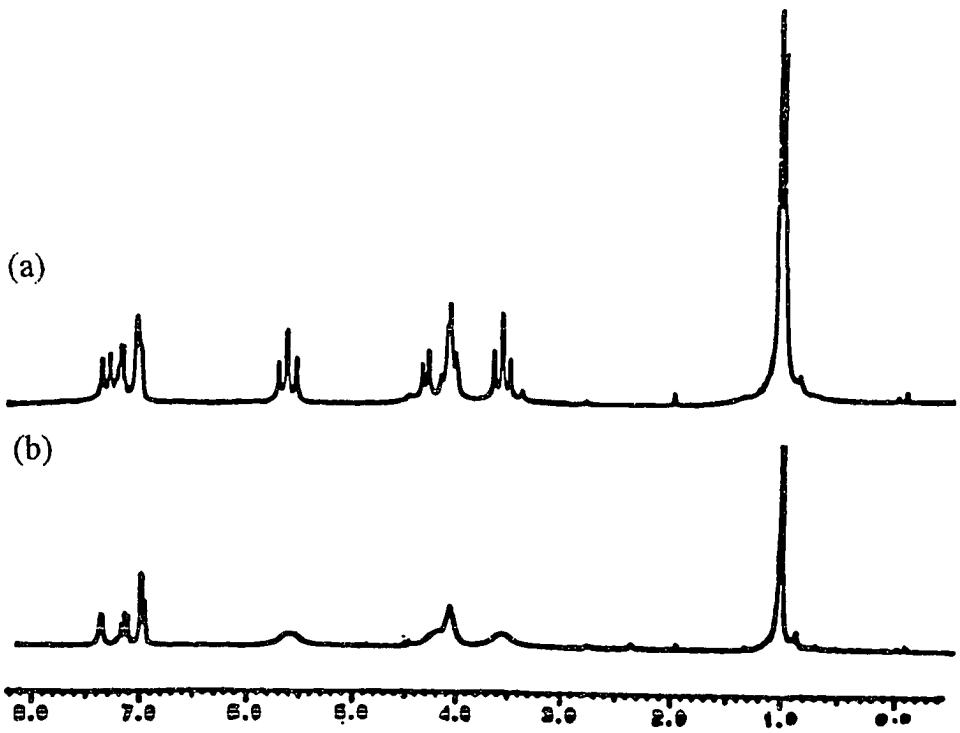

Figure B.21. 200 MHz ^{1}H NMR spectra of macrocycle **2a** measured in $CDCl_3$ at (a) 300K and (b) 250K.

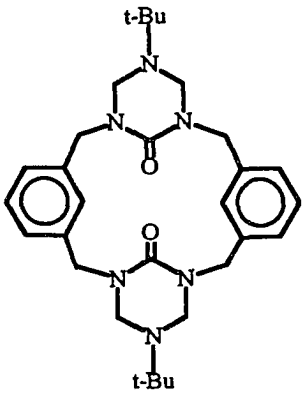

2a

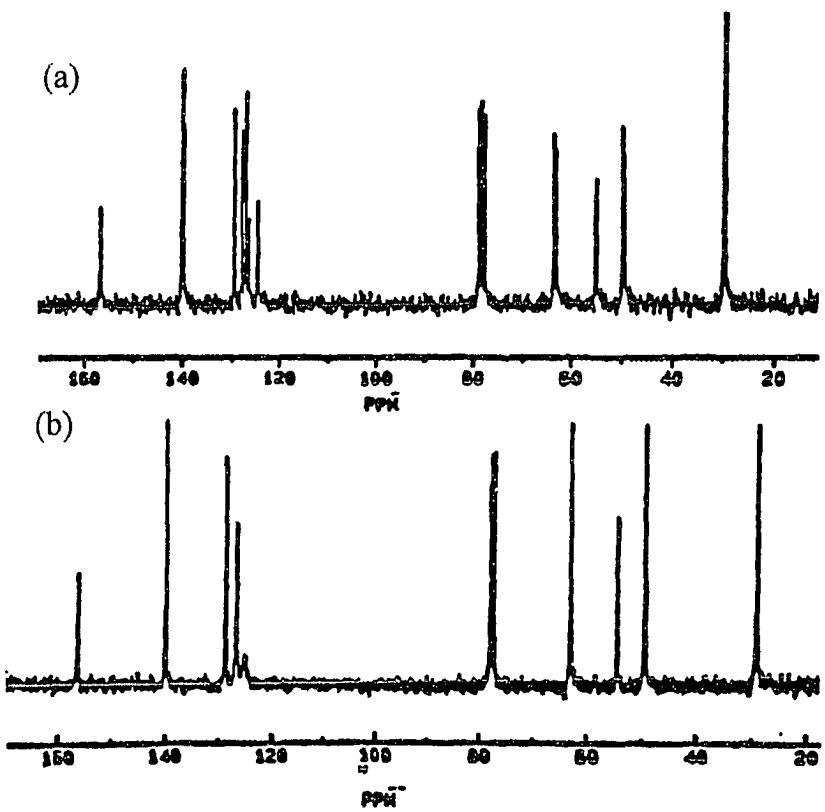

Figure B.22. 50 MHz ^{13}C NMR spectra of macrocycle **2a** measured in $CDCl_3$ at (a) 250K and (b) 300K.

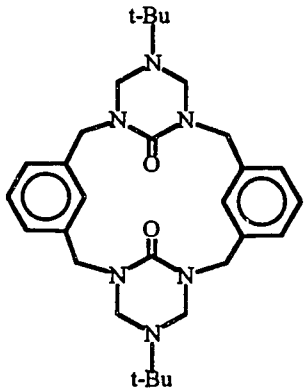

2a

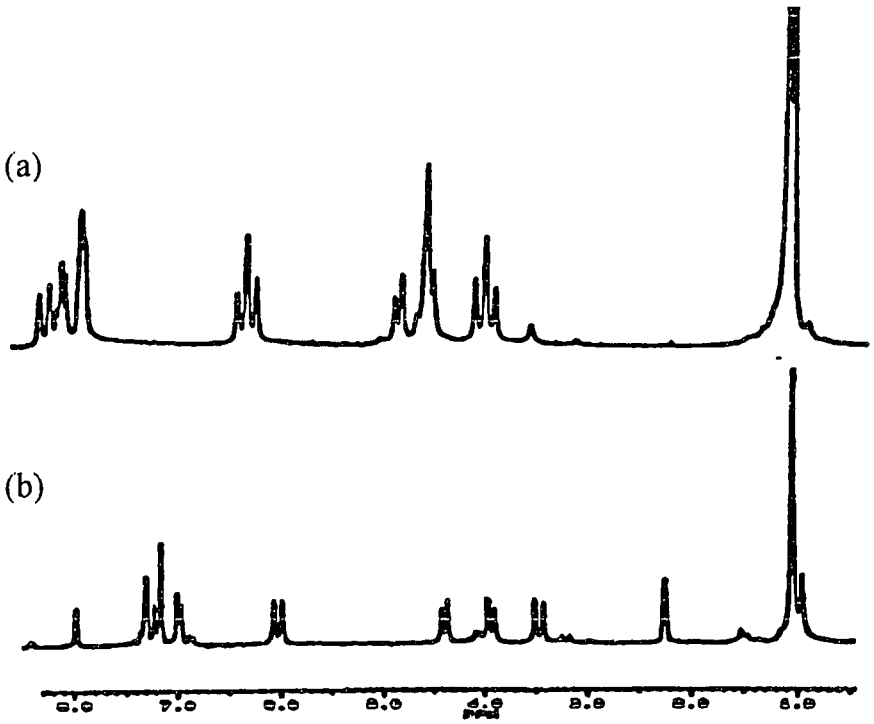

Figure B.23. 200 MHz ^{1}H NMR spectra of macrocycle **2a** measured in (a) $CDCl_3$ and (b) toluene-d_8 at 240K.

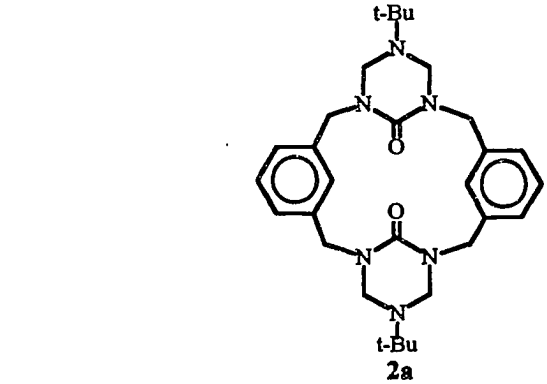

2a

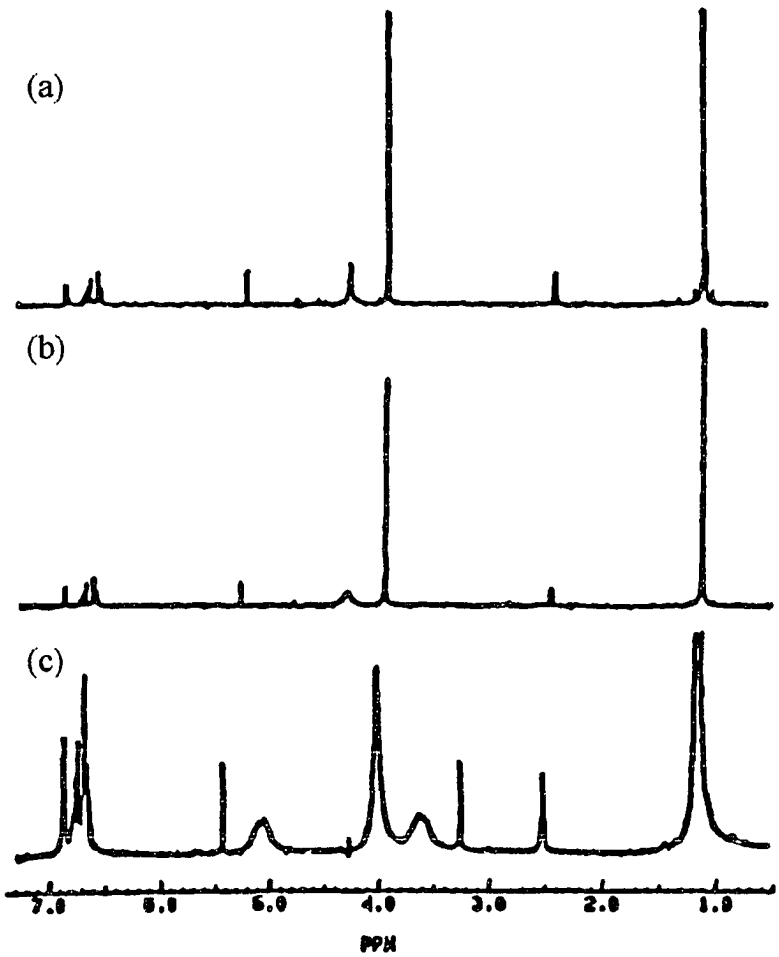

Figure B.24. 200 MHz dynamic ^{1}H NMR spectra of macrocycle **2a** measured in DMSO-d_6 at (a) 405K (b) 375K and (c) 300K.

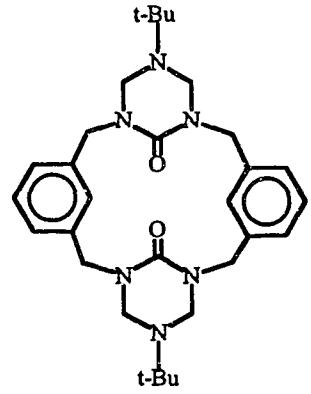

2a

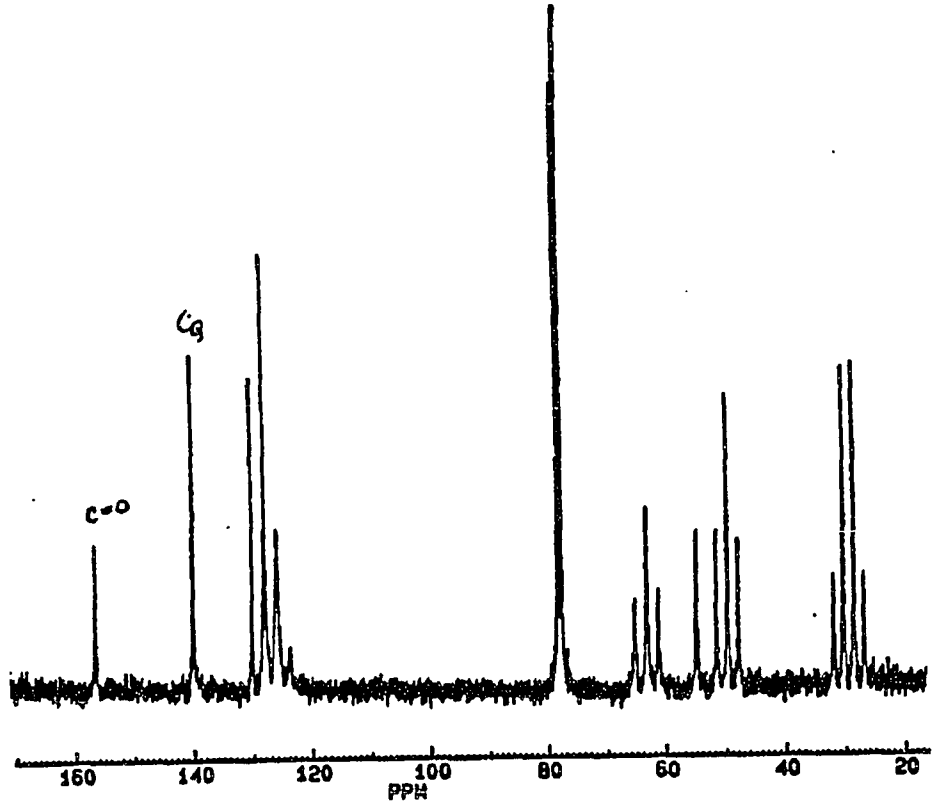

Figure B.25. 200/50 MHz ^{1}H-^{13}C coupled NMR spectrum of macrocycle **2a** measured in $CDCl_3$ at 300K.

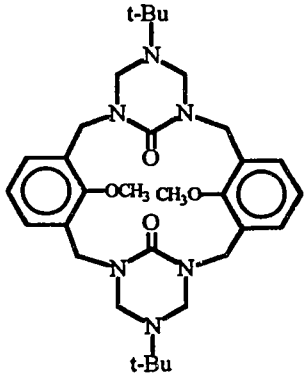

2b

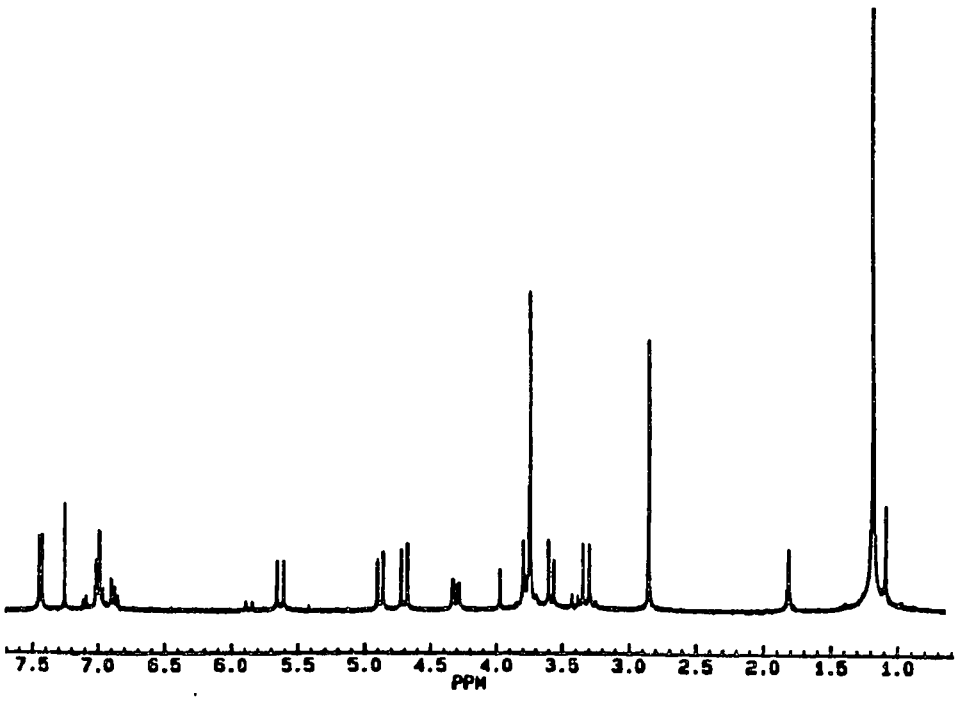

Figure B.26. 300 MHz ^{1}H NMR spectrum of macrocycle **2b** measured in $CDCl_3$ at 300K.

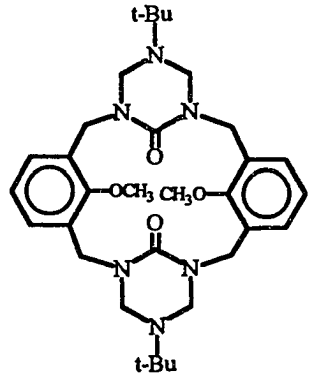

2b

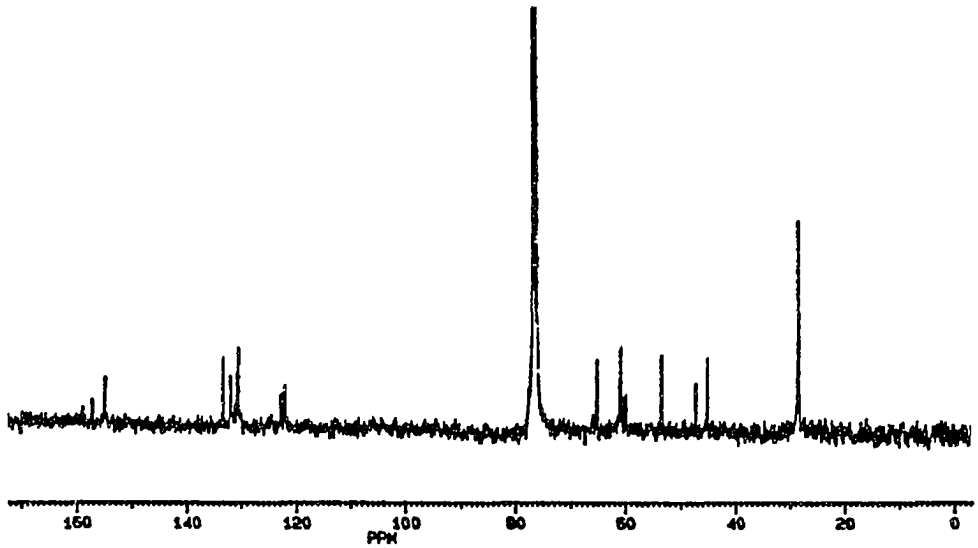

Figure B.27. 75 MHz ^{13}C NMR spectrum of macrocycle **2b** measured in $CDCl_3$ at 300K.

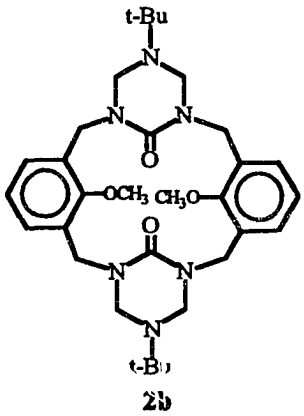

2b

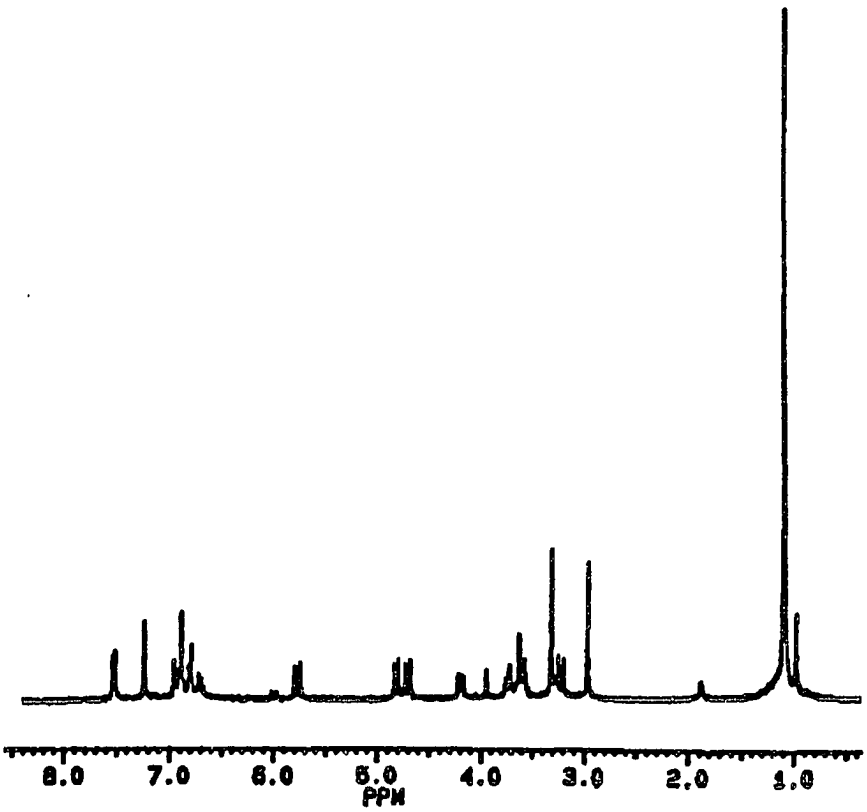

Figure B.28. 300 MHz ^{1}H NMR spectrum of macrocycle **2b** measured in C_6D_6 at 300K.

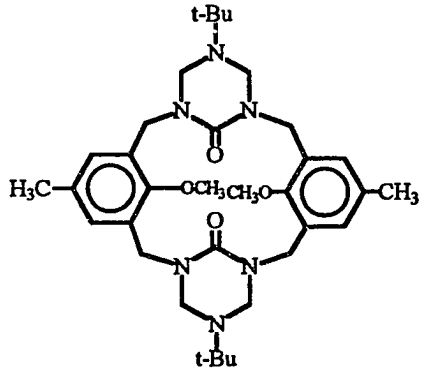

2c

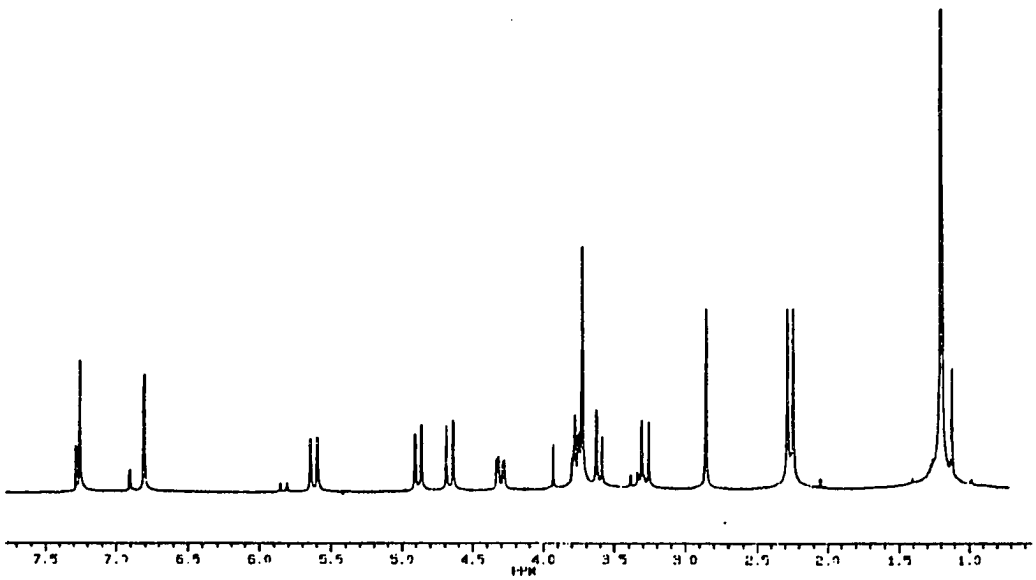

Figure B.29. 300 MHz ^{1}H NMR spectrum of macrocycle **2c** in $CDCl_3$ measured at 300K.

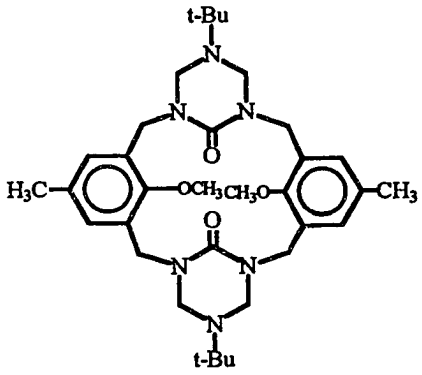

2c

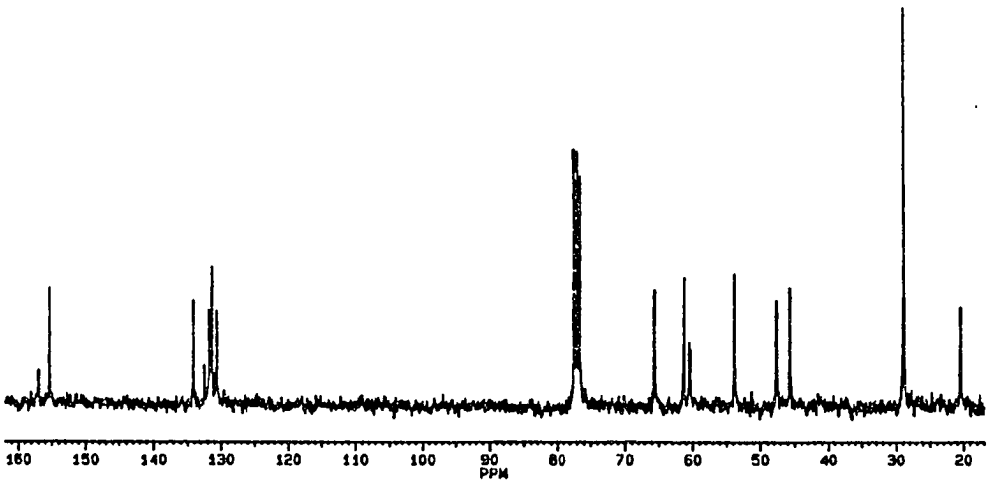

Figure B.30. 75 MHz ^{13}C NMR spectrum of macrocycle **2c** measured in $CDCl_3$ at 300K.

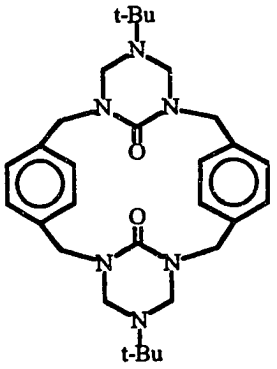

3

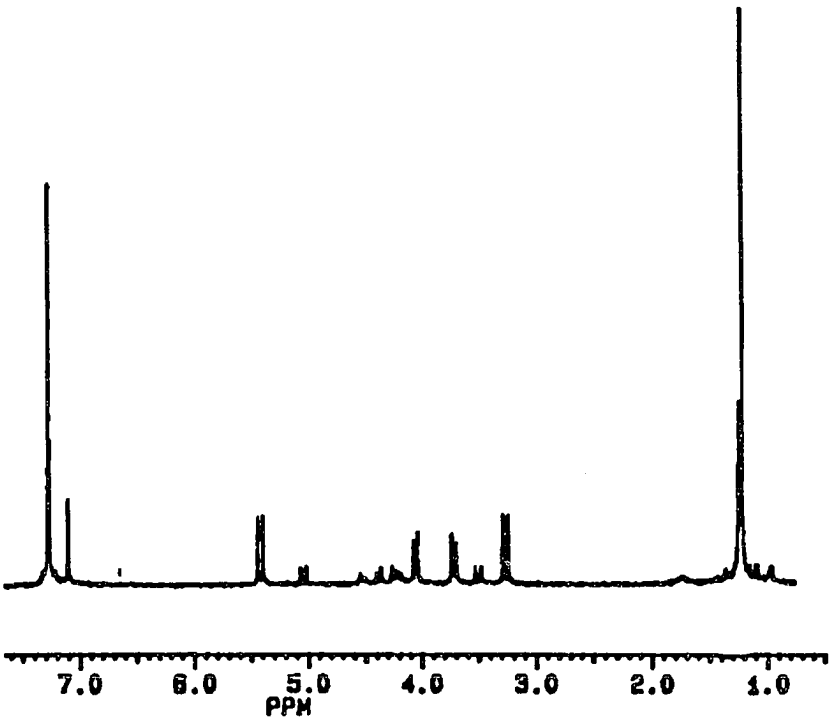

Figure B.31. 300 MHz ^{1}H NMR spectrum of macrocycle **3** measured in $CDCl_3$ at 300K.

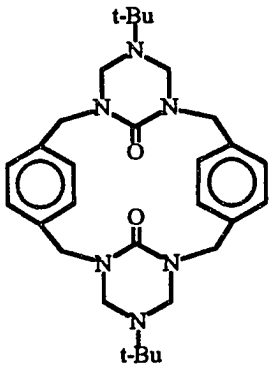

3

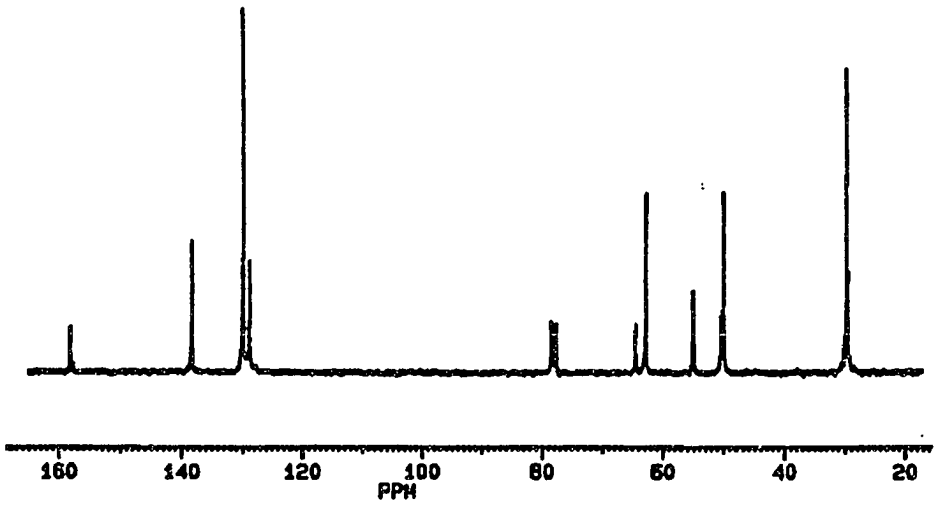

Figure B.32. 75 MHz ^{13}C NMR spectrum of macrocycle **3** measured in $CDCl_3$ at 300K.

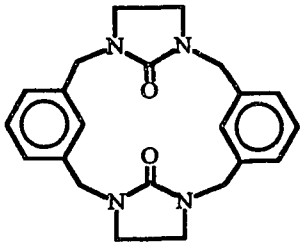

8

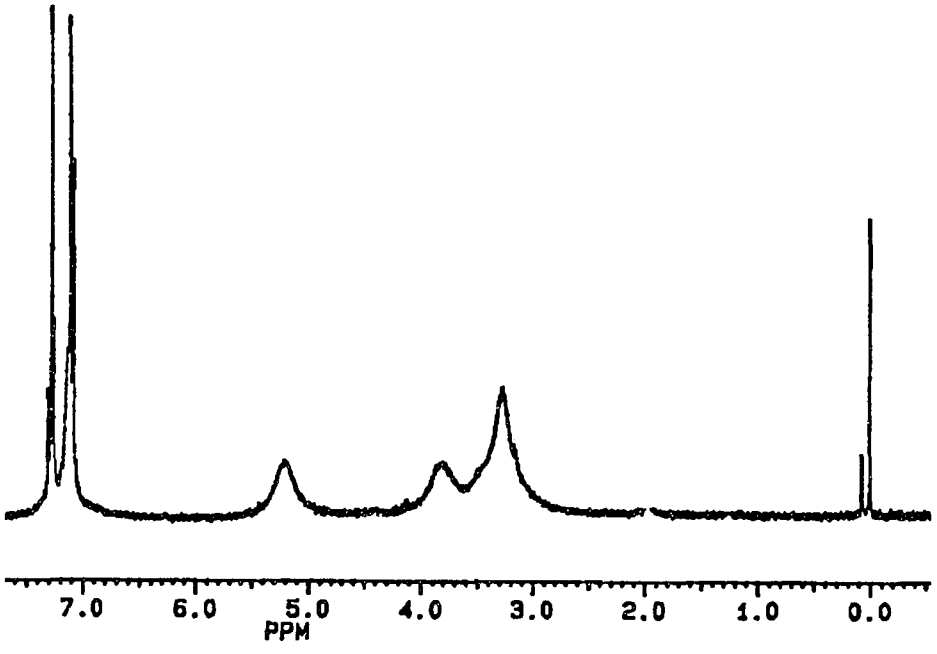

Figure B.33. 300 MHz ^{1}H NMR spectrum of macrocycle **8** measured in $CDCl_3$ at 300K.

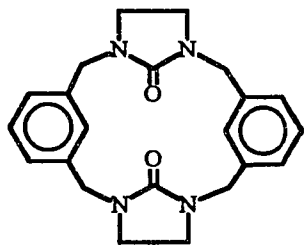

8

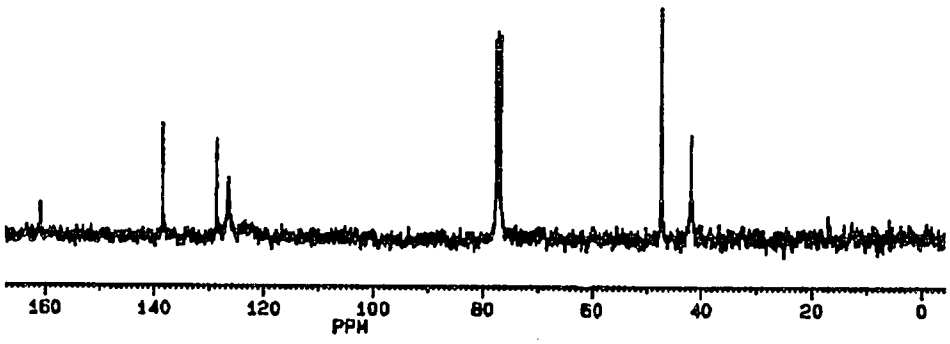

Figure B.34. 75 MHz ^{13}C NMR spectrum of macrocycle **8** measured in $CDCl_3$. at 300K.

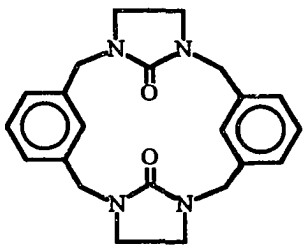

8

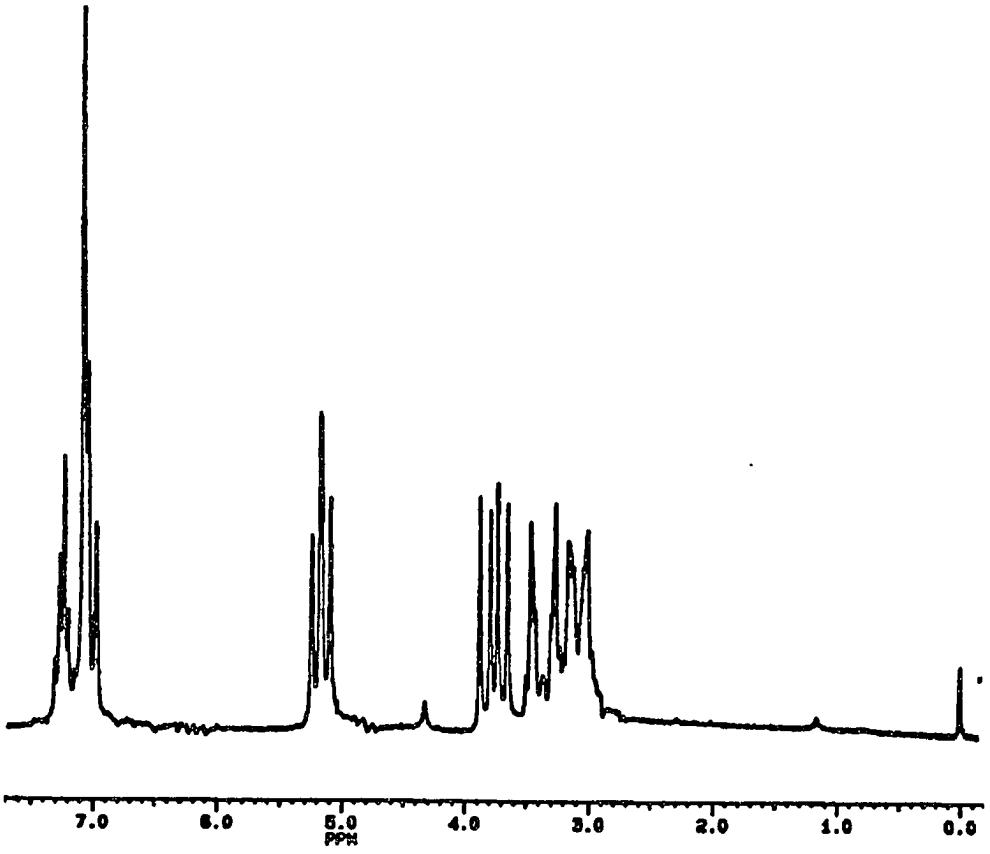

Figure B.35. 200 MHz ^{1}H NMR spectrum of macrocycle **8** measured in $CDCl_3$ at 250K.

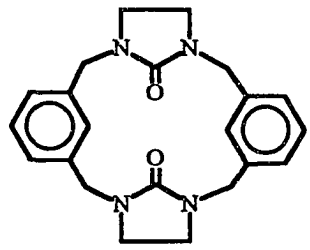

8

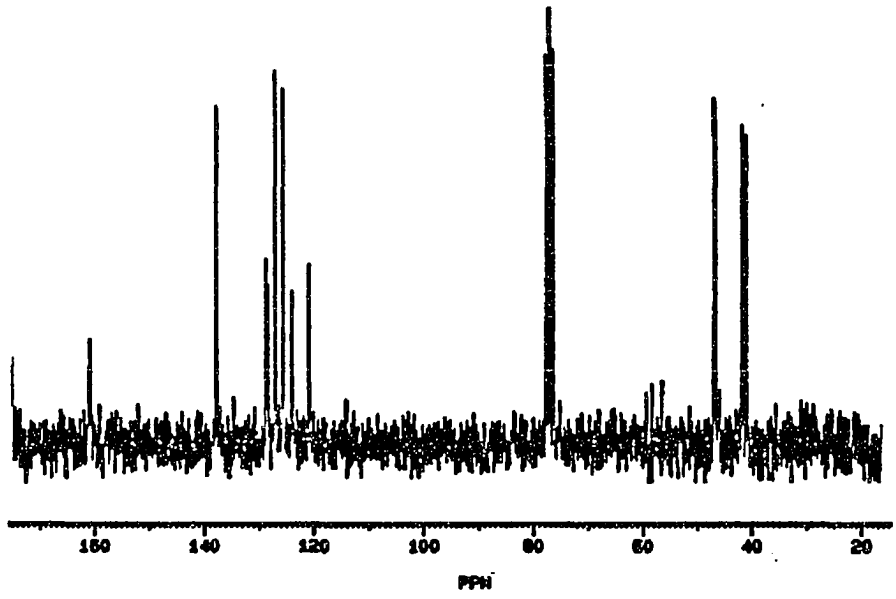

Figure B.36. 50 MHz ^{13}C NMR spectrum of macrocycle **8** measured in $CDCl_3$ at 250K.

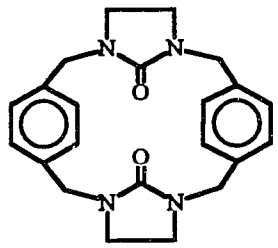

9

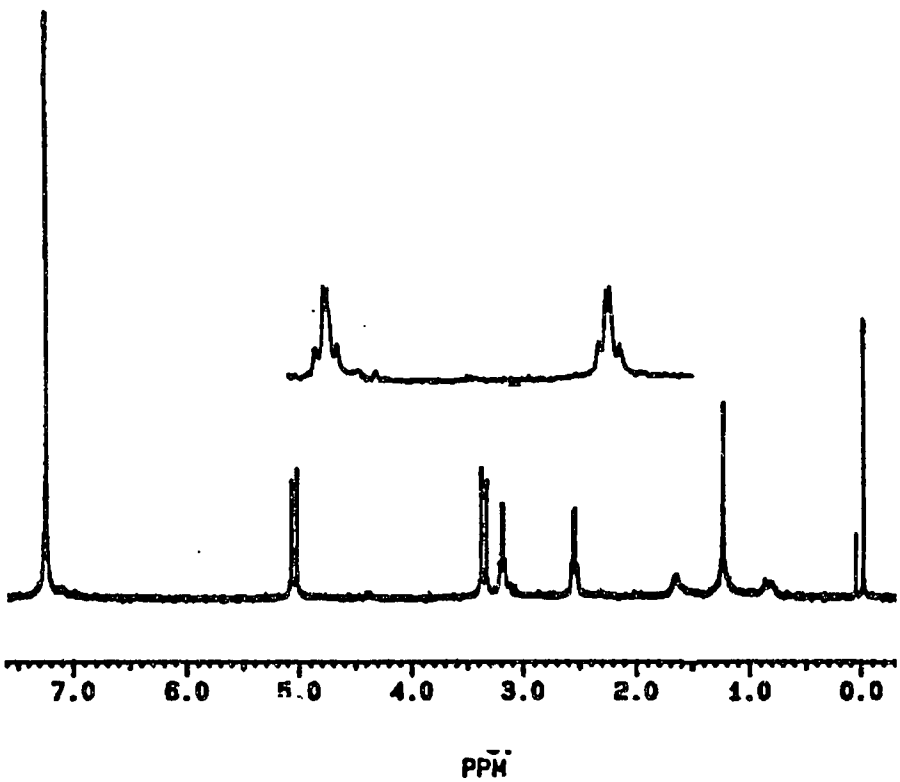

Figure B.37. 300 MHz ^{1}H NMR spectrum of macrocycle **9** measured in $CDCl_3$ at 300K.

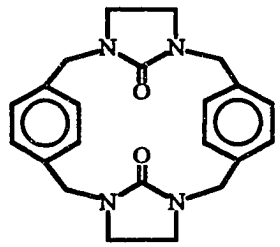

9

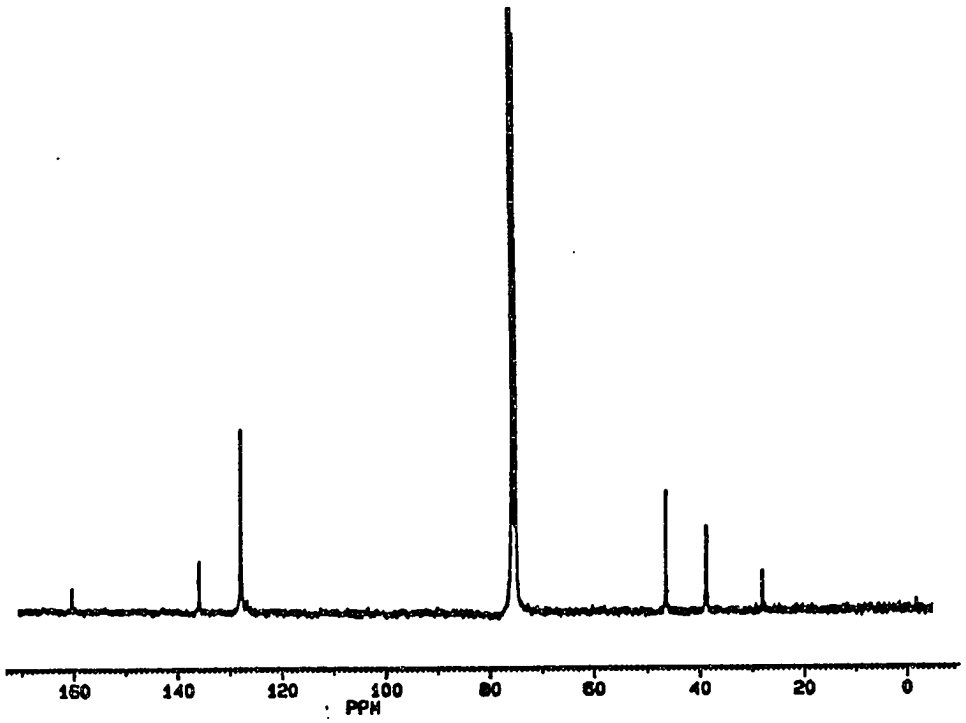

Figure B.38. 75 MHz ^{13}C NMR spectrum of macrocycle **8** measured in $CDCl_3$ at 300K.

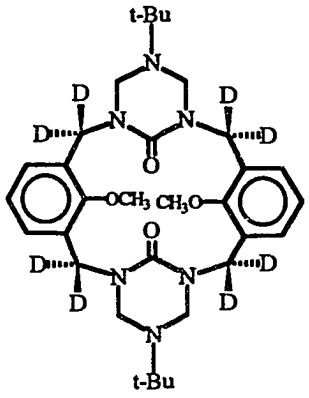

10

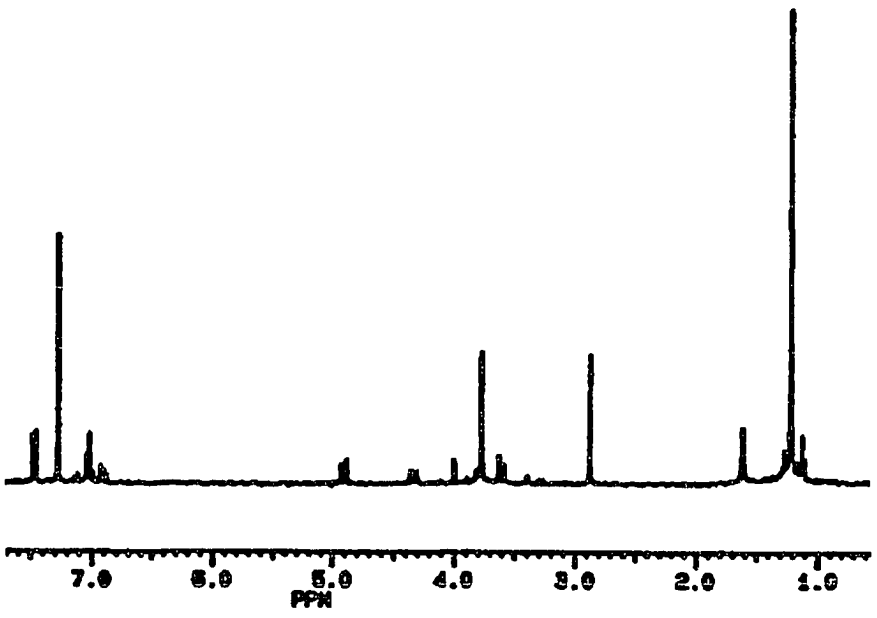

Figure B.39. 300 MHz ^{1}H NMR spectrum of macrocycle **10** measured in $CDCl_3$ at 300K.

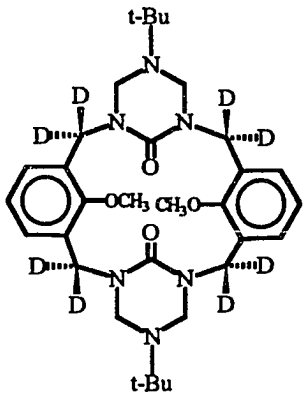

10

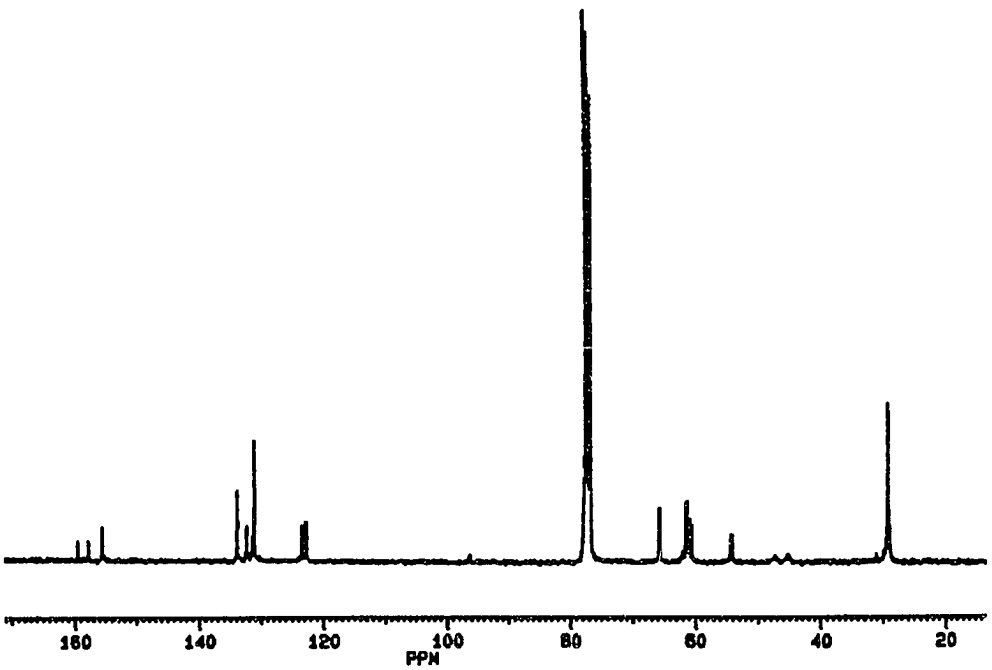

Figure B.40. 75 MHz ^{13}C NMR spectrum of macrocycle **10** in $CDCl_3$ measured at 300K.

APPENDIX C

Two-Dimensional Magnetic Resonance Spectra

Two-dimensional magnetic resonance spectra for all compounds are reproduced in this section.

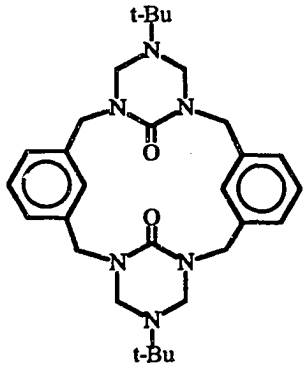

2a

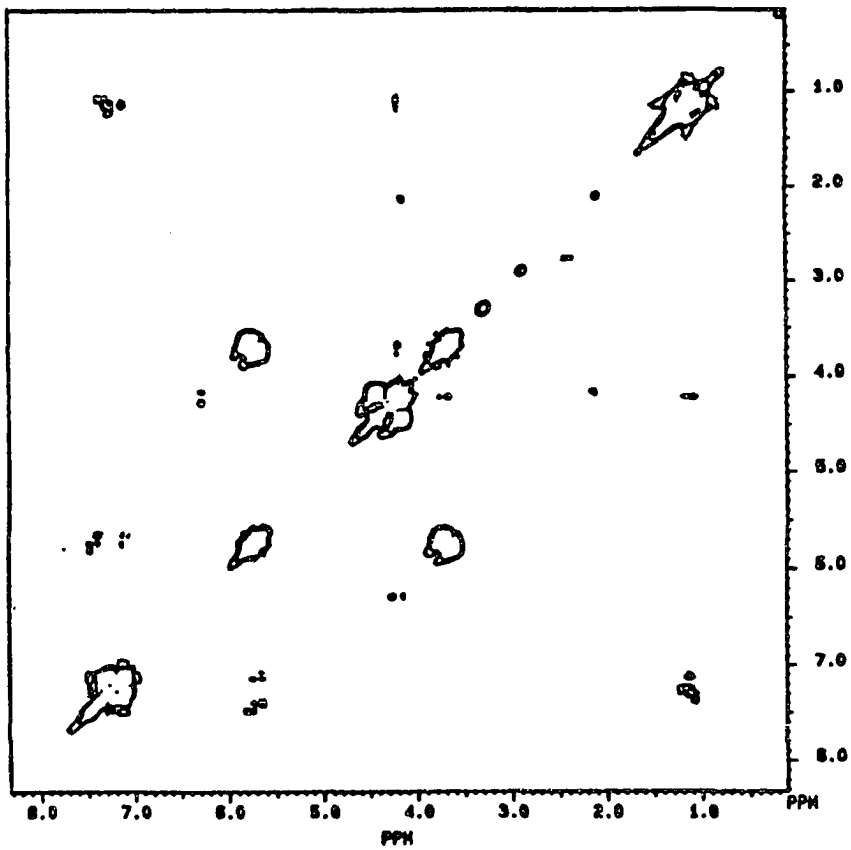

Figure C.1. Contour plot of 200 MHz ^{1}H-^{1}H correlated spectrum of macrocycle **2a** measured in $CDCl_3$ at 250K.

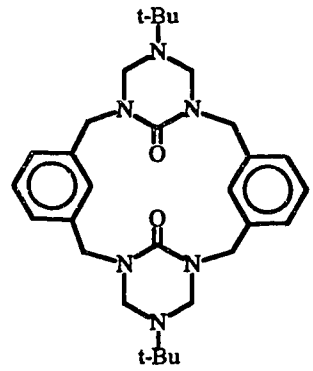

2a

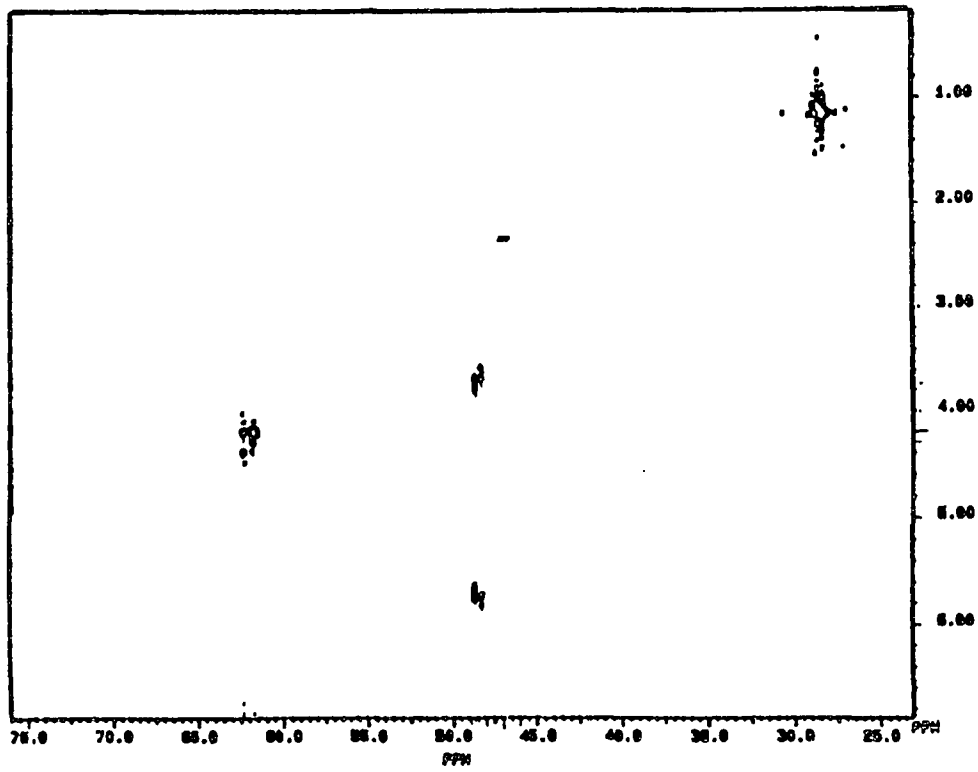

Figure C.2. Contour plot of 200/50 MHz ^{1}H-^{13}C correlated spectrum of macrocycle **2a** measured in $CDCl_3$ at 250K.

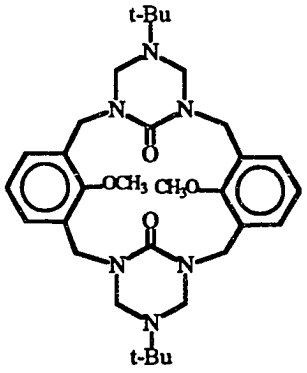

2b

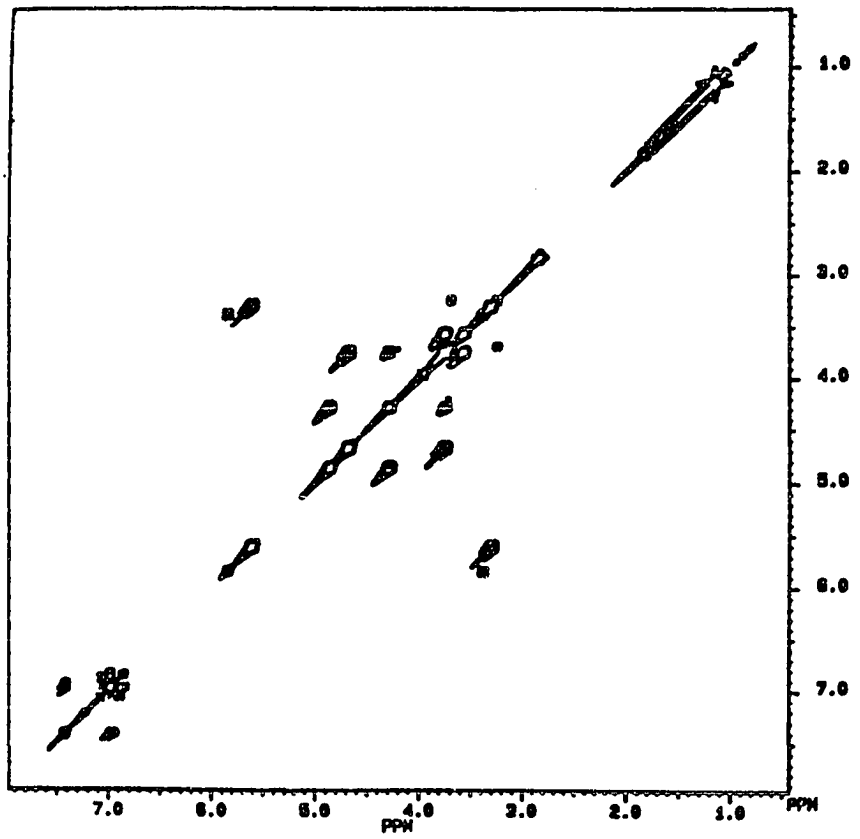

Figure C.3. Contour plot of 200 MHz ^{1}H-^{1}H correlated spectrum of macrocycle **2b** measured in $CDCl_3$ at 300K.

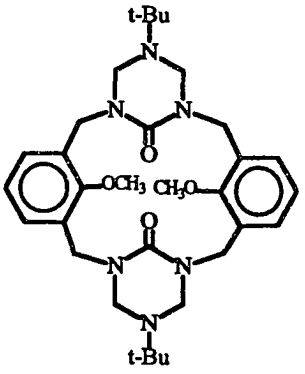

2b

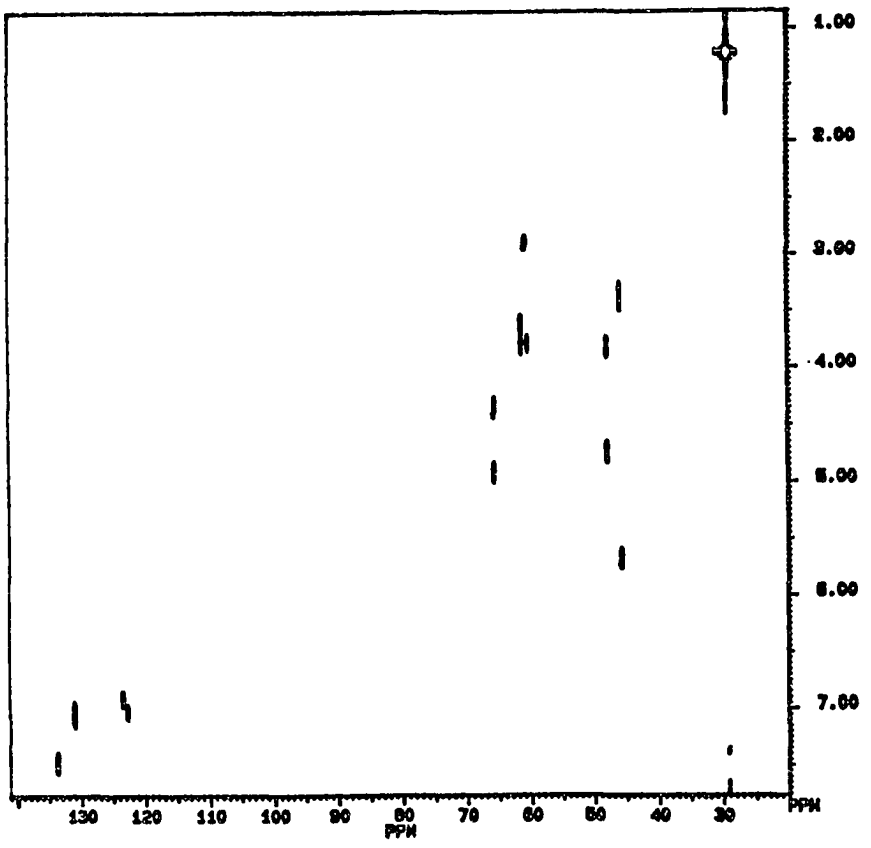

Figure C.4. Contour plot of 200/50 MHz ^{1}H-^{13}C correlated spectrum of macrocycle **2b** measured in $CDCl_3$ at 300K.

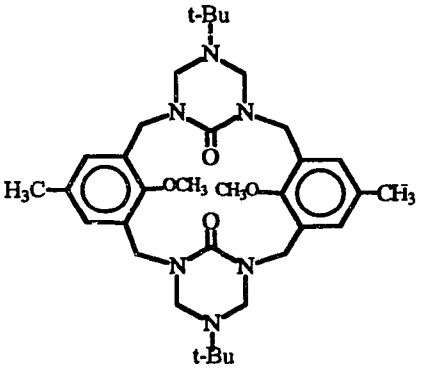

2c

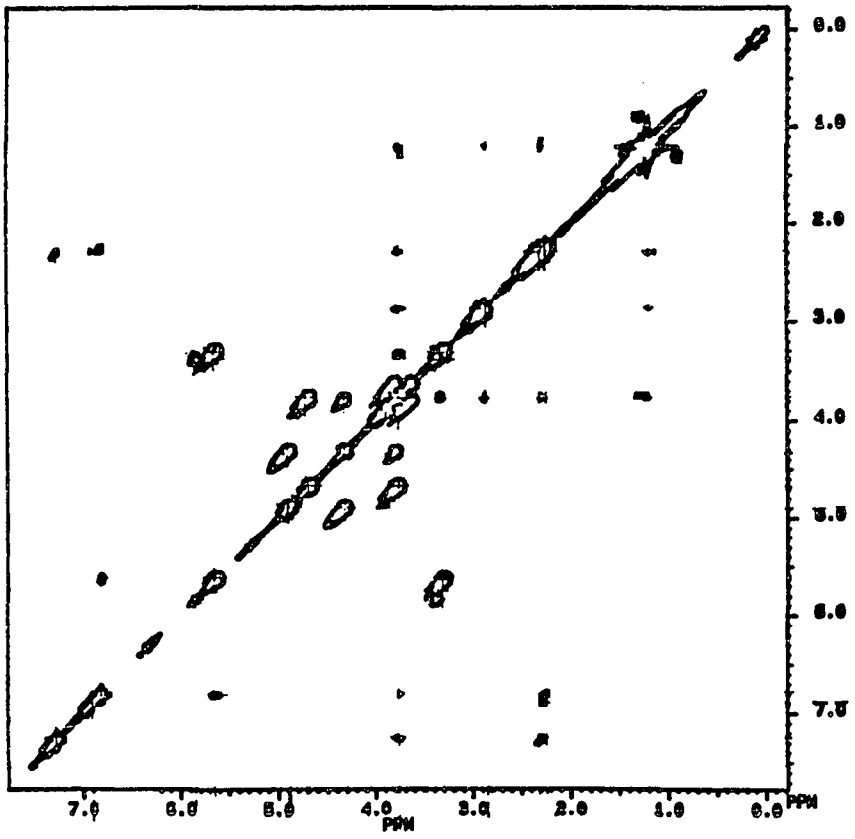

Figure C.5. Contour plot of 200 MHz ^{1}H-^{1}H correlated spectrum of macrocycle **2c** measured in $CDCl_3$ at 300K.

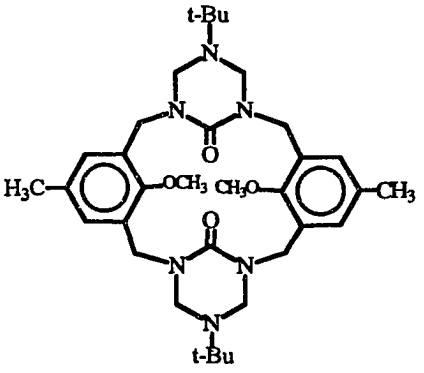

2c

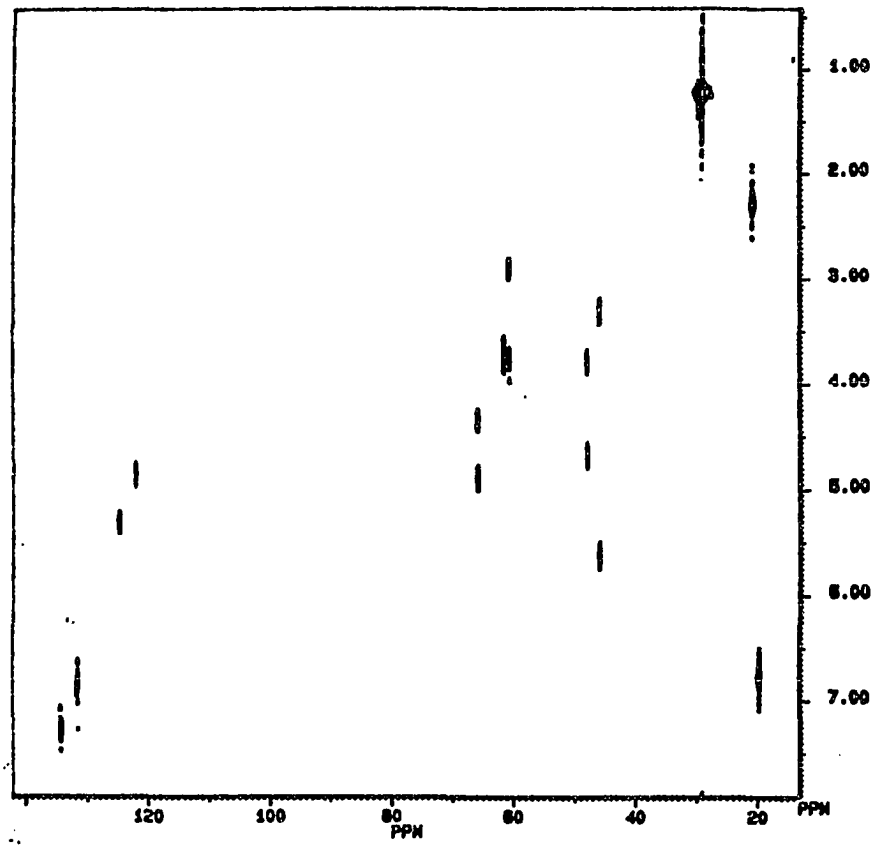

Figure C.6. Contour plot of 200/50 MHz ^{1}H-^{13}C correlated spectrum of macrocycle **2c** measured in $CDCl_3$ at 300K.

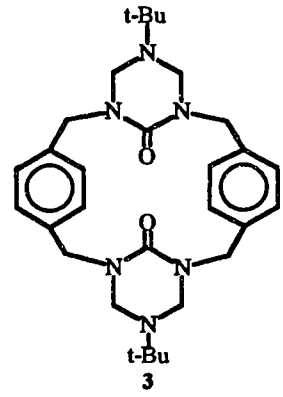

3

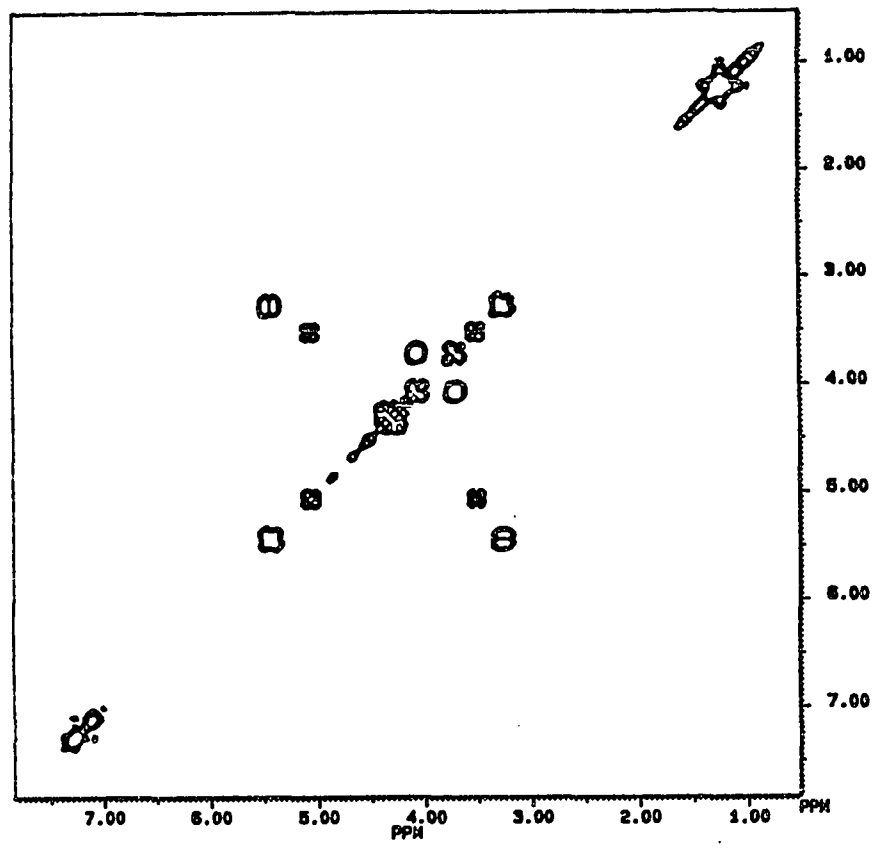

Figure C.7. Contour plot of 200 MHz ^{1}H-^{1}H correlated spectrum of macrocycle **3** measured in $CDCl_3$ at 300K.

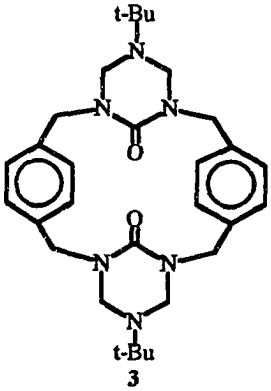

3

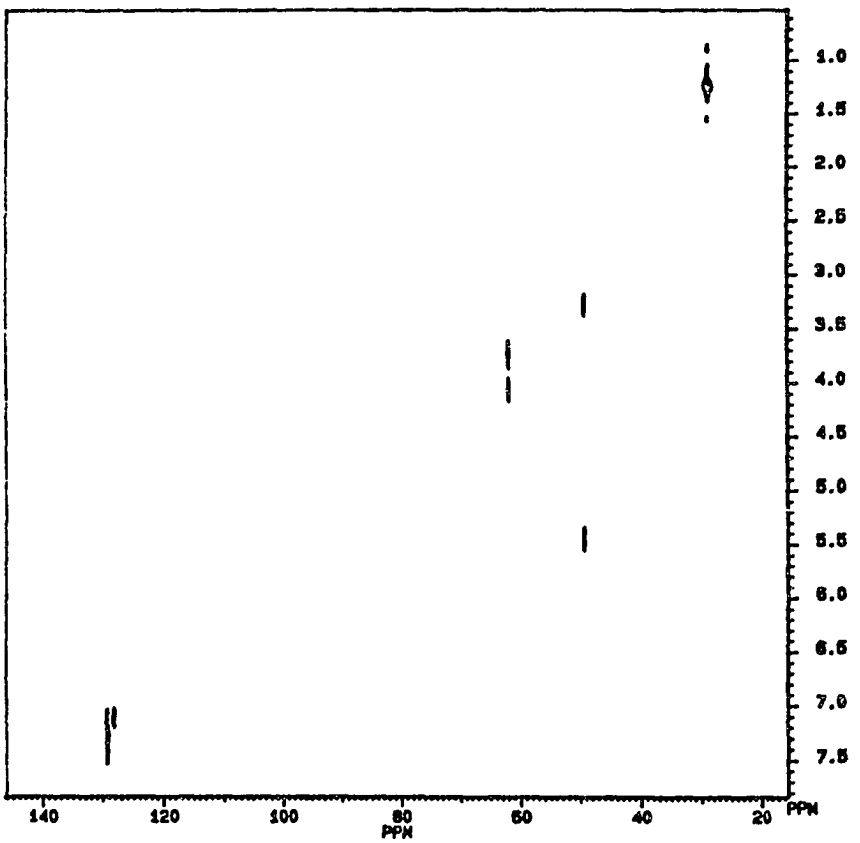

Figure C.8. Contour plot of 200/50 MHz ^{1}H-^{13}C correlated spectrum of macrocycle **3** measured in $CDCl_3$ at 300K.

APPENDIX D

X-ray Crystallography

ORTEP representations of x-ray Crystallographic measurement for macrocycles **2a-c** are reproduced in this section.

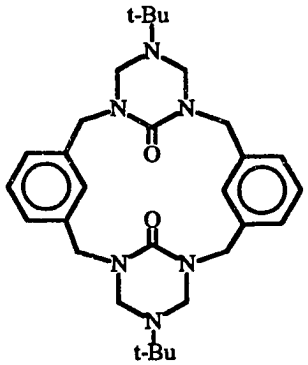

2a

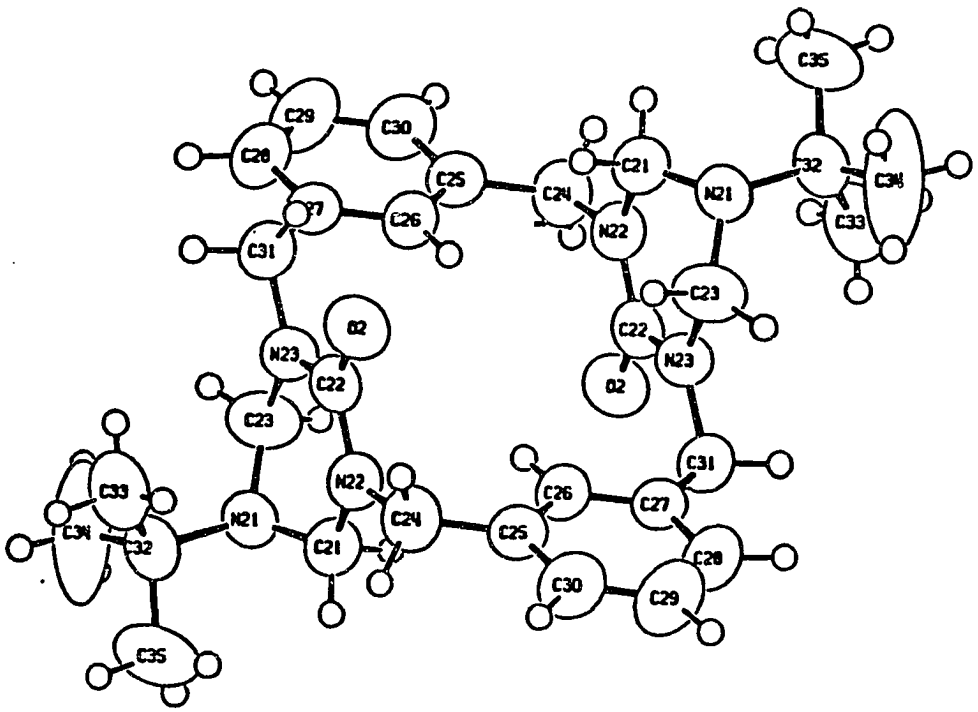

Figure D.1. ORTEP representation of macrocycle **2a**.

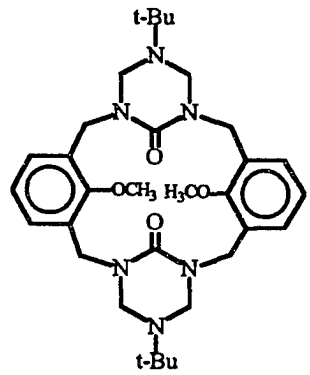

2b

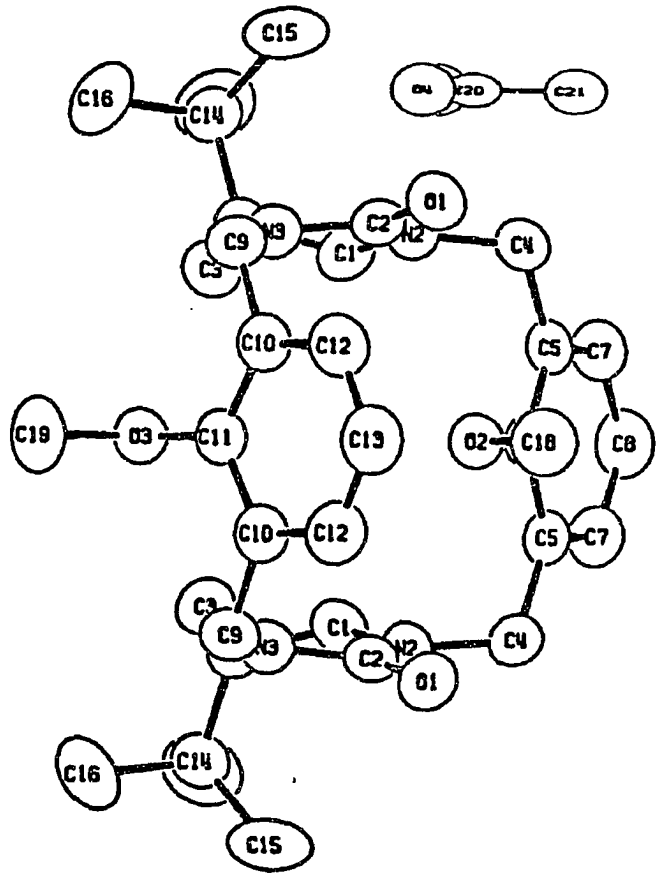

Figure D.2. ORTEP representation of macrocycle **2b**.

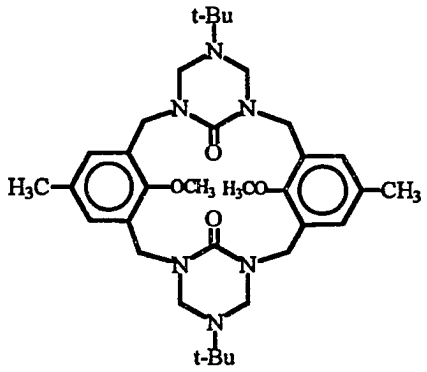

2c

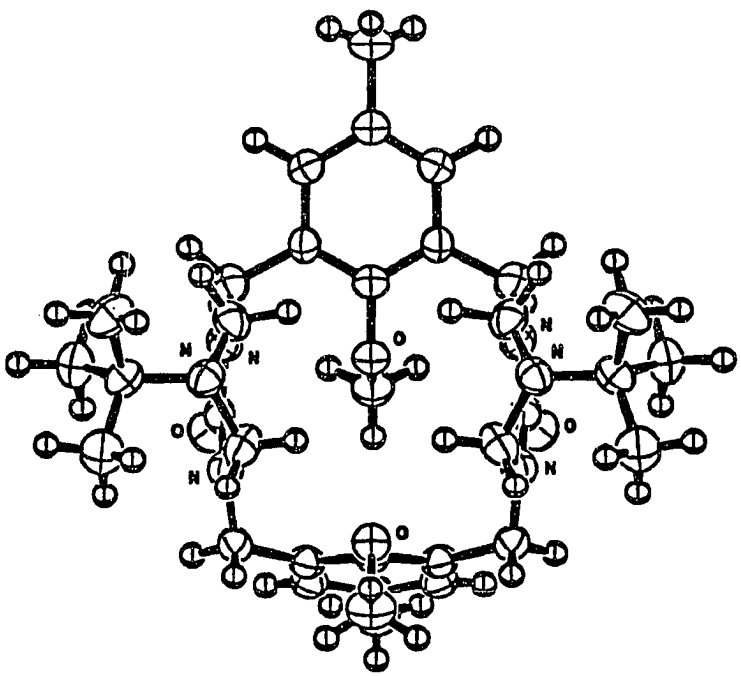

Figure D.3. ORTEP representation of macrocycle **2c**.

References

1. See for example, (a) Alster, J.; Iyer, S.; Sandus, O., *Chemistry and Physics of Energetic Materials*, Bulusu, S.N. Ed.; Kluwer Academic Publisher, Dorerecht, The Netherlands, **1990**; pp 641-652. (b) Nielsen, A.T. Polycyclic Amine Chemistry; in *Chemistry of Energetic Materials*, Olah, G.A.; Squires, D.R., Eds.; Academic Press, Inc., New York, **1991**; 95-124 (c) Olah, G.A.; Ramaiah, P; Surya Prakesh, G.K.; Gilardi, R. *J. Org. Chem.* **1993**, 58, 763.

2. Eaton, P.E. *Angew. Chemie. Int. Ed. Engl.* **1992** 31, 1421; Eaton, P.E.; Wicks, G.E. *J. Org. Chem.* **1988** 53, 5353.

3. Paquette, L.A.; Fisher, L.A.; Engle, P. *J. Org. Chem.* **1985** 50, 2524.

4. Nielsen, A.T; Nissan, R.; Chaffin, A.P.; Gilardi, R.D.; George, C. *J. Org. Chem.* **1992**, 57, 6756. Nielsen, A.T.; Nissan, R.; Vanderah, D.J.; Coon, C.; Gilardi, R. Flippen-Anderson, J.L. *J. Org. Chem.* **1990**, 55, 1459. Doyle, R.J. Jr. *Org. Mass Spectrometry.* **1991**, 26, 723.

5. Cichra, D.; Adolph, H.G. *Synthesis* **1983**, 830; Ammon, H.L.; Gilardi, R.D. Bhattacharjee, S.K. *Acta Cryst.* **1983**, C39, 1680.

6. (a) Oyumi, Y.; Brill, T.B. *Combustion Flame* **1985**, 62, 225. (b) Oyumi, Y.; Brill, T.B.; Rheingold, A.L. *J. Phys. Chem.* **1985**, 89, 4317. (c) Oyumi, Y.; Brill, T.B. *Combustion Flame* **1987**, 68, 209.

7. Oyumi, Y.; Brill, T.B.; Rheingold, A.L.; Haller, T.M. *J. Phys. Chem.* **1986**, 90, 2526.

8. Anex, D.S.; Allman, J.C.; Lee, Y.T. Studies of Initial Dissociation Processes in 1,3,3-Trinitroazetidine by Photofragmentation Translational Spectroscopy in *"Chemistry of Energetic Materials,"* Olah, G.A.; Squires, D.R. Eds.; Academic Press, Inc., New York, **1991**; p. 27.

9. Politzer, P.; Seminario, J.M. *Chem. Phys. Letters* **1993**, 207, 27.

10. Iyer, S.; Velicky, R.; Sandus, O.; Alster, J. U.S. Army Armament Research, Development and Engineering Center, Technical Report ARAED-TR-89010, June, **1989**.

11. (a) Archibald, T.G.; Gilardi, R.; Baum, K.; George C. *J. Org. Chem.* **1990**, 55, 2920 (b) Kornblum, N; Singh, H.K.; Kelly, W.J. *J. Org. Chem.* 1983, 48, 332.

12. (a) Marchand, A.P.; Rajagopal, D.; Bott, S.G. *J. Org. Chem.* **1994**, 59, 1608 (b) Marchand, A.P.; Rajagopal, D.; Bott, S.G. *J. Org. Chem.* **1994**, 59, 18, 5499.

13. see Hiskey, M.A.; Coburn, M.D. in *Alternate Synthesis of 1,3,3-Trinitroazetidine (TNAZ),* Energetics and Warheads Division Report (Explosives Section), U.S. Army ARDEC, November, **1992**.

14. (a) DEAD; diethyl azodicarboxylate (b) Lai, B.; Pramanik, B.N.; Manhas, M.S.; Bose, A.K. Tetrahedron Lett. **1977**, 1977. (c) Katritzky, A.R.; Cundy, D.J. and Chen, J. *J. Heterocyclic Chem.* **1994**, 31, 271.

15. see Schechter, H. in *Alternate Synthesis of 1,3,3-Trinitroazetidine (TNAZ),* Energetics and Warheads Division Report (Explosives Section), U.S. Army ARDEC, November, **1992**.

16. Axenrod, T.; Watnick, C.; Yazdekhasti, H.; Dave, P.R. *Tetrahedron Lett.* **1993**, 34, 6677.

17. Dave, P.R.; Ferraro, M.; Ammon, H.L.; Choi. C.S. *J. Org. Chem.* **1990**, 55, 4459.

18. Watson, W.H.; Kashyap R.P. *J. Org. Chem.* **1993**, 58, 759.

19. Gaertner, V.R. *J. Org. Chem.*, **1967**, 32, 2972.

20. Okutani, T.; Kaneko, T.; Masuda, K. *Chem. Pharm. Bull.*, **1974**, 22, 1490.

21. Gaj, B.J.; Moore, D.R. *Tetrahedron Lett.* **1967**, 2155.

22. Jenkins, H. and Cale, A.D. *German Offen.*, 1970, 1, 932, 219; *Chem. Abst.*, **1970**, 72, 100478s.

23. Higgins, R.H.; Watson, M.R.; Faircloth, W.J. *J. Heterocyclic Chem.* **1988**, 25, 383.

24. Higgins, R.H.; Eaton, Q.L.;Worth, L.; Peterson, M.V. *J. Heterocyclic Chem.*, **1987**, 24, 255.

25. Anderson, A.G. Jr; Lok, R. *J. Org. Chem.* **1972**, 37, 3953.

26. Baumann, H.; Duthaler R.O. *Helv. Chim. Acta.* **1988**, 71, 1035.

27. Nitta, Y.;Yamaguchi T.; Tanaka, T. *Heterocycles*, **1986**, 24, 25.

28. (a) Pusino, A.; Saba, A.; Desole, G.; Rosanti, V. *Gazz. Chim. Ital.* **1985**, 115, 33 (b) Sajadi, A.; Kahani, M.; Loeffler, L.J.; Hall, I.H. *J. Med. Chem.* **1980**, 23, 275.

29. Corey, E.J; Melvin, L.S. Jr.; Haslanger, M.F. *Tetrahedron Lett.* **1975**, 3117.

30. Moulines, J.; Bats, J-P.; Hautefaye, P.; Nuhrich, A.; Lamidey, A-M. *Tetrahedron Lett.* **1993**, 34, 2315.

31. Paudler, W.F.; Gapski, G.R.; Barton, J.M. *J. Org. Chem.* **1966**, 31, 277.

32. (a) Hassner, A. *The Chemistry of Heterocyclic Compounds*, Wiley-Interscience, New York, **1983**, Vol. 42, p 2, Azetidines, Lactams, Diazetidines and Diaziridines, pp 1 ff.; (b) Cromwell, N.H.; Phillips, B. *Chem. Rev.* **1979**, 79, 336.; Davies, D.E.; Storr, R.C. *Comprehensive Heterocyclic Chemistry*, Pergamon Press, New York, **1984**, Vol. 7, p 5.

33. (a) Vaughn, W.R.; Klonowski, R.S.; McElhinney, R.S.; Milward, B.W. *J. Org. Chem.* **1961**, 26, 138. (b) Shono, T.; Masumura, Y.; Uchida, K.; Nakatani, F. *Bull. Chem. Soc. Jpn.* **1988**, 61, 3029.

34. Kurteva, V.B.; Lyapova, M.J.; Pojarleff, I.V. *J. Chem. Research (S)* **1993**, 270.

35. Morimoto, A.; Okutani, T.; Masuda, K. *Chem. Pharm. Bull.* **1973**, 21, 228.

36. Searles, S.; Tamres, M. Block, F.; Quarterman, L.A. *J. Amer. Chem. Soc.* **1956**, 78, 4917.

37. Chaterjee, S.S.; Shoeb, A. *Synthesis* **1973**, 153.

38. For recent reviews see, *Supramolecular Chemistry*, Vogtle, F., John Wiley & Sons, New York **1993**; *Molecular Recognition, Clathrates* I, Weber, E., Ed.; *Top. Curr. Chem.* **1987**, 140; Rebek, J., Jr. *Science* **1987**, 235, 1478; Cram, D.J. *Angew. Chem. Int. Ed. Eng.*, **1986**, 25, 1039; Lehn, J.M. *Science* **1985**, 227, 849; Atwood, J.L.; Davies, J.E.D.; MacNicol, D.D. Eds., *Inclusion Compounds*; Academic Press: London, **1984**; Vol. 2; Vogtle, F.; Muller W.M, *J. Inclusion Phenom.* **1984**, 1, 369; Gutsche, C.D. *Acc. Chem. Res.* **1983**, 16, 161.

39. Stewart, K.D.; Miesch, M.; Knobler, C.B.; Maverick, E.F.; Cram, D.J. *J. Org. Chem.* **1986**, 51, 4327.

40. Cram, D.J.; Dicker, I.B.; Knobler, C.B.; Trueblood, K.N. *J. Am. Chem. Soc.* **1982**, 104, 6828.

41. Kaplan, L.J.; Weisman, G.R.; Cram, D.J. *J. Org. Chem.* **1979**, 44, 2226; Nolte, R.J.M.; Cram, D.J. *J. Am. Chem. Soc.* **1984**, 106, 1416.

42. Cram, D.J.; Dicker, I.B.; Lauer, M.; Knobler, C.B.; Trueblood, K.N. *J. Am. Chem. Soc.* **1984**, 106, 7150.

43. Cram, D.J.; Doxsee, K.M. *J. Org. Chem.* **1986**, 51, 5068.

44. Bryant, J.A.; Ho, S.P.; Knobler, C.C.; Cram, D.J. *J. Am. Chem. Soc.* **1990**, 112, 5837.

45. Katz, H.E.; Cram, D.J. *J. Am. Chem. Soc.* **1984**, 106, 4977.

46. Pratt, J.A.E.; Sutherland, I.O.; Newton, R.F., *J. Chem. Soc., Perkin Trans. I*, **1988**, 13.

47. Gutsche, C.D. *Acc. Chem. Res.* **1983**, 16, 161.

48. Vrielink, A.; Codding, P.W.; Gutsche, C.D.; Lin, L.G. *J. Inclusion Phenom.* **1986**, 4, 199.

49. Happel, G; Mathiasch, B.; Kammerer, H. *Makromol. Chem.* **1975**, 176, 3317.

50. Munch, J.H. *Makromol. Chem.* **1977**, 178, 69.

51. Gutsche, C.D.; Bauer, L.J. *Tetrahedron. Lett.* **1981**, 4763.

52. Gutsche, C.D.; Dhawan, B.; Levine, J.A.; No, K.H. and Bauer, L.J. *Tetrahedron* **1983**, 39, 409.

53. Peterson, H. *Synthesis* **1973**, 243.

54. Stewart, K.D.; Miesch, M.; Knobler, C.B.; Maverick, E.F. and Cram, D.J. *J. Org. Chem.* **1986**, 51, 4327.

56. Gutsche, C.D.; Dhawan, B.; NO, K.H. and Muthukrishnan, R., *J. Am. Chem. Soc.* **1981**, 103, 3782.

57. Gutsche, C.D. *Calixarenes, Monographs in Supramolecular Chemistry,vol.1*, Stoddart, J.F., Ed, RSC, Cambridge, **1989**.

58. Bauer, L.J.; Gutsche, C.D. *J. Am. Chem. Soc.* **1985**, 107, 6063.

59. Coruzzi, M.; Andreetti, G.D.; Bocchi, V.; Pochini, A.; Ungaro, R. *J. Chem. Soc. Perkin Trans. 2*, **1982**, 1133.

60. Andreetti, G.D. ; Ungaro, R.; Pochini, A. *J. Chem. Soc. Chem. Commun.* **1979**, 1005.

61. McKervey, M.A.; Seward, E.M. *J. Org. Chem.* **1986**, 51, 3581.

62. Ungaro, R.; Pochini, A.; Andreetti, G.D.; Sangermano, V. *J. Chem. Soc. Perkin Trans. 2* **1984**, 1979.

63. Ungaro, R. Pochini, A.; Andreetti, G.D.; Domiano, P. *J. Chem. Soc. Perkin Trans. 2*, **1985**, 197.

64. Uzawa, J.; Zushi, S.; Kodama, Y.; Fukuda, Y.; Nishihata, K.; Umemura, K.; Nishio, M.; Hirota, M. *Bull. Chem. Soc. Jpn.* **1980**, 53, 3623.

65. Koenig, K.E.; Lein, G.M.; Stuckler, P.; Kaneda, T.; Cram, D.J. *J. Am. Chem. Soc.* **1979**, 101, 3553.

66. Vogtle, F.; Von Newmann, P. *Tetrahedron* **1970**, 26, 5299.

67. Dave, P.R.; Doyle, G.; Axenrod, T.; Yazdekhasti, H.; Ammon, H.L. *Tetrahedron. Lett.* **1992**, 33, 1021.

68. CA Names for Compounds: **2a** = 11,23-Di-tert-butyl-1,9,11,13,21,23-hexaazapentacyclo[19.3.1.^{3,7}1.^{9,13}1^{15,19}]octacosa-3,5,7(28),15,17,19(26)-hexaene-25,27-dione; **3** = 5,16-Di-tert-butyl-3,5,7,14,16,18-hexaazapentacyclo[18.2.2.2.^{9,12}1.^{3,7}1^{14,18}]octacosa-9,11,20,22,23,26-hexaene-25,28-dione. We thank Dr. K.L. Loening of Chemical Abstract Service for supplying nomenclature.

69 Reichardt, C. *Solvents and Solvent Effects in Organic Chemistry, 2nd ed.*, VCH, New York **1989**.

70. MOPAC Manual, v. 7.0, *QCPE program 455*, **1944**; All calculations were performed on an IBM RS/6000 model 390 workstation.

71. Still, C. *MacroModel*, Columbia University Chemistry Molecular Modeling System, v. 4.5, Columbia University, New York **1994**.

72. *Chem3D Molecular Modeling and Analysis*, v. 3.1, Cambridge Scientific Computing, Inc., Cambridge, MA **1993**.

73. Cornforth, J.W.; Hart, P.D'Arcy; Nicholles, G.A.; Rees, R.J.W.; Stock, J.A.; *Br. J. Pharmacal.*, 10, 73, **1955**.